Scaled synthesis of nucleoside phosphates

CARLOTTA PAGLI

University of Durham

A Thesis Entitled

Scaled synthesis of nucleoside phosphates

Submitted by

Carlotta Pagli

Department of Chemistry

A Candidate for the Degree of Doctor of Philosophy

Durham University
Department of Chemistry

Statement of Copyright

Abstract

The research within this thesis is primarily concerned with the synthesis of phosphoanhydrides. Taking advantage of promising synthetic approaches developed in recent years in nucleoside phosphorylation, the thesis focuses on optimizing and increasing the 'usability' and 'scalability' of existing routes both in batch and in semi continuous flow systems. Specifically, the P(III)-P(V) mixed anhydride method developed by Jessen and co-workers[1] was the starting point of this work. Jessen's "one pot-three steps" synthesis of phosphoanhydrides[1] relies upon the *bis*-(fluorenylmethyl)-diisopropylamine phosphoramidite reagent.[2, 3]

Batch optimization and scale-up of phosphitylating reagent preparation was followed by translation of the process into a continuous flow method. The tetrahydrofuran-based batch approach for the preparation of *bis*-(fluorenylmethyl)-diisopropylamine phosphoramidite was completed within one hour using a simple, extractive purification process, avoiding chromatography. The approach delivered 86% yield, based on theoretical mass recovery, where the isolated material was shown to be 97% pure based on ^{31}P NMR analysis. Despite the batch process proving successful using tetrahydrofuran, a dichloromethane: tetrahydrofuran-based procedure was required for translating the process to flow. Although the mass recovery and the purity levels of *bis*-(fluorenylmethyl)-diisopropylamine phosphoramidite obtained in the batch reactions were marginally higher, the experiments performed in flow were effective, delivering 81% yield, based on theoretical mass recovery, and 87% purity based on ^{31}P NMR analysis. The flow approach was also demonstrated to be scalable, delivering 25 g of compound.

Subsequently, the synthesis of ADP from AMP using *bis*-(fluorenylmethyl)-diisopropylamine phosphoramidite in flow systems was explored. To better inform the flow platform, extensive NMR studies were performed to obtain quantitative, high sensitivity ^{31}P NMR spectra during the phosphoramidite coupling, oxidation and deprodetcion steps for the synthesis of phosphoanhydrides in DMF. NMR parameters were improved by measuring the T1 relaxation and the Ernst angle to ensure a qualitatively satisfactory analysis. Although it was not possible to gain detailed reaction kinetics data, the quantitative ^{31}P NMR methods that were developed proved to be a valuable starting point for further analytical studies and were qualitatively informative for the flow studies. Combining flow chemistry with our ^{31}P NMR work, a workflow approach was developed to deliver a robust and reliable synthesis of

nucleotides. The method was upscaled from a 0.27 mL chip to a 2.5 mL reaction coil, delivering 1 g of ADP product, with a 65% yield and a purity >99% by HPLC. The scope of our method was explored through its application to the syntheses of UDP and CDP, and these experiments gave promising starting points for future work.

In summary, starting from the Jessen's "one pot-three steps" phosphoanhydrides synthesis, an improved the batch synthesis of *bis*-(fluorenylmethyl)-diisopropylamine phosphoramidite was developed and translated to a continuous flow system. Furthermore, a reliable, robust and scalable workflow method for the synthesis of ADP in a continuous flow system was developed, supported by specific ^{31}P NMR analytical methods.

Acknowledgements

This thesis could not have been completed without the assistance of an enormous number of people. Firstly, I would like to thank Prof. David R W Hodgson for his guidance throughout my entire doctoral studies. I would like to express my entire gratitude to Prof. Ian R. Baxendale, for welcoming me to his lab and for introducing me to the field of flow chemistry. Thank you both for this opportunity. I would also like to express my gratitude for the support provided by the past and present members of the DRWH group. I would like to thank all the departmental staff, especially Dr. Juan A. Aguilar Malavia of the NMR service, the NMR kinetics chapter is all thanks to his teachings, and Dr. Aileen Congreve in HPLC, your analyses are fundamental for this work. In the end, I would especially like to thank all the people and friends I meet in the Chemistry department during all my PhD; few words, a laugh, and a smile, even hidden by the face mask, have been important.

To all the people I love.

A voi, Mamma, Babbo e Tommaso.

Memorandum

Elements of this work have been presented at:

- Online conference, 2nd Nucleosides and Nucleotides: synthetic and biological chemistry, 2021, (Poster);
- Online conference, RSC Nucleic Acids Forum, 2021, (Poster);
- Durham University Gala PG Symposium, 2022, (Oral Presentation).

Abbreviations

aaRS	Aminoacyl-tRNA synthetases
ADP	Adenosine diphosphate
AMP	Adenosine monophosphate
app	Apparent
at	Acquisition time
ATP	Adenosine triphosphate
CDP	Cytidine diphosphate
CFPS	Cell-free protein synthesis
CMP	Cytidine monophosphate
CPG	Controlled pore glass
CTP	Cytidine triphosphate
CV	Column volume
d	Doublet
dd	Doublet of doublet
d1	Relaxation delay
DBU	1,8-Diazabiciclo[5.4.0]undec-7-ene
DCC	N,N'-Dicicloesilcarbodiimmide
DCI	4,5-Dicyanoimidazole
ddATP	Dideoxyadenosine triphosphate
ddCTP	Dideoxycytidine triphosphate
ddGTP	Dideoxyguanosine triphosphate
ddTTP	Dideoxythymidine triphosphate
DMAP	4-Dimethylaminopyridine
DMF	Dimethylformammide
DMSO	Dimethyl sulfoxide
DMT	Dimethoxytrityl
DNA	Deoxyribonucleic acid
dNDPs	Deoxynucleoside diphosphates
dNTPs	Deoxynucleoside triphosphates
E2	Elimination reaction (2)
Et_2O	Diethyl ether
EtOAc	Ethylacetate
Fm	Fluorenemethylene
FR	Flow rate
GC	Gas Chromatography
GMP	Guanidine monophosphate
GSM	Global Suppression Method
GTP	Guanidine diphosphate
h	heptet
HPLC	High-performance liquid chromatography
HR-MS	High resolution–mass spectrometry
LC-MS	Liquid chromatography–mass spectrometry
m	multiplet

*m*CPBA	*meta*-Chloroperoxybenzoic acid
mRNA	messenger RNA
MS	Mass spectrometry
NCL	Native Chemical Ligation
NDP	Nucleoside diphosphate
NMP	Nucleoside monophosphate
NMR	Nuclear magnetic resonance
nt	Number of scans
NTP	Nucleoside triphosphate
OTS	Orthogonal Translation System
p1	Pulse width one
pad	Preacquisition delay
PCR	Polymerase Chain Reaction
PFA	Polyfluorinated Substances
PG	Protecting group
PPN	[bis (triphenylphosphoranylidene) ammonium] pyrophosphate
PS	Polystyrene
PTFE	Polytetrafluoroethylene
pw	Pulse width
q	quartet
RNA	Ribonucleic acid
RT	Retention time
s	Singlet
S_N	Nucleophilic substitution
SNR	Signal-to-noise ratio
t	Triplet
TBA	Tetrabutylammonium
*t*BuOOH	tert-Butyl hydroperoxide
TEAB	Triethylammonium bicarbonate
TEP	Triethyl phosphate
THF	Tetrahydrofuran
TLC	Thin layer chromatography
TMG	1,1,3,3-Tetramethylguanidine
TMP	Trimethyl phosphate
tRNAs	transfer RNA
UDP	Uridine diphosphate
UMP	Uridine monophosphate
UNAAs	Unnatural amino acids
UV	Ultraviolet

Content

1 Overview

Phosphoanhydrides are essential for life as major cellular sources of energy and as the precursors to nucleic acids.[4] Based on the fundamental biological roles of endogenous nucleosides and nucleotides, they have become important synthetic targets in medicinal chemistry, chemical biology, and material sciences over the last 50 years. The continued publication of more effective synthetic methods is due to their importance as biotechnological and therapeutic tools, which will be explored briefly in Chapter 2, section 2.1. In section 2.2, several commonly used approaches to prepare nucleoside diphosphates and triphosphates are outlined, and the advantages and disadvantages of each method are discussed. The P(III)-P(V) mixed anhydride method developed by Jessen and co-workers[1] is the starting point of the research in this thesis, and it is reviewed in section 2.3. The intent of this project, discussed in Chapter 3 is to optimize and scale the Jessen approach[1] using kinetic understanding and flow technology. The experimental results will be extensively discussed in Chapter 4, followed by conclusions and future plans in Chapter 5. The COVID-19 pandemic had significant impacts on research activity. Social distancing and the inability to room-share, prevented the timely use of NMR kinetic methods and flow systems. Thus, a nucleoside-based 'side project' and a phosphate-based 'side project' were adopted, and these are reported in Chapter 7.

2 Introduction

2.1 Nucleoside Phosphates: An Outline of Biotechnological and Therapeutic Applications

Natural nucleoside or deoxynucleoside mono-, di- and triphosphates are sugar-phosphate esters of nucleosides,[4] as shown in *Figure 1*. Namely, they are *β*-*N*-glycosides that consist of a purine (adenine or guanine) or pyrimidine (cytosine, uracil, thymine) nucleobase bonded to a pentose sugar (*β*-D-ribofuranose or 2-deoxy-*β*-D-ribose) by a *N*-glycosidic bond between C(1) of the furan ring and N(1) of cytosine or uridine or N(9) of adenine or guanine, and one-three phosphate groups bound to the C(5') of the sugar moiety**.** The first phosphate group linked to the sugar is the α-phosphate, the second is the *β*-phosphate, and the third is the *γ*-phosphate.

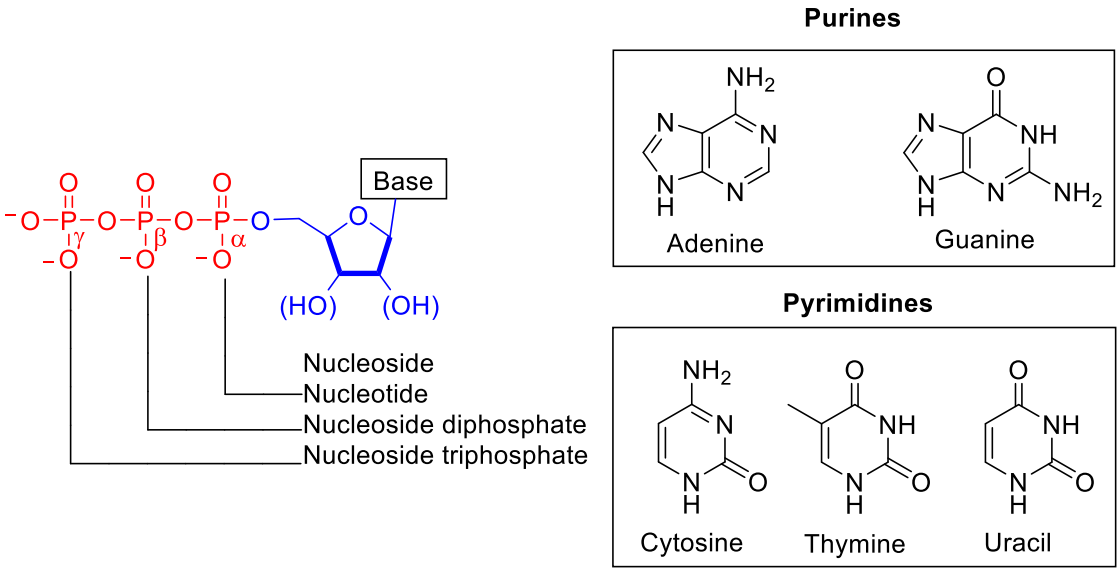

Figure 1: The structures of (deoxy)ribonucleoside phosphates.

These molecules are the primary building blocks for the enzymatic synthesis of DNA and RNA,[5-10] and they also function as energy carriers,[11-15] cofactors and signalling molecules.[16-24] Due to the fundamental biological roles of endogenous nucleosides and nucleotides, (d)NDPs and (d)NTPs and structural analogues are protagonists of the development of modern DNA sequencing methods, genetic therapies, biological probes and important classes of drug and pro-drug molecules.

The advent of genomic sequencing technologies and the rapid generation of whole-genome sequencing data for large numbers and types of organisms, including humans, has been one of the principal advances in the past two decades.

This era of sequencing, making and manipulating DNA,[25-27] which has been the focus of biological research in recent years, began with the work of Rosalind Franklin, Maurice Wilkins, Watson and Crick [28, 29] and their DNA double helix discovery, and continued with the development of chemical methods for solid-phase DNA synthesis, detection, and exploration of the genome.[30-34]

A key breakthrough in sequencing history is the well-known 'chain-termination' or dideoxy technique method, developed by Sanger and co-workers, to determinate polynucleotide sequences[35,36] in 1977 , as shown in *Figure 2*.

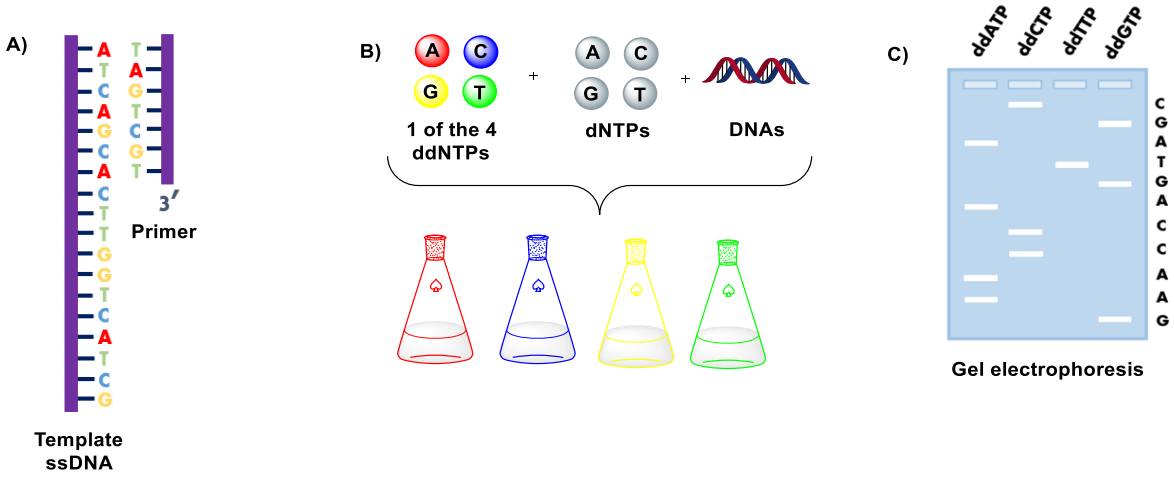

Figure 2: Overview of Sanger [37] Sequencing Technology: A) The target DNA is fragmented, amplified, denatured and bound to a primer. B) Four reaction mixtures containing different ddNTPs are performed, where elongation and termination take place. C) Gel electrophoresis to determination termination sites and, thus, sequence.

The chain-termination method is an optimization of previous studies [37-39] that led to the use of four parallel reactions carried out for each dideoxynucleoside triphosphate (ddATP, ddCTP, ddGTP and ddTTP) in the presence of a DNA polymerase[40] and a DNA primer that is extended against DNA template. Fragments were separated by polyacrylamide gel electrophoresis and the obtained sequences were read using radioisotope detection.[41]

In simple terms, this method is based on the principle that during DNA synthesis, addition of a nucleotide triphosphate requires a free hydroxyl group on the 3′ carbon of the sugar of the last nucleotide of the growing DNA strand. However, if a synthetic dideoxynucleotide that

lacks a hydroxyl group at the 3′ carbon of the sugar moiety is incorporated at the end of the growing chain, DNA synthesis stops because a phosphodiester bond cannot be formed with the next incoming nucleotide. As a result, DNA synthesis is terminated.[42] Synthetic dideoxynucleotide (ddATP, ddCTP, ddGTP and ddTTP) are the key reagents of this sequencing method, and, although the Sanger method has some limitations, its overall robustness and ease of use led to dideoxy chain-termination becoming the most common technology used to sequence DNA for many years.[30]

Hand-in-hand with the Sanger method, the Polymerase Chain Reaction (PCR),[43-45] enabled the amplification of specific DNA fragments (as shown in *Figure 3*). To date, this is one of the techniques most used in biological and biotechnological laboratories, and variants have developed based on the use of modified and synthetic dNTPs.

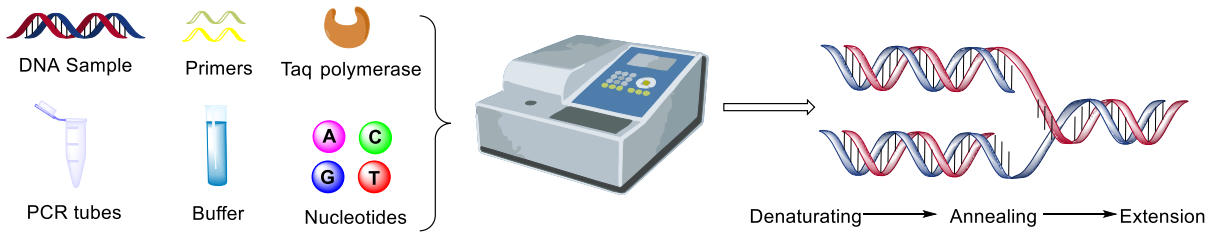

Figure 3: Schematic illustration of a PCR technology. [43-45]

The approach was designed in 1980 by Kary Mullis and colleagues.[46] The PCR assay, in much the same way as the Sanger Method, is based on reactions between a template DNA, primers, dNTPs and Taq DNA polymerase, where the reactions take place in a thermal cycler that allows repeated cycles of DNA amplification to occur through three basic heating steps (denaturation, annealing and extension). The PCR products can then be separated on the basis of their charge and size by agarose gel electrophoresis, and visualised under a UV lamp using ethidium bromide as an intercalating dye, or by Southern blotting.[47] The easy and time-effective execution of this assay means that it still forms the basis of clinical diagnostics and genomics methods, and it is an essential tool for the amplification of DNA in some Next Generation DNA Sequencing methods. [30-32, 36, 39, 41, 43, 48-50]

The Next Generation Sequencing platforms are diverse in strategies, but with conceptually similar workflows,[51-62] where the fundamental role of nucleotides in these technologies remains unchanged. It is important to underline that DNA/RNA sequencing and its optimization have underpinned many major advances in biological and biomedical research.[32, 62] The most important applications include discovery, by re-sequencing of targeted regions of

interest or whole genomes, *de novo* assemblies of bacterial genomes, cataloguing the transcriptomes of cells, tissues and organisms (RNA-seq),[63,64] genome-wide profiling of epigenetic markers and chromatin structure (ChIP-seq.),[50] and species classification and/ or gene discovery by metagenomics studies.[65]

Sequencing platforms underpin BioBrick Assembly methods, which have become standard tools that support the design and construction of synthetic genes,[66,67] and in the past five years of Biofoundries, that have enabled the rapid design, construction, and testing of genetically reprogrammed organisms for biotechnology applications and research.[68,69] The applications of sequencing technologies include studies on human diseases and the 1000 Genomes Project [70] is the result of them. The 1000 Genomes Project is a catalogue of variations across human genotype data that aims to discover genotypes and provide accurate haplotype information on all forms of human DNA polymorphism in multiple human populations. The project characterizes over 95% of variants that are in genomic regions accessible to current high-throughput sequencing technologies and that have allele frequency of 1% or higher.[70] The goal of the project is to accelerate the diagnosis of certain diseases and suggest the best therapy to follow, while also helping researchers to understand aetiology, epidemiology, and risk factors of certain diseases, as well as the discovery of future cures.

Nucleoside- and nucleotide-analogues have become indispensable to study the enzymatic pathways that involve endogenous nucleosides and nucleotides. P-modified analogues have been used to study the mechanisms and substrate specificities of enzymes such as DNA and RNA polymerases[71, 72] and protein-kinases.[73] Analogues of GTP have been employed to study signalling pathways mediated by G-protein-coupled receptors[74] and other modified compounds are promising drug candidates for targeting P2X and P2Y receptors.[75, 76]

Moreover, nucleoside and nucleotide analogues have played leading roles in drug discovery as antiviral and anticancer chemotherapeutic agents.[77-84] They exploit the same metabolic pathways as endogenous nucleosides or nucleotides and, for this reason, they are defined as antimetabolites. Inside cells, nucleoside prodrugs are phosphorylated by various kinases, to yield the active triphosphate form.

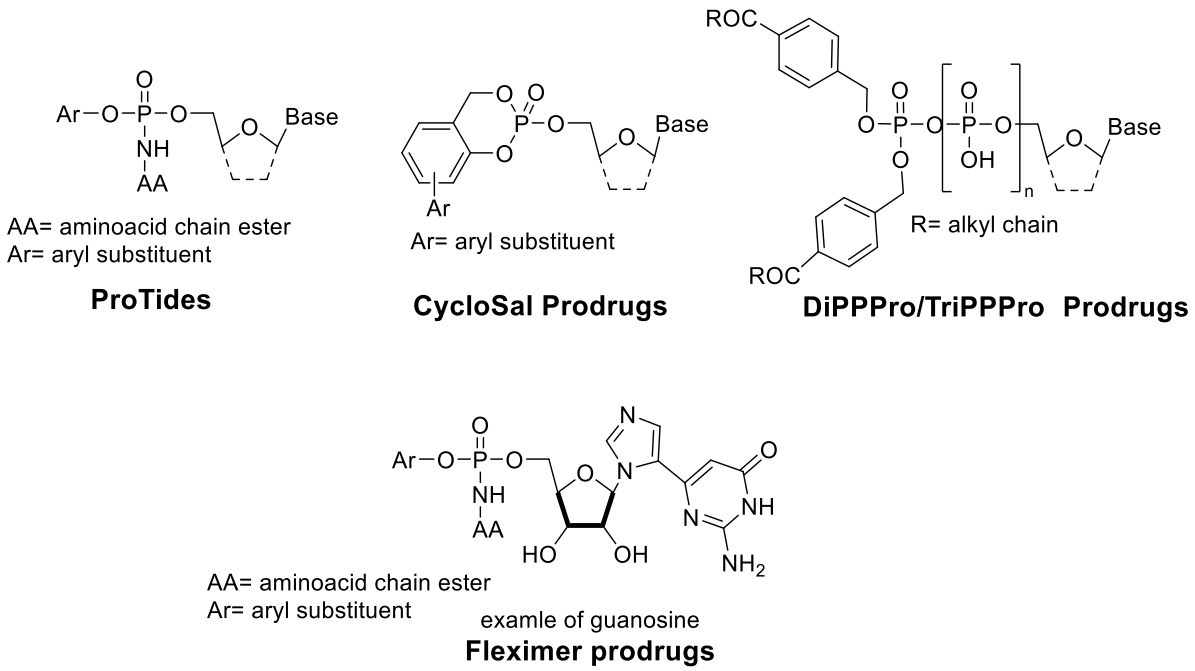

Figure 4: Four types of nucleotides prodrugs: ProTides,[85] *cycloSal*,[85-87] DiPPPro/TriPPPro[93-96] and *Flexime*[88-90] prodrugs.

The ingress of a nucleoside-based drug molecule through the phospholipidic membrane and the first 5'-phosphorylation are frequently the limiting steps of drug activation and, in order to bypass these problems, McGuigan developed the ProTide approach.[91, 92 93-95]

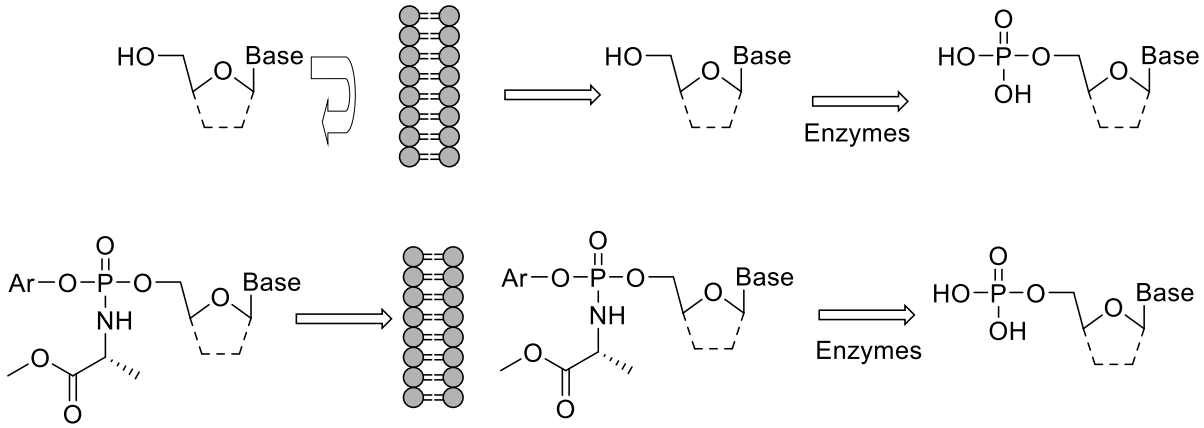

Figure 5: An example of the. ProTide strategy to allow cell entry via the phospholipidic membrane.[85]

This method is based on masking of the charges of the phosphate group with lipophilic moieties to facilitate cell penetration, and, once inside the cells, release the protected phosphate by exploiting cellular enzymes. The deprotected monophosphate may then be further activated by sequential phosphorylations to give the triphosphate. Meier and co-

workers developed a different methodology based on the delivery of masked NMP, NDP and NTP systems (*Figure 5*). The *cycloSal prodrugs*[85-87] approach (as shown in *Figure 4*) allows cellular membrane penetration thanks to a cyclic bifunctional masking group system, followed by release of the nucleotide by pH-driven chemical hydrolysis once inside the cell. *DiPPPro TriPPPro approaches* were also developed in attempts to bypass all intracellular steps of phosphorylation and immediately release active diphosphates and triphosphates[78, 96-99] (*Figure 4*). The unique concept of these powerful methodologies is the synthesis of prodrugs containing two acceptor-substituted benzyl esters linked to the β-phosphate group of the nucleoside diphosphate or the γ-phosphate group of the nucleoside triphosphate. These protecting groups allow cellular uptake of the compounds and release of the NDPs or NTPs, thus bypassing potentially limiting phosphorylation steps.[77] Research activity in this field at the same time took further and increasingly innovative directions, such as the synthesis in the early 2000s of chameleon molecules. Seley's research group introduced a new class of shape-modified nucleosides, *fleximers* (*Figure 4*). *Fleximers* are the product of dissection of the nucleobase to give flexibility to adapt to the spatial confines of the target enzyme binding site more readily.[88-90]

More recently, the COVID-19 pandemic[100-102] over the last few years has further highlighted the crucial role of nucleosides and nucleotides. Without the technologies mentioned above, scientists and clinicians would not have been able to study the genetic sequences of the SARS-CoV-2, detect antigens, create methods for virus identification in the affected people[103, 104] and, above all, generate and validate vaccines and drug treatments.[105-110]

2.2 An Overview of the Main Methods used for the Synthesis of Nucleoside Diphosphates and Triphosphates

In the last fifty years many strategies for the synthesis of (d)NDP and (d)NTP analogues have been developed due to the difficulties associated with these processes. However, a universally convenient method does not exist and remains a challenge. The paradigm of the "perfect synthesis method" can be summed up in the following phrases: clean, in that it does not lead to numerous side-products and laborious purifications; generally applicable to a broad range of nucleoside substrates; and not time consuming, in that the complete strategy should not include numerous substrate/reagent preparation and purification steps; and above all that it delivers excellent product yields. In the chemical synthesis of nucleotides, the possibility of achieving this goal becomes extremely complicated for several reasons:

- the chemical and physical characteristics of nucleosides and nucleotides (i.e., insolubility in organic solvents, low chemical stability, formation of solid-state hydrates).
- long reaction time because of the low reactivity (applies to certain strategies).
- over-reactive reagents (protecting groups needed).
- moisture sensitivity: anhydrous reagents and inert atmosphere are required to avoid the formation of side products.
- complicated, low-yielding purifications: often two orthogonal types of chromatography procedures are required (i.e., ion exchange followed by reverse-phase).

Chemically speaking, (d)NDPs and (d)NTPs are currently synthesized via two major approaches: polymer-supported synthesis and solution-phase synthesis.

Regarding the polymer-supported strategies, there are basically three approaches that exploit solid supports for the synthesis of nucleoside diphosphates and triphosphates. The first uses polymer-bound reagent which is then coupled with unprotected nucleoside. The second and the third involve the attachment of the sugar moiety or the base moiety of the substrate to the support. Anchoring reactants or substrates to a support enables reactions to be pushed to completion by using an excess of reagents. Purification of the crude reaction mixture is simplified because the spent reagents/products are immobilized on the support, which means that products and by-products can easily be separated. Controlled pore glass (CPG) and

polystyrene (PS) are commonly used for oligonucleotides synthesis. Despite their advantages, the problems found are mainly nonlinear reaction kinetics, unequal distribution and/or access to the reaction sites, solvation problems, inefficient coupling rates, and difficulties with intermediate analysis.[111-115]

The chemist's decision between solution-phase or solid support approaches towards nucleotide synthesis is not straightforward. Each method potentially remedies one problem while creating another, e.g. solution-phase methods offer faster reactions but make purification more challenging. Immobilisation requires additional, costly materials, which become cost-prohibitive when upscaled. Given that this thesis focuses on scalable production of nucleotides, the remainder of this thesis focuses on solution-phase strategies.

Solution-phase synthesis, nucleoside diphosphates and triphosphates are currently synthesized via phosphitylation (P(III) chemistry), phosphorylation (P(V) chemistry) and mixed anhydride chemistry (P(III)-P(V) chemistry). *Figure 6* shows the possible intermediates obtained during different synthetic approaches, reported in a comprehensive review published in 2016[111] by Béatrice Roy and co-workers.

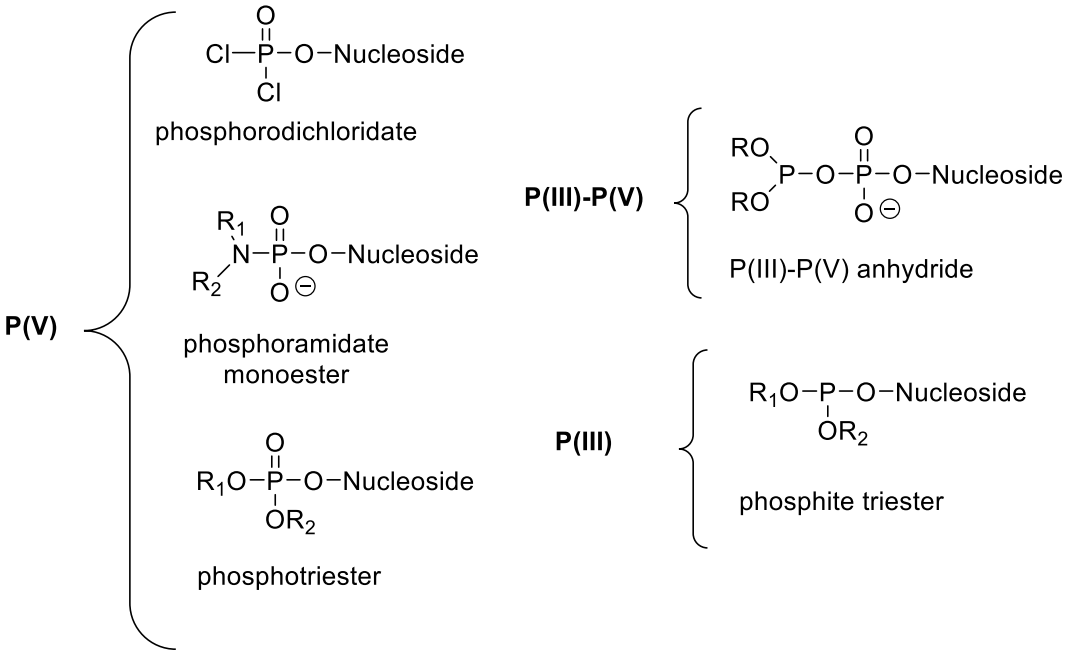

Figure 6: NDP and NTP intermediates formed by different synthetic approaches.

The following pages outline a journey through nucleotide synthesis via solution-phase chemistry. The most commonly used methods will be critically compared to understand the reasons that led us to this project and the scientific approach adopted in its course.

2.2.1 Synthetic strategies via solution-phase approaches

2.2.1.1 Synthetic strategies via P(V) approaches

The long-established P(V) synthetic approaches follow two different pathways. The first relies on a multi-step activation of a pre-formed NMP prior to treatment with either a phosphate or pyrophosphate anion (Khorana approach). The activation of the NMP is the limiting step of the entire synthetic process, critical to the success of the subsequent phosphoanhydride coupling reaction. The second uses $POCl_3$ as a partially regioselective phosphorylating agent that, in the absence of 2'/3' protection of the nucleoside, often leads to numerous by-products (Yoshikawa phosphorylation). Purifications of crude materials are difficult and multiple chromatography methods are often necessary. In the next section the most important synthetic methods will be highlighted, focussing on their advantages and disadvantages and the improvements that followed.

2.2.1.1.1 P(V) solution-phase approach via phosphoramidate intermediate

The activation of a nucleoside 5'-monophosphate as a phosphoramidate, such as morpholidate or imidazolidate using a condensing agent, followed by nucleophilic substitution at the α-P of NMP, is widely exploited for the synthesis of both (d)NDPs and (d)NTPs. Since the pioneering research of Khorana and Todd in 1953[116] and Moffatt and Khorana in the 1961[117, 118] this method continues to be used. Optimizations of the activation step and the synthesis of new pyrophosphate reagents for the coupling have increased its longevity.[119-129] In the following section, details of the parent methods of this approach and some of their modifications are presented.

Moffatt reported both the synthesis of (d)NDPs,[118] in collaboration with Khorana, and of (d)NTPs[130] through phosphoromorpholidate nucleoside intermediates, as shown in *Figure 7*.

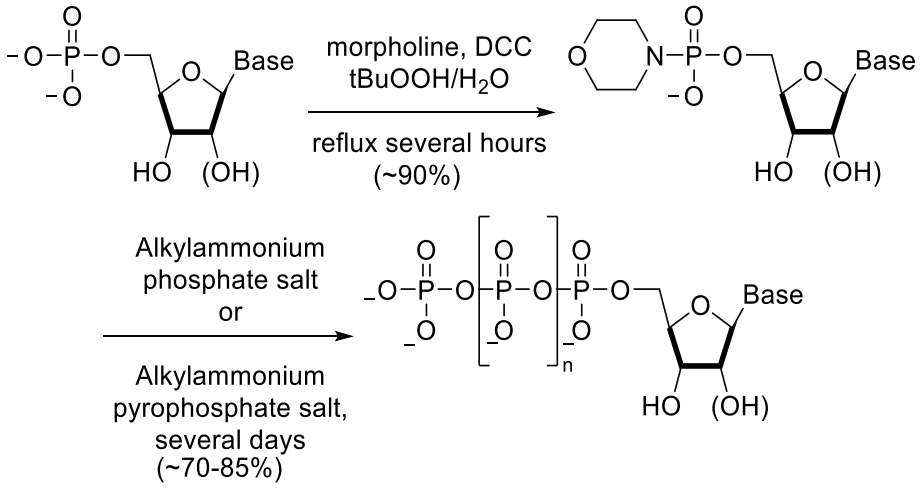

Figure 7: Moffat and Co-worker's synthetic method towards phosphoromorpholidate intermediates.[117]

The acidic form of a (d)NMP is activated with *N*,*N*-dicyclohexylcarbodiimide (DCC) in the presence of morpholine, leading to the nucleoside 5'-phosphoromorpholidate. Following this activation step, a nucleophilic substitution is performed using an orthophosphate or pyrophosphate alkylammonium salt. Maintenance of rigorous anhydrous conditions is crucial to avoid competing hydrolysis of the morpholidate intermediate over the long reaction time, however, alkylammonium phosphate salts are extremely hygroscopic. Another problem in this approach is the competing addition of the morpholine to DCC giving an intermediate that inhibits the phosphoramidate formation.[131] To overcome this problem, Van Boom proposed to generate phosphoromorpholidate intermediates by reacting NMPs with 2,2,2-tribromoethyl-morpholinochlorophosphate, for the synthesis of (d)NTPs with 65-70% of yield.[119] This, however, adds an extra step to the synthesis route and requires subsequent deprotection of the activated intermediate before the phosphorus coupling.

The strategy adopted instead by Hoard and Ott involves the use of 1,1'-carbonyldiimidazole that in the reaction with a monophosphate compound leads to the formation of a phosphorimidazolidate-activated intermediate (*Figure 8*).[129] Nucleoside phosphorimidazolidates are more reactive than the morpholidate analogues and the range of effective solvents for their formation and use is less restricted.

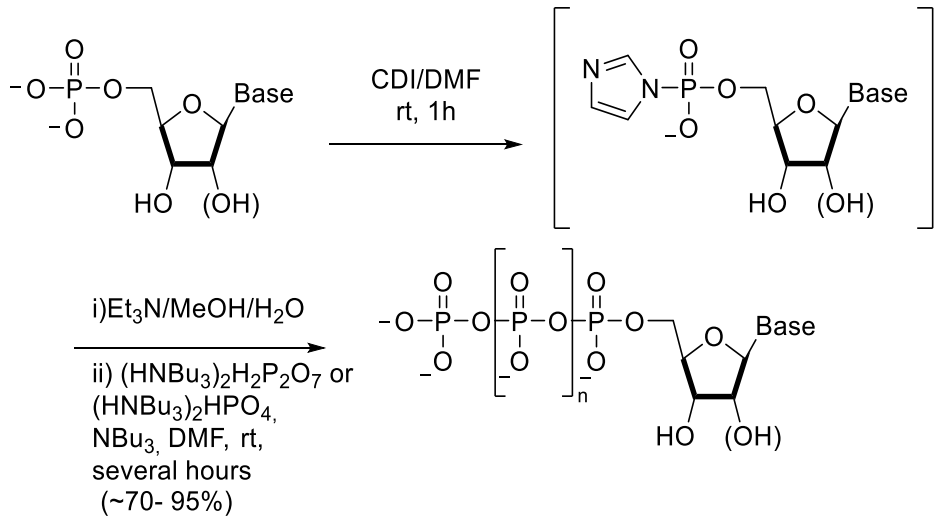

Figure 8: Hoard and Ott's method via phosphoroimidazolidate intermediate.[129]

If the starting material is a NMP, a cyclic carbonate is also formed between the 2'- and 3'-hydroxyl groups, and the resulting 2',3'-carbonate protecting group can be easily removed under basic conditions. Improved variants of this method have been developed. Some approaches rely on the use of more effective condensing systems and catalysts. A double activation of the NMPs has been used to produce the phosphoroimidazolidate intermediate in good yield.[132] For example, divalent metal ions Zn^{2+} and Mg^{2+} were adopted as catalysts for anhydride bond formation,[126, 133] and several solvents were tested to improve the solubility and reaction outcome.[134]

Although the classical methods of preparation of triphosphate nucleosides mainly proceed through nucleoside phosphoroimidazolidates or phosphoromorpholidates, alternative approaches can involve different phosphoramidates such as pyrrolidinium phosphoramidate zwitterion intermediate,[121] pyridinium phosphoramidate[124, 135] or phosphoropiperidate intermediate.[136] In fact, new precursors have been studied to overcome moderate yields and long reaction times—some of the strategies mentioned above require days to complete. These new strategies, however, rely on additional reaction steps to prepare the starting materials.

Another further frontier in this methodology optimization has been the synthesis of a new class of pyrophosphate reagent that is less hygroscopic and their use simplifies the isolation of the final products. It should always be kept in mind that the purification of this class of molecules is particularly complicated and often requires multiple, orthogonal purification steps, which are a major cause of low yields. Cleaner syntheses that do not require complicated purification processes are potentially very valuable, even if they require

additional (simple) synthetic steps. In response to this, Chaput and co-workers[125] have recently developed a new method for (d)NTP syntheses. NMPs activated with imidazole, N-methylimidazole or morpholine have been reacted with a new class of organic pyrophosphate reagents that contain a large hydrophobic moiety attached to the pyrophosphate group via a cleavable, bulky linker (as shown in *Figure 9*). The reagent's synthesis takes six reaction steps with an 85% of overall yield. Protection of the sugar base moiety is required.

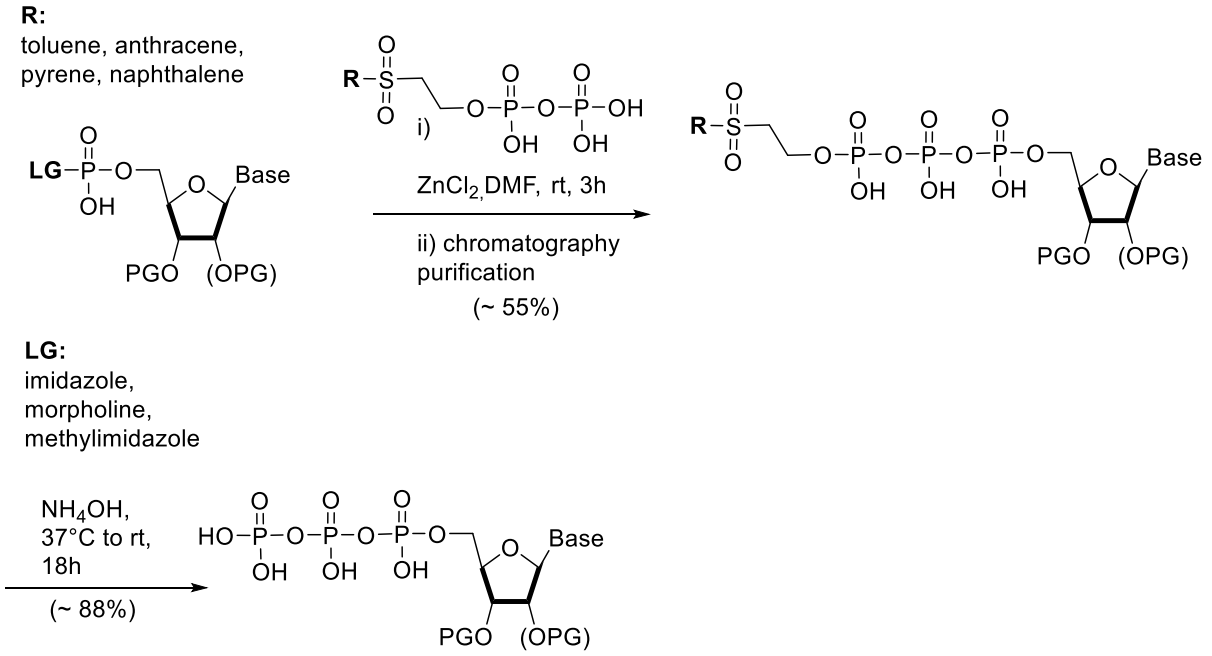

Figure 9: Highlight of the triphosphate nucleosides coupling delivered by Chaput and co-worker.[125]

Although the problem of additional steps and purifications persists, this method is not constrained to natural substrates and is scalable.

In this vein, Hodgson and co-workers[123] have described the synthesis of (d)NDPs from 5'-tosylated nucleosides using PPN [bis (triphenylphosphoranylidene) ammonium] pyrophosphate. The tosylate intermediate synthesis was developed by Poulter's group,[122] thereafter, the procedure involves nucleophilic substitution by tris(tetra-*n*-butylammonium) pyrophosphate and precipitation of the NDP product to remove PPN cation and isolate crude product. PPN salts are less hygroscopic compared to tris(tetra-*n*-butylammonium) systems and are simpler to prepare via aqueous salt exchange metathesis. Removal of PPN cation is

via precipitation with NaI in acetone (as shown in *Figure 10*), which is a well-established and simple to perform protocol for preparation of sodium salts of nucleotides.

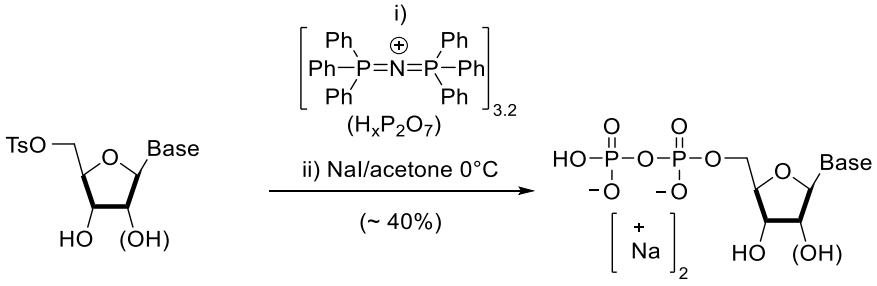

Figure 10: [Bis(triphenylphosphoranylidene)ammonium] pyrophosphate as key reagent for Hodgson and co-workers' synthetic approach.[123]

2.2.1.1.2 P(V) solution-phase approach via phosphorodichloridate intermediate

The phosphorodichloridate intermediate approach developed by Yoshikawa[137, 138] and co-workers in 1967 for the synthesis of monophosphates (NMPs) is still the most used method. This 5'-O regioselective method starts with unprotected nucleosides that are reacted with $POCl_3$ to produce corresponding phosphorodichloridates that subsequently undergo a hydrolysis process to deliver NMPs in a good yield. Through the development of Yoshikawa's monophosphorylation strategy, Ludwig[139] created a "one-pot, three-step" route to access (d)NTPs (*Figure 11*). After the phosphorylation step, before hydrolytic reaction quenching, both chloride ions are displaced to generate a cyclic intermediate using *bis*(tri-*n*-butylammonium) pyrophosphate or *tri*(tri-*n*-butylammonium) phosphate,[137] which is finally hydrolysed under basic conditions to afford (d)NDPs.

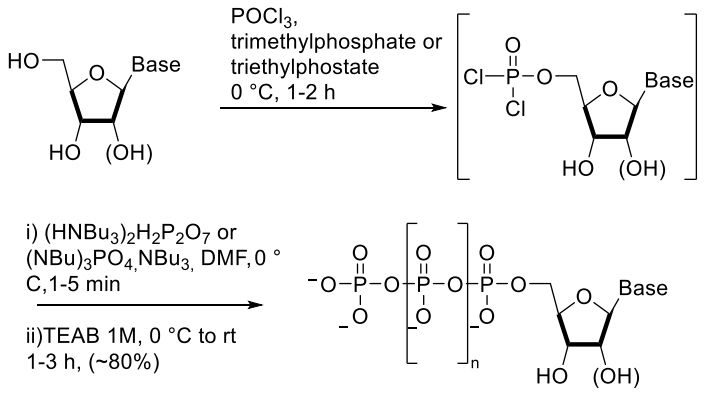

Figure 11: Ludwig's "one pot, three step" synthesis, derived from the Yoshikawa method.[139]

Although it is a simple method and applicable to a wide range of nucleoside analogues, which makes it the most widely used strategy, the formation of several by-products leads to poor-to-moderate yields of the final products. Multiple and difficult purifications are required to obtain pure (d)NTPs. The initial 5'-phosphorylation step is not completely selective to 5'-OH and the formation of 5'-monophosphate, 2'- monophosphate and 3'-monophosphate is possible. In the second step reaction, DMF reacts with the excess of $POCl_3$ to form the Vilsmeier-Haack reagent, which is much more reactive than $POCl_3$ and reacts with the sugar moiety nucleosides leading the formation of additional side products. Furthermore, the carcinogenic nature of the chloroiminium ion-based Vilsmeier-Haack reagent is an additional disadvantage. Trimethylphosphate (TMP) and triethylphosphate (TEP), which are used as solvents in the 5'-phosphorylation step, partially overcome the problems of insolubility of the nucleoside starting materials and can also accelerate monophosphorylation of nucleosides.[140] The presence of 1,8-bis(dimethylamino)naphthalene (proton sponge) accelerates the rate of the first phosphorylation.[131] Due to steric hindrance and the weak nucleophilic character proton sponge simply neutralizes the liberated HCl. Further improvements of the method have been made to decrease by-product formation. These include the use of lower temperatures and longer reaction times[141] and DMF has been replaced by acetonitrile in the second reaction step by Kore's group.[142] These improvements to the original protocol allowed the formation of a simplified method in terms of chromatographic purification thanks to 'cleaner' crude reaction products.

To summarize, both P(V) approaches, via phosphoramidate intermediate or via phosphorodichloridate intermediate, benefit from regioselectivity, in fact no protection of the

nucleobase and sugar moieties is generally required, and excess reagent can be used, however, there are multiple shortcomings. Start-to-finish reaction procedures (including preparation of dry solvents and reagents) are long and must be performed under strict anhydrous conditions. Challenging multiple purifications are often required due to the formation of side products.

2.2.1.2 Synthetic strategies via P(III) approaches

P(III) synthetic approaches are based on the use of phosphitylating reagents, such as salicyl chlorophosphite or phosphoramidite reagents,[87] which act on 5'-OH to introduce the *a*-P group. Protection of the nucleobase and sugar moieties is usually necessary because P(III) reagents are usually extremely reactive and show poor discrimination across sugar OH groups. The approach is a time-consuming because it counts on five steps: (i) selective protection of the nucleobase and sugar ring, (ii) phosphitylation, (iii) oxidation, (iv) cyclic formation and triphosphate hydrolysis and (v) purification of products. Numerous improvements have been made to the original milestone procedures and the most innovative methods will be briefly appraised and their pros and cons summarised in the next section.

2.2.1.2.1 P(III) solution-phase approach via P(III)-P(V) anhydride intermediates

One of the milestones of the P(III)-P(V) chemistry for the synthesis of nucleoside 5'-triphosphates is the strategy developed by Ludwig and Eckstein,[143] as shown in Figure *12*. It is a one pot reaction based on the phosphitylation of a protected nucleoside with salicylchlorophosphite as the phosphitylating agent. The active phosphite intermediate is than treated with bis(tri-n-butylammonium) pyrophosphate to produce a cyclic trivalent phosphorus intermediate. Oxidation of the Pα with I_2 in aqueous pyridine leads to the hydrolytic opening of the ring and subsequent deprotection releases (d)NTPs. Salicylchlorophosphite is very reactive, and it is not selective for 5'-OH. Protection of the sugar moiety is absolutely required, as is protection of the nucleobase. Nucleoside H-phosphonates are also one of the major side products, and optimizations of this method to reduce their formation and other shortcomings are reported later in this section.

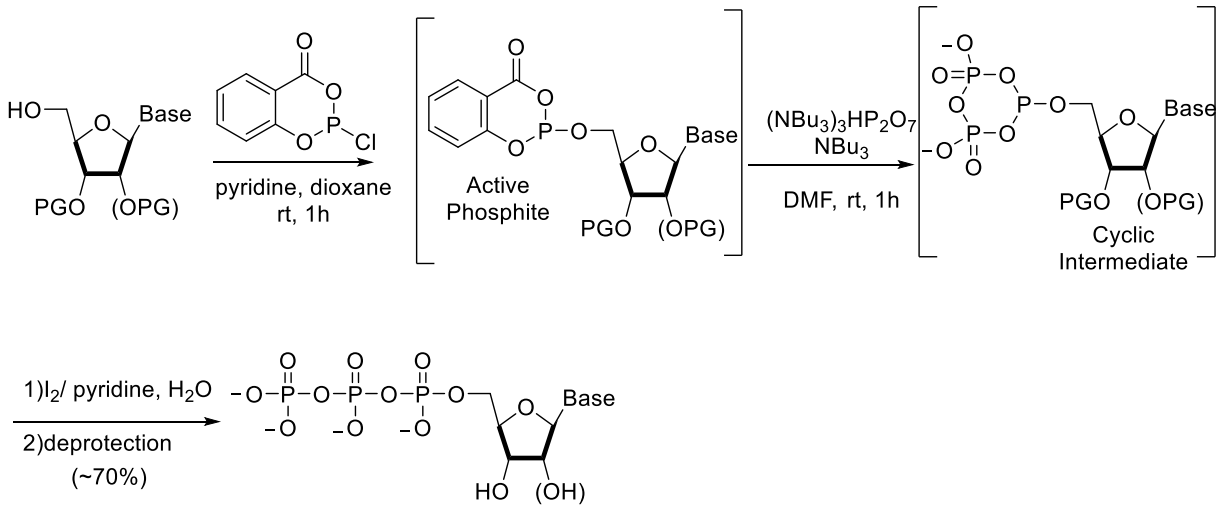

Figure 12: The Ludwig-Eckstein synthetic approach for (d)NTP synthesis.[143]

To avoid the lengthy protection and deprotection processes of the Ludwig-Eckstein method, Caton-Williams and co-workers[144] created a milder, bulkier P(III) reagent in order improve 5'-selectivity and simultaneously introduce the β- and γ-P groups, as shown in *Figure 13*.

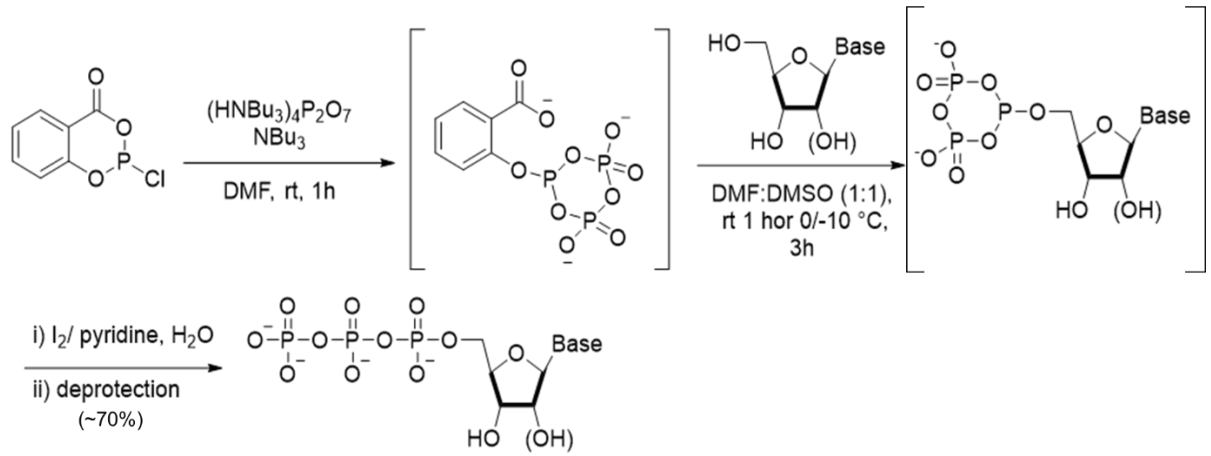

Figure 13: Caton-Williams synthetic method for (d)NTP synthesis.[144]

The phosphitylating reagent is generated *in situ* from the reaction between salicylchlorophosphite and pyrophosphate ion and the cyclic P(III)-P(V) anhydride permits high regioselectivity at the 5′-hydroxyl group for 5'-triphosphate synthesis in this one-pot coupling method. Protections of the nucleobase and of the sugar moieties are not required. The conversion of the starting material to crude product, after direct precipitation from the reaction mixture with ethanol, is ~10-50% as determined by HPLC chromatography.

In 2014 the Jessen research group reported a new synthetic procedure (*Figure 14*) for the synthesis NDPs, and NTPs[145] as well as the first iterative strategy to access phospho-anhydrides.[1] The procedure involves cycles of coupling, oxidation, and deprotection steps as shown in figure below.

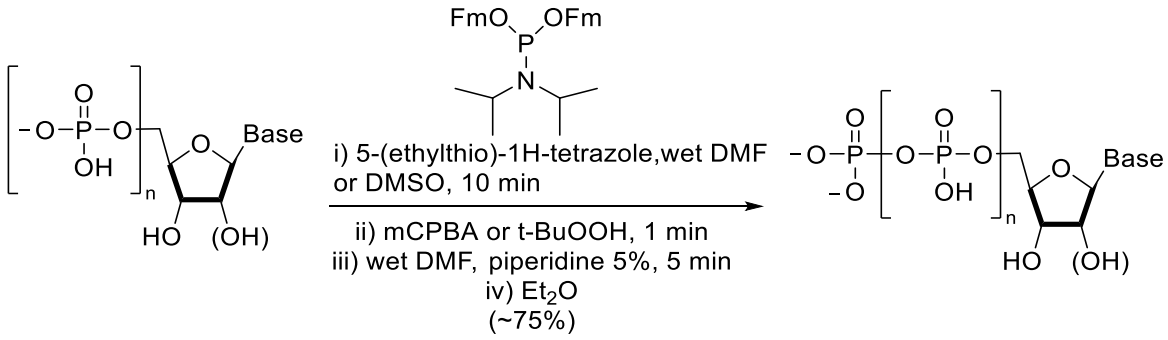

Figure 14: Jessen's synthesis of (d)NDPs, and (d)NTPs.[1, 145]

The phosphitylating reagent used is *bis*-(fluorenylmethyl)-diisopropylamine phosphoramidite which reacts with the nucleoside/nucleotide substrate by acid activation. For the synthesis of (d)NMPs using this reagent, anhydrous conditions are required. For the preparation of (d)NDPs and (d)NTPs, however, dry reagents and solvents are not required. In fact, traces of water are needed to hydrolyse the excess of phosphoramidite reagent to reduce the formation of side products. The reaction starts with unprotected nucleosides and is carried out at ambient temperature. The coupling, oxidation and deprotection reactions take place over very short time periods and chromatographic purification can be avoided, or at least, its difficulty reduced. The desired compound is isolated through precipitation upon addition of Et_2O, as a piperidinium salt. Final products are obtained in reasonable yields. With this procedure Jessen also made possible the syntheses of NMPs, NDPs, and NTPs via the sequential addition of reagents but iterative strategy required a solid support. The adoption of a solid support simplifies the purification of the crude reaction mixture, but on the other hand, the kinetics reaction cannot be linear, the analysis of intermediate can be difficult and the coupling rates are thus unclear.[111]

2.2.1.2.2 P(III) solution-phase approach via triester intermediates

In 2009, Meier's group proposed an alternative approach for the synthesis of NDPs and NTPs employing *cycloSal* as the phosphitylating agent.[146] The *cycloSal*-technique was developed previously as a prodrug concept to deliver biologically active nucleotides into the cell.[147,148] The *cycloSal* reagents are obtained from the corresponding salicyl alcohols that have been reacted with phosphorus trichloride and they are used without further purification, because they decompose easily.

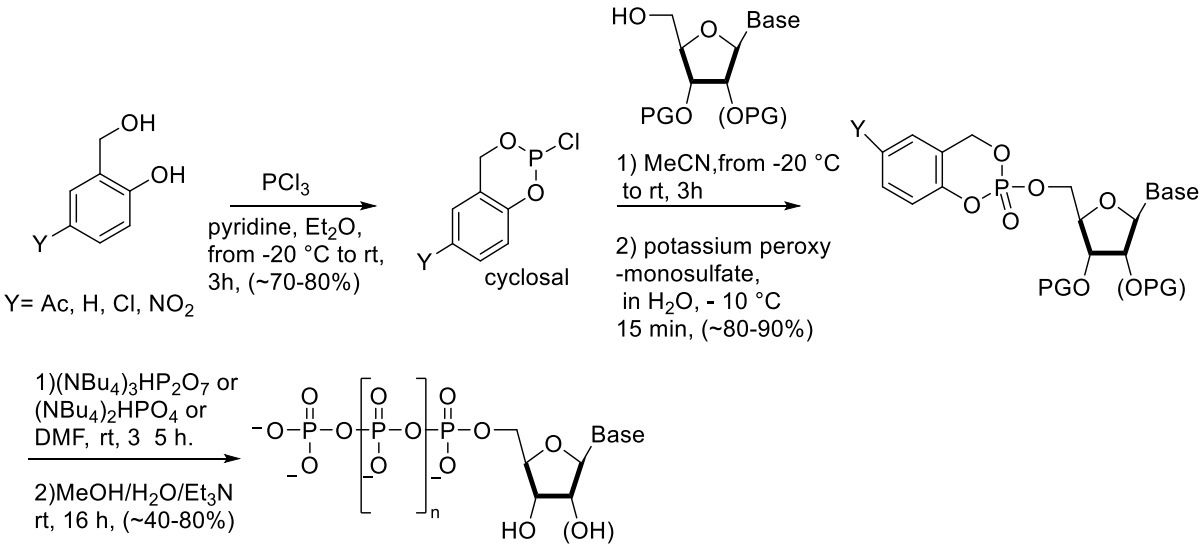

Figure 15: Synthesis of (d)NDPs (d)NTPs starting from cycloSal-phosphate triesters[146].

Even if the salicyl group decreases the reactivity of PCl_3 by displacement of two chlorides, the *cycloSal* reagents are still highly reactive and protected nucleosides are still required to ensure 5'-O-phosphitylation. After oxidation of the phosphite triester, obtained from the reaction between *cycloSal* and the protected nucleoside, to a phosphate *cycloSal* triester, an anhydride coupling reaction with phosphate or pyrophosphate salts can take place (*Figure 15*). This four-step method led to the target nucleotides in good chemical yields (40-80%).

2.3 Conclusions

In summary, both P(III) approaches, via P(III)-P(V) anhydride intermediates and via phosphite triester intermediates, require the use of highly reactive phosphitylating agents that reduce the coupling reaction time, but due to their reactivity, the formation of by-products can occur. Protection of the nucleobase and sugar moieties is often required, so the method relies on additional time-consuming steps. The phosphitylating agents are quite unstable under atmospheric conditions, so often need to be used quickly after preparation.

3 Aim of the project

The review of synthetic methodologies in the previous chapter highlights that there is no standardized, broadly satisfactory method for the synthesis of nucleoside phosphates. This is because of combinations of the chemical and physical characteristics of the nucleoside substrates, the reagents and the final product nucleotides. In addition to the issues listed in the Chapter 2 (i.e. insolubility of the starting material and reagents in organic solvents, low chemical stability of the substrates, long reaction time, low reactivity, complicated purification, moisture sensitivity), low conversion levels and hygroscopicity of reagents and products should be highlighted.

Building on the discussions above, a key goal is the development of a synthetic method towards the synthesis of phosphoanhydrides that would approach the paradigm of a clean reaction:

- avoiding laborious chromatographic purifications.
- applicability to a broad range of nucleoside substrates.
- no time-consuming steps.
- satisfactory product yields.

The idea of this project is not to create a new synthetic route, but to optimize and increase the 'usability' and 'scalability' of existing routes. After several considerations, going through the advantages and disadvantages presented by the different synthetic approaches reviewed above, Jessen's synthesis[1] (see *Figure 16*) based on the P(III)-P(V) chemistry seemed to us to be the closest to the paradigm and represented the best starting point.

Specifically, the rapid coupling, high reported levels of purity of crude products, satisfactory product yields and reaction conditions that tolerate moisture to some degrees were particularly appealing (see *Figure 16*).

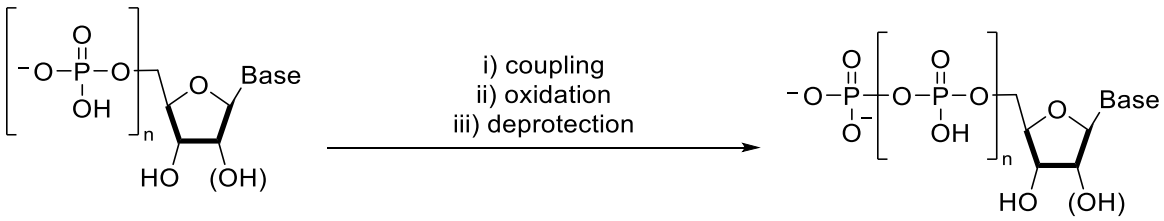

Figure 16: Key steps of Jessen's method for the phosphorylation of nucleotides.[1]

The Jessen research group adopted a bulky reagent, namely *bis*-(fluorenylmethyl)-diisopropylamine phosphoramidite to bypass one of the most important drawbacks of P(III) and P(III)-P(V) chemistry, which is the use of protecting groups on the nucleoside, due the high reactivities of most phosphitylating agents, and the resulting additional reaction steps (see section 2.2.1.2).

The steric hindrance of *bis*-(fluorenylmethyl)-diisopropylamine phosphoramidite promotes a selective coupling on the 5'-OH of the nucleoside or nucleoside-5'-phosphate and this obviates the need for protecting groups on the acceptor. The synthesis of the reagent appeared accessible 'in-batch', although long reaction times and multiple purifications steps were reported in the literature.[2]

Jessen's 'one pot-three steps' reaction (coupling, oxidation and deprotection) for the synthesis of nucleosides mono-, di- and triphosphates was reported to be compatible with non-anhydrous conditions (i.e. DMF and DMSO not actively dried) with rapid reaction times. Furthermore, their ^{31}P NMR spectroscopic analyses showed low percentage levels of unreacted starting materials (10-20% of range). Repeated precipitations after each reaction step were reported to deliver high levels of purity without extensive requirement for purification. Thus, further reverse-phase or ion-exchange chromatography purifications were either not required or relatively easy to perform because of the low levels of starting materials and by-products.

The idea of this project, as previously outlined, is to optimize and increase the 'usability' and 'scalability', I use Jessen's method as a starting point. Specifically, in this thesis, I:

- Develop and upscale the batch synthesis of *bis*-(fluorenylmethyl)-diisopropylamine phosphoramidite (sections 4.1 and 4.1.1);
- Translate into a continuous flow system using my newly-developed batch method for the synthesis of *bis*-(fluorenylmethyl)-diisopropylamine phosphoramidite (sections 4.1 and 4.1.2);

- Use *bis*-(fluorenylmethyl)-diisopropylamine phosphoramidite, prepared using upscaling methods, for the phosphitylation of nucleotides (section 4.2);
- Develop quantitative methods for reagent and product measurements (section 4.2.2.3.2.1);
- Use quantitative methods for kinetic studies to inform flow chemistry experiments (section 4.2.2.2);
- Translate the iterative addition of phosphoryl groups to nucleotides into a continuous flow system (section 4.2.2.3);
- Optimize and scale up from milligrams to grams the iterative addition of phosphoryl groups to nucleotides using the flow system (sections 4.2.2.3.2.1 and 4.2.2.3.2.2);
- Demonstrate scope across multiple nucleotide substrates (section 4.2.2.4).

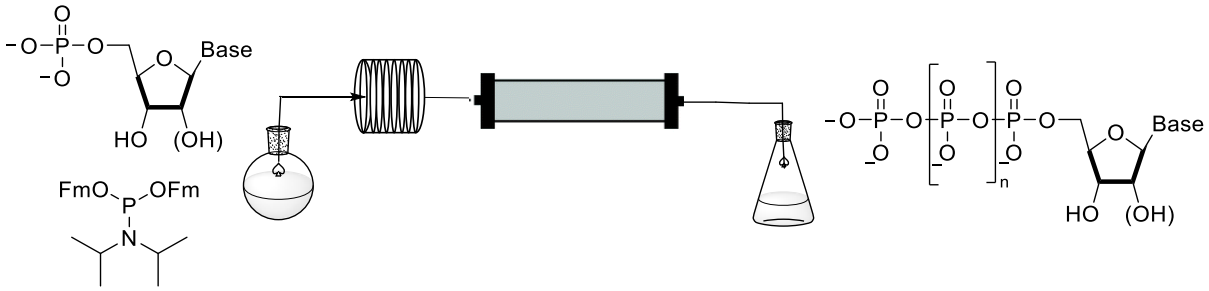

Figure 17: Schematic representation of the idea behind this project regarding the translation of the synthetic method from the batch into a continuous flow system.

The idea behind this project is reinforced by the assumption that process parameters that normally are not that easy to up-scale, can be easily controlled through software with flow apparatus (see *Figure 17*). The use of continuous flow chemistry to combine multiple synthetic steps into a single, continuous system has been extensively studied, and it has allowed the development of innovative, efficient and, most critically, scalable strategies. On the other hand, flow processes face some challenges: specifically, heterogeneity issues, such as biphasic reactions with liquid/solid components are usually not tolerated and product precipitates should be completely avoided. Start-up and shut down processes and dilution effects of additional flow streams must also be carefully considered. [149-153] Despite the fact that poor solubility of nucleosides and nucleotides in organic solvent presents a major challenge, flow chemistry, flow chemistry has recently seen some initial applications towards nucleoside-[153,154] and nucleotide-syntheses.[155] Continuous manufacturing affords the

opportunity to work under absolutely anhydrous conditions, with exquisite temperature control and consistent mixing to lead to faster, more repeatable, and readily scalable reactions.

4 Results and discussion

4.1 Development of batch and flow synthesis methods for the preparation and application of *bis*-(fluorenylmethyl)-diisopropylamine phosphoramidite (2) towards iterative, scaled phosphorylation of nucleotides

This section describes investigations of the synthesis of *bis*-(fluorenylmethyl)-diisopropylamine phosphoramidite (**2**), a phosphitylating reagent described by Jessen for one-pot, three-step phosphoanhydride formation.[1, 145] Starting from the procedures published by Bialy and Waldmann,[2] and Desmaële,[3] I explored optimization and scale-up in batch (see section 4.1.1) followed by translation of the process into a continuous flow method (see section 4.1.2).

4.1.1 Optimization of the batch synthesis of *bis*-(fluorenylmethyl) diisopropylamine phosphoramidite (2)

At the beginning of this project, I focused on the synthesis of the phosphitylating reagent, *bis*-(fluorenylmethyl)-diisopropylamine phosphoramidite (**2**). A reliable process was essential to allow sizeable quantities of material to be prepared and subsequently used during the translation to flow methods. Jessen's publications[1, 145] reported the use of Bialy and Waldmann's strategy [2] as shown in (*Figure 18*).

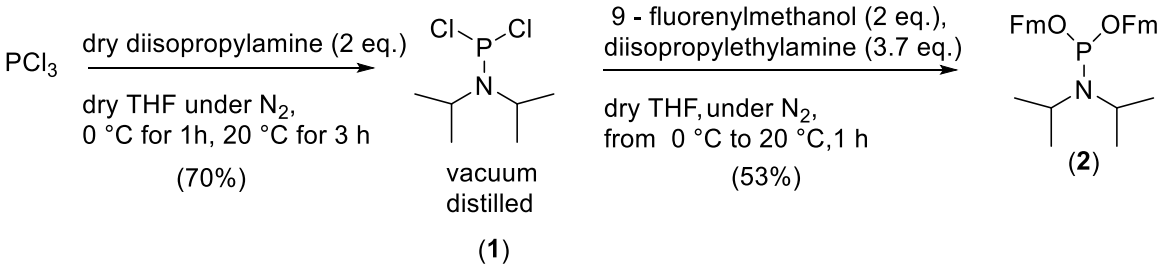

Figure 18: Two-step synthesis of *bis*-(fluorenylmethyl)-diisopropylamine phosphoramidite (**2**) reported by Bialy and Waldmann. [2]

In an initial, exploratory set of experiments according to Bialy and Waldmann's two-step synthesis procedure,[2] freshly distilled PCl_3 was reacted for 4 h with dry *N*,*N*-diisopropylamine

to form *N*,*N*-diisopropylphosphoramide dichloridite (**1**) via nucleophilic substitution of one of the three chlorides of PCl_3.[154] The resulting *N*,*N*-diisopropylphosphorodichloridite (**1**) was then successfully purified by vacuum distillation, and subsequently, 'double'-nucleophilic attack by 9-fluorenylmethanol in the presence of diisopropylethylamine (Hünig's base) was performed over 1 h to form crude *bis*-(fluorenylmethyl)-diisopropylamine phosphoramidite (**2**). Hünig's base is a sterically hindered, non-nucleophilic amine, often employed for substitution reactions to sequester the HCl that is released, whilst not competing in the substitution process.[155] The preceding nucleophilic substitution steps were both monitored by ^{31}P NMR spectroscopy until complete reaction of the respective starting material was observed. The crude reaction mixture containing *bis*-(fluorenylmethyl)-diisopropylamine phosphoramidite (**2**) was partitioned between a pH 7 phosphate buffer and EtOAc. The organic extracts were then split into two portions and the solvents were removed. The first portion was subjected to flash chromatographic purification on silica gel, using hexane/EtOAc/triethylamine (20:1:0.2) as eluent, as reported in the literature due the degradation of the molecule under acid condition. Unfortunately, the procedure led to loss of the fluorenylmethyl protecting groups. The main product (**3**), confirmed by ^{1}H NMR analysis, was derived from protecting group elimination (*Figure 19*). *Bis*-(fluorenylmethyl)-diisopropylamine phosphoramidite (**2**) is base- and acid-labile. I found it to be quite unstable on silica gel even after deactivation by pre-washing with Et_3N-containing eluent, in contradiction to the literature reports.[2, 3] Given I believed that chromatography led to degradation, I considered two possible strategies for improvement, namely: reduction of the quantity of triethylamine used during the chromatographic purification, and/or speeding up the purification to reduce product degradation. As expected, speeding up the purification and decreasing the concentration of triethylamine allowed greater quantities of the amidite (**1**) to be isolated, but still in low yields (~22%).

Basic Degradation:

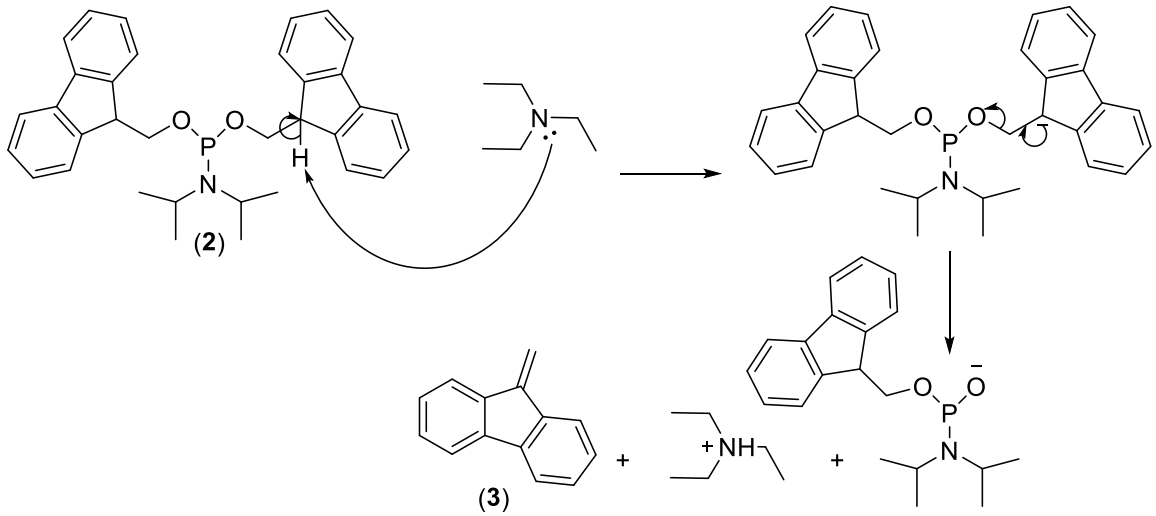

Acid Degradation:

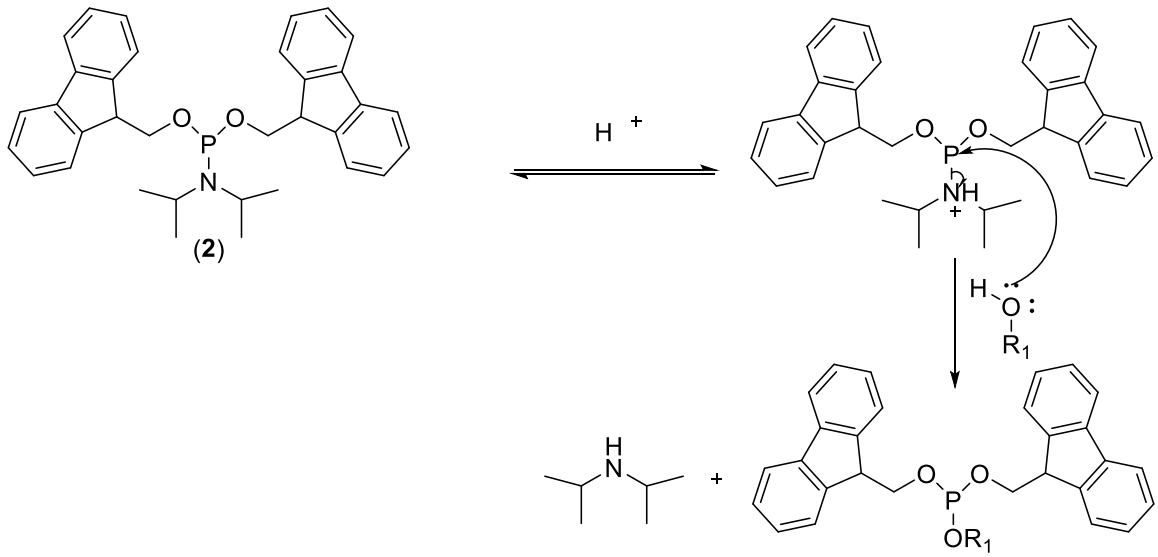

Figure 19: Proposed mechanism of acid and basic degradation of *bis*-(fluorenylmethyl)-diisopropylamine phosphoramidite (**2**).

The second portion of crude material was stored at −18°C under a N_2 atmosphere. The storage stability of *bis*-(fluorenylmethyl)-diisopropylamine phosphoramidite (**2**) was one of our concerns with regards to devising robust, reliable procedures that delivered consistent results. The compound was re-analysed after 10 and 30 days of storage and over 30-days I observed only 3% formation of by-products via ^{31} P NMR spectroscopy (peaks with ~ 15.00 and 0 ppm chemical shifts in the spectrum). Despite small traces of impurities, the crude material was ~90% product. Based on this observation, the crude material appeared to show good levels of stability with limited levels of degradation, despite the presence of reaction by-products *(Figure 20)*.

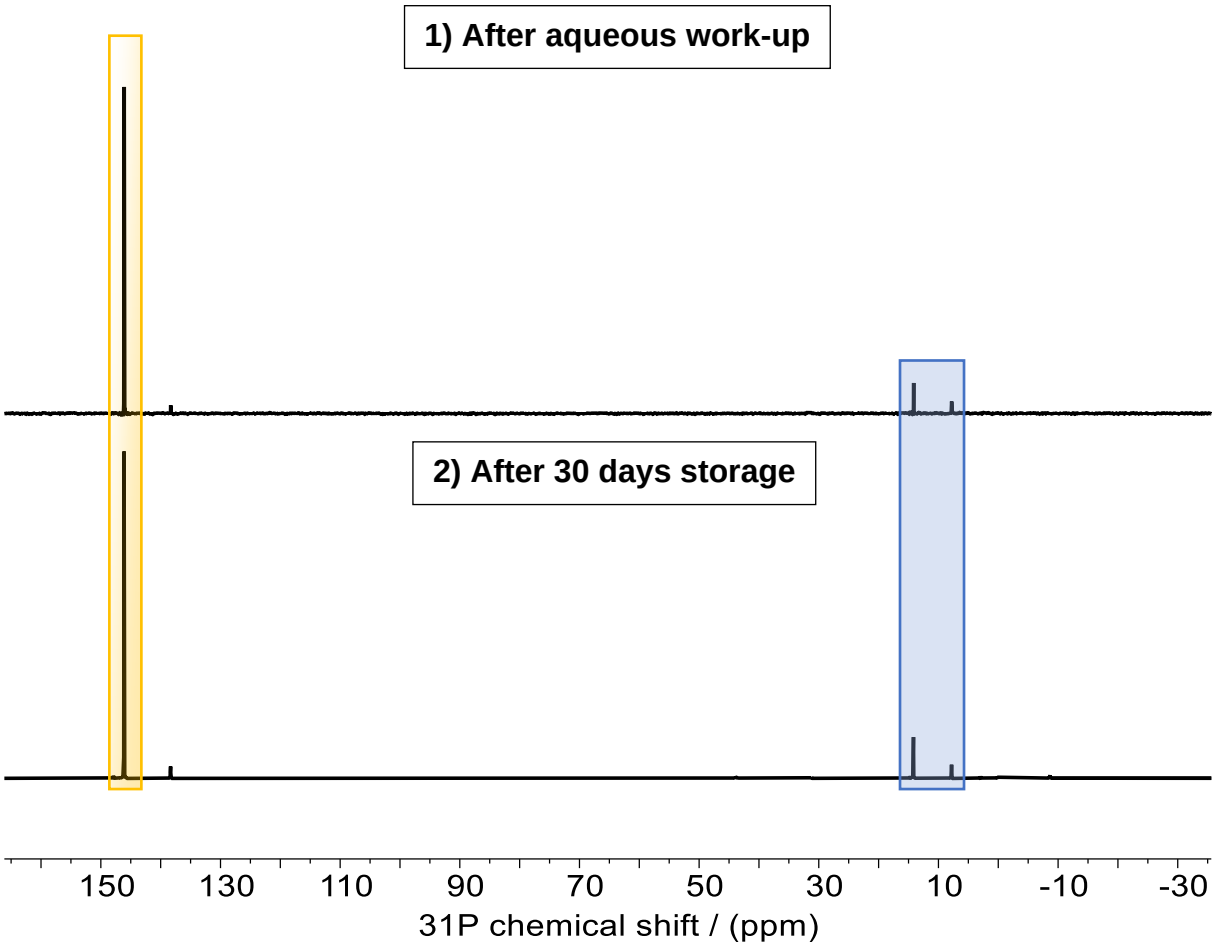

Figure 20: ^{31}P NMR spectra of *bis*-(fluorenylmethyl)-diisopropylamine phosphoramidite (**2**) (146.16 ppm chemical shift, orange labelled) in $CDCl_3$: 1) directly after the aqueous work-up (no chromatography); 2) after 30 days storage in the freezer at –18 °C.

With these preliminary results in hand, I initially tried to identify more rapid work-up methods to optimize the isolation of *bis*-(fluorenylmethyl)-diisopropylamine phosphoramidite (**2**) and to effect partial purification, while avoiding the chromatography steps that had proven to be challenging. ^{31}P NMR spectra (^{1}H coupled and decoupled) gained during reaction monitoring showed small traces of P-H-containing species between 15 and 0 ppm, and ^{1}H NMR spectra of the crude material after work-up showed small traces of unreacted 9-fluorenylmethanol. Therefore, I hypothesized that maintenance of anhydrous conditions, including during work-up, may reduce the occurrence of phosphorus-based hydrolysis products, however, this strategy alone would not address the presence of unreacted 9-fluorenylmethanol. To alleviate unreacted 9-fluorenylmethanol, I decided to focus on its physical properties, specifically, I sought to exploit differences in solubility in comparison to the desired product (**2**) in order to accomplish the isolation of unreacted 9-fluorenylmethanol.

The solubilities of both 9-fluorenylmethanol and *bis*-(fluorenylmethyl)-diisopropylamine phosphoramidite (**2**) were tested in several solvents. 9-Fluorenylmethanol proved to be highly soluble in all polar solvents, but essentially insoluble in non-polar solvents. Similarly, diisopropylethylamine hydrochloride was highly soluble in all polar solvents, and insoluble in non-polar solvents. Interestingly, the phosphoramidite (**2**) proved to be highly soluble in hexane, unlike the 9-fluorenylmethanol starting material and the diisopropylethylamine hydrochloride side product. Therefore, three work-up strategies were attempted in parallel, based on the stoichiometries described in *Figure 18*. The first experiment followed Bialy and Waldmann's procedure[2] that involved filtration to remove diisopropylethylammonium chloride, followed by the addition of 1 M phosphate buffer to the solution and extraction with EtOAc. In the second strategy, EtOAc was replaced with hexane in the extraction. In the third attempt, the THF reaction solvent was removed under vacuum and the resulting solid residues were agitated with hexane with the aim of selectively extracting product (**2**). After extraction, any precipitate suspended in the hexane was filtered off, and the solvent was removed under vacuum. The spectroscopic analyses of the materials from each of the three different work-up procedures showed no evidence of excess of reagents such as 9-fluorenylmethanol, and the mass recovery levels were almost identical (around 90% of theoretical yield). Although all three processes were equally effective in delivering materials of similar purities, direct extraction with hexane avoided time-consuming partitioning steps and, in this sense was the most efficient. With a convenient strategy for the selective extraction of amidite (**2**) in hand, I focussed on the preceding reaction processes in greater detail. Although the procedure described by Bialy and Waldmann synthesis[2] was not particularly difficult to execute, the distillation of *N*,*N*-diisopropylphosphoramide dichloridite (**1**) was a significantly time-consuming obstacle, that I hoped could be completely avoided by combining our selective hexane extraction with the one-pot approach of Desmaële.[3] Subsequently, the phosphoramidite (**2**) was prepared in a one-pot process from PCl_3, via *N*,*N*-diisopropylphosphoramidous dichloride, following a modification of Desmaële's procedure[3] (*Figure 21*).

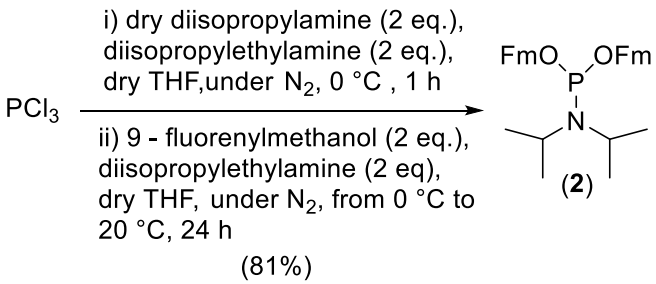

Figure 21:One-pot reaction for the synthesis of *bis*-(fluorenylmethyl)-diisopropylamine phosphoramidite (**2**).[3]

Desmaële's[3] reported reaction time was ~ 24 h, thus, with our finding that the amidite (**2**) could be selectively extracted in hexane, were started to explore modifications to the one-pot procedure. The progress of steps (i) and (ii) was monitored via ^{31}P NMR spectroscopy. On the contrary to what was expected based on Desmaële's[3] reported reaction time, the initial reaction between PCl_3 and *N,N*-diisopropylamine was observed to be complete in <20 min and the subsequent reaction with 9-fluorenylmethanol was complete in <40 min. Thus, the whole one-pot process could be completed in just 1 h instead of the reported 24 h. The crude reaction mixture was then evaporated under vacuum and the residue was subjected to extraction with hexane to yield the desired amidite (**2**). The extraction with hexane (40 mL for 2.85 mmol of PCl_3) delivered 1.250 g of amidite (**2**) in ~ 1 h from start to finish (as shown in *Figure 22*). The procedure delivered 86% yield based on theoretical mass recovery, where the isolated material was shown to be 97% pure by ^{31}P NMR and 95% pure by ^{1}H NMR methods.

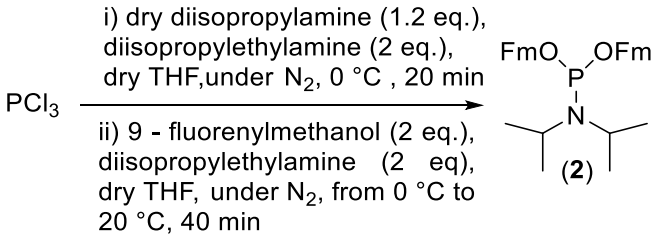

Figure 22: Optimized one-pot reaction for the synthesis of *bis*-(fluorenylmethyl)-diisopropylamine phosphoramidite (**2**).

With significant quantities of the *bis*-(fluorenylmethyl)-diisopropylamine phosphoramidite (**2**) in hand, I sought to 'use-test' the material, to check that the lack of chromatographic purification did not obstruct application to the preparation of polyphosphates. Thus, a series of parallel "one-pot three-step" reactions was carried out, respecting the stoichiometries and

the timings described by Jessen's group for the NDPs and synthesis in DMF, as shown in *Figure 23*. These 'use tests' were performed by analysing the crude materials using ^{31}P NMR spectroscopy. In the cases that I explored, I observed 80-90% conversions of ADP to ATP and 70% conversions of AMP to ADP (*Figure 23*).

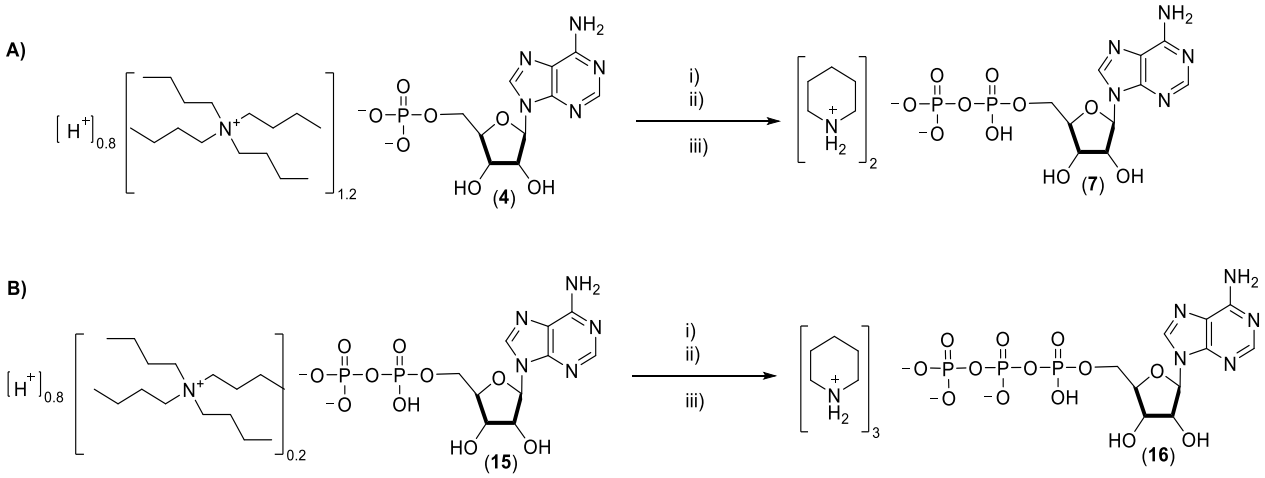

A: Conversion of AMP to ADP following Jessen's method and B: Conversion of ADP to ATP following Jessen's method. Reagents and conditions: i) bis-(fluorenylmethyl)-diisopropylamine phosphoramidite (2), 5-(ethylthio)-1H-tetrazole, wet DMF, 25 °C, 10 minutes. ii) mCPBA, wet DMF, 25 °C, 2 minutes. iii) piperidine 5% v/v, wet DMSO, 25 °C, 5 minutes.

Figure 23: A: Conversions of AMP to ADP and ADP to ATP following Jessen's method for the synthesis of NDPs and NTPs in DMF[1, 145].

Having proven the validity of the synthetic process for the preparation of amidite (**2**) and its applicability to the Jessen method, the next step was to convert the process into a continuous flow system. As discussed later in this chapter (see section 4.1.2), despite the batch process proving successful using THF, ammonium hydrochloride salts are insoluble in THF, and their precipitation would block a flow system. I performed initial screens in CH_2Cl_2 because I were aware it dissolves ammonium hydrochloride salts. These experiments were successful, and ultimately, I was forced to move forward with CH_2Cl_2 (see section 4.1.2). However, CH_2Cl_2 is a chlorinated hydrocarbon solvent whose use is limited in industrial applications due to concerns it may cause serious health issues. Thus, before proceeding further with CH_2Cl_2 I sought to identify a more benign reaction solvent by performing an additional series of batch experiments[156-162] (see *Table 1* and *Figure 24*).

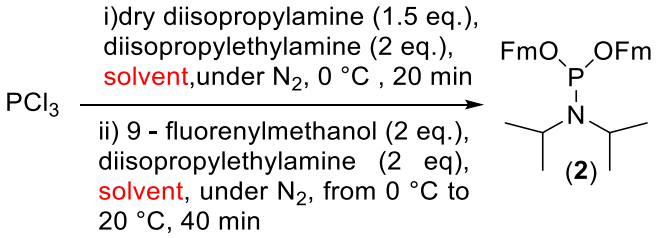

Figure 24: Solvent screening of the one-pot reaction for the synthesis of *bis*-(fluorenylmethyl)-diisopropylamine phosphoramidite (**2**).

Entry	PCl_3 (mmol)[a]	Solvent (mL)	Workup solvent (mL)	Mass recovery (%)[b]	Purity (%)[c]	Homogeneity
1	5	dry THF (20 mL)	hexane	86	97	suspension
2	5	dry CH_2Cl_2* (20 mL)*	hexane	90	84	solution
3	10	dry α,α,α-trifluorotoluene (10 mL)	hexane	95	84	suspension
4	2	Cyrene (10 mL)*	EtOAc	20	72	suspension
5	2	Cyrene (10 mL)*	hexane	7	83	suspension
7	2.5	2-methyl THF. (10 mL)	hexane	74	84	suspension
8	2.5	toluene* (10 mL)	hexane	75	98	suspension
9	2	dry hexane * (10 mL)	no workup	—	—	suspension

*Legend: *: dry THF (5 ml) was used to dissolve FmOH before addition in the second step reaction (see Figure 24).a: quantity of substrate expressed in mmol; b: mass recovery of the crude of crude phosphoramidite yield estimate based on 100% purity; c: Purity estimated by ^{31}P NMR spectroscopy.*

Table 1: 'In batch' solvent screening for the preparation of *bis*-(fluorenylmethyl)-diisopropylamine phosphoramidite (**2**).

Initial trials focused on the following systems:

- anhydrous 2-methyl-THF;
- 'wet' 2-methyl-THF (i.e. commercial, undried material, directly from a bottle without a septum);
- anhydrous α,α,α-trifluorotoluene;
- mixture of anhydrous THF/Cyrene;
- mixture of anhydrous THF/anhydrous toluene.

These solvents were chosen as CH_2Cl_2 and THF substitutes, where this selection was influenced both by availability in our laboratory and the guidelines on green solvents published in the literature.[157, 158, 160, 162, 163] 2-Methyl-THF is a biomass-derived chemical with low miscibility with water, higher boiling point, and remarkable stability compared to THF.[164] Anhydrous α,α,α-trifluorotoluene displays relatively low toxicity and a price that is comparable to CH_2Cl_2.[165] Cyrene is a bio-based substitute for toxic petrochemical-derived polar aprotic solvents that was particularly interesting because of the potential for solubilising nucleotides, and its use will be discussed in this section 4.1.1.

Hexane does not fall in any way in the green solvent categories, mainly because it is volatile and flammable. However, I wanted to explore its use not only as work-up solvent but also as reaction solvent for added convenience (as discussed in the following paragraph).

Following our modified batch procedure with each solvent (see *Figure 24*), each reaction step was monitored by ^{31}P NMR spectroscopy by diluting 0.1 ml of the crude reaction mixture into 0.5 ml of $CDCl_3$. The results showed, in most cases, complete consumption of PCl_3 and formation of *bis*-(fluorenylmethyl)-diisopropylamine phosphoramidite (**2**) with low levels of by-product formation. Although these new routes towards the batch preparation of reagent (**2**) were effective and offered potentially greener protocols, precipitation, presumably of ammonium hydrochloride salts, means these solvents are incompatible with flow apparatus. Owing to the possibility that Cyrene may also be a suitable solvent for nucleotides, thus allowing telescoping of reagent preparation with application towards phosphoanhydride formation, I spent considerable time exploring its use. Cyrene, or dihydrolevoglycosenone, is a biobased solvent synthesized from several different biomass starting materials.[166-170] The use of Cyrene as solvent has only been explored in the past few years and one of the key features of Cyrene is its high miscibility with water and organic solvents. This feature appealed to us because it could potentially allow hexane extraction and aqueous partitioning approaches. Unfortunately, in both cases, removal of the solvent from the reaction mixture

was very challenging. For the aqueous work-up, after completion of the second step, the reaction was diluted with EtOAc and washed with 1 $mol \cdot L^{-1}$ ammonium bicarbonate buffer (pH~7) and brine. Post-extraction, the crude material still contained large quantities of Cyrene. Thus, flash chromatographic purification on silica gel, using hexane/ethyl acetate 9:1 as eluent was performed, which led to pure final product, but with a mass recovery of ~20%. An even lower recovery of ~10 % was obtained after chromatographic purification following a hexane-based work-up. These lower yields after chromatographic purification were predictable since the loss of the fluorenylmethyl protecting groups had been observed in our initial set of chromatography experiments (see 4.1.1). A Cyrene removal strategy could have been lowering the pH of the aqueous solution during the partition.[167-170] In addition, the final product (**2**) is also unstable under both acidic and basic conditions (*Figure 19*). Although the use of Cyrene seemed a promising idea at the outset of our screening exercise, the results detailed above showed that further investments would be required to achieve results that are comparable to those of THF and CH_2Cl_2. At this point, I paused the use of Cyrene, however, I re-engage with its use in section 4.2.2.

As our newly developed reaction work-up is based on the use of hexane, a solvent in which the by-products are insoluble, I decided to use it not only as work-up solvent, but also as a reaction solvent for 'in batch' preparations. Although the two-step synthesis is based on S_N2 mechanisms and theoretically should require a polar solvent, a few examples in the literature [171, 172] used hexane as a solvent for the synthesis of alkylaminodichlorophosphines from PCl_3 and the respective amines. Thus, hexane was explored as a solvent for the formation of amidite (**2**), where the progress of steps (i) and (ii) was monitored via ^{31}P NMR spectroscopy. Pleasingly, the initial reaction between PCl_3 and *N*,*N*-diisopropylamine was observed to be complete in <20 min, Unfortunately, the subsequent reaction with 9-fluorenylmethanol led to the formation of a different reaction intermediate that was detected at $\delta P \sim 138$ ppm. Even after being stirred for 24 h, the reaction did not proceed beyond this point, probably due to a lack of solubility of the reagents, and thus I did not endeavour to use hexane or other alkane solvents for the displacement steps. In addition to screening alternative reaction solvents, I were also aware that hexane is unequivocally considered as undesirable solvent for work-ups. Cyclohexane and *n*-heptane are considered safer solvents than n-hexane[156, 162, 163] and I therefore explored their effectiveness during the workup, alongside solvent mixture screening. The results of these studies are reported in the next paragraph.

Moving on to CH_2Cl_2, I found that the reaction mixture was homogeneous during the initial displacement of chloride by diisopropoylamine. Thereafter, when I attempted the subsequent displacement of the remaining chlorides with 9-fluorenylmethanol, I found that 9-fluorenylmethanol was insoluble in CH_2Cl_2. Based on this observation, combined with our earlier observation that 9-fluorenylmethanol is soluble in THF, I explored the use of a mixed solvent system.

I found that the use of CH_2Cl_2-THF 4:1 led to a reaction solution with no precipitation, and, ultimately, this was the solvent system I adopted for the continuous flow system (see section 4.1.2). Following our mixed solvent protocol, the reaction solvent was evaporated, and the residues were extracted with hexane to afford the desired amidite (**2**) see *Table 2*, entry 1. In addition, *n*-heptane and cyclohexane were explored as extraction solvents on reactions using CH_2Cl_2-THF 4:1. The results from these experiments are summarised in *Table 2*, entries 2 and 3, and they show both *n*-heptane and cyclohexane were valid substitutes of hexane in the reaction work-up for the synthesis of (**2**).

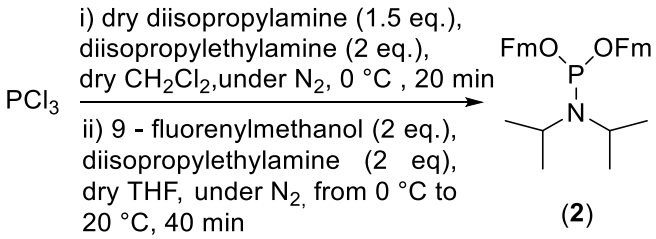

Figure 25: One-pot reaction for the synthesis of *bis*-(fluorenylmethyl)-diisopropylamine phosphoramidite (**2**) using CH_2Cl_2-THF 4:1 as reaction solvent.

Entry	PCl_3 (mmol)	CH_2Cl_2-THF 4:1 (mL)	Workup solvent (mL)	Mass recovery (%)[a]	Purity (%)[b]
1	5	20:5	hexane (20 ml)	90	84
2	5	20:5	*n*-heptane (20 mL)	96	80
3	5	20:5	cyclohexane (20 mL)	94	79

Legend: a: mass recovery of the crude phosphoramidite estimated based on 100% purity; b: purity analysed by ^{31}P NMR.

Table 2: Work-up solvent screening for the isolation of *bis*-(fluorenylmethyl)-diisopropylamine phosphoramidite (**2**).

In summary, several faster and more efficient batch syntheses of *bis*-(fluorenylmethyl)-diisopropylamine phosphoramidite (**2**) were developed (see section 4.1.1). The product (**2**) obtained with the THF-based reaction, followed by hexane extraction, proved to be an efficient phosphitylating reagent in the synthesis of ADP and ATP following Jessen's method (see sections 4.2,4.2.1,4.2.2 and 4.2.2.1).[1, 145] This result led to further optimization and the screening of greener solvents. While other solvents were able to deliver satisfactory results, I were not able to find a greener alternative solvent that maintained a homogenous reaction mixture to support flow experiments. *n*-heptane and cyclohexane also appeared to be equally effective in comparison to hexane, based on the spectroscopic data gained on the products, however, these materials were not use-tested.

4.1.2 Development and optimization of a continuous flow synthesis of *bis*-(fluorenylmethyl)-diisopropylamine phosphoramidite (2)

The use of flow technology to combine multiple synthetic steps into a single, continuous system has been extensively studied, and has allowed the development of innovative, more efficient strategies.[173] The next step for the synthesis of *bis*-(fluorenylmethyl)-diisopropylamine phosphoramidite (**2**) was the translation of the CH_2Cl_2:THF-based batch procedure to flow (*Figure 26*). These early-stage flow investigations were designed to probe the reaction viability, and the temperatures and reaction times required for the flow synthesis of the phosphoramidite (**2**).

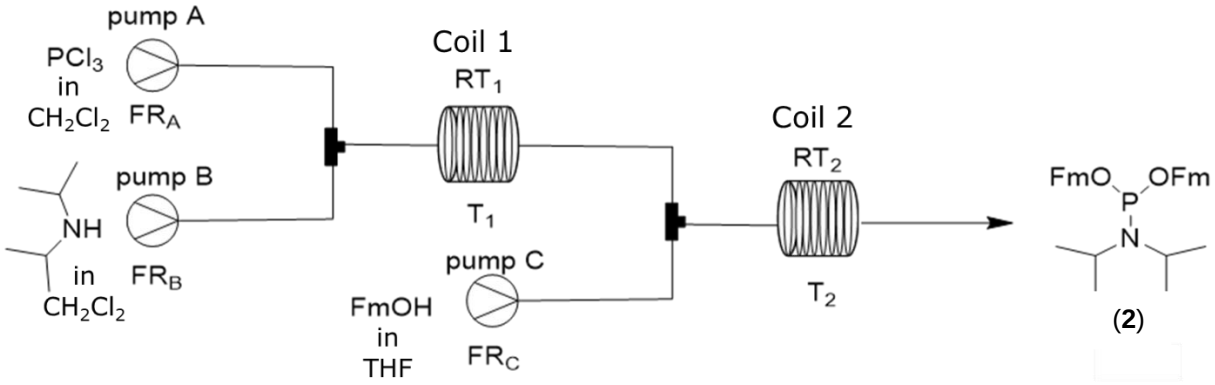

Figure 26: Proposed synthesis of *bis*-(fluorenylmethyl)-diisopropylamine phosphoramidite (2) under flow conditions.

Three reagent stock solutions were prepared:

1. PCl_3/ Hünig's base solution in dry CH_2Cl_2,;
2. N,N-diisopropylamine solution in dry CH_2Cl_2;
3. 9-fluorenylmethanol/ Hünig's base solution in dry THF.

The PCl_3 and N,N-diisopropylamine solutions in CH_2Cl_2 were reacted in coil 1 and the resulting mixture was then mixed with the 9-fluorenylmethanol solution in THF and reacted in coil 2. The reactions were performed on a Vapourtec E-series system equipped with three V-3 peristaltic pumps, an SF-10 peristaltic pump, T-mixer connections and two coil reactors with temperatures controlled by two Polar Bear Plus machines. In our first series of experiments a flow system with a 49 mL coil 1 at 0 °C, and a 51 mL coil 2 at 24 °C was used. Details of the reaction concentrations, temperatures and timings are reported in *Table 3*.

Reaction mixtures were analysed by diluting 0.1 mL of the reaction flow mixture into 0.5 mL $CDCl_3$. Thereafter, crude reaction products were isolated by removing solvents and extracting the resulting residues with hexane. The masses of the resulting materials were used to calculate each mass recovery.

Our first attempt (see Table 3, entry 1) was performed using PCl_3 and *N,N*-diisopropylamine stock solutions concentrations of 0.2 $mol \cdot L^{-1}$ (5 mmol in 20 mL dry CH_2Cl_2) for the first reaction step and 9-fluorenylmethanol 0.4 $mol \cdot L^{-1}$ (10 mmol in 20 mL dry THF) anhydrous THF for the second reaction step, mimicking the batch conditions reported in section 4.1.1. For both the three solutions, flow rates of 0.6 $mL \cdot min^{-1}$ were applied to give an approximate residence time of 40 min in the first coil and of 28 min in the second coil. On analysis of the resulting materials, I found low mass recovery and poor levels of purity. I hypothesised that the reaction was incomplete, either at the step 1 or step 2. Therefore, to increase the rate of reactions I increased the concentrations of reagents to 1 and 2 $mol \cdot L^{-1}$ (see Table 3, entries 2 and 3).

The first result obtained did not produce high product yield, but at higher solutions concentration of 1 $mol \cdot L^{-1}$ and 2 $mol \cdot L^{-1}$ of PCl_3, the reaction performance improved. Subsequently, a higher flowrate of 1 $mL \cdot min^{-1}$ and a subsequent higher mixing efficiency within the coil were successfully employed, with a step 1/coil 1 residence time of 25 min instead of 40 min, and a step 2/coil 2 residence time of 17 min instead of 28 min, further decreasing reaction times compared to batch (see Table 3, entry 4).

Because operating the all-reaction process at room temperature would have been advantageous and more translatable to an industrial process at this point a second tier of experiments was then performed (entries 5-7) with coil 1 held at 24 °C rather than 0 °C. The flowrate was maintained at 1 $mL \cdot min^{-1}$ and using 2 $mol \cdot L^{-1}$ of PCl_3 solution. The best result in terms of yield (81%) and purity (84% based on ^{31}P NMR) of amidite **2** was obtained under these conditions (see Table 3, entry 5). Several repetitions under these conditions proved very successful and consistent. Thus, I decided to scale up the reaction. Using 50 mmol of PCl_3 in a 2 $mol \cdot L^{-1}$ stock solution, and I formed amidite (**2**) with a mass recovery of 71% and a purity of 82% (see Table 3, entry 7). The last tier of experiments (entries 8-11) centred on changing the length of the first coil, from 49 mL to 14 mL and 20 mL but the reaction performance was less encouraging.

As previously mentioned at the beginning of this section, these early-stage flow investigations listed in *Table 3* were designed to probe the reaction viability,

temperatures and reaction times required. Because each experiment was not allowed to reach steady-state by equilibrating the flow reactors with 2 CV before the collection, I expect higher mass recovery and purity level of the desired compound (**2**) when collected under steady-state eqilibrium.[174]

Entry	$FR_A=FR_B=FR_C$ ($mL \cdot min^{-1}$)[a]	T_1 (°C)[b]	T_2 (°C)[c]	RT_1 (min)[d]	RT_2 (min)[e]	PCl_3 ($mol \cdot L^{-1}$)[f]	Mass recovery (%)[g]	Purity (%)
1	0.6	0	24	40	28	0.2	52	68
2	0.6			40	28	1	66	84
3	0.6			40	28	2	73	80
4	1			25	17	2	54	84
5	1	24		25	17	2	81	84
6	0.6			40	28	2	80	82
7	1			25	17	2	71	82
8	1			10	17	2	73	82
9	1			7	17	2	54	84
10	1			7	17	1	50	87
11	1			10	17	1	70	80

Legend: a FR: flow rate each pump. b T1: reaction temperature in the first coil. c T2: reaction temperature in the second coil. d RT1: residence time of the first reaction step. E RT2: residence time of the second reaction step. F C: concentration. g mass recovery of the crude phosphoramidite estimate based on 100% purity.

Table 3: Flow parameters for the synthesis of *bis*-(fluorenylmethyl)-diisopropylamine phosphoramidite (**2**).

These materials were successfully 'use-tested' for the batch synthesis of ADP (see sections 4.2.2 and 4.2.2.1) and then used for the flow synthesis of NDPs, and the results of these experiments are discussed in detail in section 4.2.2.3

In summary, a faster, more efficient batch synthesis of *bis*-(fluorenylmethyl)-diisopropylamine phosphoramidite (**2**) was developed (see section 4.1.1) that was subsequently translated into a continuous flow process (see section 4.1.2). Both processes avoided chromatography to deliver reagent that proved effective in the Jessen coupling[1], thanks to a simple work up. I found extraction with hexane, *n*-heptane and cyclohexane, to afford good yields and high levels of purity. Several additional 'greener' reaction solvents

were tested as alternatives to THF and CH_2Cl_2. Unfortunately, I found CH_2Cl_2 to be the only viable candidate for continuous flow, alongside THF as co-solvent.

A series of flow experiments were conducted using different reactant concentrations, coil temperatures and flow rates. Although the mass recovery and the purity levels of amidite (**2**) obtained in the batch reactions were marginally higher, probably because the experiments performed in flow were not under steady-state equilibrium, they were still effective and, critically, showed scope for scalability. I did not increase reaction concentration in batch, instead focusing on the opportunities offered by our flow approach. Specifically, our scaled batch process to deliver 25 g of amidite (**2**) took place in a reaction volume of 250 mL, compared to the flow reaction that instead took place in a 75 mL reaction volume. I was able to successfully increase coil temperature, thus increasing the reaction rate, and reactant concentrations in flow, thus reducing solvent burden and reaction times.

4.2 Development of Jessen's "one-pot three-step" phosphorylation reaction

As mentioned at the beginning of this chapter, I chose to 'use-test' the phosphitylating reagent, *bis*-(fluorenylmethyl)-diisopropylamine phosphoramidite (**2**) made with our convenient batch method, without further purification or processing in "one-pot three-step" phosphoanhydride formation reactions.[1, 145] Initially, our 'use-test' was to form ATP from ADP, where ADP was used as a partial tetra-*N*-butyl ammonium salt (**15**) results from this study are described in 4.2.1. The coupling effectiveness of *bis*-(fluorenylmethyl)-diisopropylamine phosphoramidite (**2**) was assessed in the presence of an acid activator to introduce a γ-phosphate onto ADP and subsequently form tris-piperidinium ATP (**16**) as shown in

Figure 27 (see section 4.2.1).

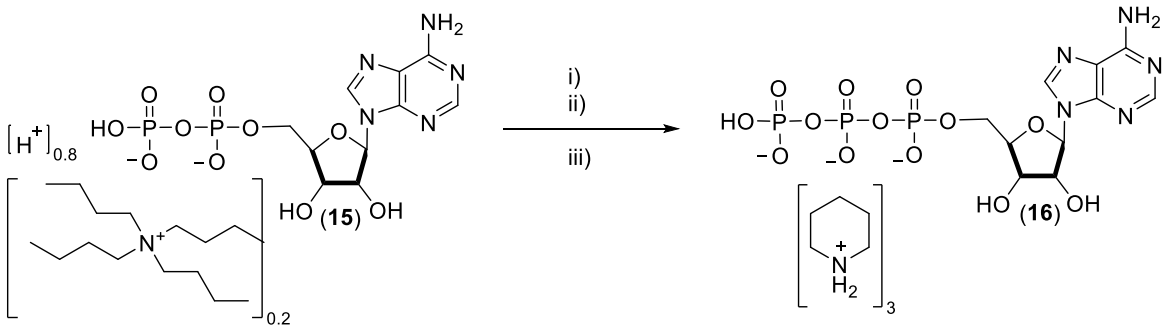

*Reagents and conditions: i) bis-(fluorenylmethyl)-diisopropylamine phosphoramidite (**2**), 5-(ethylthio)-1H-tetrazole, wet DMF, 25 °C. ii) mCPBA, wet DMF, 25 °C. iii) piperidine 5% v/v, wet DMSO, 25 °C.*

Figure 27: One-pot three-step reaction for the synthesis of ATP (**16**) from ADP (**15**).

The overarching purpose of this project is to translate phosphoanhydride formation to a scalable, continuous flow system. Testing and optimisation of flow chemistry often requires access to larger quantities of substrates and reagents. Access to large quantities of phosphitylating agent (**2**) was described in section 4.1, however, ADP (acid form) was only available in relatively small quantities at relatively high cost (~£75/ 5 g). Owing to the lower cost and large-scale availability (~£50 /100 g) of AMP (acid form), I moved away from ATP synthesis to focus on the synthesis of ADP from AMP as or test-bed system as shown in

Figure 28 (see section 4.2.2).

Initially, batch reactions (section 4.2.2.1) were explored to validate the approach and analytical methods, before being transferred to a flow system (section 4.2.2.3). In addition, to gain some level of understanding about reaction times, ^{31}P NMR kinetic studies were performed on the coupling and oxidation steps during the conversion of AMP to ADP (section 4.2.2.2). Eventually, the method I developed was applied towards the preparation of UDP from UMP, and CDP from CMP to show generality (section 4.2.2.4).

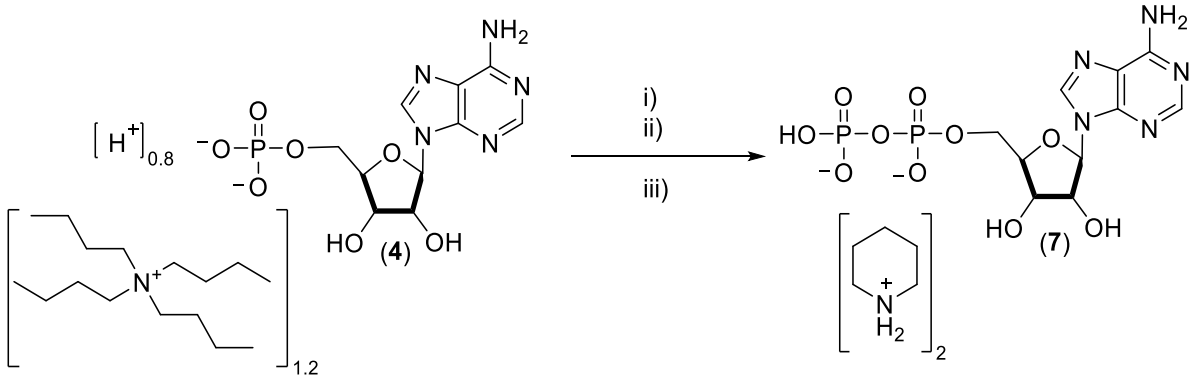

Reagents and conditions: i) bis-(fluorenylmethyl)-diisopropylamine phosphoramidite (**2**), 5-(ethylthio)-1H-tetrazole, wet DMF, 25 °C. ii) mCPBA, wet DMF, 25 °C. iii) piperidine 5% v/v, wet DMSO, 25 °C.

Figure 28: One-pot three-step reaction for the 5'-adenosine diphosphate synthesis (**7**)[1, 145].

4.2.1 Batch-based “one-pot three-step” synthesis of ATP

As highlighted in the introduction to this section (section 4.2), initial phosphoanhydride formation reactions were performed using ADP salts as substrates (**16**), following the procedure developed by Jessen’s group.[1, 145]

Thus, ADP tetrabutylammonium salt (**16**) was dissolved in DMF and 5-(ethylthio)-1*H*-tetrazole was added. Amidite reagent (**2**) ‘titre-corrected’ to account for the purity level, was then added to the solution. After 15 min, substantial conversion of ADP to the *bis*-Fm protected P(III)-P(V)-P(V) anhydride (**17**), was observed by ^{31}P NMR spectroscopy. The P(III)-P(V)-P(V) anhydride (**17**) was then oxidised to bis-Fm protected P(V)-P(V)-P(V) anhydride (**18)** using *meta*-chloroperoxybenzoic acid (*m*CPBA). The protected anhydride (**18**) was precipitated by the addition of hexane/diethyl ether and collected by centrifugation. After dissolution of the solid in DMSO, cleavage of the Fm protecting groups was performed by addition of 5% v/v piperidine solution in DMF. Upon deprotection, the ATP product (**16)** was precipitated as its piperidinium salt after further addition of diethyl ether. The entire process was complete in less than 30 min.

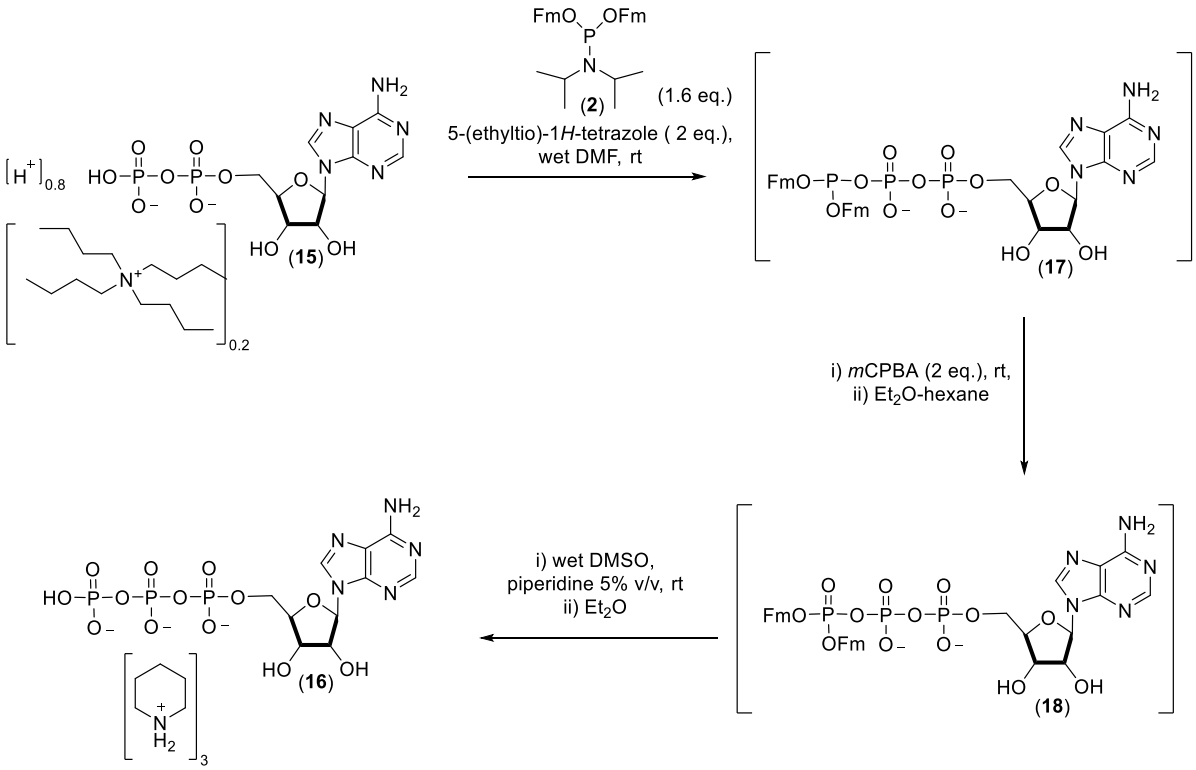

Figure 29: Reaction scheme for the "One-pot three-step" synthesis of 5'-adenosine triphosphate (**16**) in batch.

I attempted to optimise the coupling reaction by changing the numbers of equivalents of amidite, activator and oxidising reagent with respect to the nucleotide substrate. Using ^{31}P NMR spectroscopy with D_2O lock tube as our primary measure of reaction effectiveness, I found the use of additional numbers of equivalents of the amidite reagent compared to Jessen's reported[1] 1.6 equivalents did not affect the complete conversion of the starting material, but increased by-product formation, especially of the H-phosphonate detected ~1-3 ppm by ^{31}P NMR spectroscopy, with a J_{P-H} = 611.3 Hz (see Figure 30). Interestingly, on the ^{31}P NMR spectrum of the coupling step, three small peaks corresponding to the α-β-γ phosphate of Fm-protected ATP (**16**) were observed. What I expected to see at this stage were only the peaks of the intermediate P(III)-P(V)-P(V) anhydride (**17**) rather than the P(V)-P(V)-P(V) (**18**) system. Based on this observation, I hypothesized that DMSO could have some oxidizing power towards the P(III) reaction intermediate (**17**), but, at this stage, I did not explore this idea further, based on the low levels of (**18**) formed. In addition to the potential effect of the DMSO on the P(III) intermediate, I also had concerns that DMSO may oxidise the reagent amidite (**2**). While this parallel process may not be a problem in batch processes where coupling is occurring in competition with reagent oxidation, this could be a significant shortcoming when making stock solutions of reagent in DMSO for flow experiments.

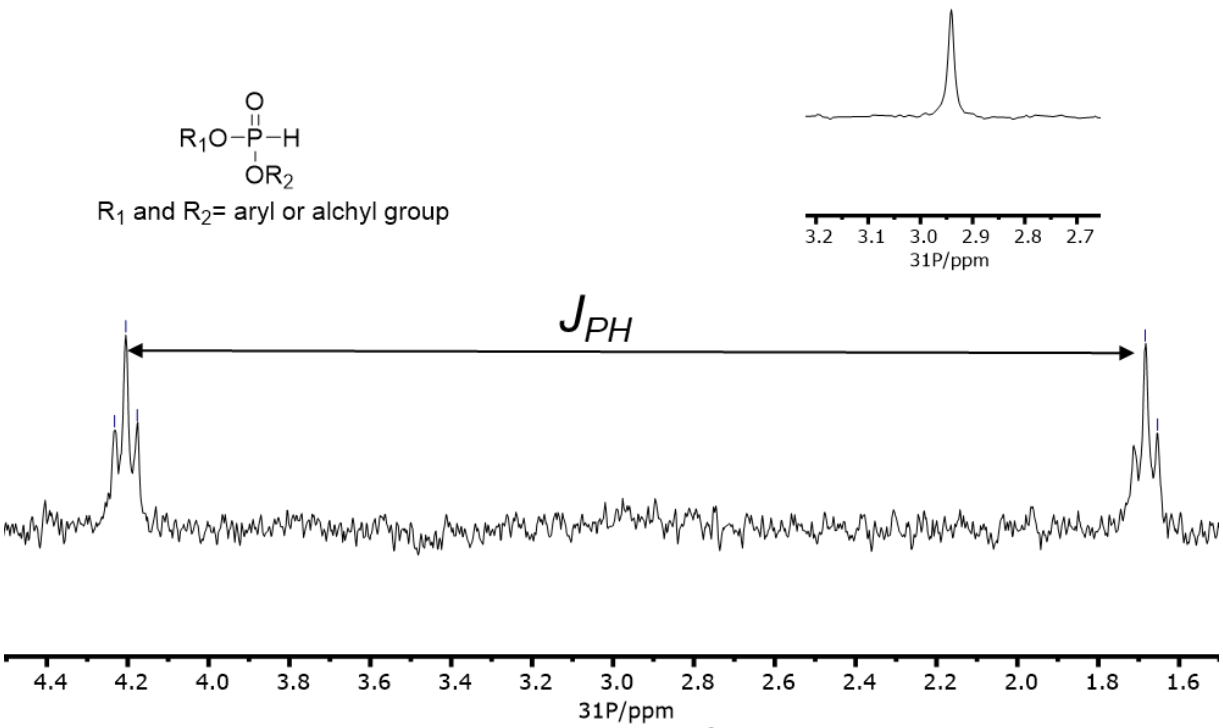

Figure 30: H-phosphonate structure (top left), $^{3}1P^{-1}H$ coupled (main figure) and ^{31}P-^{1}H decoupled (inset) NMR spectra run with D_2O lock tube.

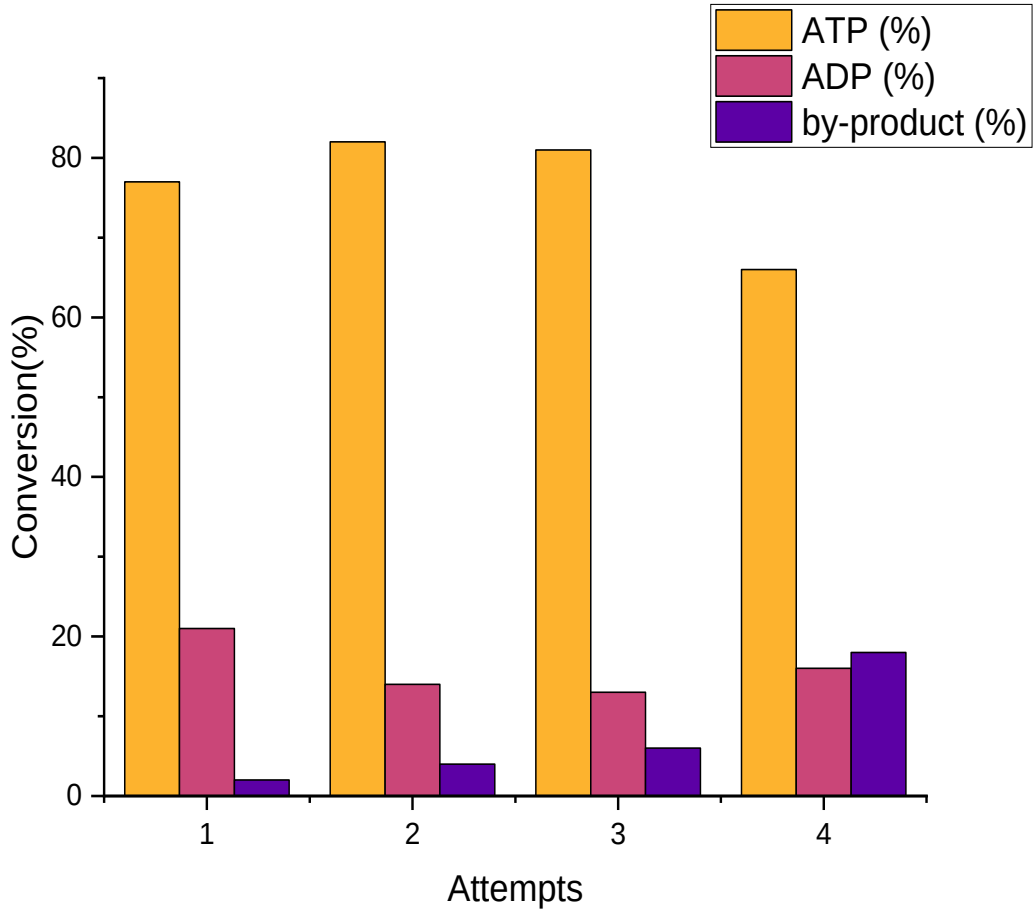

Entry	ADP(TBA)$_{0.2}$H$_{.8}$ (15) (equiv.)[a]	Amidite (2) (equiv.)[a]	Activator (equiv.)[a]	*m*CPBA (equiv.)[a]
1	1	1.6	2.0	2.0
2	1	2.0	2.5	2.5
3	1	2.5	3.1	3.1
4	1	3.2	4.0	4.0

Table 4: Summary of numbers of equivalents of reagents used for ATP synthesis with related graph of % conversions of ADP into ATP. Each set of conditions was trialled once.

Having shown that increasing the number of equivalents of 2, 5-(ethylthio)-1*H*-tetrazole and *m*CPBA only led to small improvements to conversion levels with significantly increased by-product formation and reagent consumption, I focused our attention on reaction timing. First,

I explored the duration of the first coupling step (step 1, *Figure 29*) that leads to the formation of the P(III)-P(V)-P(V) anhydride (**17**), by monitoring the reaction progress five times over the course of 1 h. The highest level of conversion was recorded after only 5 min of coupling, with a ratio of starting material/product of ca. 1/3.5. After 1 h, however, the ratio was reduced to ca. 1/1, with a slight increase of by-products. This reduced ratio of conversion could be potentially traced back to the instability of P(III)-P(V)-P(V) anhydride (**17**), which probably undergoes hydrolysis at the γ-phosphorus at prolonged reaction times.

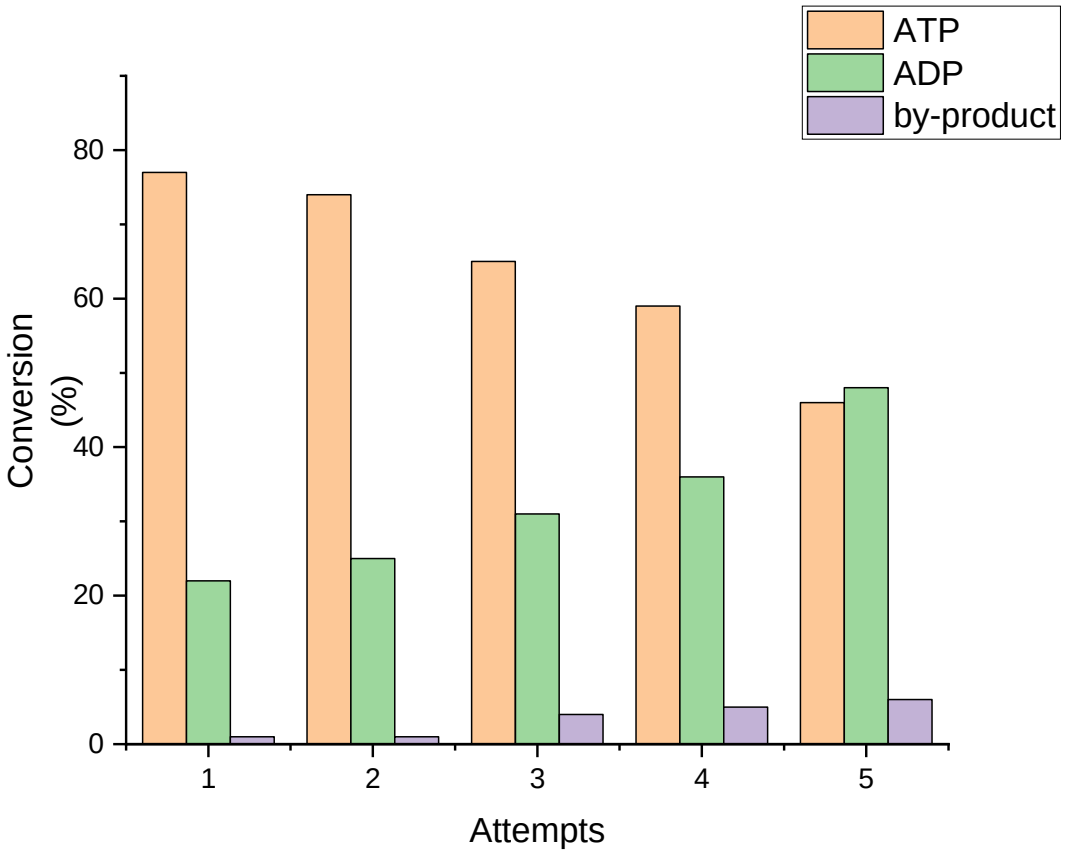

Entry	Time (min)	ATP (16) %	ADP (15) %	by-product %
1	5	77	22	~1
2	10	74	25	~1
3	20	65	31	4
4	40	59	36	5
5	60	46	48	6

Table 5: Summary of different coupling times for ATP synthesis (**16**) with related graph of % conversions during time. Each set of conditions was trialled once.

The preliminary results detailed above for the synthesis of tris-piperidinium ATP (**16**) confirmed the effectiveness of our phosphitylating reagent (**2**), accessed through our simple ~1 h batch procedure. Furthermore, the rapidity of the P(III)-P(V)-P(V) coupling highlighted

the potential opportunity offered by flow technologies, where short contact times can be reliably and repeatably accessed with good mixing. Given that larger quantities of nucleotide starting materials were expected to be required to allow exploration and optimisation of flow methods, I moved to AMP instead of ADP as the substrate, as ~100 g quantities of the acid form could be purchased at reasonable cost (see section 4.2).

4.2.2 "One-pot three-step" synthesis of ADP

As mentioned previously (4.2.1), the choice to set aside the ATP synthesis and focus on ADP arose from practical needs. Starting material monophosphates such as AMP can be supplied in much larger quantities than diphosphates, at significantly lower cost. Despite the change of direction, I maintained the goal of optimizing the synthetic method for phosphoanhydride formation both in batch and in flow.

4.2.2.1 Testing and Optimisation of the "one-pot three-step" batch synthesis of ADP

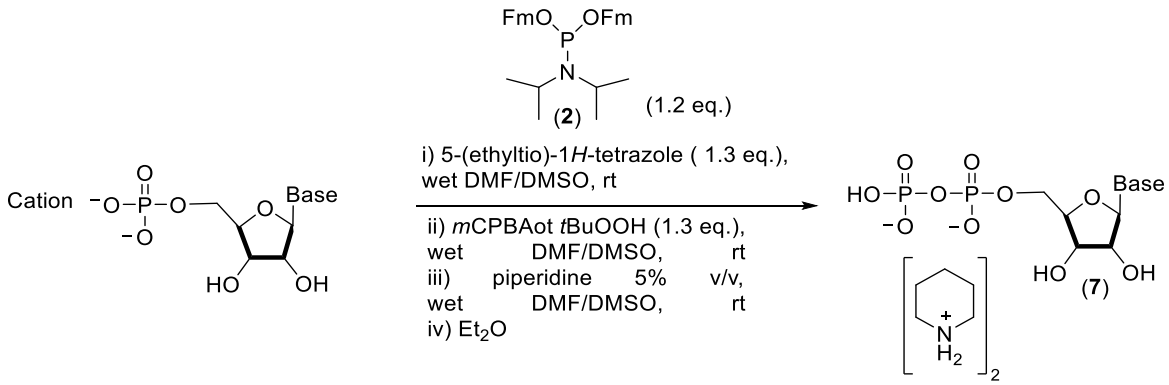

Figure 31: Bis-piperidinium NDP synthesis reported by Jessen's group.[1, 145]

Based on our previous results for ATP[1] synthesis, I carried out an initial screening of reagent, substrate, and activator concentrations for ADP synthesis. Jessen's group[1] reported several procedures to make NDPs. They differ in the choice of solvent (DMF or DMSO), activators (5-phenyl-1*H*-tetrazole or 5-(ethylthio)-1*H*-tetrazole), and oxidizing agents (*m*CPBA or *t*BuOOH in decane).

In the first general method, Jessen reported the dissolution of the 1.0 equiv. of NMP trihexylammonium or pyridinium salt in DMSO (or DMSO-d6) before the addition of 1.2 equiv. of *bis*-(fluorenylmethyl)-diisopropylamine phosphoramidite (**2**), activated with 1.2 equiv. of 5-phenyl-1*H*-tetrazole[1]. The subsequent oxidation step was carried out with 5 equiv. of *t*BuOOH (5 mol·L^{-1} in decane) and then the Fm protecting groups were cleaved with 5% v/v piperidine in DMF. The product, precipitated upon addition of Et_2O, was isolated by centrifugation, washed with Et_2O and dried in vacuo.

In Jessen's second general method, 1.0 equiv. of NMP with ca. 1.2 tetra-n-butyl ammonium counterions was dissolved in DMF. Thereafter, 1.2 equiv. *bis*-(fluorenylmethyl)-diisopropylamine phosphoramidite (**2**) was added and immediately after its dissolution, 1.3 equiv. of 5-(ethylthio)-1*H*-tetrazole was added. After completion of the anhydride coupling, 1.3 equiv. of *m*CPBA was added in the oxidation step followed by deprotection and precipitation with 5% v/v piperidine in DMF and Et_2O leading to NDP.[1]

Specifically, AMP trihexylammonium was the salt chosen by Jessen[1] for the synthesis of ADP in DMSO, with 75% of isolated yield on a scale of 100 mg of starting material.

To identify a method that was congenial in terms of solubility for application in flow, I first tested the solubilities of trihexylammonium, pyridinium and tri-*n*-octylammonium salts of AMP in 1.5 mL of DMSO-d6. Although both salts appeared reasonably soluble, I found that pyridinium and trihexylammonium AMP solution was fully clear, whereas the tri-*n*-octylammonium showed some turbidity. The one pot-three steps reaction with pyridinium and trihexylammonium AMP salts as substrates were performed in parallel. During the deprotection step, by contrast with the pyridinium AMP substrate reaction mixture, no precipitation occurred at the addition of piperidine in reaction mixture with trihexylammonium AMP salt as substrate, making the isolation the final product more difficult. Thus, in future DMSO-based experiments, I used the pyridinium AMP salt. I checked the solubility of 5-(ethylthio)-1*H*-tetrazole activator in DMSO and found it to be soluble at 0.23 $mol \cdot L^{-1}$

Moving to DMF, I found tetrabutylammonium AMP was fully soluble at a concentration of 0.17 $mol \cdot L^{-1}$, and 5-(ethylthio)-1*H*-tetrazole was soluble at a concentration of 0.23 $mol \cdot L^{-1}$.

Our initial decision to explore reactions using DMSO (see sections 4.2.2.2.1 and), and subsequently to move on the use of DMF (see section 4.2.2.2.3.2) will be discussed through this chapter.

DMF is, however, considered an undesirable solvent for several reasons,[160, 175-177] thus I tested the solubilities of tetrabutylammonium AMP in potentially greener solvents.

Specifically, I screened four polar, aprotic solvents (see below). In the cases of trifluorotoluene and 2-methyl-tetrahydrofuran, I had already shown their effectiveness for the preparation of *bis*-(fluorenylmethyl)-diisopropylamine phosphoramidite (**2**), thus, I hoped that if nucleotides showed solubility in these two solvents, I may be able to form, and then use the reagent with nucleotide substrate *in situ*.

1. Cyrene;[166-170]
2. acetonitrile;
3. trifluorotoluene;
4. 2-methyl-tetrahydrofuran.[164, 178]

Unfortunately, screening the solubility of AMP tetrabutylammonium salt in all four solvents, showed poor solubility levels, thus precluding their use for flow-based anhydride formation. Despite the insolubility of the AMP salts in the four solvents, I continued with the suspended AMP salts in attempts to perform phosphoanhydride formation in batch, as shown in *Figure 32*, with the hope that as reaction occurred, materials may slowly react and dissolve. In this way, I hoped to be able to potentially move away from the use of DMF in batch, if not flow.

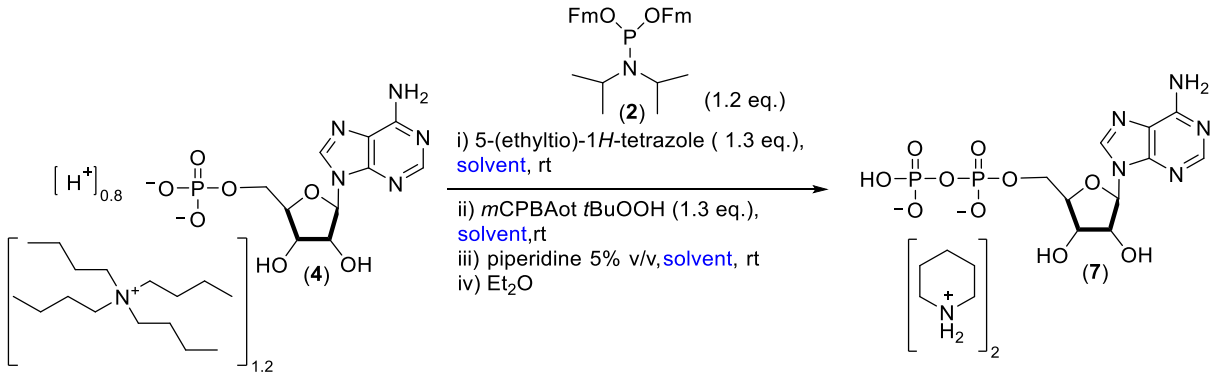

Figure 32: Solvent screening for the "one pot-three steps" synthesis of bis-piperidinium ADP (**7**).

The reactions carried out in acetonitrile, trifluorotoluene and 2-methyl-tetrahydrofuran showed no conversion of AMP to ADP by ^{31}P NMR spectroscopy.

With Cyrene, the tetrabutylammonium AMP salts proved fully soluble, however, the addition of the phosphitylating agent to the reaction led to the formation of a clear gel. Despite this potential problem, I continued with the reaction to synthesize *bis*-(fluorenylmethyl)-

diisopropylamine phosphoramidite (**2**), as described in section 4.1.1, followed by direct addition of AMP to the mixture. Reaction analysis by ^{31}P NMR spectroscopy showed poor conversion of AMP to ADP, and the formation of several by-products. This poor result may be a result of the unusual solubility phenomena observed in the reaction.

Although I aspired to make the phosphoanhydride formation greener while maintaining full solubility for flow protocols, this was not our absolute priority. Thus, in order to progress the flow aspects of the project, I reverted to the use of DMF and DMSO as originally demonstrated by the Jessen group.[1, 145]

4.2.2.2 Kinetic studies of the "one-pot three-step" synthesis of ADP by ^{31}P NMR spectroscopy

Through this section, I will develop methods to quantitatively analyse the coupling (step 1) and oxidation (step 2) processes for the synthesis of ADP via ^{31}P NMR spectroscopy (see *Figure 31*). As mentioned in the section 4.2.2.1, our initial decision to explore reactions using DMSO will be discussed in detail in section 4.2.2.2.1 and 4.2.2.2.2, providing an overall view of the reasons why I subsequently moved on the use of DMF (see section 4.2.2.2.3). I found that a ^{31}P NMR spectroscopy method for quantitative time-course analysis became necessary (see details in section 4.2.2.3.2.1). T_1 studies of the oxidation reaction (step 2) for the synthesis of ADP were then performed under the guidance of Dr. Juan A. Aguilar Malavia and the results are discussed in section 4.2.2.2.3.1 and 4.2.2.2.3.2. The results proved to be fundamental to the development of a specific, quantitative, and robust ^{31}P NMR spectroscopy method for determinations of concentrations of P-containing species, as discussed in sections 4.2.2.2.3.2 and 4.2.2.3.2.1 Although the observed fast reaction times (see section 4.2.2.2.3.2) made it difficult to analyse the reaction kinetic trends extensively, an appreciation of the time scales of reactions was still gained. I hoped these data would enable us to make informed decisions about reaction times and reduce by-product formation in semi-continuous flow systems. Knowledge of T_1 values also allowed us to make quantitative assessments of concentrations of species in stock solutions.

4.2.2.2.1 ^{31}P NMR spectroscopic analyses of the coupling and oxidation steps of "one-pot three-step" synthesis of ADP in DMSO

As mentioned in section 4.2.2, initially I opted to explore reactions using DMSO as the solvent for two reasons:

1. Based on Jessen's report, DMSO-d6 was also expected to be an effective solvent. I hoped this would facilitate ^{31}P NMR analyses without requiring the addition of 'lock tubes' containing a deuterated solvent;
2. The cost of DMSO-d6 (~350 £/ 100 g). is much lower compared to DMF-d7 (~500 £/ 10 g).

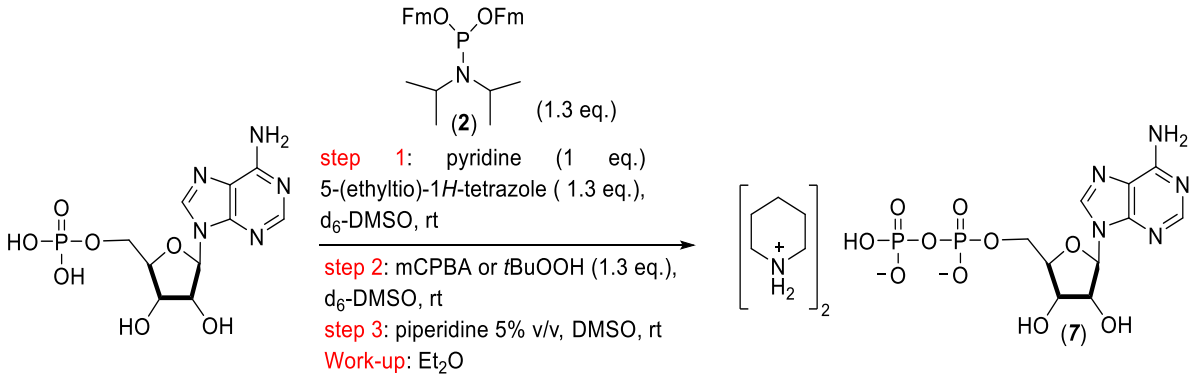

Figure 33: "One pot-three steps" synthesis of bis-piperidinium ADP synthesis (**7**), following the DMSO method reported by Jessen's group.[1]

Preliminary experiments were analysed by single acquisition experiments on a Bruker Neo-400 spectrometer. I used a simple mixing protocol, in a vial, which is described here for clarity. As our studies progressed, I realised that this protocol, although simple and accessible with our facilities, was insufficiently rapid to gain complete kinetic understanding. In a 5 ml vial, 50 mg of AMP pyridinium salt (1 equiv.) was dissolved in DMSO-d6 (0.350 mL). Then, solid 5-(ethylthio)-1*H*-tetrazole was added to the AMP solution, followed by amidite (**2**) dissolved in of DMSO-d6 (0.300 mL). The mixture was then transferred from the mixing vial to an NMR tube. The progress of the coupling reaction (step 1) between AMP and amidite (**2**), (see *Figure 33*) was then assessed after 5, 10, 20, 30 and 60 min of reaction. From the resulting ^{31}P NMR spectra, I were able to observe the consumption of AMP and amidite (**2**) and the emergence of new sets of signals, including the distinctive $^{2}J_{P\text{-}P}$ coupled signal of the P(III)-P(V) anhydride (**8**). The highest level of conversion was recorded after 5 min. of coupling, with a ratio of starting material/product of *ca.* 1/3.6. After 1 h, however, the ratio

was reduced to *ca.*1/2.2, with a slight increase of by-products. This reduced ratio could potentially be traced back to the instability of the P(III)-P(V) anhydride (**8**).

Next, the effectiveness of the coupling reaction was analysed in further detail by changing the numbers of equivalents of the reagents. The use of additional numbers of equivalents of amidite (**2**) (1.5 equiv. instead of 1.2 equiv.) still led to complete consumption of AMP, however, by-product formation increased significantly. Therefore, I opted for an intermediate value, 1.3 equiv. of amidite (**2**), that could increase the reaction rate whilst still giving relatively low levels of by-products.

Regarding oxidation of the mixed P(III)-P(V) (**8)** system to P(V)-P(V) (**9**), i.e step 2, (see *Figure 33*), the kinetics of reactions with *m*CPBA and *t*BuOOH 5 M in decane were assessed. Both NMR analyses (timepoints of 5, 10, 20, 30, 60 min.) showed that the oxidation of the P(III) (**8**) to P(V) (**9**) was complete within 5 min. Overnight storage of the resulting solutions showed the resulting P(V)-P(V) Fm-protected anhydride (**9**) to be stable, especially compared to the P(III)-P(V) anhydride (**8**). In summary, our brief exploration of conditions confirmed the effectiveness of the method proposed by Jessen.[1, 145]

Based on the preliminary analyses discussed above, quantitative kinetic analyses of coupling (step 1) and oxidation (step 2) processes of the "one-pot three-step" ADP synthesis[1, 145], were run on a 500 MHz spectrometer. These experiments were initiated because I found the summation of integrals of P-containing species to be inconsistent across the time course. Figure 34 gives a schematic representation of a ^{31}P time course pulse sequence. The important parameters to be considered during the settings of a time course experiment, and which I will often mention through this chapter, are:

1. number of scan (ns or nt, depending on machine manufacturer);
2. relaxation delay (d1): a delay period in the pulse sequence between scans, expressed in seconds;
3. acquisition time (at): the length of time that the receiver is actually acquiring data;
4. preacquisition delay (pad): an additional delay time at the start of the acquisition before there are any pulses. This parameter is expressed in seconds;
5. pulse 'width': (pw) the time in microseconds of the pulse for the experiment;
6. pulse width one (p1); a second pulse width parameter that can be applied when different initial and subsequent pulse widths are required;
7. The repetition time, the total time between pulses = d1 + at + pad.

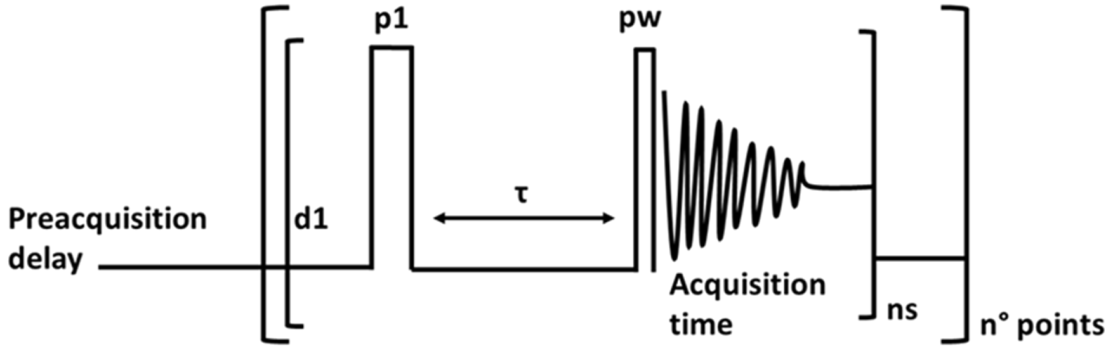

Figure 34: ^{31}P time course pulse sequence.

In our first set of experiments, reactions were monitored over the course of 4 h using an automated programme, where each time-point was assessed by acquiring a 6 scan (nt) ^{31}P experiment, with 10 s preacquisition delay (pad) +2 s relaxation delay (d1) + 1.5 s acquisition time (at).

In the same way as the single spectrum acquisition experiments acquired on the Bruker Neo-400 spectrometer discussed previously, the time course samples were prepared by dissolving in a vial 50 mg (0.14 mmol) of the diacid form of AMP in 350 µL of DMSO-d6. Then, 1.2 equiv. of pyridine (12 µL, 0.17 mmol) was added to the nucleotide solution followed by 1.2 equiv. of *bis*-(fluorenylmethyl)-diisopropylamine phosphoramidite (**2**) (mass adjusted based on purity level measured by ^{31}P NMR spectroscopy, 0.17 mmol) and 1.2 equiv. of 5-(ethylthio)-1*H*-tetrazole (25 mg, 0.18 mmol). Trimethyl phosphate was added to the reaction at the outset as a reference of known concentration (17 µL, 0.14 mmol). The reaction was monitored using ^{31}P NMR spectroscopy on a 500 MHz spectrometer at 25 °C. At the end of the run, 1.2 equiv. of *m*CPBA (31 mg, 0.18 mmol) was added to the coupling solution and the kinetics of the oxidation step were investigated by returning the sample to the NMR magnet.

As shown in *Figure 35*, by the time the first time point of the coupling reaction had been acquired by the spectrometer, ~50% conversion to P(III)-P(V) anhydride product (**8**) (^{31}P signals ~125.18 ppm and ~–12.82 ppm) was observed, however, the signals quickly reduced over time, confirming the intermediate to be quite unstable. Indeed, the necessary time to prepare and insert the sample into the spectrometer and launch the time-course was at least 1 min, thus compromising attempts to understand the kinetics.

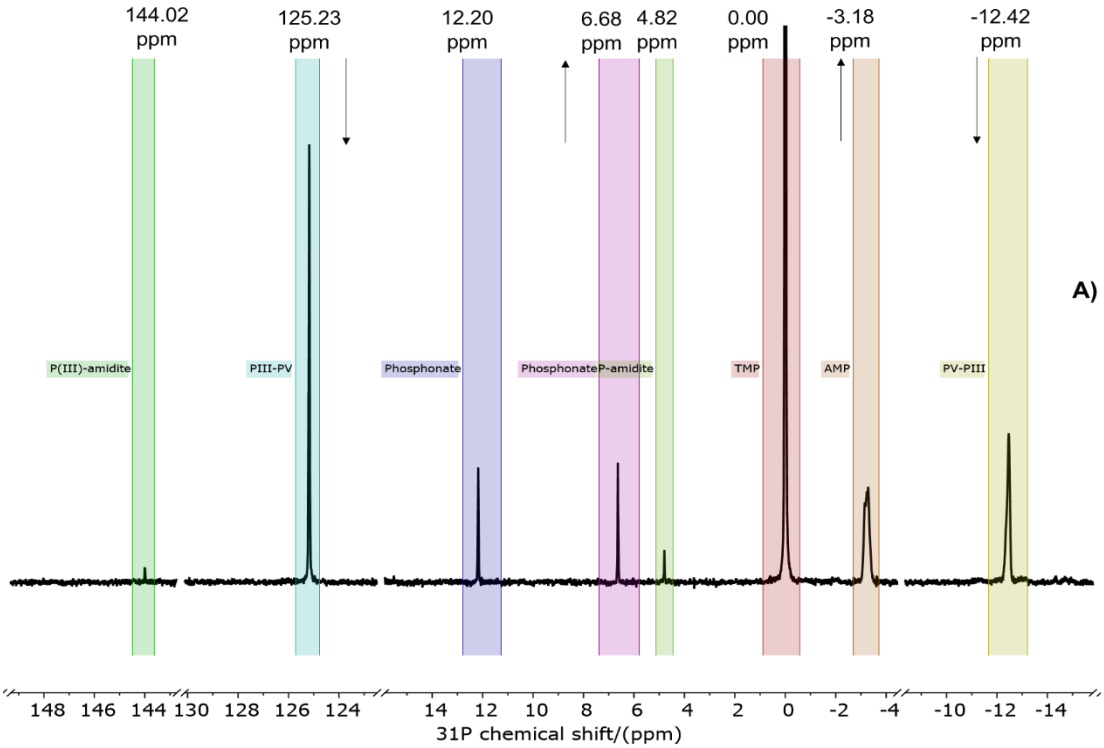

A)

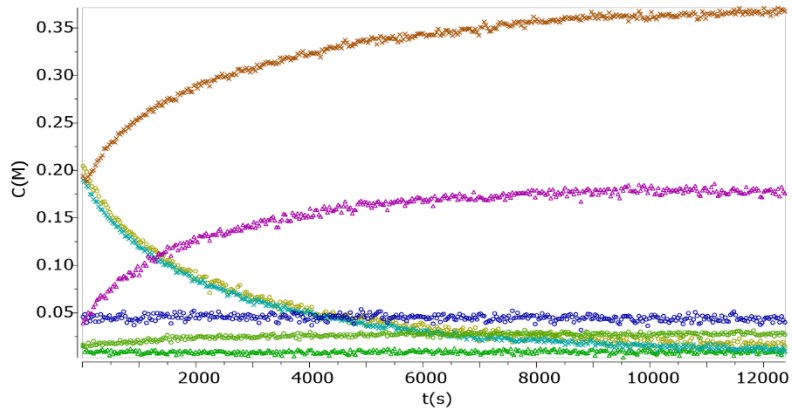

B)

Chemical structures corresponding to the peak label of signals spectrum:

C)

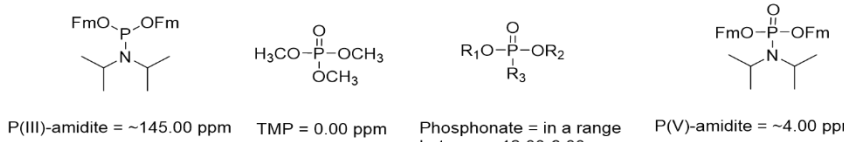

P(III)-amidite = ~145.00 ppm

TMP = 0.00 ppm

Phosphonate = in a range between ~12.00-6.00 ppm

P(V)-amidite = ~4.00 ppm

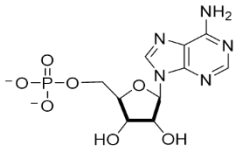

AMP =~ -3.50 ppm

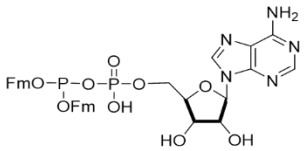

P(III)-P(V) = ~125.00 ppm
P(V)-P(III) =~ -12.00 ppm

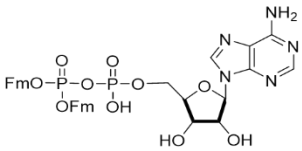

P(V)-P(V) =~ -14.00 ppm

Figure 35:A) Highlight of an exemplar ^{31}P NMR spectrum of AMP-amidite coupling reaction time-course in DMSO with B) related concentration C(M) over time t(s) graph. Data series are as follows: AMP (orange cross), P(V)-P(III) (yellow hollow circles), P(III)-P(V) (light blue crosses, Phosphonate (magenta hollow triangles), Phosphonate

(blue hollow circles), P(V)-amidite (light green hollow circles), P(III)-amidite (green hollow triangles). C) chemical structures.

While the ^{31}P NMR signals of P(III)-P(V) anhydride product (**8**) (~125.18 ppm and ~ –12.82 ppm) were decreasing in intensity, signals at ~ –3.85 ppm and 6.52 ppm increased. The lack of early time points in the time course made it difficult to see the product formation in comparison to by-product formation. Based on their chemical shift values, I hypothesized that the by-products could be phosphate esters or phosphoramidates (i.e., P(V) species). To gain additional insight, I explored our reagent's interactions with other components within the coupling and the oxidation reactions.

Thus, ^{31}P NMR spectra of the following mixtures were obtained in the presence of trimethyl phosphate:

- *bis*-(fluorenylmethyl)-diisopropylamine phosphoramidite (**2**) and oxidant;
- *bis*-(fluorenylmethyl)-diisopropylamine phosphoramidite (**2**), 5-(ethylthio)-1*H*-tetrazole and oxidant;
- *bis*-(fluorenylmethyl)-diisopropylamine phosphoramidite (**2**) and 5-(ethylthio)-1*H*-tetrazole.

The data were collected by acquiring ^{31}P NMR experiments with the same ^{31}P time-course pulse parameters described above [6 scans (nt), 2 s relaxation delay (d1) + 1.5 s acquisition time (at)]. The chemical shift of trimethyl phosphate was adjusted to 0.00 ppm in each NMR spectrum. The data were then compared to the ^{31}P NMR spectra of the AMP pyridinium salt time-course coupling reaction in DMSO-d6 (see *Figure 35*). As shown in *Figure 36*, the first significant piece of information gleaned from the results was the correspondence between the side product signal ~6.52 ppm (red spectra, number 1), with the product signal from the reaction between *bis*-(fluorenylmethyl)-diisopropylamine phosphoramidite reagent (**2**), 5-(ethylthio)-1*H*-tetrazole and the oxidant (green spectra, number 2). While the shifts were consistent, it should be borne in mind that the coupling reaction step does not involve the addition of an oxidant until the second reaction step. I hypothesised that adventitious entry of atmospheric oxygen into our system or oxidation of the P(III) reagent (**2**) by DMSO to be the potential cause(s).

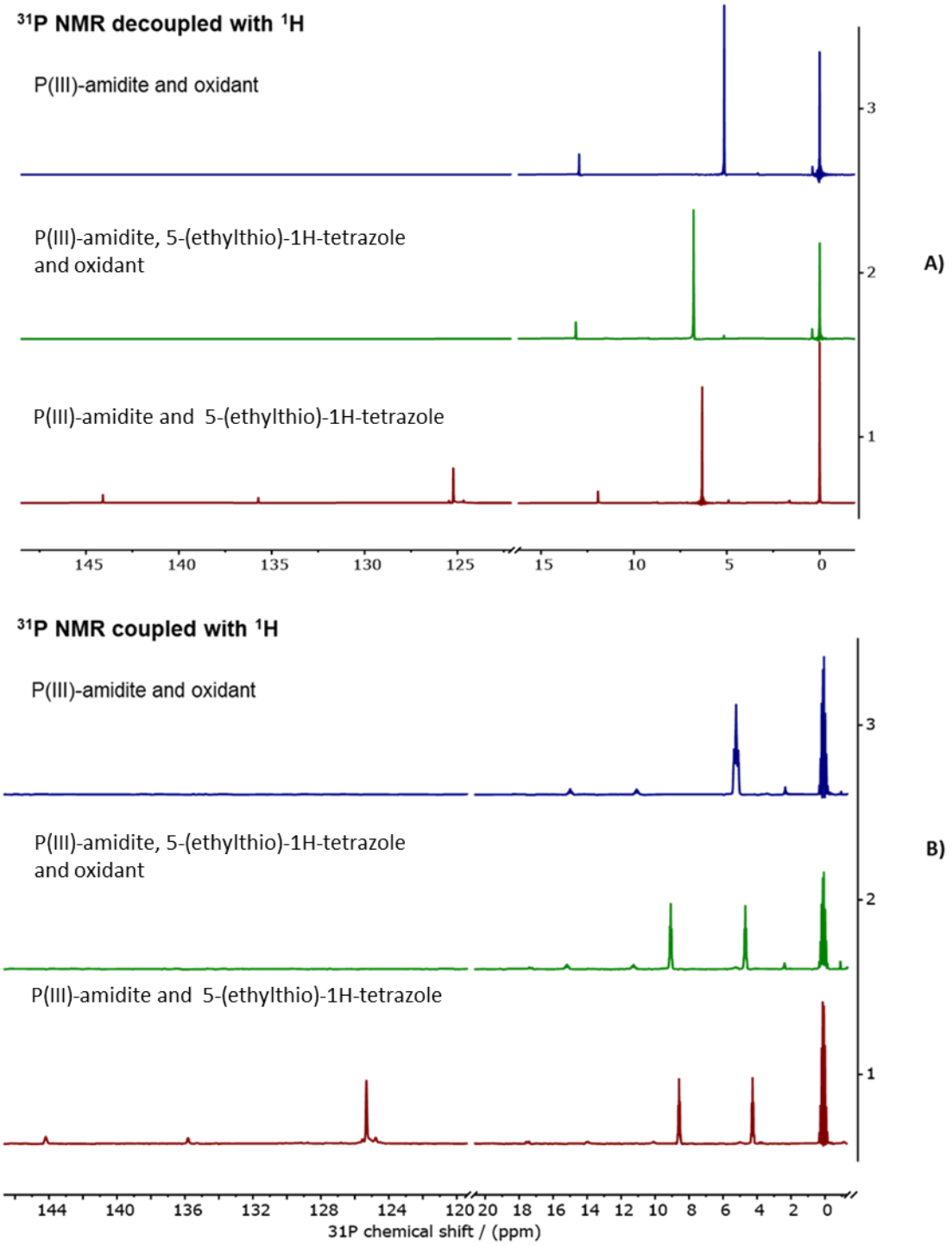

Figure 36: Highlight of ^{1}H-decoupled (A) and ^{1}H coupled (B) ^{31}P NMR spectra with D_2O lock tube, in presence of TMP as standard (0.00 ppm), of the *bis*-(fluorenylmethyl)-diisopropylamine phosphoramidite(**2**) reacted respectively with with 5-(ethylthio)-1*H*-tetrazole (1, red spectra) with 5-(ethylthio)-1*H*-tetrazole and oxidant (2, green spectra) and oxidant (3, blue spectra) in DMSO.

I expected the mixture of amidite (**2**) and 5-(ethylthio)-1*H*-tetrazole to produce some level of P(III) tetrazolide (**19**), with a ^{31}P chemical of ~ 126 ppm. (red spectra, number 1, *Figure 36*).

Instead of detecting the peak of the amidite (**2**) at ~ 145 ppm, I observed another signal with much lower chemical shift at ~6.35 ppm. The shift value is similar to that one observed for the mixture of amidite (**2**), 5-(ethylthio)-1*H*-tetrazole and oxidant, which should produce a P(V) tetrazolide, ~6.78 ppm. From the ^{1}H coupled ^{31}P NMR spectra of the reaction between *bis*-(fluorenylmethyl)-diisopropylamine phosphoramidite (**2**) with with 5-(ethylthio)-1*H*-tetrazole (red spectra number 1, *Figure 36*) and with 5-(ethylthio)-1H-tetrazole and oxidant (green spectra, number 2, *Figure 36*), the peaks with chemical shift around ~6.00 and 7.00 ppm predicted to be H-phosphonates, with a $J_{P\text{-}H}$= 700 Hz. Instead, the peak corresponding to the oxidized form of amidite (**2**) at ~ 5.12 ppm shows a very distinct coupling patterns in ^{31}P coupled with ^{1}H spectrum (blue spectrum, number 3, *Figure 36* B).

We, thus, believe that the P(III) tetrazolide (**19)** was oxidised to H-phosphonate, with DMSO presumably acting as the oxidant. During the NMR time course analyses for the coupling step to form P(III)-P(V) anhydride (**8**), in DMSO and in DMF (discussed in section 4.2.2.2.2) the peak at ~6.35 ppm was never observed. In these cases, where a nucleophilic substrate was present, I believe that coupling of the P(III) tetrazolide (**19**) was more rapid than its oxidation by DMSO. Recent studies have proven that phosphoramidite activation is the rate-determining step in the phosphitylation reactions, where activation takes place on timescales of seconds at commonly-employed reaction concentrations.[179] When 5-(ethylthio)-1*H*-tetrazole and P(III) reagent (**2**) are mixed, tetrazolide (**19**) formation likely takes place quickly, with subsequent oxidation by DMSO taking place more slowly in the absence of a parallel coupling option.

I also explored the natures of the signals with negative chemical shift values, which appeared over the coupling time course. I hypothesized a possible reversion to AMP due to instability of the P(III)-P(V) intermediate (**8**). A DMSO-d6 solution of AMP (diacid form) in the presence of trimethyl phosphate was analysed by ^{31}P NMR spectroscopy using the parameters employed for the previous time course study. The spectrum obtained was then compared to the previous time course result, as shown in *Figure 37*.

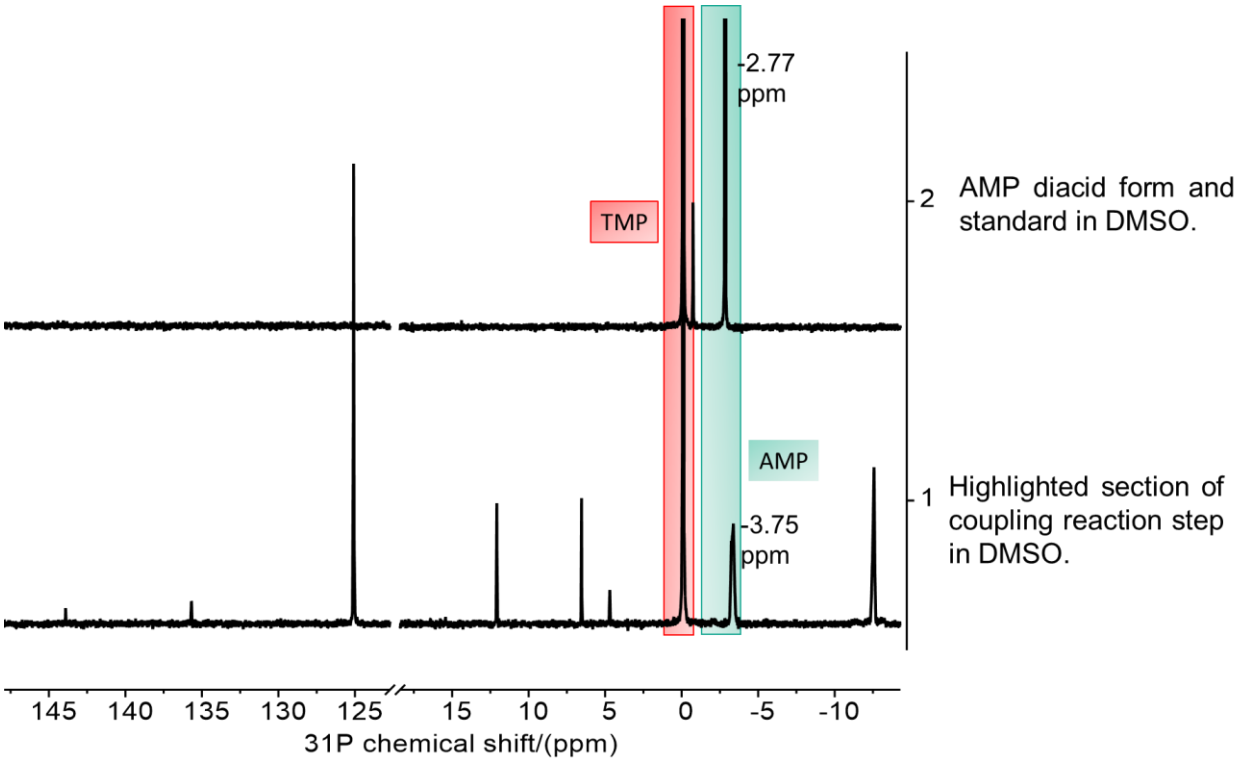

Figure 37: Comparison of ^{1}H-decoupled ^{31}P NMR spectra of AMP-amidite (**2**) coupling reaction mixture in DMSO and a DMSO-d6 solution of AMP diacid. Both samples contained trimethyl phosphate as a standard, which was set to 0.00 ppm.

Even though the chemical shifts of the two peaks highlighted in light blue are not the same (~ –2.77 ppm and ~ –3.75 ppm, highlighted in light green), I I thought that different speciation could cause the shift difference. A subsequent AMP (diacid form) 'spike' added to the time course sample led to superposition of the peaks. These results gave strong evidence in support of our hypothesis that reversion of the P(III)-P(V) intermediate (**8**) to AMP was occurring.

I repeated several single acquisition experiments that were discussed in section 4.2.2.1. A coupling reaction between AMP and amidite (**2**), in the presence of trimethyl phosphate standard was performed and single aliquots of the resulting P(III)-P(V) mixture were quenched after 1, 5, 15, 30 min of coupling with *m*CPBA. The chart below (*Figure 38*) highlights the changing concentrations of product and by-products over time. Concentrations were determined by measuring integral values and comparing them to the known concentration of trimethyl phosphate standard.

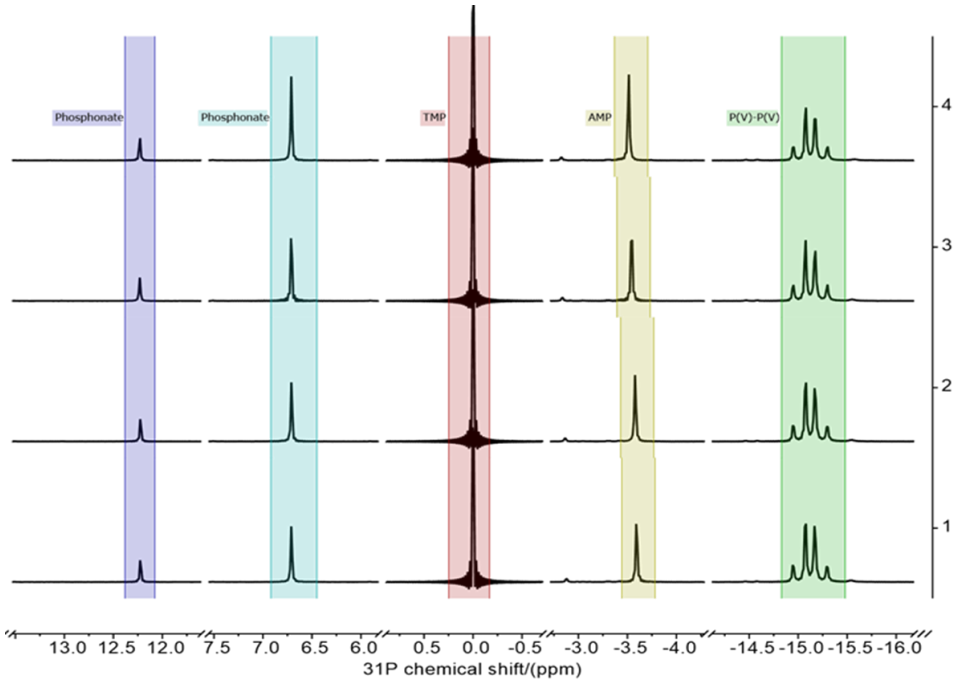

A)

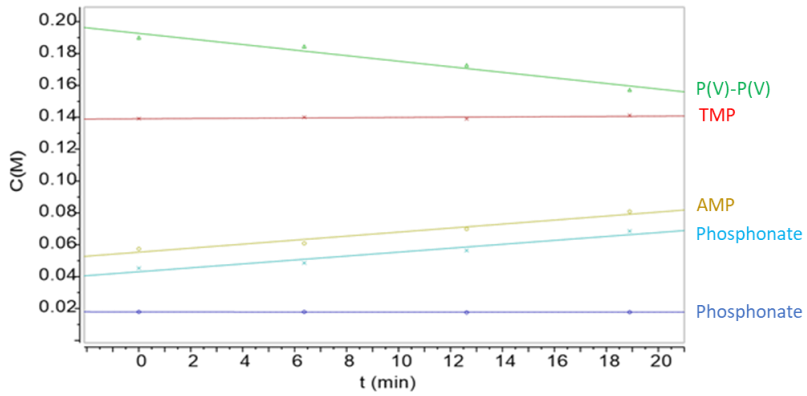

B)

Chemical structures corresponding to the peak label of signals spectrum:

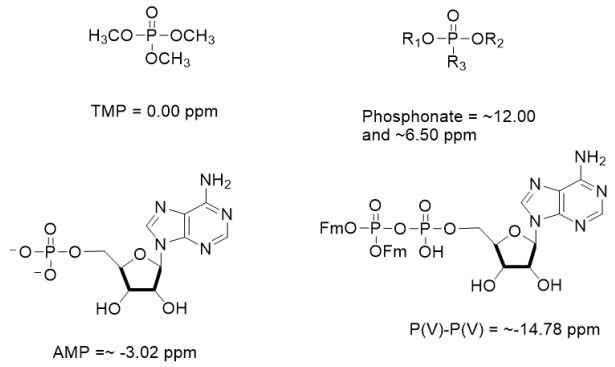

C)

Figure 38: A) ^{31}P NMR spectra of the time-course gained from discontinuous (aliquots withdrawn and quenched) coupling reaction between AMP and amidite (**2**) in DMSO-d6 1 min after initiation (stacked spectrum number 1), 5 min after initiation (stacked spectrum number 2), 15 min after initiation (stacked spectrum number 3), and 30 min after initiation (stacked spectrum number 4). and B) related concentration C(M) over time t(min) graph. The graph is reported as follows: P(V)-P(V) green line, TMP red

line, AMP yellow line, phosphonate blue light blue line. A single replicate of the experiment was conducted. C) chemical structures legenda.

The data reported in *Figure 38* showed the highest observed level of conversion and the lowest level of by-products occurred after a contact time of less than 100 s.

Therefore, based on these findings, I concluded that the coupling took place over a timeframe of only seconds. While the detailed natures of P(V) phosphoramidate by-products and reverted AMP were not confirmed by isolation, ^{31}P NMR studies using mixtures of reagents gave strong evidence to support our hypotheses. I questioned at this point if the solvent itself was in some regards responsible for the P(III)-P(V) intermediate (**8**) instability, and for the reversion reaction to AMP. This hypothesis arose from observations gathered during our experiments towards ADP and ATP syntheses, discussed in this section and sections 4.2.1 and 4.2.2.1. From the analyses conducted on ATP synthesis (see section 4.2.1) I had already considered the possibility of DMSO oxidising the P(III)-P(V) coupling reaction intermediate (**8**). In addition, during the oxidation step for the synthesis of ADP in DMSO, a strongly exothermic reaction was observed upon the addition of *m*CPBA, with a concomitant high percentage of by-products. The exothermicity suggested that *m*CPBA and DMSO reacted, thus, to test this hypothesis, *m*CPBA was added to a coupling ADP solution mixture in DMF and no heating occurred (data not shown).

At this point, I began comparative studies in DMSO and DMF of the “one-pot three-step” synthesis of ADP, with a view to moving away from the use of DMSO because of the potential problems outlined in the foregoing paragraphs.

4.2.2.2.2 ^{31}P NMR spectroscopic analyses of the coupling and oxidation steps of "one-pot three-step" syntheses of ADP performed in DMSO and DMF

The ^{31}P NMR time-course data of coupling and oxidation steps of the one-pot three-step ADP synthesis in DMSO revealed instability problems of the P(III)-P(V) anhydride intermediate (**8**), causing reversion to AMP starting material. As discussed in 4.2.2.1, a solvent screening was conducted to identify a method that was congenial in terms of solubility for the application in flow, and both DMSO and DMF dissolved all materials. The initial choice to explore reactions using DMSO as the solvent relied on the cost of DMSO-d6 compared to DMF-d7. Due to the results discussed in section 4.2.2.1, I questioned this choice, performing comparative DMF and DMSO reaction experiments using D_2O lock tube to analyse them on a Bruker Neo-400 spectrometer.

At first, both coupling reactions steps were performed and analysed every 10, 30, 60 min and after 1 day to compare the stability of the P(III)-P(V) anhydride (**8**). As highlighted in *Figure 39*, despite the slightly different shifts of the peaks due the nature of the solvent, some differences were already clear after 10 min of coupling.

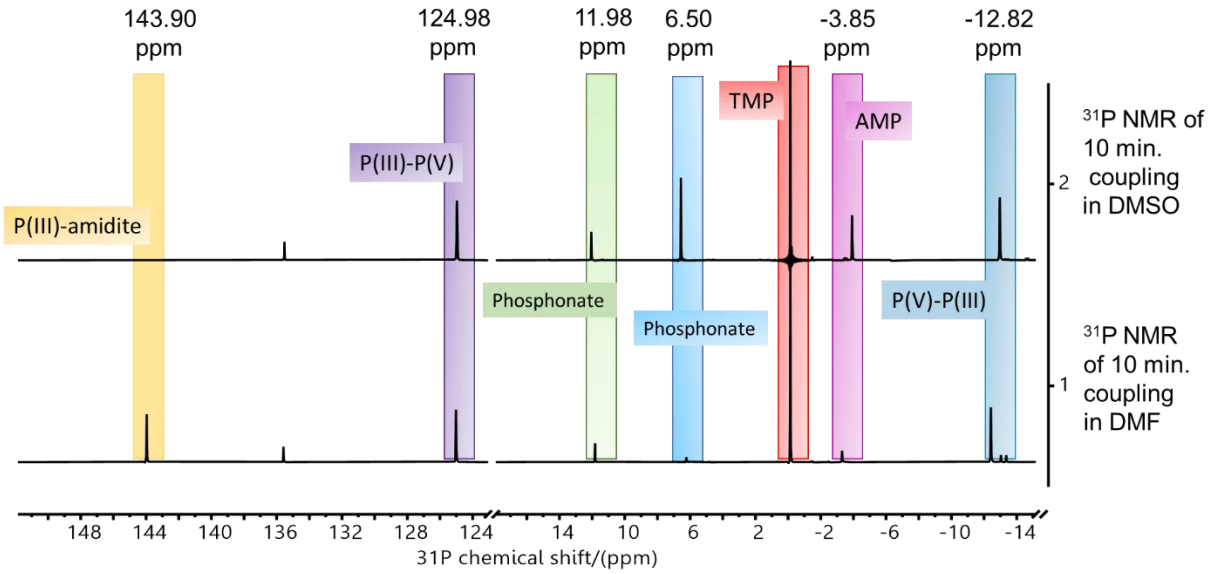

Figure 39: ^{31}P NMR spectrum of AMP-amidite coupling reaction (10 min) in DMSO compared to coupling reaction (10 min) in DMF. The TMP peak (red) was normalized to 0.19 M and the other peaks are given as a relative to TMP.

In both the reaction mixtures, the P(III)-P(V) anhydride (**8**) signals were evident at ~125.18 and ~ –12.85 ppm (highlighted inpurpe and blue). In the DMF reaction, the signal at ~ 146.18

ppm (highlighted in orange), corresponding to phosphitylating reagent was still intense, in the DMSO reaction the reagent signal was not detected. Simultaneously, the by-product signal at ~ 6.52 ppm (highlighted in light blue), was barely detected in the DMF reaction compared to an intense signal DMSO. The peak at at ~ 135 ppm, that appeared in almost all the spectra is a not-isolated by-product from the synthesis of the phosphitylating reagent (**2**). Thus, *Figure 39* shows clear evidence that although the reaction of DMF is a slower compared to the one performed in DMSO, the DMF reaction appeared cleaner.

Furthermore, the stability of the P(III)-P(V) phosphate anhydride (**8**) was subsequently tested by acquiring ^{31}P spectra of the crude reaction mixtures after 1 day of coupling (*Figure 40*).

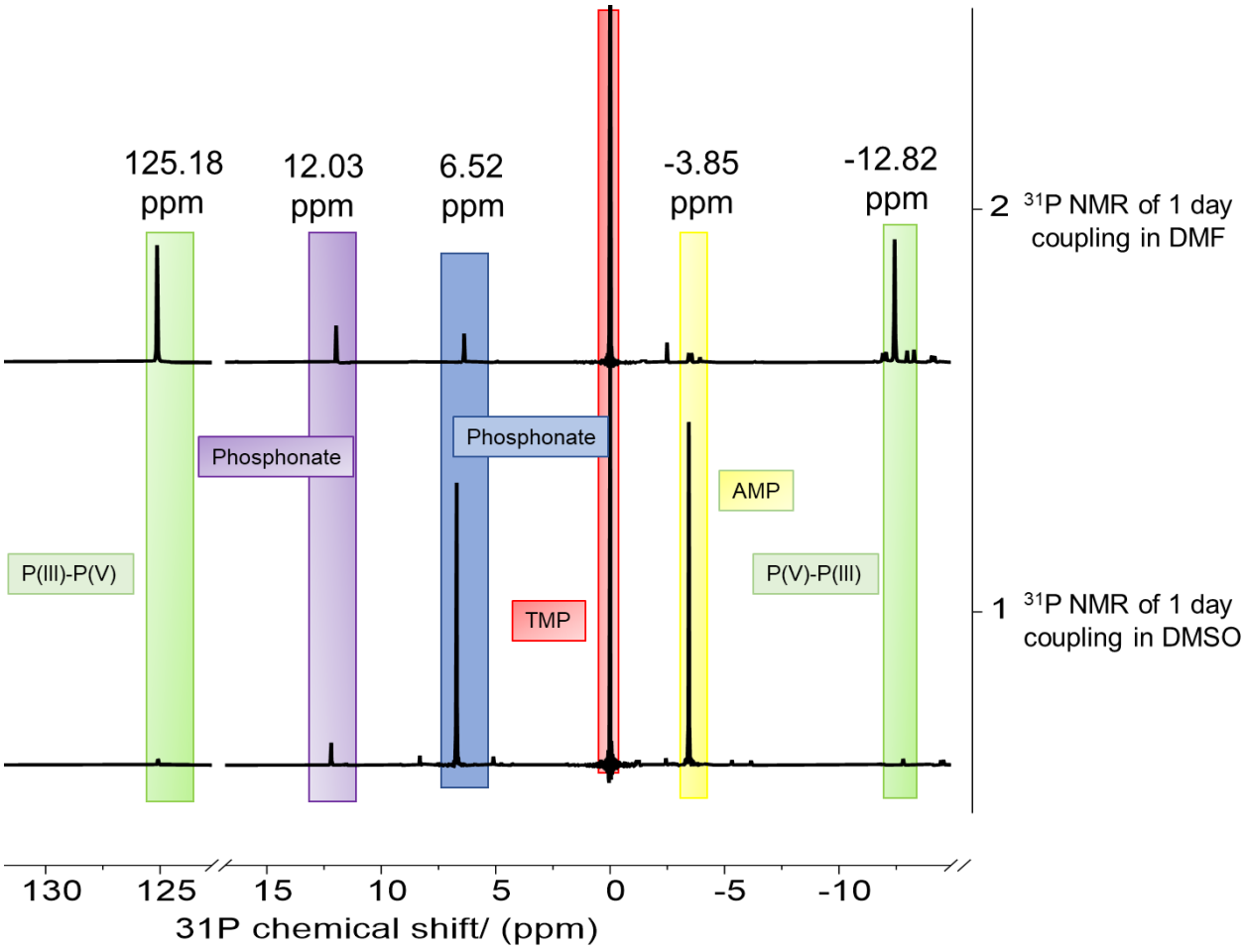

Figure 40: Highlight of exemplar ^{31}P NMR spectra of AMP-amidite coupling reactions after (1) 1 day in DMSO compared to (2) coupling reaction after 1 day in DMF.

As shown in *Figure 40*, the ^{31}P signals corresponding to the P(III)-P(V) anhydride (**8**) peaks (~125.18 and ~ –12.85 ppm) were not detected in the DMSO reaction, whereas in DMF these

signals were still intense (highlighted in green). In DMF, the signals corresponding to the P-H phosphonates by-product at ~ 6.52 ppm (highlighted in blue) and to AMP at ~ –3.85ppm (highlighted in yellow), were barely detectable, but in DMSO they were even more intense.

The ^{31}P NMR spectrum after 1 day of coupling in DMF appeared more complex compared to after 10 min of coupling, however, the P(III)-P(V) anhydride (**8**) signals did not change significantly, suggesting the intermediate to be reasonably stable over the 1-day time span. After oxidation of the DMSO- and DMF-based reaction mixtures with *t*BuOOH 5 M in decane, the mixture in DMF gave higher levels of conversion to the desired P(V)-P(V) intermediate (**9**), in part because of the improved performance in the coupling step.

In summary, based on comparisons of ^{31}P NMR results of the "one-pot three-step" reaction in DMSO versus DMF, the DMF method for the synthesis of ADP appeared to be more effective. Specifically, the stability of the P(III)-P(V) anhydride intermediate (**8**) in DMF as compared to DMSO, appeared to be particularly significant, thus subsequent reactions were performed in DMF. Furthermore, the (unconfirmed) observation of P(III) reagent (**2**) being oxidised to P(V), coupled with sample heating upon addition of larger quantities of oxidant for rapid reaction quenching, re-affirm our preference for DMF over DMSO.

4.2.2.2.3 ^{31}P NMR spectroscopy analysis of the coupling and oxidation steps of the "one-pot three-step" synthesis of ADP in DMF

With a clear decision to use the DMF-based "one-pot three-step" method for the synthesis of ADP in our hands, I focussed on the optimization of an NMR-based kinetic method. I needed to determine NMR parameters to obtain quantitative data with high levels of sensitivity. Preliminary studies to determine T_1 values were performed on each reaction component, in addition to an Ernst angle study, discussed in section 4.2.2.2.3.1, to ensure a qualitatively satisfactory analysis method.[180-187]

4.2.2.2.3.1 ^{31}P NMR spectroscopy T_1 relaxation times studies

As already mentioned (see section 4.2.2.2.1), the important parameters to be considered for setting up a time-course NMR experiment are: the number of scans (nt), the relaxation delay (d1), the acquisition time (at) and the preacquisition delay (pad) before the acquisition of a new time point.

However, to obtain quantitative NMR information, it is necessary to set the repetition time (d1 + at + pad) to be > 5 × longest T_1. T_1 is the spin-lattice relaxation constant, which quantifies how quickly the net magnetization of a nucleus returns to equilibrium. To ensure quantitative determination of integral values for each species, knowledge of T_1 values is essential. Each nucleus in a molecule has a different T_1 value.[182]

One of our initial aims was to develop quantitative kinetic methods to inform flow chemistry experiments, thus T_1 studies of single reaction components were conducted on a 500 MHz spectrometer. A T_1 inversion recovery pulse sequence [180, 182, 188 189] was used that consists of an inversion pulse followed by a variable delay (τ) and a 90° reading pulse (*Figure 41*).

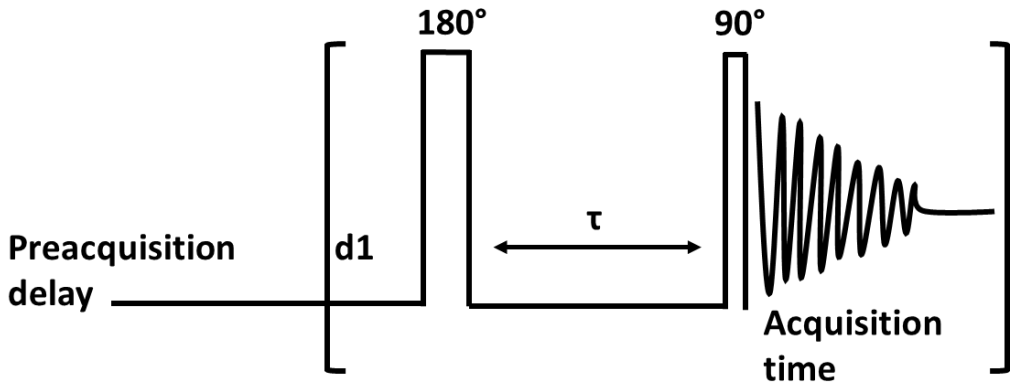

Figure 41: T_1 inversion recovery pulse sequence.

Since the reaction mixture composition may change the T_1 constants, instead of running NMR samples of individual components, I opted for an oxidation reaction mixture containing substrate, reagents, and intermediates (see *Figure 42*).

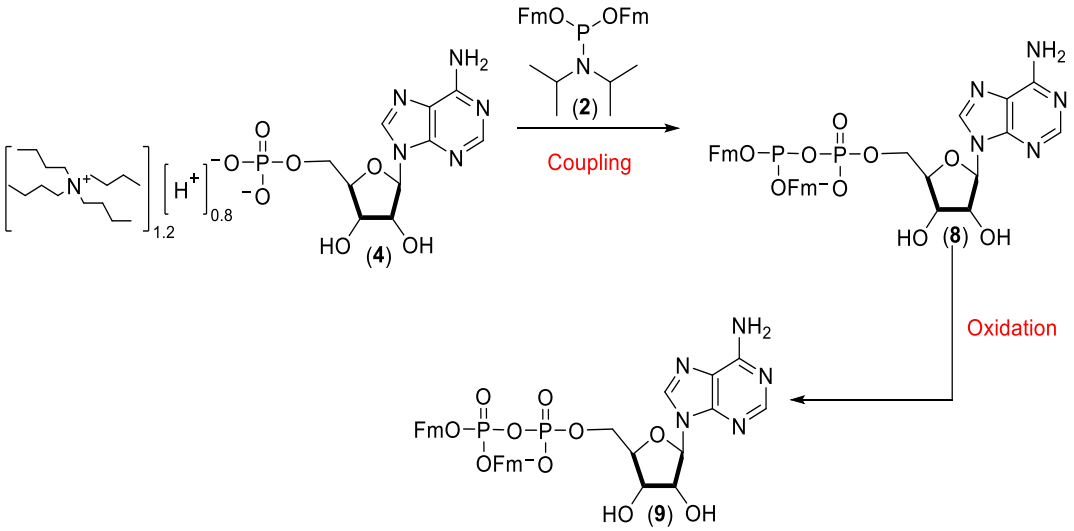

Figure 42: The main species (AMP (**4**), amidite (**2**), P(V)-P(V) anhydride (**9**) and P(III)-P(V) anhydride (**8**) analysed during the inversion pulse experiment. These are substrates and products respectively of the first two reaction steps, coupling and oxidation step, of the "one-pot three-step synthesis" of ADP [1, 145].

The sample was prepared by dissolving 5'-AMP $TBA_{1.2}H_{0.8}$ (**4**) (0.088 g, 0.14 mmol) in 0.375 mL of DMF followed by 5-(ethylthio)-1*H*-tetrazole (2 equiv.). *Bis*-(fluorenylmethyl)-diisopropylamine phosphoramidite (**2**) (mass adjusted based on purity level measured by ^{31}P

NMR spectroscopy, 0.18 mmol, 1.3 equiv.) dissolved in DMF (0.375 mL) was then added to the nucleotide solution. The coupling reaction mixture was shaken at room temperature and after 10 min, *t*BuOOH 5 M in decane (36 µL, 0.18 mmol, 1.3 equiv.) was added to the solution. The oxidised mixture was then transferred to an NMR tube with D_2O lock tube and trimethyl phosphate as standard (0.00 ppm) (20 mg, 17 µl, 0.14 mmol, equiv.). A ^{31}P NMR experiment, with H-decoupling only during the acquisition time, was then set up at 25 °C on a 500 MHz spectrometer. The T_1 values of the phosphorus nuclei were measured by recording the inversion recovery ^{31}P NMR spectra in a series of experiments involving different d1 ranging from 100 ms to 20 s.

The ^{31}P signals of the main species were integrated and their intensities were plotted against the delay time. The results gave the T_1 relaxation times of each component, as reported in *Table 6*.

Peak	**^{31}P ppm**	**T_1 (s)**
P(III) reagent (**2**)	146.11	0.88 ± 0.01
trimethyl phosphate	0.00	8.25 ± 0/07
AMP $(TBA)_{1.2}H_{0.8}$ (**4**)	–2.25	0.69 ± 0.02
P(V)-P(V) anhydride (**9**)	–12.50	0.40 ± 0.01
P(V)-P(V) anhydride (**9**)	–13.01	0.44 ± 0.02
P(III)-P(V) anhydride (**8**)	–12.82	0.53 ± 0.01
P(III)-P(V) anhydride (**8**)	125.18	0.54 ± 0.01

Table 6: T_1 values for the species present in the reaction depicted in *Figure 42*. Data obtained using a 500 MHz spectrometer at 25 °C.

The longest T_1 belonged to the standard compound trimethyl phosphate (8.25 s), as shown in Table 6. To obtain quantitative data, the NMR sample should be in the magnet for at least 5 times the longest T_1 value to allow all nuclei to polarize before starting to acquire data—in this case, 5 × 8.25 s, thus at least d1= 41s.

Subsequently, the minimum number of scans necessary to produce an adequate signal-to-noise ratio was determined and, when using 0.14 mmol 5'-AMP $TBA_{1.2}H_{0.8}$ (**4**) in 0.750 mL of DMF, a single scan proved to be sufficient.

In our first time-course experiment, I used a repetition time of d1=51 s, and a preacquisition delay (pad) of 10 s between blocks of single-scan (nt=1) acquisitions. Unfortunately, these parameters proved to be inadequate to monitor the relatively fast reaction, delivering too few time points at early reaction times to allow assessment of curvature. In order to gain useful 'early' time points, I had to take practical decisions:

1. I decided to use a repetition time value based on $5T_1$ of the *analyte* with the longest T_1 value. This was the P(III) amidite reagent with $T_1 = 0.88 \pm 0.01$ s, thus ~ 5 s;
2. To obtain quantitative results, I performed time course runs first using d1 based on $5T_1$ belonging to the standard compound trimethyl phosphate (i.e. 5 × 8.25 s) and then $5T_1$ belonging to P(III) reagent (i.e. 5 × 0.88 ± 0.01 s) to calculate a correction factor. The correction factor was found, on average, to be 1.33. This was then used to quantitatively correct for the poorer relaxation rate of the trimethylphosphate standard.;
3. A preacquisition delay (pad) of 10 s was used between blocks of acquisitions. Proton decoupling was only used during acquisitions to avoid problem with nOe variations;
4. These parameters led to a total repetition time 15 s (3.5 s relaxation delay (d1) + 1.5 s acquisition time (at) + 10 preacquisition delay (pad) = 15 s in total), which is > $5T_1$(P(III) reagent) of 5 s. This compromise ensured all analyte signals were fully relaxed, and I applied the correction factor to the signal for the trimethylphosphate standard.

The Ernst angle [186, 187, 189] is the tip angle that leads to maximal signal to noise (S/N) of a particular spin for a given repetition time.[186] Thus, based on using relaxation delay, d1= 3.5 s

+ acquisition time, at= 1.5 s acquisition time, and the known T_1 (0.88 ± 0.01 s) for the P(III) reagent, the Ernst angle,[186, 187, 189] was determined for the T_1 parameter adopted. Experimental data were acquired with pulse angles of 63°, 67.7° 75.6°, 83° and 86°. Subsequently, S/N values were compared with data acquired with a 90° pulse angle, and the signal-to-noise ratio at a 90° pulse angle appeared to be sufficient for us to be confident that all species with significant populations were being detected adequately.

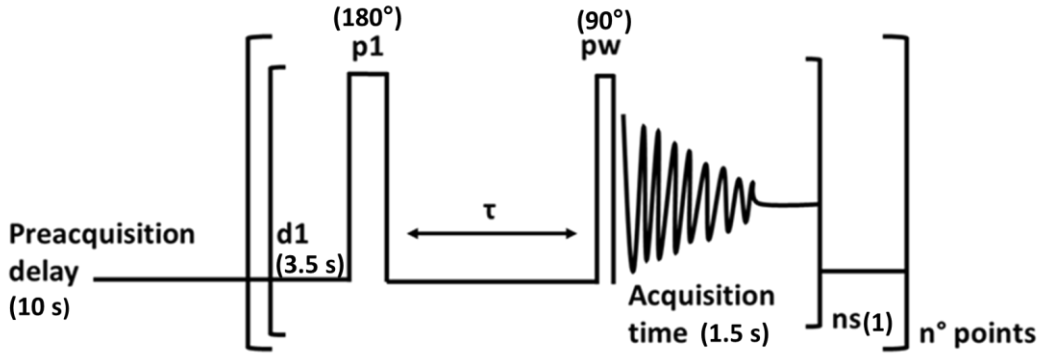

Figure 43: The pulse sequence developed for acquisition of 31P NMR time-course data.

With a quantitative experiment in place, time-course studies of the coupling reaction of AMP $(TBA)_{1.2}H_{0.8}$ (**4**) with amidite (**2**) and the oxidation reaction of the resulting P(III)-P(V) intermediate (**8**) were set up. In summary (*Figure 43*), the following parameters I employed: preacquisition delay, pad=10 s; relaxation delay, d1=3.5 s; pulse width one, p1=180°; pulse width, pw=90°; acquisition time, at=1.5 s and number of scans, nt=1, over a period of 100 min.

4.2.2.2.3.2 Analyses of ^{31}P NMR kinetic studies of the coupling and oxidation steps of the "one-pot three-step" synthesis of ADP in DMF

In this section, I report our attempts towards ^{31}P NMR kinetic studies for the coupling and oxidation steps for the synthesis of ADP from AMP in DMF-h7 and DMF-d7, using the NMR acquisition parameters discussed in the previous section. Ultimately, the NMR platform used for measurements proved to be too slow on the timescale of the reactions, however, the data collected gave us an appreciation of reaction timescales that were useful when translating to a continuous flow approach.

Preliminary, comparative time-course experiments were set up in DMF-d7 (*Figure 44* and *Figure 46*) and non-deuterated DMF with D_2O lock tube (*Figure 47* and *Figure 48*) to prove demonstrate the reliability of the D_2O lock tube strategy (see section 4.2.2.2.3.1). The samples for ^{31}P NMR analyses were prepared, (as mentioned in sections 4.2.2.2.3.1 and 6.4.1.1.1, 6.4.1.1.2), by dissolving 5'-AMP $TBA_{1.2}H_{0.8}$ (**4**) (0.088 g, 0.14 mmol) in 0.375 mL DMF-h7 or DMF-d7. 5-(ethylthio)-1*H*-tetrazole (2 equiv.) was added to each nucleotide solution followed by a solution of *bis*-(fluorenylmethyl)-diisopropylamine phosphoramidite (**2**) (0.18 mmol, 1.3 equiv.) dissolved in 0.375 mL DMF-h7 or DMF-d7. Each reaction mixture was then transferred to an NMR tube (with D_2O lock tube in case of DMF-d7) and 1 equiv. of trimethyl phosphate was added as internal standard. ^{31}P spectra were recorded at 25 °C with a single scan (nt=1) and a relaxation delay of d1=3.5 s over a period of 100 min. At the end of the run, 1.3 equiv. of *t*BuOOH 5 M in decane was added to the solution and a new time course experiment was acquired using the same NMR parameters to observe the oxidation process.

Figure 44 and *Figure 46* summarise the ^{31}P NMR spectra of the coupling reaction and the oxidation time-courses in DMF-d7. As shown in the related concentration graph (*Figure 44*), the coupling reaction between AMP (~ –3.68 ppm) and P(III) reagent (**2**) (~148.95 ppm) to form the P(III)-P(V) anhydride intermediate (**8**) (signals ~ 125.18 ppm and –12.82 ppm) is bi-phasic, with the second phase commencing after ~1500 s, with essentially complete conversion of AMP to the P(III)-P(V) anhydride (**8**) after ~5500 s.

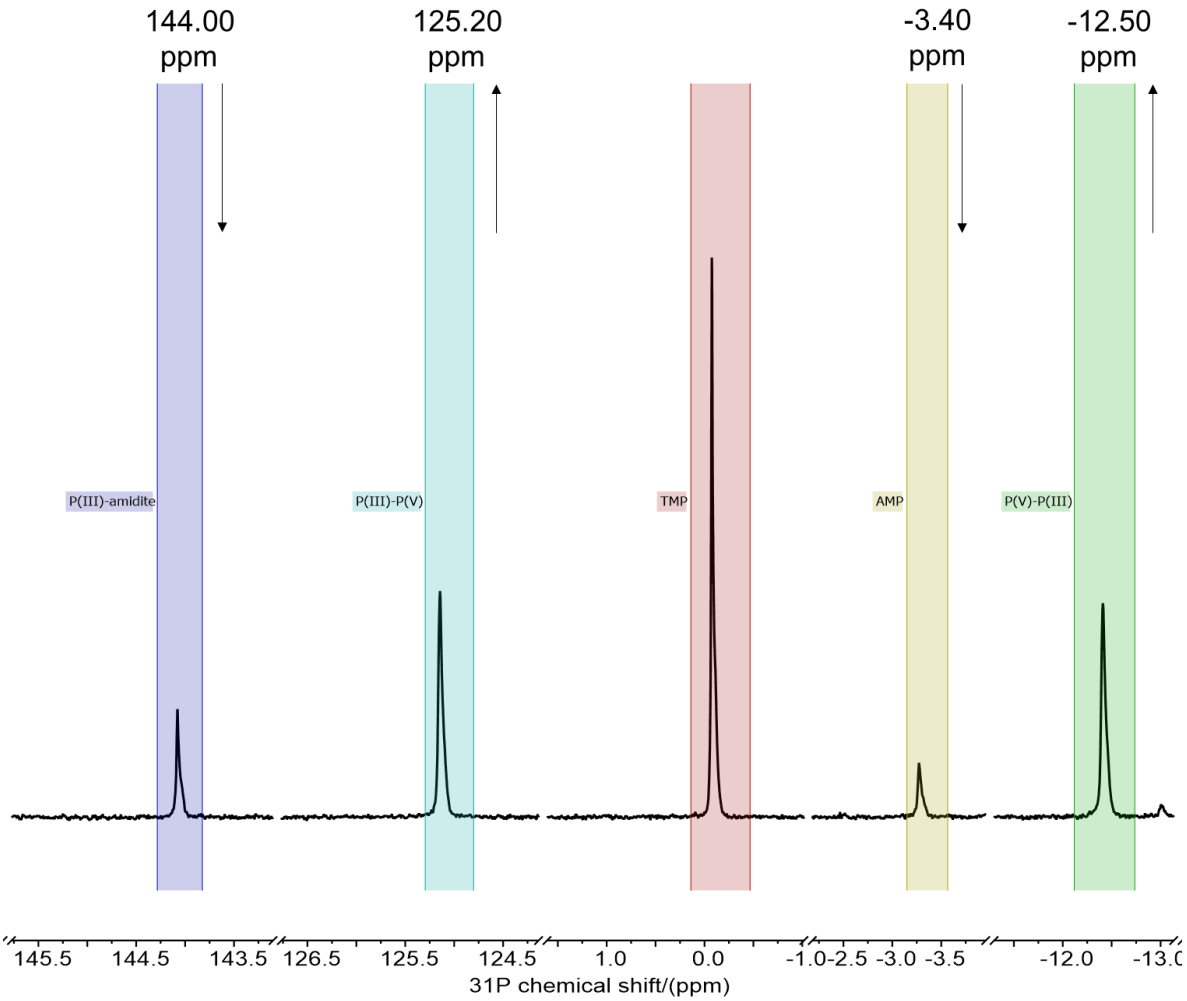

A)

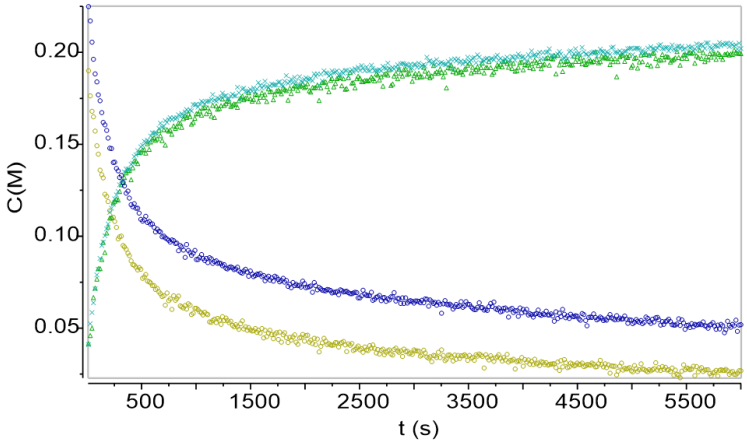

B)

Chemical structures corrisponding to the peak label of signals spectrum:

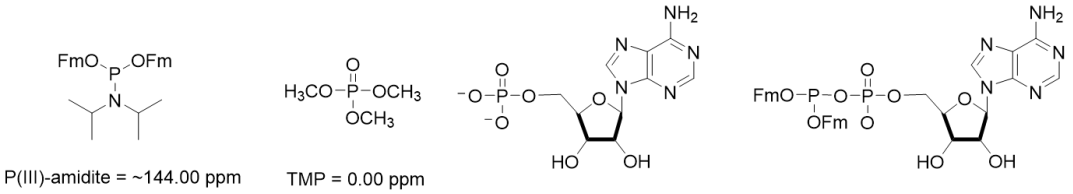

P(III)-amidite = ~144.00 ppm

TMP = 0.00 ppm

AMP = ~-3.40 ppm

P(III)-P(V)=~125.20 ppm
P(V)-P(III)=~12.50 ppm

C)

Figure 44: A) Highlights of an exemplar ^{31}P NMR spectrum of AMP-amidite coupling reaction time-course in DMF-d7 with B) related concentration C(M) over time t(s) graph. Data series are as follows: AMP (yellow hollow circles), P(V)-P(III) (green triangles) , P(III)-P(V) (light triangles blue crosses), P(V)-amidite. C) chemical structures.

As previously mentioned in section 4.2.2.2.3, the phosphoramidite activation is the rate-determining step in the first coupling (see Figure 45), thus I did not see evidence of P(III)-tetrazolide intermediate (**19**) at ~126 ppm (see *Figure 36*) in the time-course.

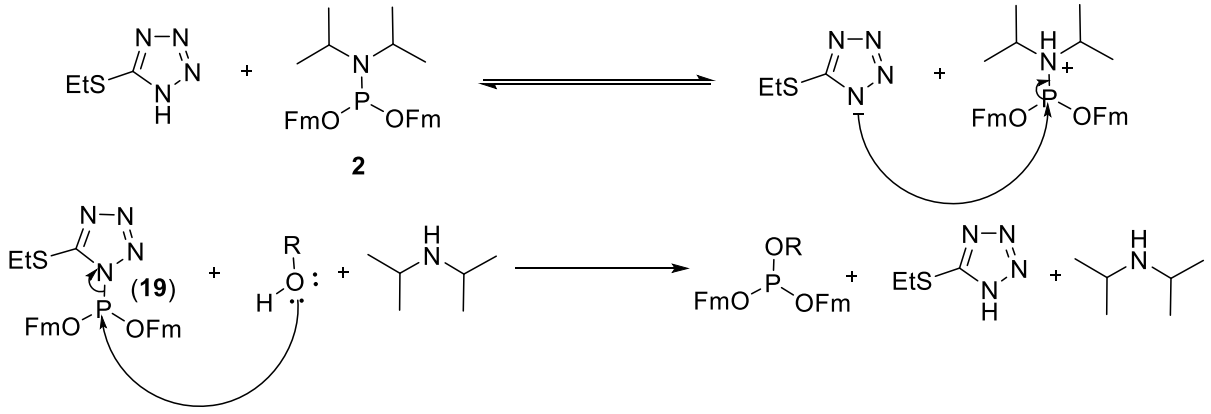

Figure 45: Mechanism of activation and coupling of a phosphoramidite (**2**) with 5-(ethylthio)-1*H*-tetrazole as an activator.

The P(III) tetrazolide peak (**19**) (at ~126 ppm, *Figure 36*)) was not observed during our time course studies in DMF. In the recent report by Fiona J. Laraman *et al.*[179] activation kinetics of traditional and modified deoxyribonucleoside phosphoramidites was monitored by ^{1}H NMR with the support of a stopped flow platform. The data obtained showed that the activation took place over the course of tens of seconds. It was also demonstrated that doubling the concentration of activator in comparison to phosphoramidite led to an equilibrium shift towards the active form, as I observed in DMSO (see section 4.2.2.2.2), owing to an enhanced forward rate of equilibration. Our observation, in concert with the work of Laraman *et al.*, demonstrated that sample preparation and data acquisition in a standard spectrometer was too slow to allow full kinetic analysis. The time between mixing solutions and acquisition of initial data was several minutes in our system, meaning that the coupling process was significantly progressed towards the region plateau before I even began observations in the spectrometer.

A new coupling solution was then prepared (see sections 4.2.2.2.3.1 and 6.4.1.1.1, 6.4.1.1.2) to be used to monitor the oxidation process. The coupling reaction mixture was shaken at room temperature over a period of 10 min and tBuOOH 5 M in decane (36 μL, 0.18 mmol, 1.3 equiv.) was then added. The oxidation mixture was then transferred to an NMR tube with 1 equiv. trimethyl phosphate as internal standard. ^{31}P spectra were recorded at 25 °C with a single scan (nt=1) and a relaxation delay of d1=3.5 s over a period of 100 min.

The coupling step was not finished after 10 min, in the reported NMR spectrum (*Figure 46*), thus, AMP (signal ~ –3.68 ppm, decreasing), P(III) reagent (**2**) (signal ~ –145.89 ppm, decreasing) and its oxidised form, P(V)-amidite (signal ~ 5.06 ppm) are visible. Critically, in respect of the oxidation process, the concentration graph shows complete conversion of the P(III)-P(V) intermediate (**8**) (signals ~ 125.18 ppm and –12.82 ppm) to the P(V)-P(V) protected intermediate (**9**) (signal ~ –14.98 ppm), with a plateau after 500 s (as shown in *Figure 46*).

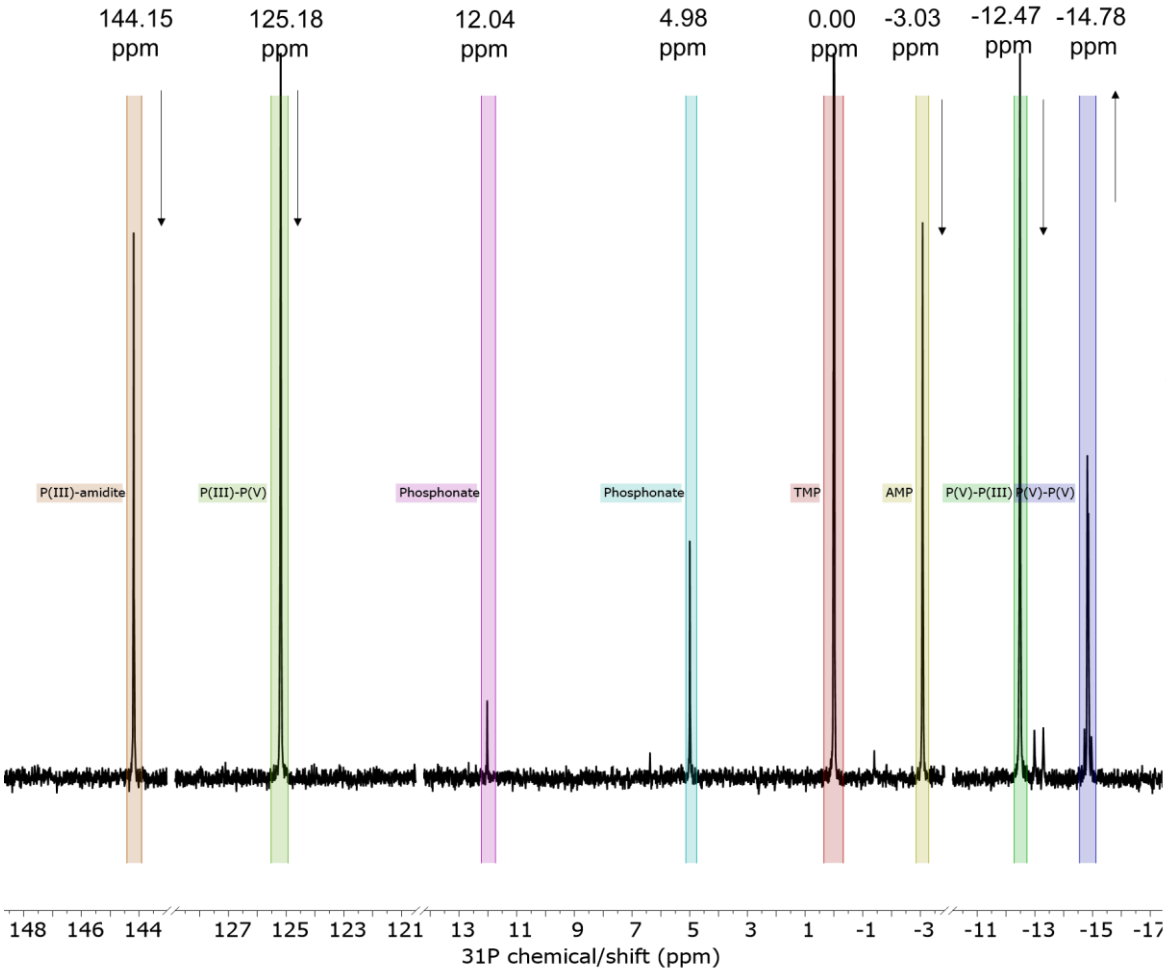

A)

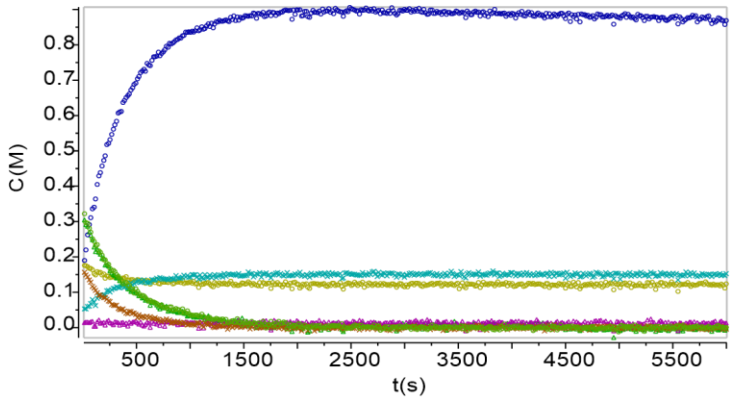

B)

Chemical structures corresponding to the peak label of signals spectrum:

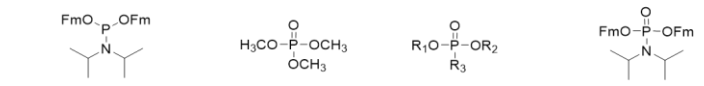

P(III)-amidite = ~144.15 ppm

TMP = 0.00 ppm

Phosphonate = ~12.00 and ~6.50 ppm

P(V)-amidite= ~4.98 ppm

C)

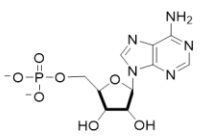

AMP =~ -3.02 ppm

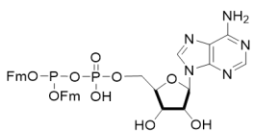

P(III)-P(V) = ~125.18 ppm
P(V)-P(III) = ~-12.47 ppm

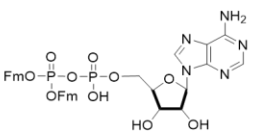

P(V)-P(V) = ~-14.78 ppm

Figure 46 :A) Highlight of an exemplar ^{31}P NMR spectrum of P(III)-P(V) intermediate (**8**) oxidation reaction time-course in DMF-d7 with B) related concentration C(M) over time t(s) graph. Data series are as follows: AMP (yellow hollow circles), P(V)-P(III) (green triangles), P(III)-P(V) (light green triangles), Phosphonate (magenta hollow triangles), Phosphonate (light blue crosses), P(V)-amidite (light green hollow circles), P(III)-amidite (orange crosses). C) chemical structures.

A new experiment was to monitor the coupling and oxidation steps for the ADP synthesis (**7**) in non-deuterated DMF, using a D_2O lock tube. Sample preparation was performed in a similar manner to the previous example (see sections 4.2.2.2.3.1 and 6.4.1.1.1, 6.4.1.1.2). ^{31}P spectra were recorded at 25 °C with a single scan (nt=1) and a relaxation delay of d1=3.5 s over a period of 100 min (*Figure 47*). At the end of the run, 1.3 equiv. of *t*BuOOH 5 M in decane was added to the solution and a new time course experiment was acquired using the same setting NMR parameters to monitor the oxidation process (*Figure 48*).

In the coupling step (see *Figure 47*), the formation of P(III)-P(V) intermediate (**8**) with signals at ~ 125.18 ppm and –12.82 ppm could be observed, with concomitant decreases in the signals for AMP ~ –3.68 ppm and P(III) reagent (**2**) ~ 148.95 ppm. The coupling reaction reached a plateau after 1000 s. Incomplete conversion of AMP to the P(III)-P(V) anhydride (**8**) was observed, with the supply of P(III) reagent (**2**) seemingly being exhausted. This observation contributed to us concluding that our abilities to accurately prepare solutions with defined concentrations of reaction components were compromised.

Each sample in the initial series of NMR experiments was prepared by weighing reagents and substrate. In particular, the weighing of *bis*-(fluorenylmethyl)-diisopropylamine phosphoramidite (**2**) was complicated due of its sticky consistency. As discussed in section 4.2.2.3.2.1, the preparation of stock solutions that could be accurately determined, became essential. Furthermore, quantitative correction for the amidite reagent's purity needed to be put in place and this purity level could also be subject to decreases through improper reagent storage. Together, these factors were the likely sources of inconsistency between intended reactant concentrations and those observed in the ^{31}P NMR spectra.

During the oxidation step, 'clean' formation of the P(V)-P(V) intermediate (**9**) with signals ~ –14.98 ppm with concomitant reduction in signals for P(III)-P(V) intermediate (**8**) ~ 125.18

ppm and – 12.82 ppm was observed, with the process reaching a plateau after 500 s (see *Figure 48*).

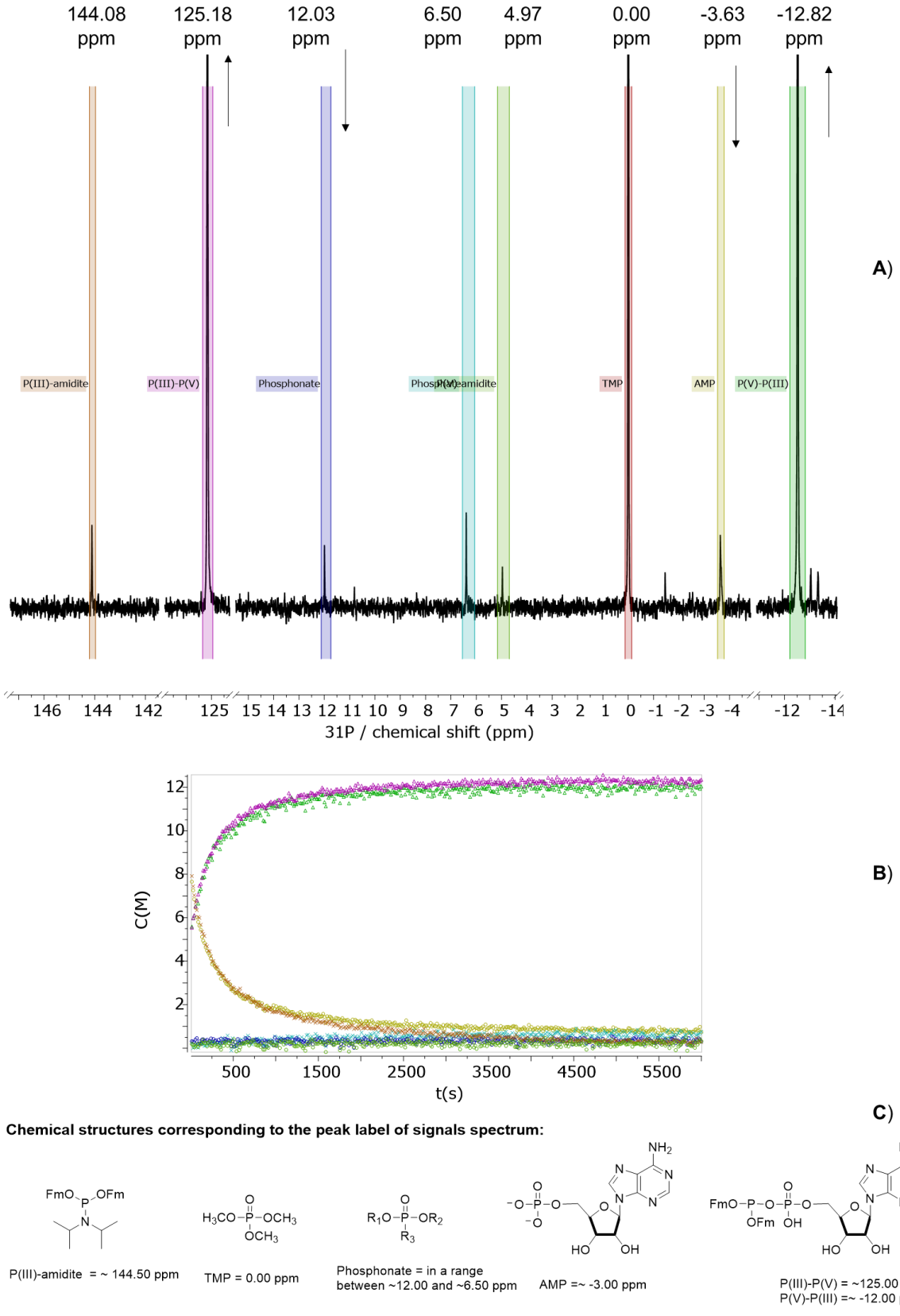

Figure 47: A) Highlights of an exemplar ^{31}P NMR spectrum of AMP-amidite coupling reaction time-course in DMF with D_2O lock tube with B) related concentration C(M) over time t(s) graph. Data series are as follows: AMP (yellow hollow circles), P(V)-P(III) (green triangles), P(III)-P(V) (magenta triangles), Phosphonate (purple hollow

triangles), Phosphonate (light blue crosses), P(V)-amidite (green hollow circles), P(III)-amidite (orange crosses).and C) chemical structures.

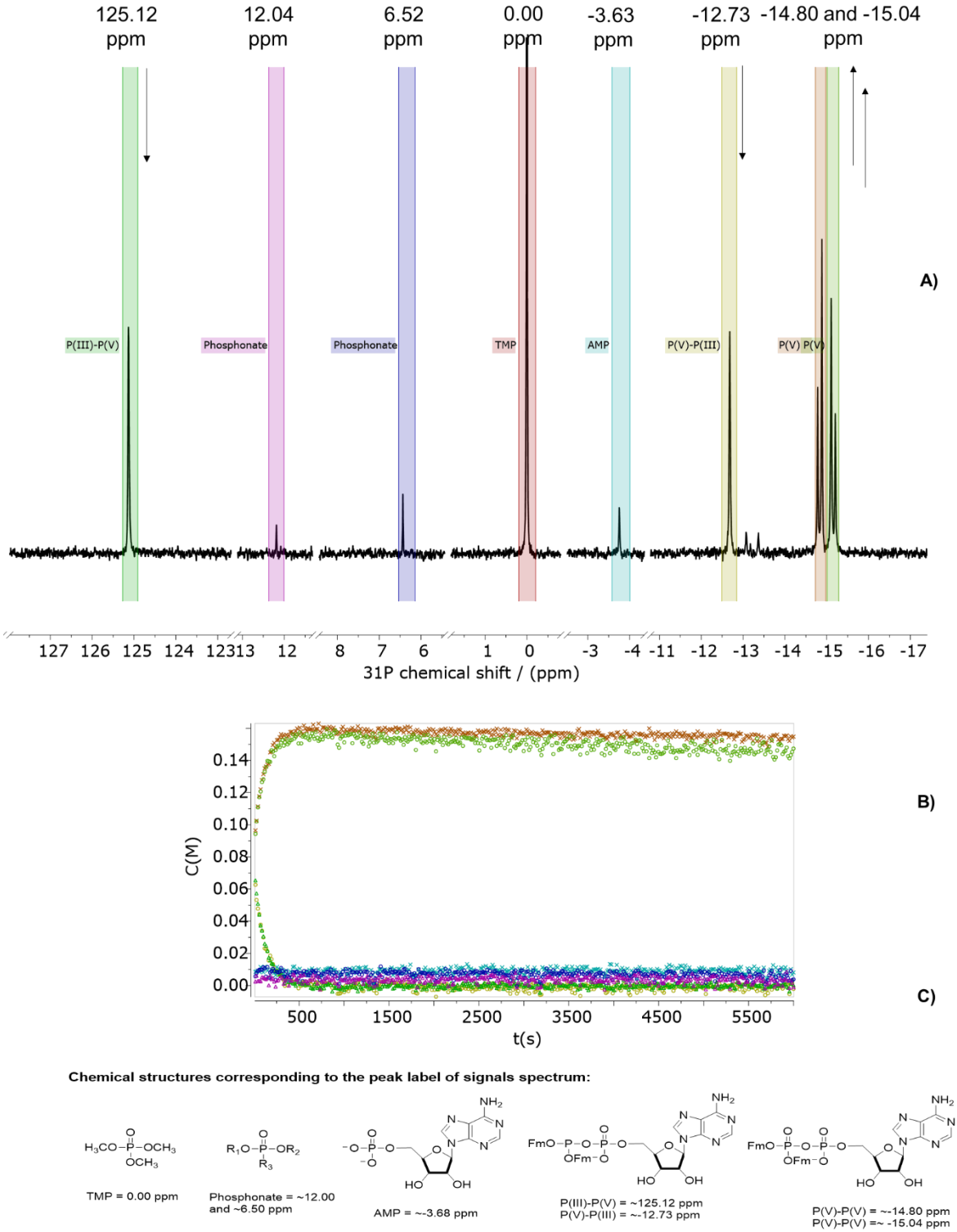

Figure 48: A) Highlights of an exemplar ^{31}P NMR spectrum of P(III)-P(V) intermediate (**8**) oxidation reaction time-course in DMF with D_2O lock tube with B) related concentration C(M) over time t(s) graph. Data series are as follows: AMP (light blue

crosses), P(V)-P(III) (green triangles), P(III)-P(V) (yellow hollow circles), Phosphonate (magenta triangles), Phosphonate (blue hollow circles), P(V)-P(V) (light green hollow circles), P(V)-P(V) (orange crosses).and C) chemical structures.

In summary, a specific ^{31}P NMR spectroscopy method to quantitatively analyse the coupling (step 1) and oxidation (step 2) processes for the synthesis of ADP has been developed.

The poor results obtained from the coupling reaction in DMSO, led us to conduct investigations on the nature of the by-products and highlighted the importance of T_1 and Ernst angle studies to obtain quantitative ^{31}P NMR integral values. The set of results obtained showed both the coupling and the oxidation processes were quite rapid. For practical reasons associated with sample preparation time, it was not possible to gain early time points on kinetic analyses using the conventional NMR spectrometer setup. With this finding in mind, I did not pursue quantitative kinetic analyses any further.

I also found that initial experiments performed by weighing relatively small masses of crude, sticky materials created inconsistent ^{31}P NMR results. Thus, although these experiments were not quantitative, they were qualitatively informative for the flow studies described in section 4.2.2.3.2.1. In addition, our initial NMR kinetic experiments were performed at similar concentrations to those applied by Jessen's group, however, I subsequently found that these concentrations were too high for applications in flow (see section 4.2.2.3.2.1

Although detailed kinetic studies proved impractical, the quantitative ^{31}P NMR methods I developed were a good starting point for a quantitative method for reagent and substrate stock solution preparations. In the future, the adoption of a stopped flow NMR platform could give reliable real-time results, avoiding the limitations of classical NMR.[190]

4.2.2.3 Translation of the "one-pot three-step" synthesis of ADP to a semi-continuous flow system

The results reported in section 4.2.2.1 were the starting point for translating the batch method to a continuous flow system. Our initial strategy was to perform the coupling of the amidite reagent (**2**) to AMP in flow, and then, after reaching the steady state reaction equilibrium, quench the reaction mixture by delivering the flow into an excess of oxidant. Initially, *t*BuOOH 70% in H_2O was adopted as the oxidant because of supply problems with *t*BuOOH 5 M in decane. Thereafter, deprotection and crude product isolation were performed in batch by the addition of piperidine or other amine base, and precipitation of the desired product by addition of Et_2O (*Figure 49*).

At the outset, I aimed to optimize the yield of the flow-based coupling reaction and then convert the second oxidation step into a flow-based process, with the resulting reaction mixture being delivered into a piperidine solution in DMF to effect deprotection. In the final analysis, I did not convert the oxidation step into a flow process because a batch-based 'quench' into excess oxidant proved effective and could be easily scaled.

The "one-pot three-step" synthesis of ADP was initially performed using a 0.27 mL chip flow reactor, with freshly made solutions of reagents (*Figure 49*), and this will be discussed in section 4.2.2.3.1.

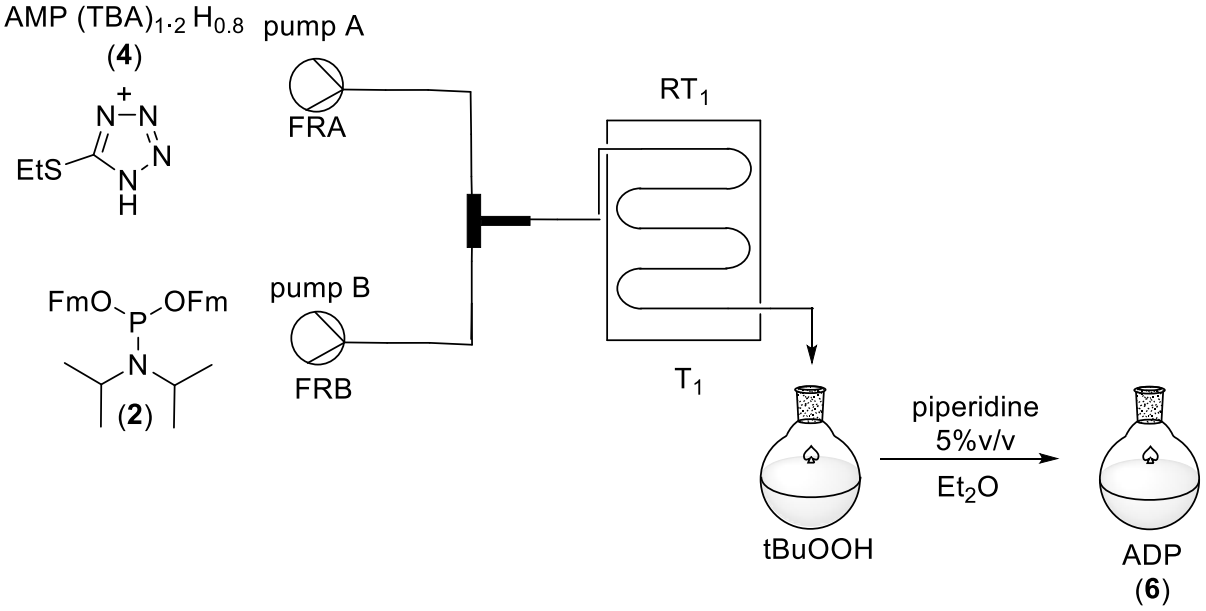

Figure 49: Overarching approach towards the synthesis of ADP under Flow Conditions

This method, however, although delivering promising results, gave inconsistent outcomes. Therefore, I subsequently developed a workflow to deliver a reliable method (see section 4.2.2.3.2.1) and then translated it to a larger coil reactor (2.5 mL), see section 4.2.2.3.2. Experiments exploring variation of reaction flow rates, concentrations, and scale, to optimize the flow process using a 2.5 mL coil reactor will be discussed in section 4.2.2.3.2.2. Ultimately, the results obtained for the flow synthesis of ADP encouraged us to apply the approach towards the synthesis of UDP and CDP, and the results with these systems are discussed in section 4.2.2.4.

4.2.2.3.1 Translation of the "one-pot three-step" synthesis of ADP (7) to a 0.27 mL chip flow reactor

Synthetic studies were performed using a *Uniqsis* FlowSyn system equipped with two SF-10 peristaltic pumps, T-mixer connections, and 0.27 mL chip reactor. A freshly made solution of AMP $(TBA)_{1.2}H_{0.8}$ (**4**) in DMF, containing 5-(ethylthio)-1*H*-tetrazole, was pumped into the reactor with a 40 μl/min flowrate, where it was reacted with *bis*-(fluorenylmethyl)-diisopropylamine phosphoramidite (**2**) dissolved in DMF, pumped into the reactor at the same flowrate (40 μl/min). After establishing stable flow (approximately 2 coil volumes), the reaction mixture was then quenched into 5 equiv. of *t*BuOOH 70% in H_2O and deprotected with 5% v/v piperidine in DMF followed by precipitation with Et_2O. With a fixed residence time of ~ 7 min. and a chip reactor temperature of 25 °C, different reagent concentrations were investigated, as summarized in *Table 7*.

Entry	Activator (equiv.)[a]	Amidite (2) (equiv.)[a]	Consumption of AMP before deprotection (%)[b]	Consumption of AMP after deprotection (%)[b]
1	1.3	1.3	88	94
2	2	1.3	82	90
3	2	2	clog	clog

Legend: a equiv.: equivalents. b % of AMP consumed in the rection mixture by ^{31}P NMR. AMP consumption: $([AMP]_0–[AMP]_{obs})/[AMP]0$, where [AMP]obs is the concentration before or after deprotection step and $[AMP]_0$ is total AMP concentration at the start of the process.

Table 7: Parameters for initial attempts towards the synthesis of ADP using a 0.27 mL chip.

Our first attempt (see *Table 7*, entry 1) was performed using AMP $(TBA)_{1.2}$ $H_{0.8}$ (**4**) solution with a concentration of ~1.8 mmol·mL^{-1} with 1.3 equiv. of activator and a ~2.3 mmol·mL^{-1} solution of amidite (**2**) (1.3 equiv.). Reached the steady state equilibrium, the P(III)-P(V) anhydride mixture was then quenched into 5 equiv. of *t*BuOOH 70% in H_2O to form the Fm-protected P(V)-P(V) anhydride (**9**) and the product mixture was analysed by ^{31}P NMR. On analysis of the quenched materials, I found there was 12% AMP. Subsequently, the Fm-

protected P(V)-P(V) anhydride (**9**) was reacted with 5% v/v piperidine in DMF followed by precipitation with Et_2O. The crude material was then analysed by ^{31}P NMR spectroscopy. The results showed an increase in AMP level to 18%. I hypothesised that the reaction was incomplete in the coupling step (step 1) and that the instability of the intermediate anhydrides had caused their hydrolysis and therefore reformation of AMP, either at the oxidation step (step 2) or at the deprotection step (step 3). Therefore, to increase the rates of desired reactions I increased the numbers of equivalents of the activator (see *Table 7*, entry 2) and both the activator and the amidite reagent **2** (see *Table 7*, entry 3). The use of higher numbers of equivalents of both activator and amidite reagent 2 caused clogging of the flow reactor. On the contrary, on the analysis of the reaction with 2 equiv. of activator after oxidation, I found only 4% AMP, and 10% AMP after deprotection, see Table 3, entry 3.

The kinetic data discussed in section 4.2.2.2.3.2, validated this set of results. The higher level of consumption of AMP in the presence of 2 equiv. of activator instead of 1.3 equiv. is probably due to the effect of the higher levels of activator on the pre-equilibrium formation of the active tetrazolide intermediate (**19**) (see *Figure 40*).

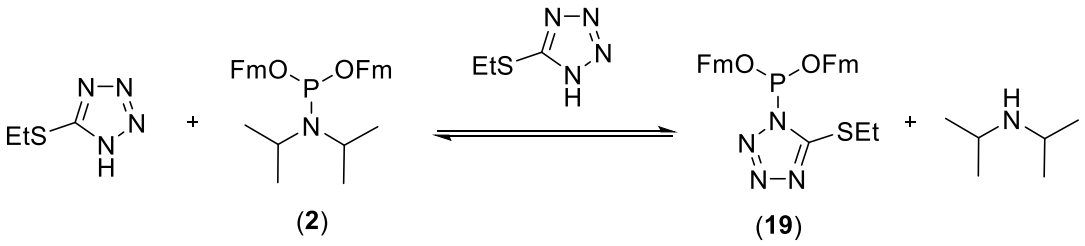

Figure 50: Proposed equilibrium formation of the tetrazolide intermediate (**19**) that acts as the active phosphitylating reagent.

The reactions described in the previous paragraph were carried out without accurate calibration of the pumps or titration of the amidite reagent (**2**) or AMP substrate (**4**), however, they allowed the development of sampling methods and the opportunity to become familiar with the flow system. Despite the imperfect execution, the results obtained were promising from the outset. After testing several flow rates, a careful calibration of the pumps was performed, and the next run delivered 98% consumption of AMP after the oxidation step. Despite the pump calibration studies, the reaction performance was still not robust and reliable. At this point, I sought to review the molar concentrations of the individual reagents,

especially of the phosphitylating reagent because it had not been purified by chromatography and I were already aware that its titre was only ~85-90%. This problem was resolved using the ^{31}P NMR assay methods described in sections 4.2.2.3.2 and 4.2.2.3.2.1.

4.2.2.3.2 Translation of the “one-pot three-step” synthesis of ADP into a 2.5 mL coil flow reactor from batch synthesis

In the following sections the “one-pot-three-step” synthesis of ADP (**6**) using a 2.5 mL coil flow will be discussed. First, our workflow method, which is based on the preparation of stock solutions analysed with our quantitative ^{31}P method, is discussed in detail. Then, as mentioned in section 4.2.2.3, further experiments exploring reaction flowrate, concentrations and scale up, to optimize the flow process for the “one-pot three-step” synthesis of ADP, are discussed in detail in section 4.2.2.3.2.1.

4.2.2.3.2.1 Workflow to deliver a reliable method for the "one-pot three-step" synthesis of ADP using semi-continuous flow chemistry

Our first step to create a robust method was to prepare reagent and substrate stock solutions at well-defined concentrations between 0.20 and 0.25 M.

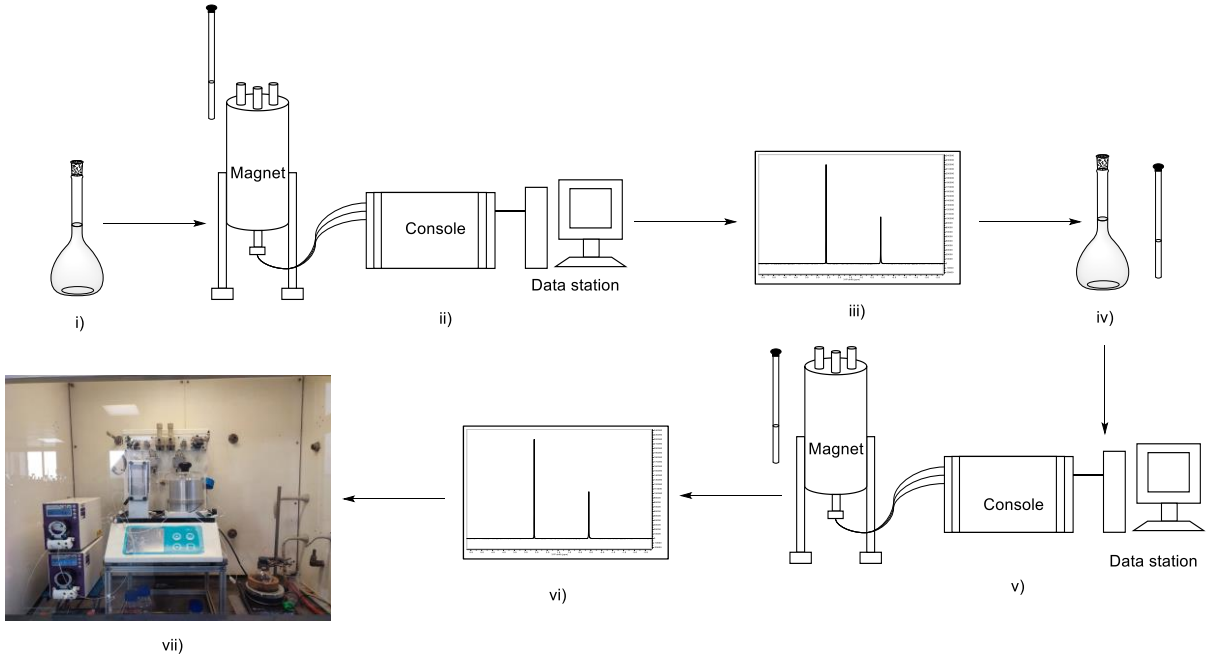

Legend: Preparation of stock solutions of reagents by quantitative ^{31}P NMR spectroscopy using trimethyl phosphate as an internal standard of known concentration. i): Prepare initial stock solution with concentration in excess of desired target concentration. ii) Perform ^{31}P NMR spectroscopy using trimethyl phosphate as an internal standard of known concentration. iii) Data analysis of the spectrum to determine concentration of analyte with respect to known concentration of TMP standard. iv) Dilution of analyte stock solution to desired concentration. v) Re-analyse diluted analyte solution by ^{31}P NMR spectroscopy. vi) Data analysis of the spectrum to confirm desired analyte solution concentration has been achieved. vii) Use analyte solution in flow reaction.

Figure 51: Workflow for the preparation of stock solutions of known concentrations prior reactions in a flow system.

The solubility properties of the crude *bis*-(fluorenylmethyl)-diisopropylamine phosphoramidite (**2**) forced us to reduce concentrations—over the course of a few hours, the *bis*-(fluorenylmethyl)-diisopropylamine phosphoramidite (**2**) solution tended to become a suspension. Thus, amidite (**2**) solutions were analysed immediately prior to use by a single ^{31}P acquisition, with the repetition time at least $5T_1$, where T_1 studies are reported in section 4.2.2.2.3.1. I employed a single ^{31}P run and a fixed, known concentration of trimethyl phosphate (0.25 M in DMF) as internal standard, keeping in mind that the T_1 of trimethyl phosphate was about 8 seconds, the parameters adopted for the acquisition were a d_1=51.5 s

and a.t.=18 s to ensure complete relaxation of all ^{31}P nuclei. The reagent stock solutions were then diluted based on the ^{31}P NMR data and, prior to use, were analysed again by a single ^{31}P spectrum acquisition (see *Figure 51*). The latter experiment was used to confirm that dilution had been performed correctly and that the reagent still retained its integrity.

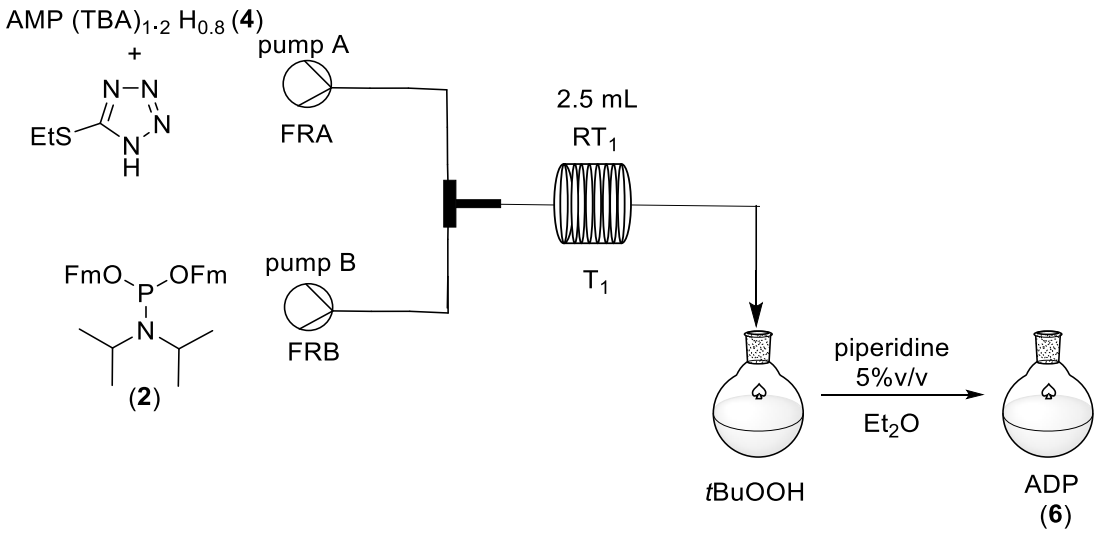

Figure 52: Synthesis of ADP pyridinium salt under flow conditions in a 2.5 mL coil.

I subsequently opted for a coil of 2.5 ml volume (see *Figure 52*). When I used the 0.27 mL chip I processed a volume of 5 ml in total over 75 min, The adoption of the bigger coil allowed us to run 40 ml of solution in less than 1 h.. When the flow apparatus

had reached a steady state, with flowrate of A (FRA)= flowrate of B (FRB)=300 μL·min^{-1} and a fixed temperature of 25 °C, two experiments were run, and the reaction conditions are reported in Table 8. After oxidation of the P(III)-P(V) intermediate (**8**), the Fm protecting groups were cleaved by stirring the reaction mixture with 5% v/v piperidine for 10 min. After deprotection, the product was precipitated upon addition of Et_2O and mixed for 10 min. The precipitate was then isolated by centrifugation, washed with Et_2O and dried in vacuo. The progress of each reaction step was followed by ^{31}P NMR spectroscopy. From these analyses it emerged that ADP was converted back to AMP as determined by decreasing ADP and increasing AMP signalss on ^{31}P NMR spectra.

Entry	*t*BuOOH 70% in H_2O (eq.)[b]	piperidine %v/v[c]	Consumption of AMP before dep.(%)[d]	Consumption of AMP after dep.(%)[d]
1	5	5	97	87
2	1.3	5	98	92

a C: concentration. b equiv.: equivalents. c %v/v.: percentage solute volume over DMF solution volume d % of AMP detected by ^{31}P NMR. AMP consumption: $([AMP]_0–[AMP]_{obs})/[AMP]0$, where [AMP]obs is the concentration before or after deprotection step and $[AMP_]_0$ is total AMP concentration at the start of the process.

Table 8: Oxidation reaction conditions and subsequent deprotection reaction outcomes for the synthesis of ADP from AMP.

4.2.2.3.2.2 Optimisation of the "one-pot three-step" synthesis of ADP using semi-continuous flow chemistry

Our efforts to increase the conversion levels to ADP after the Fm-deprotection step arose from the observation that the levels of AMP increased after the Fm deprotection step. The presence of water, although minimal, in the *t*BuOOH solution, I believed could cause the hydrolysis of the unstable P(III)-P(V) anhydride (**8**) in parallel with the deprotection process. Thus, with this hypothesis in mind, a single coupling reaction mixture conducted in flow was divided into 3 portions of 10 ml. Each portion was then treated with a different oxidant (see *Table 9* below).

One flow coupling reaction split in three portions (12 mL) to explore the use of different oxidant reagents:

5'-AMP $TBA_{1.2}H_{0.8}$ (4) (mmol·mL^{-1})[a]	Activator (eq.)[b]	Amidite (2) (eq.)[b]
0.05	2	1.3

Entry	Oxidant reagent (eq.)[b]	Consumption of AMP before dep.(%)[d]	Consumption of AMP after dep.(%)[d]
1	*m*CPBA (1.3 eq.)	77	50
2	*t*BuOOH 5 M in decane (1.3 eq.)	~99	60
3	*t*BuOOH 70% in H_2O (0.95 eq.)	~99	56

a C: concentration. b equiv.: equivalents. d (%) Conversion rate by ^{31}P NMR. AMP consumption: $([AMP]_0–[AMP]_{obs})/[AMP]0$, where [AMP]obs is the concentration before or after deprotection step and $[AMP]_0$ is total AMP concentration at the start of the process.

Table 9: Oxidation experiments on P(III)-P(V) intermediate (**8**) in the synthesis of ADP (**6**) from AMP (**4**).

Our attempts involved the use of 1.3 equiv. of *m*CPBA (Table 3, entry 1), 1.3 eq of *t*BuOOH 5 M in decane (*Table 10*, entry 2) and 0.95 equiv. of *t*BuOOH 70% in H_2O, (Table 3, entry 3). The resulting reaction mixtures were then analysed by ^{31}P NMR spectroscopy, and the levels of AMP were assessed. Then each mixture was subjected to deprotection using 5% v/v piperidine in DMF, followed by ^{31}P NMR spectroscopic analyses. The level of AMP after the oxidation with *m*CPBA (23%), is in line with what I had previously observed during our ^{31}P NMR kinetic studies (see section 4.2.2.2.3.2). The level of AMP after oxidation with *t*BuOOH 70% in H_2O and *t*BuOOH 5 M in decane, on the other hand, were both ~ 1%, which showed that the presence of water, in small quantities, did not affect the outcome of the oxidation reaction.

With a reasonably firm conclusion that water was not the cause of the reversion to AMP during oxidation, I focused on the Fm-deprotection step. I formulated the following areas to explore with a view to averting decomposition back to AMP:

1. Reaction time and temperature;
2. The stoichiometry of piperidine addition;
3. Fm-deprotection reaction temperature;
4. The amine base adopted as deprotecting reagent.

A single flow experiment was performed to generate the P(V)-P(V) Fm-protected anhydride (**9**). The reaction mixture was then divided into 3 portions that were treated with 5% v/v piperidine in DMF for different times as described in *Table 10*.

One flow coupling reaction split into 3 portions (12 mL each) to explore piperidine deprotection time.

5'-AMP $TBA_{1.2}H_{0.8}$ (4) (mmol·mL^{-1})[a]	Activator (eq.)[b]	Amidite (2) (eq.)[b]	*t*BuOOH 70% in H_2O (eq.)[b]
0.05	2	1.3	1.3

Entry	Piperidine 5% v/v[c] stirring time	Consumption of AMP before dep.(%)[d]	Consumption of AMP after dep.(%)[d]
1	~ few seconds	~98	92
2	~1 min		93
3	10 min		93

a C: concentration. b equiv.: equivalents. c %v/v.: percentage solute volume over DMF solution volume d Conversion rate by ^{31}P NMR. AMP consumption: $([AMP]_0–[AMP]_{obs})/[AMP]0$, where [AMP]obs is the concentration before or after deprotection step and $[AMP]_0$ is total AMP concentration at the start of the process.

Table 10: Deprotection experiments exploring stirring time for the Fm-deprotection step of the synthesis of ADP.

Each reaction product mixture was analysed by ^{31}P NMR spectroscopy, and the percentage of AMP after Fm-deprotection step was compared to the percentage before the Fm-deprotection step. I found (entries 1-3) that the deprotection reaction time had essentially no effect on the outcome, with AMP level increasing from ~2% before Fm-deprotection to 7-8% post-deprotection.

I then considered the stoichiometry of piperidine addition and the effect of temperature. The volume of 5% v/v piperidine solution corresponded to 15 equiv. of piperidine with respect to AMP starting material. For each equivalent of AMP converted to Fm-protected ADP, 4 equivalents of piperidine are expected to be needed, as shown in *Figure 53*.

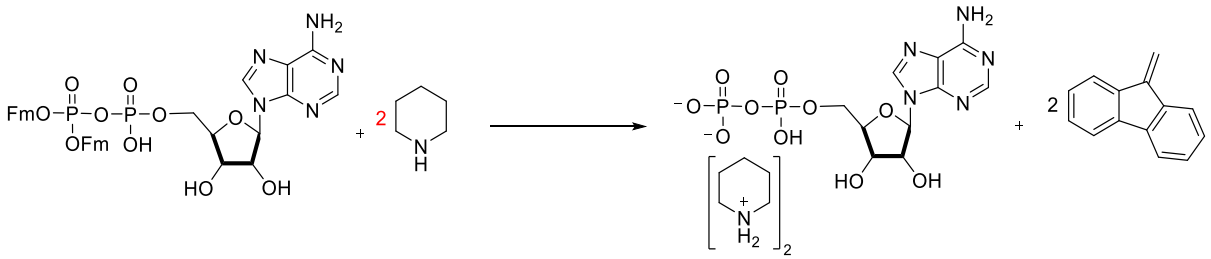

Figure 53: "One-pot three-step" balanced deprotection reaction.

Thus, two experiments were performed with reduced numbers of equivalents (5 and 10 equivalents). In addition, a further experiment was performed at reduced temperature of 0 °C (see *Table 11* below).

One flow coupling reaction split in 4 portions (10 mL) to explore the use of piperidine equivalents and temperature:

5'-AMP $TBA_{1.2}H_{0.8}$ (4) ($mmol \cdot mL^{-1}$)[a]	Activator (eq.)[b]	Amidite (2) (eq.)[b]	*t*BuOOH 5 M in decane (eq.)[b]
0.05	2	1.3	5

Entry	piperidine (eq.)[b]	temperature (°C)[c]	Consumption of AMP before dep.(%)[d]	Consumption of AMP after dep.(%)[d]
1	5	25	96	76
2	10			80
3	15			82
4	15	0		81

a C: concentration. b equiv.: equivalents. c °C: degree Celsius. d Conversion rate by ^{31}P NMR. AMP consumption: $([AMP]_0-[AMP]_{obs})/[AMP]0$, where [AMP]obs is the concentration before or after deprotection step and $[AMP]_0$ is total AMP concentration at the start of the process.

Table 11: Experiments exploring numbers of the equivalents of piperidine and temperature of the Fm-deprotection step for the synthesis of ADP from AMP.

Once again, a single flow experiment was performed to generate the P(V)-P(V) Fm-protected anhydride (**9**). The solution was analysed before Fm-cleavage by ^{31}P NMR spectroscopy, and the AMP level was ~ 4%. The reaction mixture was then divided into four portions of 5 mL each, and treated with piperidine in DMF (5, 10, 15 equiv. at 25 °C and 15 equiv. at 0 °C as shown in *Table 11*. The results show that the reaction temperature did not affect the outcome (entry 3 vs entry 4). The adoption of 5 equiv. led to a poorer outcome compared to the use of 10 or 15 equiv. of piperidine (76% vs 80-82%).

Finally, several secondary and tertiary amine bases were screened (see *Table 12*). The choice of amine was based in part on availability in the laboratory. Thereafter, I selected a range of secondary and tertiary structures across as wide a range of pK_{aH} as possible to test the effects of base strength.[191]

- Piperidine: secondary cyclic amine base, pK_{aH} (H_2O) 11.22;
- Morpholine: secondary cyclic base, pK_{aH} (H_2O): 8.0;
- DBU (8-diazabicyclo[5.4. 0]undec-7-ene): strong, non-nucleophilic amidine, pK_{aH} (H_2O) 13.5;
- TMG (Tetramethylguanidine): strong, amidine, pK_{aH} (H_2O) 13.0;
- Triethylamine: strong, tertiary amine, pK_{aH} (H_2O) 10.65;
- Hünig's base (*N*,*N*-Diisopropylethylamine): strong, non-nucleophilic tertiary amine base, pK_{aH} (H_2O) 10.5;[191]

One flow coupling reaction split in 6 portions (5 mL) to explore different deprotection bases:

5'-AMP $TBA_{1.2}H_{0.8}$ (4) (mmol·mL^{-1})[a]	Activator (eq.)[b]	Amidite (2) (eq.)[b]	*t*BuOOH 5M in decane (eq.)[b]
0.05	2	1.3	5

Entry	Base 5% v/v	Consumption of AMP before dep.(%)[c]	Consumption of AMP after dep.(%)[c]
1	Piperidine	~ 99	83
2	DBU		~ 98
3	TMG		~ 98
4	Morpholine		83
5	Triethylamine		92
6	Hünig's base		75

a C: concentration. b equiv.: equivalents. c % Conversion rate by ^{31}P NMR. AMP consumption: $([AMP]_0 - [AMP]_{obs})/[AMP]0$, where [AMP]obs is the concentration before or after deprotection step and $[AMP]_0$ is total AMP concentration at the start of the process.

Table 12: Fm-deprotection experiments using a range of 2° and 3° amine bases for the synthesis of ADP.

As before, the oxidised solution was split into six portions of 5 mL each and each portion was then reacted simultaneously with a different amine base. Upon the addition of piperidine, DBU and TMG, the solutions became white, pink and yellow suspensions, respectively (as shown in *Figure 54*). Precipitation was not observed upon the addition of morpholine, triethylamine and Hünig's base, however, after 10 min some cloudiness had appeared (as shown in *Figure 55* and *Figure 56*).

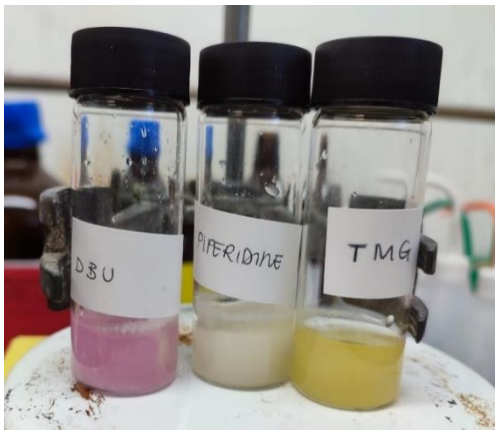

Figure 54: Picture of the solutions directly after the addition of DBU, piperidine and TMG.

Figure 55: Picture of the solutions after 10 min from the addition of morpholine, triethylamine and Hünig's base.

Figure 56: Picture of $CMP(TBA)_{1.2}(H)_{0.8}$ (**6**) and activator stock solution.

Et_2O was added to each reaction mixture to ensure complete precipitation of nucleotides before analysis. The resulting materials were then analysed by ^{31}P NMR spectroscopy (see *Table 12*). Minimal reversion to AMP was observed with TMG and DBU. While I did not investigate why these systems gave better performances, I noted both TMG and DBU are amidines with relatively high pK_{aH} (H_2O) values.[192] Amidines are more basic than alkyl amines because the two nitrogen atoms work together to donate electron density onto each other.[193] Delocalization of one nitrogen's lone pair onto the other, and the resulting stabilization of the protonated amidinium ion, makes amidines particularly basic, with a pK_{aH} values of about 13.[191] Guanidines, with three nitrogen atoms donating lone pair electrons, are even more basic, and, given the higher propensity for precipitation with more basic amines, there may be opportunity to avoid the addition of Et_2O altogether.[193, 194] I decided to proceed using TMG, however, DBU should also be explored in the future.

I found TMG and piperidinium nucleotide salts display poor solubilities in water. This poor solubility proved to be an issue during analyses of reaction mixtures and, more critically, could cause problems with future anion exchange chromatographic purifications or iterative phosphorylation processes. Thus, I sought to perform cation exchange to improve the solubility of TMG and piperidinium salts in water to aid analysis and chromatography. The residue was exchanged by suspending the crude material in a solution of NaI (5 M in acetone-H_2O; 9:1), with stirring, overnight. The following day, both the reaction mixtures were centrifuged at 4 °C, 400 rpm for 20 min and then decanted to obtain a yellow solid for the TMG reaction and a white solid from the piperidine reaction. By ^{31}P NMR spectroscopy the

conversion levels of AMP into ADP (**10**) of both reactions were analysed. The ^{31}P NMR spectra showed for the reaction using piperidine as deprotecting base a consumption rate of AMP of 98% after oxidation and 92% after deprotection and for the reaction using TMG as deprotecting base a consumption rate of AMP of 99% after oxidation and 97% after deprotection.

In parallel to reaction development, I explored a preparative chromatography method. I initially used mixtures of commercial samples of AMP and ADP to develop an anion exchange chromatography method that delivered good separations of AMP and ADP using a linear gradient from 0.05 M to 1 M TEAB buffer pH 8 on a 15.5 g RediSep Rf Gold® Amine column with a flowrate of 30 mL/min or on a 5 g RediSep Rf Gold® Amine column with a flowrate of 13 mL/min (see *Figure 58*).

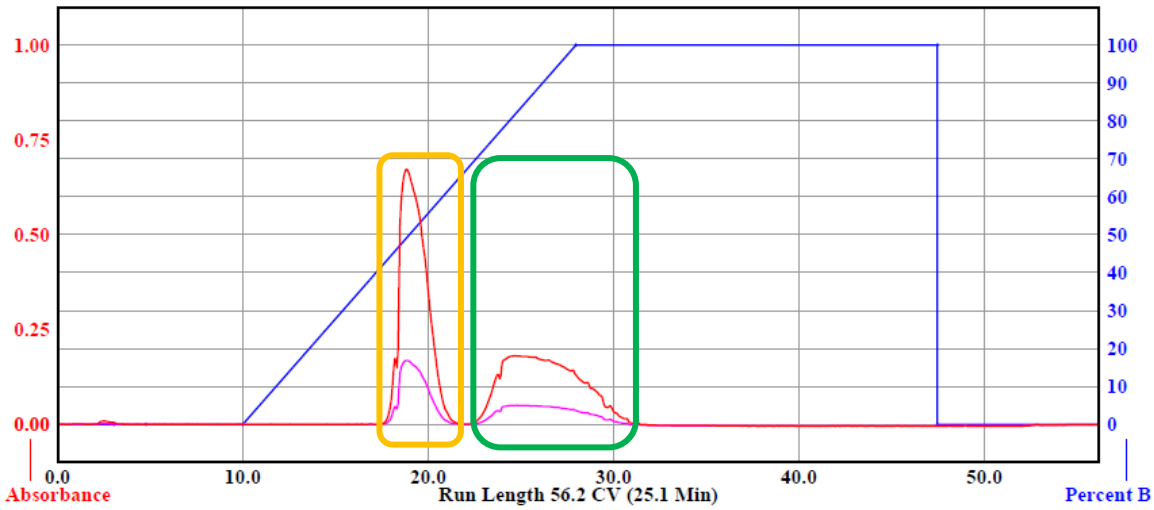

Figure 58: Chromatogram of a mixture of commercial AMP and ADP purified using Teledyne CombiFlash NextGen 100 system and 15.5 g RediSep Gold® Amine column with gradient elution using triethylammonium bicarbonate buffer (from 0.05 M to 1 M). AMP is highlighted in orange, ADP in green. 10 mg of NaAMP and 10 mg of NaADP were used in the mixture.

The crude reaction mixtures from TMG- and piperdine-based deprotections were then resolved using the same approach. In each case ~50 mg of crude material was loaded onto the column. As shown in *Figure 59* and *Figure 60*, the chromatograms obtained from both purifications highlighted the reliability of the method with good resolution of AMP and ADP. The method thus seemed to be robust and ready to be adopted as the last step in our scaled ADP synthesis.

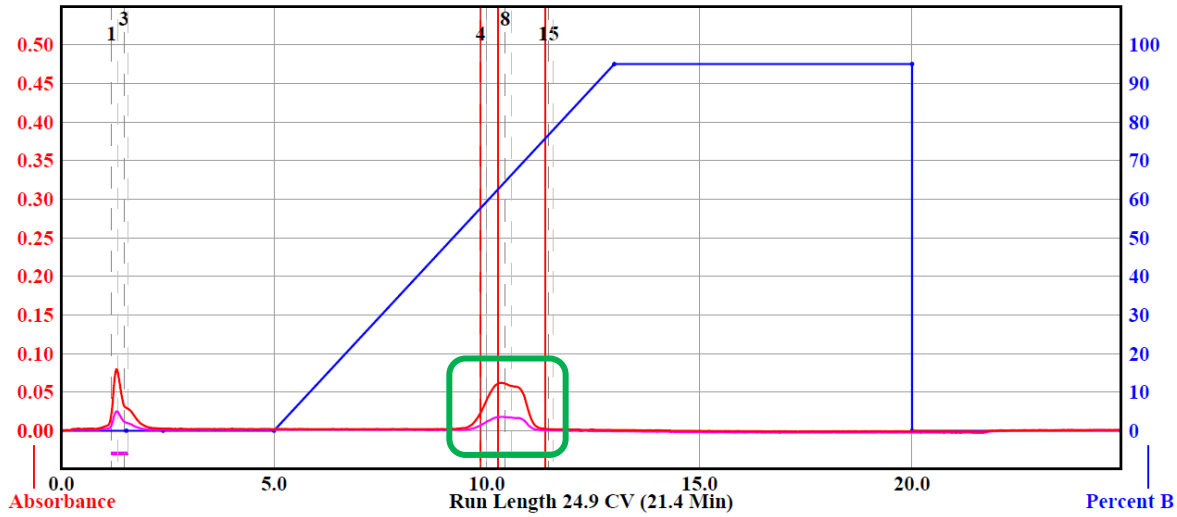

Figure 59: Chromatogram of the ADP (TMG as deprotecting base) crude material using Teledyne CombiFlash NextGen 100, on 15.5 g RediSep Gold® Amine column with gradient elution using triethylammonium bicarbonate buffer (from 0.05 M to 1 M). AMP is highlighted in orange, ADP in green.

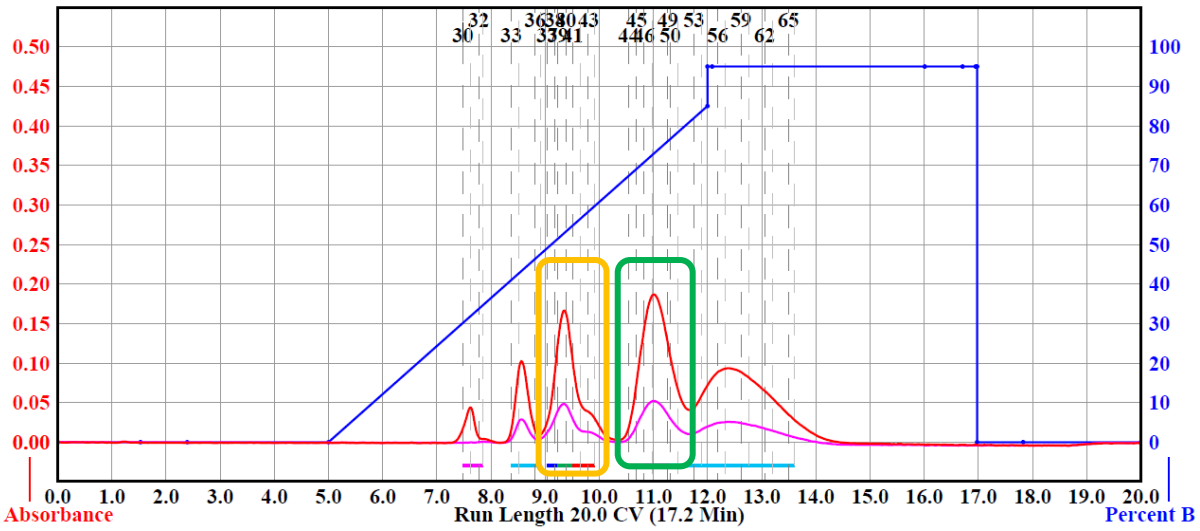

Figure 60: Chromatogram of the ADP (piperidine as deprotecting base) crude material using Teledyne CombiFlash NextGen 100, on 15.5 g RediSep Gold® Amine column with gradient elution using triethylammonium bicarbonate buffer (from 0.05 M to 1 M). AMP is highlighted in orange, ADP in green.

The chromatograms, shown in *Figure 59* and *Figure 60*, showed that the crude material obtained from TMG deprotection compared to the crude material obtained from piperidine detection was much less complex, thus making the purification easier, with potential for faster elution and enhanced productivity.

Based on these assessments, an up-scaled synthesis of ADP (**6**) was performed using TMG as deprotection reagent and purification of the crude was performed using the same anion exchange protocol, but on a larger column.

In the foregoing sections, flow reaction experiments for the synthesis of ADP on the 0.27 mL chip reactor and 2.5 mL coil were performed on scales of 0.25 mmol [~ 150 mg of AMP $TBA_{1.2}H_{0.8}$ (**4**)] and 1 mmol [~ 500 mg of AMP $TBA_{1.2}H_{0.8}$ (**4**)], respectively. In our up-scaled process, I used ~ 2 g of AMP $TBA_{1.2}H_{0.8}$ (**4**) as substrate.

A DMF solution of 5'AMP $TBA_{1.2}H_{0.8}$ (**4**) (0.05 $mol \cdot L^{-1}$, 60 mL, 1.0 equiv.) with 5-(ethylthio)-1*H*-tetrazole (2 equiv.) and a DMF solution of *bis*-(fluorenylmethyl)-diisopropylamine phosphoramidite (0.065 $mol \cdot L^{-1}$, 60 mL, 1.3 equiv.) (**2**) were pumped (FRB = FRA = 0.30 $mL \cdot min^{-1}$ flowrate) into a 2.5 mL coil reactor; for 4 min (120 mL total solution in 320 min total) under temperature control of 25 °C. After establishing stable flow (approximately 2 coil volumes), the resulting coupling mixture was then quenched into a solution of *t*BuOOH 5 M in decane (1.3 equiv.) in dry DMF (2.5 mL). Following complete oxidation (determined by ^{31}P NMR spectroscopy), the Fm protecting groups were cleaved with 5% v/v TMG in DMF. After deprotection, the product was precipitated upon addition of Et_2O. The precipitate was isolated by centrifugation, washed with Et_2O and dried in vacuo. The ^{31}P NMR spectra showed 95% consumption of AMP after oxidation and 90% after deprotection. The residue formed after deprotection with TMG was cation exchanged overnight by suspending the crude material in 10 mL of a solution of NaI (5 M in acetone-H_2O; 9:1) and the resulting solid was purified by anion exchange chromatography on a 100 g RediSep Rf Gold® Amine column, with a linear gradient of 1 M TEAB buffer pH 8, and a flow rate of 60 mL/min. (see *Figure 61*), followed by freeze drying. After freeze drying, 1.0 g of 5'ADP $Et_3NH_{1.4}$ $H_{0.6}$ (**11**) was collected (1.8 mmol, 65%).^{31}P and ^{1}H NMR analyses showed the resulting material to be 97% or 98% pure respectively.

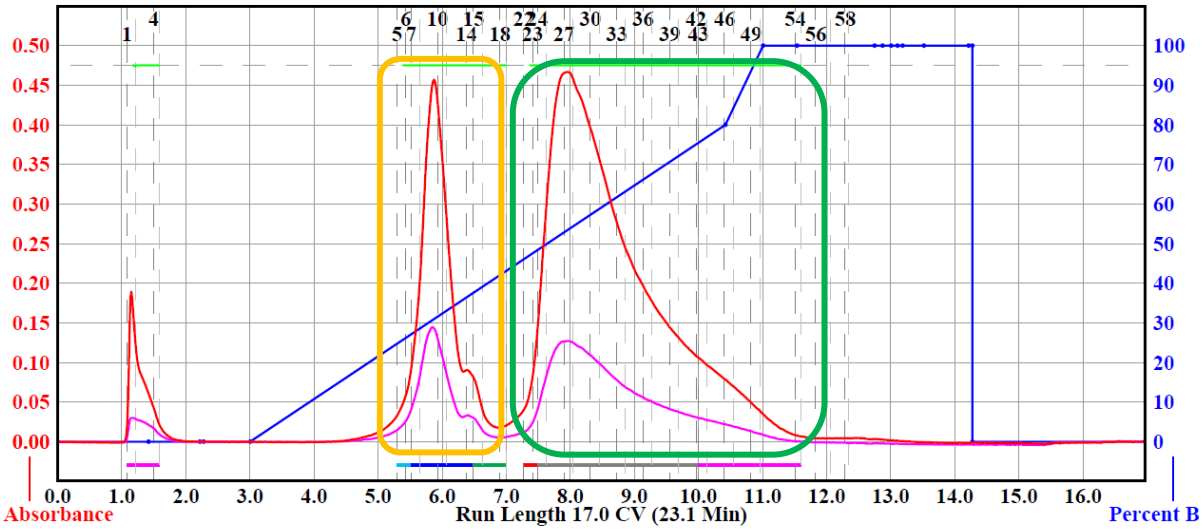

Figure 61: Chromatogram of the purification of ~2 g scale synthesis of ADP using Teledyne CombiFlash NextGen 100, on 100 g RediSep Gold® Amine column with gradient elution using triethylammonium bicarbonate buffer (from 0.05 M to 1 M). AMP is highlighted in orange, ADP in green.

Subsequently, the material was analysed by HPLC to corroborate the ^{31}P and ^{1}H NMR assessments of purity. A Cogent UDA column (4 µm, 100 Angstroms, 100 mm × 2.1 mm), with a flowrate of 0.4 mL/min, eluent A = 100% 23 mM ammonium acetate and B = 90% MeCN,10% 16 mM ammonium acetate, was run with a linear gradient over 30 min to resolve nucleotides. Two runs were performed: first our purified material and then, a mixture of commercial AMP, ADP and ATP to confirm the retention times of the analytes I expected to detect. Pleasingly, as shown in *Figure 62* and *Figure 63*, the level of purity of our compound was >99%.

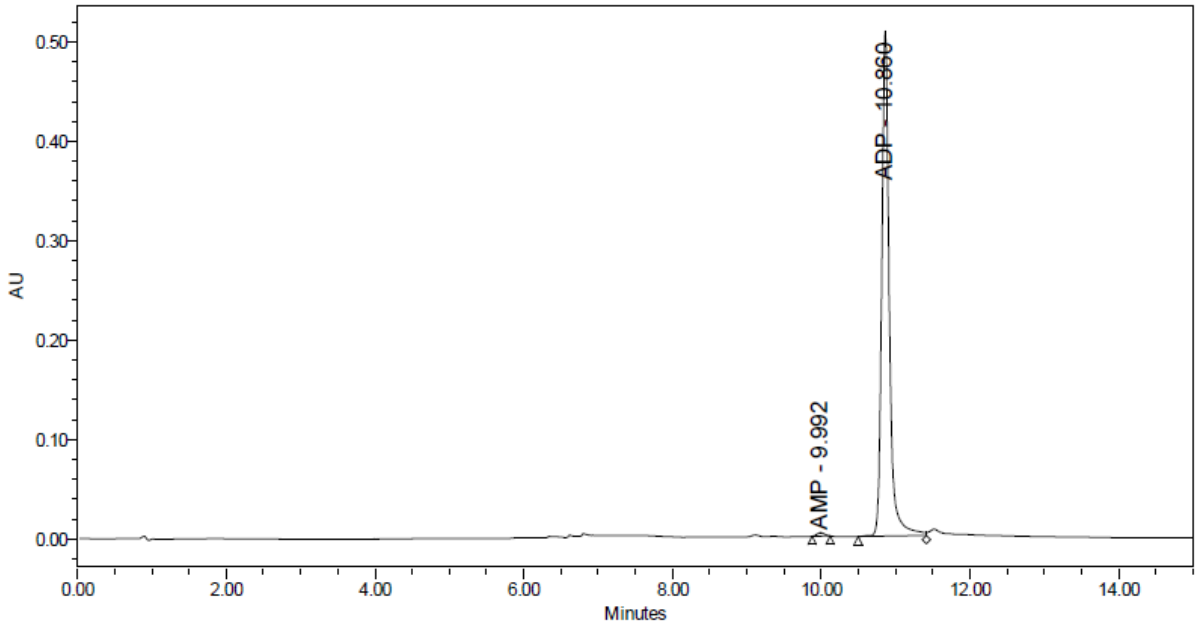

	Peak Name	RT	Area	% Area	Height
1	AMP	9.992	24916	0.69	3569
2	ADP	10.860	3601099	99.31	507991
3	ATP	11.350			

Figure 62: HPLC chromatogram of the chromatographically purified materials from the scaled ADP synthesis (see 4.2.2.3.2.2).

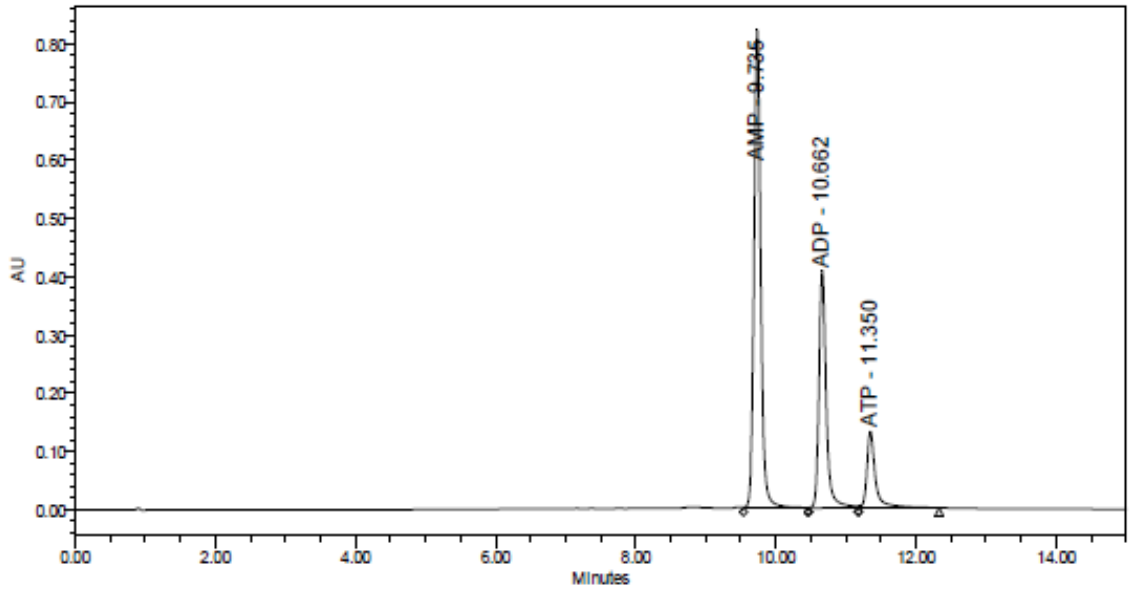

	Peak Name	RT	Area	% Area	Height
1	AMP	9.735	5506145	57.56	821063
2	ADP	10.662	2939305	30.73	407942
3	ATP	11.350	1120668	11.71	130957

Figure 63: HPLC chromatogram of the AMP, ADP and ATP standards mixture.

The results for the scaled synthesis and purification validate the robustness of our workflow method for the synthesis of ADP using a continuous flow system, leading to pure product on gram scale.

4.2.2.4 Application of the "one-pot three-step" semi continuous flow process towards the synthesis of UDP and CDP

To explore the scope of our method, I also applied it to the synthesis of the other nucleoside diphosphates.

I began with the synthesis of UDP, from UMP because I expected UMP to be more soluble than the other readily available nucleoside monophosphates. Synthetic studies were performed using the Uniqsis FlowSyn system with a 2.5 mL coil reactor. A stock solution of 5'-UMP $TBA_{1.6}$ $H_{0.4}$ (0.05 mol·L^{-1}) (**5**) with 5-(ethylthio)-1*H*-tetrazole and a stock solution of amidite (**2**) (0.065 mol·L^{-1}) were reacted and the resulting clear coupling mixture, established stable flow (approximately 2 coil volumes), was then quenched into a solution of *t*BuOOH. The Fm protecting groups were then removed and the product precipitated using 5% v/v piperidine, according to the procedure used for ADP synthesis (see sections 4.2.2.3.2). The conversion levels of UMP after oxidation and after deprotection were then analysed by ^{31}P NMR spectroscopy. Pleasingly, 90% of the UMP was observed to have been consumed after oxidation, and, after deprotection 85% of UMP was seen to have been consumed. During preparation of the stock solution of UMP salt and the subsequent flow procedure, no precipitation or clogging were observed. In summary, the procedure proved effective for the formation of UDP from UMP.

Moving to CMP, however, problems with solubility during the process were encountered. The first difficulties arose during preparation of $CMP(TBA)_{1.2}(H)_{0.8}$ (**6**) and activator stock solution. As shown in *Figure 64*, upon the addition of the activator to the diluted $CMP(TBA)_{1.2}(H)_{0.8}$ (**6**) solution, a gel formed instantaneously. Given that $CMP(TBA)_{1.2}(H)_{0.8}$ (**6**) was soluble in the absence of 5-(ethylthio)-1*H*-tetrazole, I chose to include the tetrazole activator in the amidite (B) stock solution instead of the nucleotide substrate solution.

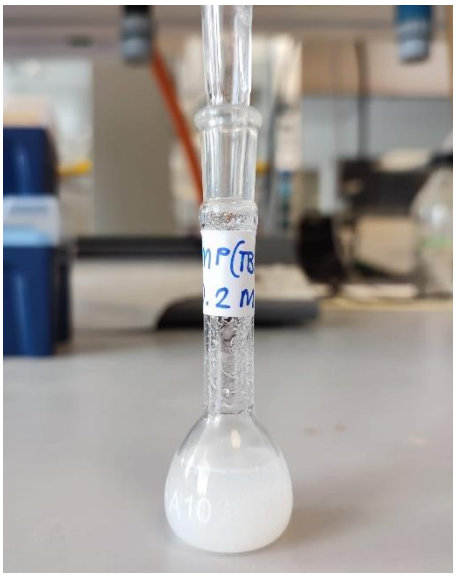

Figure 64: Picture of $CMP(TBA)_{1.2}(H)_{0.8}$ (**6**) and activator stock solution.

Figure 65: Picture of $CMP(TBA)_{1.2}(H)_{0.8}$ (**6**) and a 5-(ethylthio)-1*H*-tetrazole and to the amidite (**2**) stock solution.

The resulting solutions of $CMP(TBA)_{1.2}(H)_{0.8}$ (**6**) in DMF and amidite reagent (**2**) with 5-(ethylthio)-1*H*-tetrazole were both clear and free of particles and gelatinous materials as shown in *Figure 65.*

Thus, 5'-CMP $(TBA)_{1.2}(H)_{0.8}$ (**6**) (0.05 $mol \cdot L^{-1}$ in DMF) was reacted in a 0.27 mL chip with amidite (**2**) (0.065 $mol \cdot L^{-1}$) mixed with 5-(ethylthio)-1*H*-tetrazole (2 equiv.). Unfortunately, when the two solutions contacted each other, gelation occurred causing the flow reactor to become clogged. Our next move was to further dilute the stock solutions of nucleotide and reagent plus activator and adopt a larger, 2.5 mL reactor coil.

I hoped that even if the gelation were to occur, the combination of larger flow rates (0.6 $mL \cdot min^{-1}$) and larger coil tubes (2.5 mL) may avoid clogging. As reported in *Table 13* *Legenda*: a °C: coil temperature. b C.: concentration. c % rate conversion of CMP detected by ^{31P} NMR.

Table 13 below, several different concentrations were explored. In addition, elevated reactor temperatures were also explored in efforts to increase solubility and avoid gelation.

Entry	**T (°C)[a]**	**$CMP(TBA)_{1.3}$ (6) ($mol \cdot L^{-1}$)[b]**	**(%)[c] CMP unreacted**
1	25 °C	0.05	35
2	25 °C	0.025	60
3	50 °C	0.025	74

Legenda: a °C: coil temperature. b C.: concentration. c % rate conversion of CMP detected by ^{31}P NMR.

Table 13: Attempts towards the flow synthesis of CDP from CMP in a 2.5 mL coil reactor.

The data gathered showed that a combination of diluted reagent stock solutions, the adoption of a larger reactor and higher flow rates prevented clogging and led to reasonable levels of conversion to CDP (**13**), despite the relatively poor solubility of substrate in combination with reagent solutions (See *Table 13*, entry 1). Further dilution (see *Table 13*, entry 2,), however, led to reduced conversion levels, at least at the flow rate I explored. There was visual evidence of gelation in the system which was apparent when the mixture emerged from the flow system. The use of an increased temperature (see *Table 13*, entry 3), further reduced conversion level, possibly because of increased rates of decomposition of the *bis*-(fluorenylmethyl)-diisopropylamine phosphoramidite reagent. This hypothesis was supported by evidence of H-phosphonate formation garnered from ^{31}P NMR spectroscopy (*Figure 66*).

Although I did not further optimise the syntheses of CDP (**13**) and UDP (**12**), these preliminary results are promising for future research.

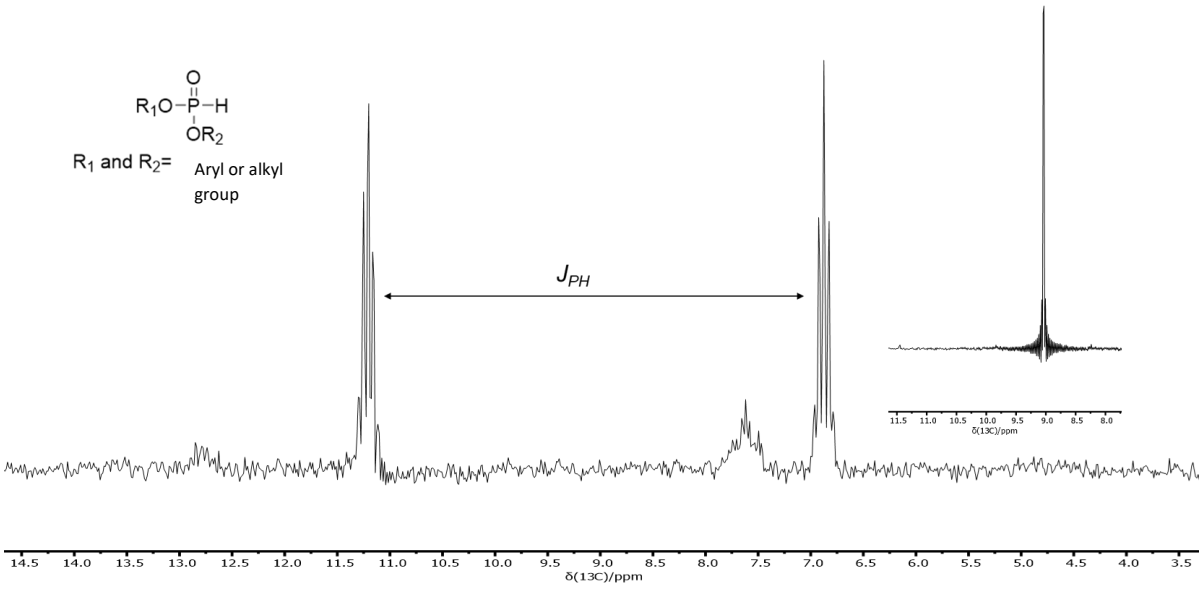

Figure 66: H-phosphonate structure, with a highlight on the ^{31}P-^{1}H couple and ^{31}P-^{1}H decoupled NMR spectra.

In summary, in this chapter I have discussed the steps that led us to deliver a robust and reliable flow method for the synthesis of ADP (section 4.2.2.3.2.2) from AMP. Specific, quantitative ^{31}P NMR methods were set up to analyse reagent stock solutions and each reaction step (sections 4.2.2.2.3.2 and 4.2.2.3.2.1). These results were combined with those obtained from the synthesis in flow (section 4.2.2.3.2.1) to make our method repeatable and scalable (up to ~ 2 g of AMP substrate). The same method was tested for the synthesis of CDP from CMP and UDP from UMP. The results obtained for the CDP and UDP synthesis

(section 4.2.2.4), were promising starting points for future work. I chose not to explore GMP as a substrate because of the problems encountered with CMP, where CMP is usually viewed as being more soluble than GMP.

5 Conclusions and Future Plans

This chapter summarises the results presented and discussed in Chapter 4, draws conclusions, and suggests future plans.

As discussed in Chapter 2, phosphoanhydrides are essential for life as major cellular sources of energy and as precursors of nucleic acids. Thanks to the fundamental biological roles of endogenous nucleosides and nucleotides, they have become essential scientific tools. In Chapter 3, methodologies for their synthesis were reviewed, highlighting that there is no standardized, broadly satisfactory method for the synthesis of nucleoside phosphates. This lack of a general satisfactory method arises because of problems associated with insolubility of the starting materials and reagents in organic solvents, low chemical stability of the reagents (especially P(III) systems), long reaction times/low reactivity (especially morpholidate systems), complicated purifications and moisture sensitivity. The idea behind this project, as discussed in Chapter 4, is not to create a new synthetic route, but to optimize and increase the 'usability' and 'scalability' of existing routes, in particular the Jessen's phosphoanhydride synthesis based on the P(III)-P(V) chemistry[1]. I sought to develop and optimize the batch and flow syntheses of the phosphitylating reagent, *bis*-(fluorenylmethyl)-diisopropylamine (**2**), and subsequently, Jessen's "one pot-three steps" phosphorylation reaction. [1, 145]

Our targets for the synthesis of *bis*-(fluorenylmethyl)-diisopropylamine (**2**) were:

1. Develop and upscale the batch synthesis of *bis*-(fluorenylmethyl)-diisopropylamine phosphoramidite (see 4.1.1);
2. Translate into a continuous flow system, our newly-developed batch method for the synthesis of *bis*-(fluorenylmethyl)-diisopropylamine phosphoramidite (see section 4.1.2);
3. Use *bis*-(fluorenylmethyl)-diisopropylamine phosphoramidite, prepared using upscaling methods, for the phosphitylation of nucleotides (see sections 4.2, 4.2.1 and 4.2.2 ,4.2.2.1);

Our targets for the batch and flow development of Jessen's "one pot-three steps" phosphorylation reaction[1, 145] were:

1. Develop quantitative methods for reagent and product measurements (see section 4.2.2.2.3.1);

2. Use quantitative method for kinetic studies to inform flow chemistry experiments (see section 4.2.2.3.2.1);
3. Translate the iterative addition of phosphoryl groups to nucleotides into a continuous flow system (see section 4.2.2.3);
4. Optimize and scale up from milligrams to grams the iterative addition of phosphoryl groups to nucleotides using the flow system (see section 4.2.2.3.2.2);
5. Demonstrate scope across multiple nucleotide substrates (see section 4.2.2.4).

5.1 Conclusions and Future Plans for the Development of batch and flow synthesis methods for the preparation and application of *bis*-(fluorenylmethyl)-diisopropylamine phosphoramidite (see Chapter 4, section 4.1.1)

5.1.1 Conclusions

In Chapter 4, section 4.1.1, starting from the procedures published by Bialy and Waldmann, [2] and Desmaële,[3] a faster, more efficient batch synthesis of *bis*-(fluorenylmethyl)-diisopropylamine phosphoramidite (**2**) was developed (see section 4.1.1), and subsequently translated into a continuous flow process (see section 4.1.2).

In an initial, exploratory set of experiments according to Bialy and Waldmann's two-step synthesis procedure,[2] I initially tried to identify much more rapid work-up methods to optimize the isolation of the phosphoramidite (**2**) while avoiding the chromatography steps which had proven to be challenging.

The solubilities of 9-fluorenylmethanol, *bis*-(fluorenylmethyl)-diisopropylamine phosphoramidite (**2**) and diisopropylethylamine hydrochloride were tested in several solvents. 9-Fluorenylmethanol and diisopropylethylammonium hydrochloride salts proved to be highly soluble in all polar solvents, but essentially insoluble in non-polar solvents, while the phosphoramidite (**2**) proved to be highly soluble in hexane. Therefore, three work-up strategies were attempted in parallel:

1. Filtration to remove diisopropylethylammonium chloride salts, followed by the addition of 1 M phosphate buffer to the solution and extraction with EtOAc following Bialy and Waldmann's procedure;[2]
2. EtOAc was replaced with hexane in the extraction;
3. THF reaction solvent was removed under vacuum and the resulting solid residues were agitated in hexane, with the aim of selectively extracting product (**2**).

After extraction, any precipitate suspended in the hexane was filtered off, and the solvent was removed under vacuum. The spectroscopic analyses of the materials from each of the three different work-up procedures showed similar mass recovery levels and purity of the amidite (**2**). Although all three processes were equally effective in delivering materials of similar purities, direct extraction with hexane avoided time-consuming partitioning steps and, in this sense, was the most efficient.

The extraction has been performed with safer solvents than hexane: *n*-heptane and cyclohexane, that appeared to be equally effective in comparison to hexane, based on the spectroscopic data gained on the products obtained with good yields and high levels of purity.

With a convenient strategy for the selective extraction of amidite (**2**) in hand, I focussed on the preceding reaction processes, combining our selective hexane extraction with the ~24 h one-pot, two step approach of Desmaële.[3] Desmaële's strategy[3] was performed and monitored via ^{31}P NMR spectroscopy. On the contrary to what was expected based on Desmaële's reported reaction time, the process was completed in just 1 h instead of the reported 24 h. The procedure delivered 86% yield based on theoretical mass recovery, where the isolated material was shown to be 97% pure by ^{31}P NMR and 95% pure by ^{1}H NMR methods.

The product (**2**) obtained with the THF-based reaction, followed by hexane extraction, was then demonstrated to be an efficient phosphitylating reagent in the synthesis of ADP and ATP following Jessen's method (see section 4.2.1 and 4.2.2).[1, 145]

Having proven the validity of the synthetic process for the preparation of amidite (**2**) and its applicability to the Jessen method[1, 145], the next step was to convert the process into a continuous flow system. Despite the batch process proving successful using THF, ammonium hydrochloride salts are insoluble in THF and their precipitation would clog a flow system. I performed initial solvent screening in batch to find an alternative solvent system that maintained a homogenous reaction mixture to support flow experiments:

- anhydrous 2-methyl-THF;
- 'wet' 2-methyl-THF (i.e. commercial, undried material, directly from a bottle without a septum);
- anhydrous α,α,α-trifluorotoluene;
- mixture of anhydrous THF/Cyrene;
- mixture of anhydrous THF/anhydrous toluene;
- mixture of anhydrous THF/anhydrous CH_2Cl_2.

I found CH_2Cl_2 to be the only viable candidate for continuous flow, alongside THF as co-solvent.

A series of flow experiments were conducted using different reactant concentrations (from 0.2 $mol \cdot L^{-1}$ to 2 $mol \cdot L^{-1}$, coil lengths, temperatures (from 0 ºC to 24 ºC) and flow rates (from 0.6 $mL \cdot min^{-1}$ to 1 $mL \cdot min^{-1}$).

The results from these experiments showed that I were able to successfully increase reactant concentrations in flow, reducing solvent used. Increased coil temperature delivered increased reaction rate and reduced reaction time. Although the mass recovery and the purity levels of amidite (**2)** obtained in the batch reactions were marginally higher, the experiments performed in flow were still effective (81% mass recovery and 87% purity) and scalable, delivering 25 g of amidite (**2**).

5.1.2 Future plans

Our synthetic method development for the synthesis of *bis*-(fluorenylmethyl)-diisopropylamine phosphoramidite (**2**) delivered material that was effective in Jessen's method for the synthesis of diphosphates and triphosphates.[1, 145]

However, more in-depth solvent screening studies should be conducted. The best crude reaction outcome achieved from our preliminary studies involved the use of dry α,α,α-trifluorotoluene. Anhydrous α,α,α-trifluorotoluene proved to be effective for the batch process, with a mass recovery of 95 % and purity level of 84%, but not suitable for the flow process due the precipitation of side products. Further studies with this system could improve safety and more sustainability, while improving efficiency and productivity on large scales. Thereafter, alternative work-up solvents, such as methyl tert-butyl ether, should be tested.

In respect of developing a continuous flow method for the syntheses of *bis*-(fluorenylmethyl)-diisopropylamine phosphoramidite (**2**) and phosphoanhydrides, further solvent screening studies should be conducted to try to identify a candidate that supports both processes. Unfortunately, dry DMF, which was used to perform the synthesis of phosphoanhydrides both in batch and in flow (see Chapter 4, section 4.2), cannot be used to perform the synthesis of *bis*-(fluorenylmethyl)-diisopropylamine phosphoramidite (**2**) because it will react with PCl_3.

The *bis*-(fluorenylmethyl)-diisopropylamine phosphoramidite (**2**) I prepared should also be consistently tested across a broader range of nucleoside mono- and di-phosphate substrates, particularly using our flow methods.

5.2 Conclusions and future plans for the Development of Jessen's "one pot-three steps phosphorylation reaction (see Chapter 4, section 4.2)

5.2.1 Conclusions

In Chapter 4, section 4.2, I discussed the steps that led us to deliver a robust and reliable flow method for the synthesis of ADP from AMP.

Initial phosphoanhydride formation reactions were performed using ADP salts as substrates (**15**) (see Chapter 4, section 4.2.1), following the procedure developed by Jessen's group[1, 145] to 'use-test' the phosphitylating reagent, *bis*-(fluorenylmethyl)-diisopropylamine phosphoramidite (**2**) made with our convenient batch and flow methods. For practical needs I then moved away from ATP synthesis to focus on the synthesis of ADP from AMP.

Based on our previous results for ATP synthesis, initial screening of reagent, substrate, and activator concentrations for ADP synthesis were carried out to identify a method that was congenial in terms of solubility for application in flow. Different AMP salts were tested (i.e. tri-*n*-octylammonium, trihexylammonium, pyridinium and tetrabutylammonium), oxidants (*m*CPBA or *t*BuOOH in decane or *t*BuOOH 70% in H_2O), and different polar, aprotic solvents (i.e., DMSO, DMF, α,α,α-trifluorotoluene, 2-methyl-tetrahydrofuran, Cyrene and acetonitrile). Although I aspired to make the phosphoanhydride formation greener while maintaining full solubility for flow protocols, this was not our absolute priority. Thus, in order to progress the flow aspects of the project, I reverted to the use of DMF and DMSO as demonstrated by the Jessen group[1, 145] (see Chapter 4, section 4.2.2.1).

In Chapter 4, section 4.2.2.2.1, the initial decision to explore reactions using DMSO is discussed. The use of DMSO-d6 facilitated ^{31}P NMR analyses without requiring the addition of 'lock tubes' containing a deuterated solvent and the cost of DMSO-d6 is much lower compared to DMF-d7.

The development of quantitative methods for reagent and product concentration measurements and for kinetic studies was one of our initial research targets, see Chapter 4, section 4.2.2.2.1. Preliminary ^{31}P NMR experiments were analysed using an automated 'walk-

up' spectrometer to gauge approximate reaction times. The progress of the coupling reaction between AMP and amidite (**2**), was then assessed after 5, 10, 20, 30 and 60 min of reaction. Subsequently, the effectiveness of the coupling reaction was analysed in further detail by changing the numbers of equivalents of the reagents. The same concept was applied to analyse the progress of the oxidation step.

Based on the preliminary results from these experiments, quantitative kinetic ^{31}P NMR spectra of coupling (step 1) and oxidation (step 2) processes of the "one pot-three steps" ADP synthesis[1, 145] were on a dedicated spectrometer, thermostated at 25 ºC, using specific acquisition parameters to gain more quantitative insights. Trimethyl phosphate (0.00 ppm) was also adopted as internal standard with fixed concentration.

The P(III)-P(V) anhydride intermediate (**8**) (^{31}P signals ~125.18 ppm and ~ –12.82 ppm) appeared to quickly decompose into what I hypothesized to be phosphate ester by-products; however, their nature was not confirmed. The ^{31}P NMR data gained in respect of the oxidation step showed the P(V)-P(V) anhydride (**9**) to be stable over the time of the experiment. Furthermore, by using oxidant to quench the coupling reaction after various time periods, I found the highest level of conversion to occur after ~1 min. Importantly, our studies have proven that reversion of the P(III)-P(V) intermediate (**8**) to AMP was occurring, due the high instability of P(III)-P(V) anhydride intermediate (**8**). Analysis of the ^{31}P NMR spectra acquired for the DMSO-based "one pot-three steps" reaction showed that the coupling step was extremely rapid, however, when using excess oxidant to quench the reaction (i.e., oxidise P(III) species), I found that the oxidant reacted exothermically with DMSO. With this factor in mind, I abandoned further studies with DMSO (see Chapter 4, sections 4.2.2.2.2 and 4.2.2.2.3).

I then moved to using DMF for the "one pot-three steps" synthesis of ADP[1, 145] studies, where ^{31}P NMR analyses were then performed using trimethyl phosphate as internal standard and alongside a D_2O lock tube. Single acquisition NMR spectra were acquired using an automated 'walk-up' spectrometer to gauge approximate reaction times. The progress of the coupling step was then assessed after 5, 10, 20, 30 and 60 min of reaction, and then every hour. The results showed the DMF reaction to be slower compared to the DMSO reaction, however the P(III)-P(V) anhydride (**8**) was significantly more stable. This enhanced stability appeared to afford overall improvements in the performance in the coupling step. The oxidation reaction

in DMF, performed with *t*BuOOH, ran smoothly, leading to stable P(V)-P(V) species (**9**) without any cross-reactivity with the solvent (see Chapter 4, section 4.2.2.2.3).

Extensive NMR studies were then performed in DMF to obtain quantitative, high sensitivity ^{31}P NMR spectra during the "one pot-three steps" ADP synthesis protocol. Preliminary studies of T_1 were performed on each reaction components, as well as an Ernst Angle study to ensure a qualitatively satisfactory analysis method. To obtain quantitative information, was necessary to set the scan repetition rate (d1 + the acquisition time in some cases, d1 + acquisition time + the waiting period in others) to a time longer than $5T_1$. The longest T_1 belonged to the integration standard compound trimethyl phosphate (8.25 s), whereas the other species involved in the reactions had smaller T_1 values (0.44-0.88 s), however, a single scan proved to be adequate to gain sufficient quantitative information. The T_1 value of 8.25 s was then used to calculate the repetition time (51 s), but this resulted NMR experiments that were too slow in comparison to the reaction, which was essentially complete within few min. Thus, to improve the time-responsiveness of our NMR experiments, I considered the longest T_1 of our analytes (excluding the trimethyl phosphate standard), which are all under 1 s (the largest was for the P(III) reagent at 0.88 ± 0.01 s). Thereafter, a correction factor was applied to the integrals of signals for trimethyl phosphate before plotting and analysing datasets (see Chapter 4, section 4.2.2.2.3.1).

The NMR experiments of both the coupling and oxidation steps were set to record ^{31}P spectra at 25 °C with a single transient (nt=1), an acquisition time of 1.5 s and a relaxation delay of 3.5 s between acquisitions over a period of 100 min. After applying the correction factor to trimethyl phosphate, I obtained quantitative results where the summation of integrals across all P species at a given timepoint was constant. This constant value demonstrated that all P species were being accounted for throughout the time-course. Inconsistent results prevented analysis of the reaction rate kinetics. This inconsistency was a product of not using stock solutions for the respective reagents and practical time constraints; the reaction occurred on a shorter timescale than that of sample preparation and data acquisition in the standard spectrometer (see Chapter 4, section 4.2.2.2.3.2).

The translation of the batch "one pot-three steps" ADP synthesis method into a semi-continuous flow system (Chapter 4,4.2.2.3.1) was initiated by performing the coupling reaction in a *Uniqsis* FlowSyn, 0.27 mL chip flow reactor, with freshly made solutions of

reagents. This method, however, although delivering promising results (i.e. up to 94% AMP consumption detected by ^{31}P NMR after oxidation step and up to 94% AMP consumption after deprotection step), gave inconsistent outcomes.

Therefore, I subsequently developed a workflow approach to reliably deliver stock solutions of each reagent via a quantitative ^{31}P NMR method, devised using the T_1 values mentioned above. A robust method to prepare reagent and substrate stock solutions at well-defined concentrations between 0.20 and 0.25 M was then created.

With this robust workflow in place the "one pot-three steps" ADP synthesis was translated to a 2.5 mL flow coil. At the end of each oxidation and deprotection step, the crude material was analysed using a quantitative ^{31}P NMR method. From these analyses it emerged that the percentage conversion of AMP to ADP was reduced after the deprotection step, compared to the level of AMP consumption that was observed directly after the oxidation step. Efforts to increase the conversion levels to ADP after the Fm-deprotection step started by testing different concentrations of *t*BuOOH 70% in H_2O, and testing different oxidants systems, (i.e.*t*BuOOH 5M in decane and *m*CPBA). The results showed poorer performance with *m*CPBA, and similar performances between *t*BuOOH 70% in H_2O and *t*BuOOH 5M in decane. With a reasonably firm conclusion that water was not the cause of the reversion to AMP, I focused on the piperidine Fm-deprotection step, exploring:

1. Reaction time (~ few seconds, ~ 1 min, ~ 10 min).
2. The stoichiometry of piperidine addition (5, 10, 15 equiv. of piperidine)
3. Fm-deprotection reaction temperature (0 ºC, 25 ºC)
4. The amine base adopted as deprotecting reagent.

Different tiers of experiments were set up against each point, leading to the following conclusions:

1. The deprotection reaction time had essentially no effect on the outcome;
2. The base addition temperature did not affect the outcome;
3. The adoption of 5 equiv. led to a poorer outcome compared to the use of 10 or 15 equiv. of piperidine (76% vs 80-82%);
4. The screening of different deprotecting reagents showed:
    - Piperidine (99% AMP consumption detected by ^{31}P NMR after oxidation step and 83% AMP consumption after deprotection step);

- Morpholine (99% AMP consumption detected by ^{31}P NMR after oxidation step and 83% AMP consumption after deprotection step);
- DBU (99% AMP consumption detected by ^{31}P NMR after oxidation step and 98% AMP consumption after deprotection step);
- TMG (99% AMP consumption detected by ^{31}P NMR after oxidation step and 98% AMP consumption after deprotection step);
- Triethylamine (99% AMP consumption detected by ^{31}P NMR after oxidation step and 92% AMP consumption after deprotection step);
- Hünig's base (99% AMP consumption detected by ^{31}P NMR after oxidation step and 75% AMP consumption after deprotection step).

The best results were obtained with TMG and DBU, and the next set of ADP synthesis experiments were carried out using TMG as deprotecting reagent (see Chapter 4, 4.2.2.3.2.2).

Comparative experiments between TMG and piperidine deprotecting agents were performed and the crude materials were purified using Teledyne CombiFlash NextGen 100 under our purification method [(15.5 g RediSep Gold® Amine column using gradient elution with triethylamine bicarbonate buffer (from 0.05 M to 1 M)]. The crude material obtained from TMG deprotection showed a relative higher purity level compared to the crude material obtained from piperidine purification, and, on this basis, an up-scaled ADP synthesis was performed using TMG as deprotection reagent.

Until that point, the flow experiments for the synthesis of ADP, had been performed using a 0.27 mL chip reactor and 2.5 mL coil, on a scale of 0.25 mmol (~ 150 mg of AMP $TBA_{1.2}$ $H_{0.8}$) and 1 mmol (~ 500 mg of AMP $TBA_{1.2}$ $H_{0.8}$) respectively. In the scale-up, 2 g of AMP $TBA_{1.2}$ $H_{0.8}$ was used as substrate, delivering 1 g of ADP product, with purity >99% by HPLC (see Chapter 4, section 4.2.2.3.2.2).

The smaller scale method was also applied towards the syntheses of CDP from CMP and UDP from UMP (see Chapter 4, section 4.2.2.4). The results obtained for UDP synthesis proved the procedure to be effective (90% UMP consumption detected by ^{31}P NMR after oxidation step and 85% UMP consumption after deprotection step using piperidine). The synthesis of CDP presented solubility problems. Several different concentrations of substrate were explored, alongside different temperatures and coil lengths without delivering significant improvement. This result, 65% CMP consumption detected by ^{31}P NMR after oxidation step, is still a promising starting point for future work.

I chose not to explore GMP as a substrate because of the problems encountered with CMP, where CMP is usually viewed as being more soluble than GMP.

5.2.2 Future plans

Thanks to the promising results obtained, I are able to suggest both short- and long-term plans for the future of this project.

First, moving further along the path towards translation of the "one pot-three steps" ADP synthesis into a semi- continuous flow system, both the coupling and the oxidation steps should be performed in flow, with quenching of the oxidized reaction into a solution of TMG 5% v/v in DMF (as shown in *Figure 67*). Moreover, thanks to the interesting results observed from the screening of different deprotecting reagents, also DBU should be more explored as deprotecting reagent alongside TMG.

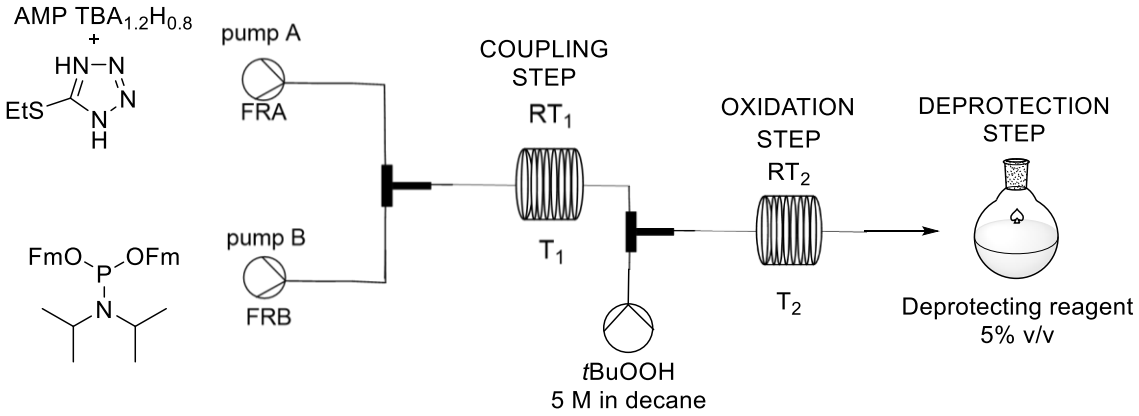

Figure 67: Suggested representation of the coupling and oxidation steps of the one pot-three steps ADP synthesis in a semi-continuous flow system.

Additionally, after optimization of the oxidation step in flow, a further step forward would be the translation of the deprotection reaction from batch into the continuous flow system. Upon the addition of piperidine and TMG, precipitation of the deprotected material is observed. These precipitations would clog a flow system, however, triethylamine as deprotecting reagent only showed signs of precipitation after 30 min of stirring. Thus, the translation of the deprotection step into flow, as suggested in *Figure 68*, could be possible, with the product triethylammonium nucleotide also lending itself to re-solubilisation and iterative phosphorylation.

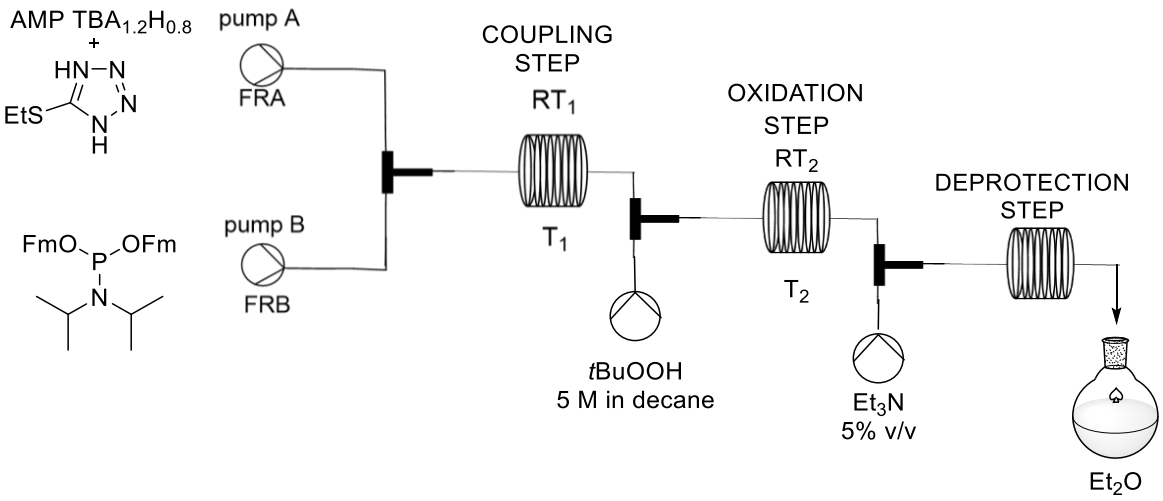

Figure 68: Suggested representation of the "one pot-three steps" ADP synthesis performed into a continuous flow system.

As with our previous developments, the method should be tested and optimized using AMP as substrate before deploying it against a wider range of nucleotides.

Alongside with these flow studies, a broader screening of green solvents should be conducted to find better candidates than DMF. As mentioned above, this would make both the manufacturing safer and more sustainable.

The ion exchange chromatography method, used for the purification of the scaled synthesis of ADP, should be tested across different substrates, buffers, gradients, and media.

The adoption of our ^{31}P NMR method on a stop flow NMR platform would give real-time results, avoiding the limitations of classical NMR and allowing reliable measurement of the kinetic process.

In summary, an effective, robust method for addition of phosphates has been demonstrated, and a significant number of our initial aims have been achieved.

6 General experimental procedures

Unless otherwise stated, all solvents were purchased from Fisher Scientific and used without further purification. Dry solvents were were purchased from SigmaAldrich and used without further purification. Substrates, their precursors, and reagents were purchased from either Alfa Aesar, Sigma-Aldrich, TCI, Carbosynth or Acros Organics. Reactions were conducted in flow using the following equipment Vapourtec Vapourtec E-series system equipped with three V-3 peristaltic pumps, an SF-10 peristaltic pump, two Polar Bear Plus machines and *Uniqsis* FlowSyn system along with standard PTFE tubing and reactor coils. Chromatography was performed on a Teledyne CombiFlash NextGen 100 system. For TLC, Sigma-Aldrich plates were used, and visualisation was performed using UV-irradiation.

All reactions using air sensitive, or moisture sensitive reagents were carried out under nitrogen atmosphere. Nuclear Magnetic Resonance (NMR) spectra were recorded on a Bruker Neo-400 spectrometer with operating frequencies of 400.20 MHz for ^{1}H, 100.63 MHz for ^{13}C and 162.00 MHz for ^{31}P at 25 °C and Varian VNMRS-600 spectrometer with operating frequencies of 599.242 MHz for ^{1}H, 92.01 MHz for ^{2}H, 150.72 MHz for ^{13}C and 242.65 MHz for ^{31}P at 25 °C. Nuclear Magnetic Resonance (NMR) time course spectra were recorded on a Varian DD2-500 spectrometer with operating frequencies of 499.53 MHz for ^{1}H and 202.21 MHz for ^{31}P at 25 °C. Chemical shifts of species (^{1}H and ^{31}P NMR) were related to known compounds or compared with samples of commercially available compounds. Low resolution liquid chromatography mass spectrometry (LC-MS) was performed using a Waters TQD mass spectrometer and an Acquity UPLC BEH C18 1.7µm column (2.1 mm x 50 mm) in ESI mode with a MeCN:Water (0.1% formic acid) as mobile phase in gradient conditions (ramping from 95:5 to 5:95 MeCN:Water (0.1% formic acid) in 4 minutes). ESI-HRMS was performed using a Waters QtoF Premier mass spectrometer. For accurate mass measurements the deviation from the calculated formula is reported in ppm and mDa.

6.1 Synthesis of *bis*-(fluorenylmethyl)-diisopropylamine phosphoramidite (2)

This section reports the procedures followed for the synthesis of *bis*-(fluorenylmethyl)-diisopropylamine phosphoramidite (**2**). First, I report the procedures followed and developed for the synthesis of **2** in batch, see section 6.1.1, and subsequently the procedure developed for the flow synthesis, see section 6.1.2.

6.1.1 Batch syntheses of *bis*-(fluorenylmethyl)-diisopropylamine phosphoramidite (2)

Our experiments built on the two-step procedure published by Bialy and Waldmann[1, 2, 145] and on the one pot synthesis developed by Dësmale[3] (see procedures reported in Chapter 4, section 4.1.1 and 4.1.2).

6.1.1.1 Synthesis of *N,N*-diisopropylphosphoramide dichloridite (1) based on Bialy and Waldmann's procedure[1, 2, 145]

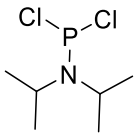

Under an inert atmosphere, anhydrous diisopropylamine (20.4 mL, 145.6 mmol, 2 equiv.) was added dropwise to an ice-cooled solution of phosphorus trichloride (26.4 mL, 72.8 mmol, 1 equiv.) in anhydrous THF (100 mL) over the course of 1 h. The ice bath was removed, and the mixture was stirred at room temperature for a further 3 h, then filtered under vacuum. The solids were washed with anhydrous THF, and the filtrate was collected. The filtrate was concentrated under reduced pressure on a rotary evaporator to give a yellow oil, which was distilled at 164 °C, under 1 atm to give *N*,*N*-diisopropylphosphoramide dichloridite (3.3 g, 22%).

^{31}P NMR (162 MHz, $CDCl_3$): δP =169.5;

^{1}H NMR (400 MHz, $CDCl_3$)**:** δH = 3.89–3.99 (app h. J= 6.7 Hz, 2 H).1.29 (d, J = 6.85 Hz, 12 H).

6.1.1.2 Attempted synthesis of *bis*-(fluorenylmethyl)-diisopropylamine phosphoramidite (2) from N,N-diisopropylphosphoramide dichloridite (1) using Bialy and Waldmann's procedure[1, 2, 145]

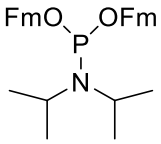

product expected (**2**)

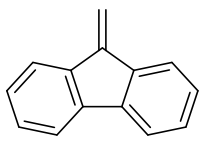

product formed (**3**)

Under an inert atmosphere, *N*,*N*-diisopropylphosphoramide dichloridite (**1**) (0.50 g, 2.50 mmol, 1 equiv.) was added dropwise to an ice-cooled solution of 9-fluorenylmethanol (0.98 g, 5.0 mmol, 2 equiv.) and diisopropylethylamine (1.6 mL, 9.25 mmol, 3.7 equiv.) in anhydrous THF (5 mL). The ice bath was removed, and the mixture was stirred for 1 h at room temperature. Over the course of the reaction a white precipitate formed. The mixture was diluted with phosphate buffer (1 M, pH 7, 5 mL) and EtOAc (10 mL). The layers were separated, and the aqueous layer was extracted with EtOAc (10 mL). The combined organic extracts were dried (Na_2SO_4), filtered and concentrated under reduced pressure on a rotary evaporator to give an oily residue. Chromatography on silica gel (cyclohexane/EtOAc/Et_3N 20:1:0.2) was attempted. The major fraction based on UV-vis detection was concentrated under reduced pressure, however, the material did not show the expected signal at 146.11 ppm in the ^{31}P NMR spectrum. ^{1}H NMR analysis revealed the material to be fluorene (**3**).

^{1}H NMR (400 MHz, $CDCl_3$): δH = 7.82-7.63 (m. 4H), 7.46-7.32 (m, 4H) 6.11 ppm (s, 2H).

(Traces of hexane and EtOAc were apparent in the ^{1}H NMR spectra).

6.1.1.2.1 Synthesis of *bis*-(fluorenylmethyl)-diisopropylamine phosphoramidite (2) from *N*,*N*-diisopropylphosphoramide dichloridite (1 with hexane-based extraction of crude product (see section 6.1.1.2)

Under an inert atmosphere, *N*,*N*-diisopropylphosphoramide dichloridite (0.50 g, 2.50 mmol, 1 equiv.) was added dropwise to an ice-cooled solution of 9-fluorenylmethanol (0.98 g, 5.0 mmol, 2 equiv.) and *N*,*N*-diisopropylethylamine (1.6 mL, 9.25 mmol, 3.7 equiv.) in anhydrous THF (5 mL). The mixture was stirred for 1 h at room temperature, whereupon a white precipitate formed. The solvent was removed under reduced pressure on a rotary evaporator and the resulting pale-yellow solid was extracted with freshly distilled hexane (10 mL). The insoluble *N*,*N*-diisopropylethylamine hydrochloride salt was removed via vacuum filtration, and washed with hexane (20 mL). The filtrate was concentrated under reduced pressure on a rotary evaporator to give the crude phosphoramidite as a yellow oil (1.04 g, 80% mass recovery, 90% purity by ^{31}P NMR spectroscopy).

^{31}P NMR (162 MHz, $CDCl_3$): δP =146.11 (138.26, 121.81, 14.11 impurities).

^{1}H NMR (400 MHz, $CDCl_3$): δH = 7.82-7.79 (m, 4 H), 7.74-7.59 (m, 4 H), 7.47-7.39 (m, 4 H), 7.38-7.31 (m, 4 H) 4.5 (t, J = 6.9 Hz, 2 H), 4.11-4.05 (m, 2 H), 3.91-3.85 (m, 2 H), 3.73–3.68 (m, 2 H), 1.22 (d, J = 7.1 Hz, 12 H).

^{13}C NMR (101 MHz, D_2O): δC = 144.99 (C ×2), 144.70 (C ×2), 141.44 (C ×2), 141.32 (C ×2), 127.48 (CH×4), 127.44 (CH×4), 126.91 (CH×4), 126.88 (CH×4), 125.52 (CH×4), 125.27 (CH×4),, 119.94(CH×4), 119.84 (CH×4), 66.05 (CH_2), 65.88 (CH_2), 49.25 (d, $^{3}J_{C\text{-}P}$ = 7.8 Hz, CH×2), 49.20 (CH×2), 43.08 (d, $^{2}J_{C\text{-}P}$ = 7.8 Hz, CH×2) 24.70 ((d, $^{3}J_{C\text{-}P}$ = 7.4 Hz, CH_3×4) [found traces of hexane at 31.69, 22.76, 14.25].

HR-MS calculated for $C_{34}H_{37}NO_2P$ 522.2554, found 522.2562 (Δ = –0.8 mDa; –1.5 ppm).

6.1.1.3 Synthesis of *bis*-(fluorenylmethyl)-diisopropylamine phosphoramidite (2) based on Dësmale's method [3]

Under an inert atmosphere, *N*,*N*-diisopropylethylamine (1.48 g, 11.5 mmol, 2 equiv.) was added to an ice-cooled solution of PCl_3 (0.79 g, 5.7 mmol, 1 equiv.) in anhydrous THF (20 mL). *N*,*N*-Diisopropylamine (1.50 mL, 10.7 mmol, 1.7 equiv.) was then added over the course of 10 min. The mixture was stirred at 0 °C for 1 h, then another portion of *N*,*N*-diisopropylethylamine (1.48 g, 11.5 mmol, 2 equiv.) was added while maintaining the reaction mixture at 0 °C, followed by the addition of 9-fluorenylmethanol (2.24 g, 11.5 mmol, 2 equiv.) in anhydrous THF (5 mL). The reaction mixture was stirred at room temperature for 24 h then concentrated under reduced pressure. The residue was suspended in 1 M phosphate buffer solution at pH 7 (20 mL) and the mixture was extracted with EtOAc (4 × 50 mL). The combined organic layers were washed with phosphate buffer (1 M, pH 7, 20 mL), dried with $MgSO_4$ and concentrated under reduced pressure on a rotary evaporator to give a yellow oil (2.41 g, 81% mass recovery and 85% purity by ^{31}P NMR spectroscopy).

6.1.1.3.1 Syntheses of the *bis*-(fluorenylmethyl)-diisopropylamine phosphoramidite (2) using different solvents, adapted from the procedure reported in section 6.1.1.2.1

Based on the batch procedure reported in 6.1.1.2.1, the synthesis of *bis*-(fluorenylmethyl)-diisopropylamine phosphoramidite (**2**) was explored in several solvents (See *Table 14* for details).

Under an inert atmosphere, anhydrous, distilled *N*,*N*-diisopropylethylamine (2 equiv.) was added dropwise to an ice-cooled solution of PCl_3 (see *Table 14* for details of the mmol amount) in the chosen solvent (see *Table 14* for details and volumes). Additional anhydrous, distilled *N*,*N*-diisopropylamine (1.2 equiv.) was added to the mixture over a period of 5 min. After the mixture had been stirred at 0 °C for 20 min, a third portion of *N*,*N*-diisopropylethylamine (2 equiv.) was added followed by a solution of 9-fluorenylmethanol (2 equiv.) in anhydrous THF (5 mL). The mixture was allowed to warm to room temperature, with stirring, over 30 min. During this period, aliquots (0.5 mL) were removed from the reaction mixture every 10 min, diluted with $CDCl_3$ (0.25 mL) and analysed by ^{31}P NMR spectroscopy to monitor the progress of the reaction. At the end of the reaction, as determined by ^{31}P NMR spectroscopy, the solvent was removed under reduced pressure on a rotary evaporator and the resulting pale-yellow solid was extracted with freshly distilled hexane (40 mL). The insoluble *N*,*N*-diisopropylethylamine hydrochloride salt was removed by vacuum filtration, and washed with *hexane* (2 × 20 mL). The filtrate was concentrated under reduced pressure on a rotary evaporator to give the crude phosphoramidite as a yellow oil. The crude yields of the materials were measured, and the materials were analysed by ^{31}P NMR spectroscopy to estimate purity.

Entry	PCl_3 (mmol)[a]	Reaction solvent (mL)	Workup solvent (mL)	Mass recovery (%)[b]	Purity (%)[c]	Homogeneity
1	5	dry THF (20 mL)	hexane	86	97	suspension
2	5	dry CH_2Cl_2 (20 mL)*	hexane	90	84	solution
3	10	dry α,α,α-trifluorotoluene (10 mL)	hexane	95	84	suspension
4	2	Cyrene (10 mL)*	EtOAc	20	72	suspension
5	2	Cyrene (10 mL)*	hexane	7	83	suspension
7	2.5	2-methyl THF. (10 mL)	hexane	74	84	suspension
8	2.5	toluene* (10 mL)	hexane	75	98	suspension
9	2	dry *hexane* * (10 mL)	no workup	—	—	suspension

a: quantity of substrate expressed in mmol; b: mass recovery of the crude of crude phosphoramidite yield estimate based on 100% purity; c: Purity estimated by 31P NMR spectroscopy.

Table 14: Results of experiments for the optimization of the synthesis of *bis*-(fluorenylmethyl)-diisopropylamine phosphoramidite (**2**) based on modification of the procedure reported in section 6.1.1.3.1.

6.1.1.3.2 Batch syntheses of the *bis*-(fluorenylmethyl)-diisopropylamine phosphoramidite (2) using varying concentrations of reagents in CH_2Cl_2-THF 4:1 based on the procedure reported in section 6.1.1.3.1

The batch procedure reported in section 6.1.1.3.1 (*Table 14,* entry 2) was adapted to explore the synthesis of *bis*-(fluorenylmethyl)-diisopropylamine phosphoramidite (**2**) through a series of experiments where the reaction solvents were CH_2Cl_2-THF 4:1 (see *Table 15* for details), and PCl_3 and other reagent concentrations were varied to explore whether the reaction mixture

remained homogeneous. Furthermore, the effectiveness of different post-reaction extraction solvents was also explored.

Under an inert atmosphere, anhydrous, commercially available distilled *N*,*N*-diisopropylethylamine (2 equiv.) was added dropwise to an ice-cooled solution of PCl_3 (see *Table 15* for mmol amounts) in commercially available anhydrous CH_2Cl_2 (see *Table 15* for mL volumes). Additional commercially available, anhydrous, distilled *N*,*N*-diisopropylamine (1.2 equiv.) was added to the mixture over a period of 5 min. After the mixture had been stirred at 0 °C for 20 min, a third portion of *N*,*N*-diisopropylethylamine (2 equiv.) was added followed by a solution of 9-fluorenylmethanol (2 equiv.) in anhydrous THF. The mixture was allowed to warm to room temperature, with stirring, over 30 min. During this period, aliquots (0.5 mL) were removed from the reaction mixture every 10 mins, diluted with $CDCl_3$ (0.25 mL) and analysed by ^{31}P NMR spectroscopy to monitor the progress of the reaction. At the end of the reaction, as determined by ^{31}P NMR spectroscopy, the solvent was removed under reduced pressure on a rotary evaporator, and the resulting pale-yellow solid was agitated with solvent (see *Table 15* for details and volumes). The insoluble diisopropylethylamine hydrochloride salt was removed by vacuum filtration, and the filter paper was washed with hexane (2 × 20 mL). The solution was concentrated under reduced pressure on a rotary evaporator to give the phosphoramidite as a yellow oil (mass recovery and purity levels are reported in *Table 15*).

Entry	PCl_3 (mmol)[a]	CH_2Cl_2: THF = 4:1 (mL)	Workup solvent (mL)	Mass recovery (%)[b]	Purity (%)[c]
1	10	40:10	hexane (40 mL)	72	84
2	10	10:2.5	hexane (40 mL)	86	86
3	5	20:5	hexane (20 mL)	90	84
4	50	200:50	hexane (100 mL)	97	85
5	5	20:5	*n*-heptane (20 mL)	96	80
6	5	20:5	cyclohexane (20 mL)	94	79

Legend: a: quantity express in mmol of starting material; b: mass recovery of the crude of crude phosphoramidite yield estimate based on 100% purity; c: purity analysed by ^{31}P NMR.

Table 15: Set of experiments for the synthesis of *bis*-(fluorenylmethyl)-diisopropylamine phosphoramidite (**2**) using CH_2Cl2-THF 4:1 based on modification of the procedure reported in section 6.1.1.3.2.

6.1.2 Flow synthesis of *bis*-(fluorenylmethyl)-diisopropylamine phosphoramidite (2) using CH_2Cl_2-THF 4:1

The procedures developed for the synthesis in flow of *bis*-(fluorenylmethyl)-diisopropylamine phosphoramidite (**2**) are reported below. Only one synthetic route is described in its entirety. Different conditions were screened: coil lengths for the first reaction step, flow rates, reaction timing and concentrations of the reagents (all reaction details and results are listed in *Table 16*). Full details of the results and discussion can be found in Chapter 4, section 4.1.2.

The following solutions were prepared in anhydrous CH_2Cl_2: PCl_3 (2 mol·L^{-1}) containing *N*,*N*-diisopropylethylamine (4 mol·L^{-1}), and *N*,*N*-diisopropylamine (2.4 mol·L^{-1}). A stock solution of 9-fluorenylmethanol (4 mol·L^{-1}) containing *N*,*N*-diisopropylethylamine (4

mol·L^{-1}) was prepared in commercially available anhydrous THF. PCl_3 containing *N*,*N*-diisopropylethylamine and *N*,*N*-diisopropylamine solutions were pumped from their flasks into a Vapourtec E-series system equipped with three V-3 peristaltic pumps, an SF-10 peristaltic pump, T-mixer connections and two coil reactors with temperatures controlled by two Polar Bear Plus machines. The solutions were pumped through a suction needle at flow rate A (FRA = see *Table 16*) and flow rate B (FRB = FRA) using pumps A and B, respectively, and mixed in a 49 mL coil (PTFE). The 9-fluorenylmethanol solution was pumped from its flask at the same flow rate (FRC = FRA) and mixed in a 51 mL coil (PTFE) with the *N*,*N*-diisopropylphosphoramide dichloridite intermediate generated from the first coiled reactor. The reacted materials were collected, the solvents were removed under reduced pressure on a rotary evaporator and the resulting pale-yellow solid was agitated with freshly distilled *hexane* (40 mL). The precipitated diisopropylethylamine hydrochloride salt was removed by vacuum filtration, and the solids were washed with *hexane* (2 × 20 mL) to extract the desired compound. The solution was concentrated under reduced pressure on a rotary evaporator to give the title compound as a yellow oil, and the resulting materials were analysed by ^{31}P NMR spectroscopy (see *Table 16* below for individual results).

Entry	$FR_A=FR_B=FR_C$ ($mL \cdot min^{-1}$)[a]	T_1 (°C)[b]	T_2 (°C)[c]	RT_1 (min)[d]	RT_2 (min)[e]	PCl_3 ($mol \cdot L^{-1}$)[f]	Mass recovery (%)[g]	Purity (%)
1	0.6	0	24	40	28	0.2	52	68
2	0.6			40	28	1	66	84
3	0.6			40	28	2	73	80
4	1			25	17	2	54	84
5	1	24		25	17	2	81	84
6	0.6			40	28	2	80	82
7	1			25	17	2	71	82
8	1			10	17	2	73	82
9	1			7	17	2	54	84
10	1			7	17	1	50	87
11	1			10	17	1	70	80

Legend: a FR: flow rate each pump. b T1: reaction temperature in the first coil. c T2: reaction temperature in the second coil. d RT1: residence time of the first reaction step. e RT2: residence time of the second reaction step. f C: concentration. g mass recovery of the crude phosphoramidite estimate based on 100% purity.

Table 16: Flow reaction experiments for the synthesis of *bis*-(fluorenylmethyl)-diisopropylamine phosphoramidite (**2**) using CH_2Cl_2-THF 4:1 as solvents.

6.2 Workflows for One Pot-Three Steps Nucleoside Diphosphate (NDP) syntheses in batch and flow

6.2.1 Synthesis of the NMP TBA_xH_{2-x} salts

Adenosine, uridine and cytidine monophosphates were converted to their TBA salts to facilitate solubilization in DMF.

6.2.1.1. Adenosine monophosphate $TBA_{1.2}$ $H_{0.8}$ (4)

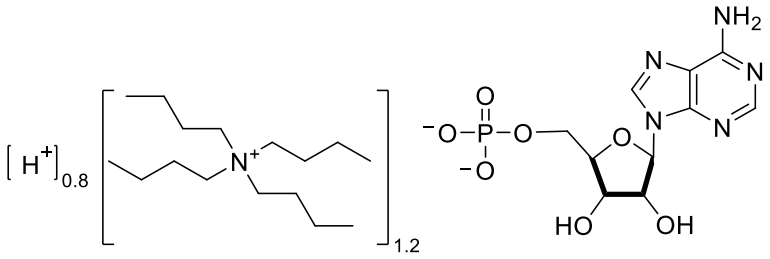

5'-AMP (acid form, 5.0 g, 14.4 mmol) was dissolved in purified H_2O (10 mL) at room temperature. Tetrabutylammonium hydroxide (40% v/v solution in water, 4.49 g; 17.3 mmol, 1.2 equiv.) was added to the solution and the mixture was stirred at room temperature for 20 min. The product was isolated as a white solid by overnight freeze drying (8.90 g, 97%).

^{31}P NMR (242.65 MHz, D_2O): $\delta P = 1.22$.

^{1}H NMR (599.42 MHz, D_2O): δH = 8.33 (s, 1H), 7.99 (s, 1H), 5.91 (d, J = 5.8 Hz, 1H), 4.57 (t, J = 5.5 Hz, 1H), 4.34-4.32 (m, 1H), 4.21 – 4.20 (m, 1H), 3.94-3.92 (m, 2H), 3.00 – 2.98 (m, 10H), 1.48-1.42 (m, 10H), 1.20-1,14 (h, J = 7.3 Hz, 11H), 0.76 (t, J = 7.5 Hz, 16H).
^{13}C NMR (150.72 MHz, D_2O): δC = 155.23 (C), 152.54 (C), 148.77 (C), 139.79 (C), 118.28 (C), 86.80 (CH), 84.18 (d, $^{4}J_{C,P}$= 8.8 Hz, CH), 74.38(CH), 70.44(CH), 64.03 (d, $^{3}J_{C-P}$ = 4.8 Hz, CH_2), 58.0 – 57.96 (m, CH_2), 23.00 (CH_2), 19.04 – 19.02 (m, CH_2), 12.72(CH_3).

HR-MS calculated for $C_{10}H_{15}N_5O_7P$ 348.0706, found 348.0709 (Δ = –0.3 mDa; –0.9 ppm).

6.2.1.2 Uridine monophosphate $TBA_{1.4}H_{0.6}$ (5)

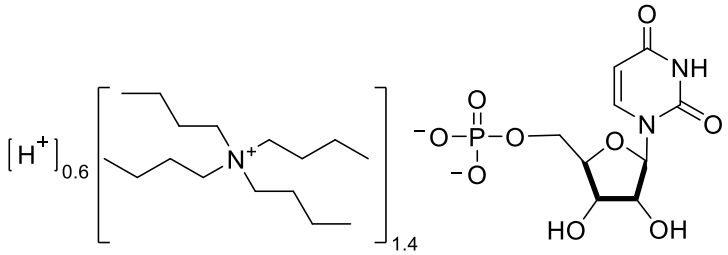

5'-UMP (acid form, 2.0 g, 5.4 mmol) was dissolved in distilled H_2O (5 mL) at room temperature. Tetrabutylammonium hydroxide (40% v/v solution in water, 3.5 g; 6.48 mmol, 1.2 equiv.) was added to the solution and the solution was stirred for 20 min at room temperature. The product was isolated as a white solid by overnight freeze drying (3.6 g, 95%).

^{31}P NMR (242.65 MHz, D_2O): $\delta P = 1.26$.

^{1}H NMR (599.42 MHz, D_2O): $\delta H = 7.88$ (d, J = 8.5 Hz, 1H), 5.84 (d, J = 5,3 Hz, 1H), 5.81 (d, J = 8.5 Hz, 1H), 4.23 (t, J = 5.3 Hz, 1H), 4.20– 4.18 (m, 1H), 4.13 – 4.11 (m, 1H), 3.97 – 3.94 (m, 1H), 3.91– 3.87 (m, 1H), 3.06–3.03 (m, 11H), 1.53 – 1.47 (m, 11H), 1.24 – 1.18(h, J = 7.4 Hz, 10H), 0.80 (t, J = 7.4 Hz, 17H).

^{13}C NMR (150.72 MHz, D_2O) δC: 166.19 (C), 151.77 (C), 141.71 (CH), 102.51 (CH), 88.27 (CH), 83.64-83.58 (d,$^{4}J_{C,P}$= 8.90 Hz, CH_2), 73.79 (CH), 69.78 (CH), 63.67 (d,$^{3}J_{C,P}$= 4.8 Hz, CH_2), 58.06 – 58.02 (m, CH_2), 23.05 (CH_2), 19.07– 19.05 (m, CH_2), 12.73 (CH_3).

HR-MS calculated for $C_9H_{14}N_2O_9P$ 325.0439, found 325.0437 (Δ = 0.2 mDa; 0.6 ppm).

6.2.1.3 Cytidine monophosphate $TBA_{1.2}H_{0.8}$ (6)

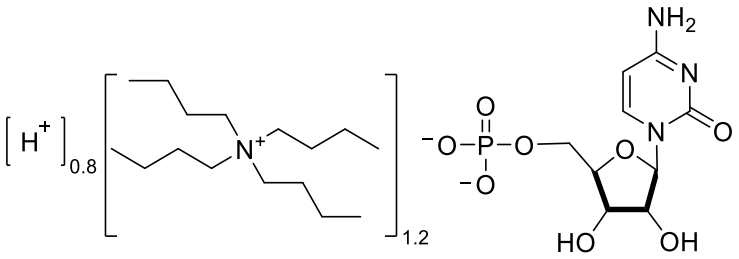

5'-CMP (acid form, 3.0 g, 9.1 mmol) was dissolved in distilled H_2O (5 mL) at room temperature. Tetrabutylammonium hydroxide (40% v/v solution in water, 7.1 g; 10.9 mmol, 1.2 equiv.) was added to the solution and the solution was stirred for 20 min at room temperature. The product was isolated as a white solid by overnight freeze drying (5.2 g, 96%).

^{31}P NMR (242.65 MHz, D_2O): δP = 0.81.

^{1}H NMR (599.42 MHz, D_2O): δH = 7.86 (d, J = 7.3 Hz, 1H), 5.96 (d, J = 7.3 Hz, 1H), 5.84 (d, J = 4.4 Hz, 1H), 4.18–4.15 (m, 2H), 4.12– 4.07 (m, 1H), 4.01 – 3.98 (m, 1H), 3.92 – 3.89 (m, 1H), 3.05– 3.02 (m, 10 H), 1.52 – 1.47 (m, 10H), 1.24 – 1.17(h, J = 7.3 Hz, 10H), 0.79 (t, J = 7.3 Hz, 15H).

^{13}C NMR (150.72 MHz, D_2O) δ 166.19 (C), 151.77 (C), 141.71 (CH), 102.51 (CH), 88.27 (CH), 83.63 (d,$^{4}J_{C,P}$= 8.90 Hz, CH_2), 73.79 (CH), 69.78 (CH), 63.67 (d,$^{3}J_{C,P}$= 4.90 Hz, CH_2), 58.06 – 58.02 (m, CH_2), 22.97 (CH_2), 19.07 – 19.05 (m,CH_2), 12.69 (CH_3).
HR-MS calculated for $C_9H_{15}N_3O_8P$ 324.0590, found 324.0597(Δ = –0.7 mDa; –2.2 ppm).

6.2.2 Batch Synthesis of NDPs following Jessen reported procedures[1]

The batch syntheses of NDPs listed below were initially based on the protocols reported by the Jessen group[1, 145] and our own findings for the preparation of ATP from ADP. In the first set of experiments, the solvents DMSO, DMSO-d6 and DMF were compared in terms of solubility (see Chapter 4, section 4.2.2.1). Yields were not recorded, however, outcomes based on NMR spectra are reported in Chapter 4, section 4.2.2.1.

6.2.2.1 Procedure for the synthesis of Adenosine Diphosphate, following the Jessen's DMSO reported procedures for the synthesis of NDPs[1] (see Chapter 4, section 4.2.2.1)

To identify a method that was congenial in terms of solubility for application in flow, I first tested the solubilities of the tri-*n*-octylammonium, trihexylammonium and pyridinium salts of AMP in 1.5 mL of DMSO-d6 as described in Chapter 4, section 4.2.2.1. The results obtained are discussed in Chapter 4, section 4.2.2.1. The pyridinium salt of AMP was used as substrate for the DMSO-based experiments.

5'-AMP (acid form, 100.0 mg, 0.28 mmol) was added to 1.0 mL of DMSO (or DMSO-d6) and tri-*n*-octylamine or trihexylamine or pyridine (0.28 mmol, 1.0 equiv.). 5-(ethylthio)-1*H*-tetrazole (47 mg, 0.36 mmol, 1.3 equiv.) was added to the reaction mixture followed by a solution of *bis*-(fluorenylmethyl)-diisopropylamine phosphoramidite (**2**) (from 1.2 to 1.5 equiv.) of DMSO (or DMSO-d6) (0.500 mL). After ~ 10 min, *t*BuOOH 70% in H_2O (49 μL, 0.36 mmol, 1.3 equiv.) or *m*CPBA (63 mg, 0.36 mmol, 1.3 equiv.) were added carefully to the mixture. Approximately 5 min after the addition of oxidant, the Fm protecting groups were cleaved using piperidine (75 μL of a 5% v/v solution in DMSO). After stirring for ~ 10 min, the product was precipitated by the addition of Et_2O (5 mL). The precipitate was isolated by centrifugation or filtration, washed with Et_2O and dried *in vacuo*. The resulting materials were analysed by ^{31}P NMR spectroscopy.

Entry	5'-AMP counterion	Consumption of AMP after deprotection (%)[a]	Homogeneity during reaction
1	pyridinium	53%	clear solution
2	tri-n-octylammonium)	40%	cloudy solution
3	trihexylammonium	55%	clear solution

Legend: a: (%) Conversion rate by ^{31}P NMR.

Table 17: ^{31}P NMR spectroscopy results and homogeneity of the ADP synthesis from the tri-*n*-octylammonium, trihexylammonium and pyridinium salts of AMP as substrates.

6.2.2.2 Procedure for the synthesis of Adenosine Diphosphate, following Jessen's DMF reported procedures for the synthesis of NDPs[1] (see Chapter 4, section 4.2.2.1)

The procedure reported below describes the synthesis of ADP in DMF. The reaction outcomes were compared to earlier results (see section 6.2.2.1) obtained using DMSO as solvent. These reactions were carried out to identify the best synthetic method in terms of solubility for application in flow.

5'-AMP $TBA_{1.2}H_{0.8}$ (**4**) (178.0 mg, 0.28 mmol) was dissolved in DMF (1.0 mL). 5-(ethylthio)-1*H*-tetrazole (47 mg, 0.36 mmol, 1.3 equiv.) was added to the reaction mixture followed by a solution of *bis*-(fluorenylmethyl)-diisopropylamine phosphoramidite (**2**) (188.0 mg, 0.36 mmol, 1.3 equiv.) in DMF (0.500 mL). After ~ 10 min, *t*BuOOH 70% in H_2O (49 µL, 0.36 mmol, 1.3 equiv.) or *m*CPBA (63 mg, 0.36 mmol, 1.3 equiv.) were added and the mixture was stirred for < 5 min. The Fm protecting groups were cleaved using piperidine (75 µL of a 5% v/v solution in DMF). After stirring for ~ 10 min, the product was precipitated by addition of Et_2O (5 mL). The precipitate was isolated by centrifugation or filtration, washed with Et_2O and dried *in vacuo.* The resulting materials were analysed by ^{31}P NMR spectroscopy which showed 56% consumption of AMP after the deprotection step.

6.2.3 Semi Continuous Flow Synthesis of Nucleoside Diphosphates (NDPs) (see Chapter 4, see section 4.2.2.3)

Nucleoside Diphosphates (NDPs) synthesis flow method optimizations are reported below. In the most part, crude reaction mixtures were analysed by ^{31}P NMR spectroscopy to determine levels of consumption of starting nucleotide, conversion to product nucleotide and fate of reagent. In section 6.2.4.2.2.2.3, a scaled-up of synthesis of triethyl-ammonium ADP (1.0 g isolated) was performed, and the crude reaction products were resolved by preparative anion exchange chromatography.

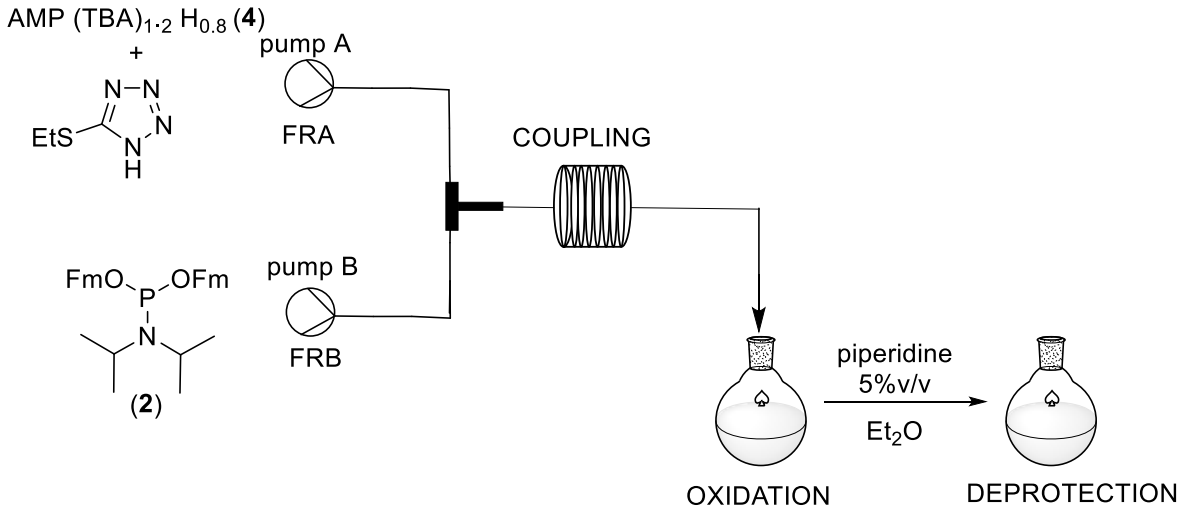

Figure 69: Scheme of semi-flow synthesis setup for NDPs.

As illustrated in *Figure 69*, the coupling step of the one pot three step reaction for the synthesis of NDPs was performed using a flow reactor, followed by the oxidation and the deprotection steps performed in batch. The development of the flow chemistry was discussed in Chapter 4. Our initial experiments focused on using 5'-AMP $TBA_{1.2}H_{0.8}$ (**4**) as the substrate and DMF as the reaction solvent. Coupling reactions were initially carried out with freshly prepared stock solutions, where the *bis*-(fluorenylmethyl)-diisopropylamine phosphoramidite (**2**) was weighed out. Subsequently, to create a robust and reliable method, stock solutions were prepared, analysed by quantitative NMR methods and their concentrations were then standardized before use (see section 6.2.4 and section 6.2.4.1). After optimization, UDP synthesis was also carried out following the same method.

6.2.3.1 Semi continuous flow synthesis of bis-piperidinium ADP (7) using a 0.27 mL chip reactor and substrate/stock solutions prepared by weighing (see Chapter 4, section 4.2.2.3.1)

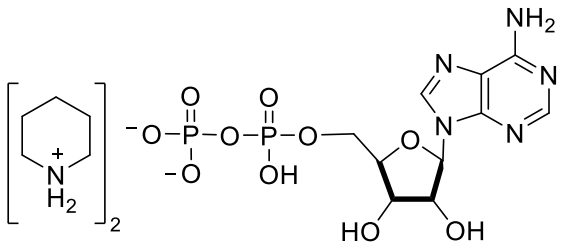

A solution containing 5'-AMP $TBA_{1.2}H_{0.8}$ (**4**) (0.18 mol·L^{-1}, 1.0 equiv.) and 5-(ethylthio)-1*H*-tetrazole (see *Table 19*) in anhydrous DMF (2.5 mL), and a solution of *bis*-(fluorenylmethyl)-diisopropylamine phosphoramidite (**2**) (0.36 or 0.23 mol·L^{-1}, 2.0 or 1.3 equiv.) in anhydrous DMF (2.5 mL) were pumped from their flasks through a suction needle at flow rate A (FRA = 0.040 mL·min^{-1}) and flow rate B (FRB = FRA) using pumps A and B, respectively. These were combined in a glass mixing chip held at 25 °C (0.27 mL, *Uniqsis* FlowSyn system). After establishing stable flow (approximately 2 coil volumes), the resulting coupling mixture was then quenched directly into a solution of *t*BuOOH 70% in H_2O (0.46 mL, 5 equiv.) in dry DMF (2.5 mL). Following complete oxidation as confirmed by ^{31}P NMR analysis, the Fm protecting groups were cleaved with piperidine (5% v/v solution in DMF, 0.25 mL). After deprotection, the product was precipitated by addition of Et_2O. The precipitate was isolated by centrifugation or filtration, washed with Et_2O and dried *in vacuo*, (see *Table 18* below for individual results).

Entry	Amidite (2) (eq.)[a]	Activator (eq.)[a]	Consumption AMP after ox. (%)[b]	Consumption AMP after dep. (%)[b]
1	1.3	1.3	90	84
2	1.3	2	88	82
3	2		–	-–
4	1.3		96	90
5	1.5		93	90

Legend: a eq: equivalents; b: (%) Conversion of AMP determined by ^{31}P NMR Spectroscopy.

Table 19: Set of flow reaction experiments for the synthesis of bis-piperidinium ADP (**7**) using a 0.27 mL chip and stock solutions of substrate and reagents prepared by weighing.

6.2.4 Workflow for the Semi continuous flow synthesis of Nucleoside Diphosphates (NDPs) using volumetric stock solutions of substrate and reagent prepared using a quantitative ^{31}P NMR method

Before performing the coupling step of the one pot-three steps synthesis of nucleoside diphosphates (NDPs), I prepared volumetric stock solutions of substrate and reagent. This involved an initial solution preparation in DMF, where the concentration of the substrate/reagent was in excess of the target value. Then a quantitative ^{31}P NMR analysis of the solution was performed, followed by dilution to the target concentration. Finally, a further quantitative ^{31}P NMR analysis of the solution was performed to confirm that the desired solution concentration had been achieved. (See *Figure 70* and section 6.4.1.2).

The procedures for the preparation of reagent stock solutions, and syntheses of NDPs are reported below. The development of the steps outlined in *Figure 70* and the parameters used for the ^{31}P NMR analysis are reported in sections 6.4, 6.4.1.2, and widely discussed in the Chapter 4, section 4.2.2.3.2.1.

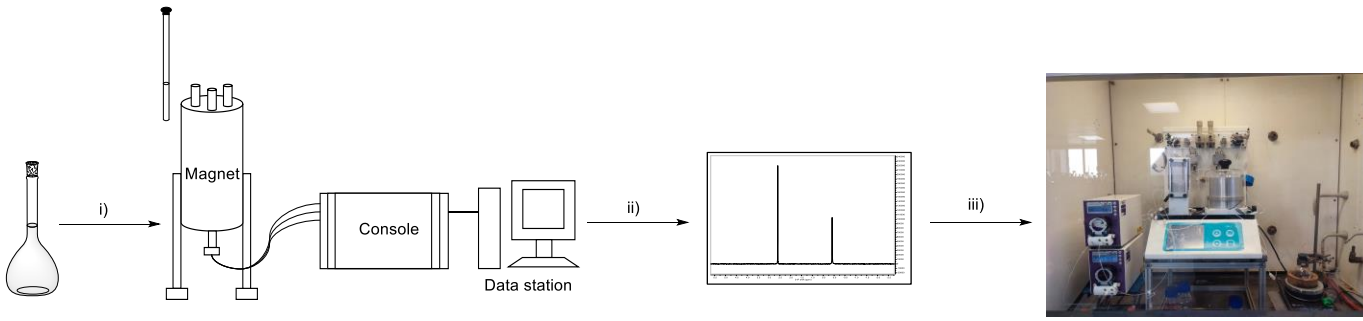

Legend: Preparation of stock solutions of reagents by quantitative ^{31}P NMR spectroscopy using trimethyl phosphate as an internal standard of known concentration. i): Prepare initial stock solution with concentration in excess of desired target concentration. ii) Perform ^{31}P NMR spectroscopy using trimethyl phosphate as an internal standard of known concentration. iii) Use analyte solution in flow reaction.

Figure 70: Simplified diagram of the workflow for the preparation of stock solutions prior to use in a flow system.

6.2.4.1 Preparation of Standardized Stock Solutions of Reagents prior to semi continuous flow synthesis of Nucleoside Diphosphates (ADP and UDP)

6.2.4.1.1 Volumetric solution of trimethyl phosphate

A 0.25 mol·L^{-1} solution of trimethyl phosphate was prepared to confirm concentrations of 5'-AMP TBA salt and *bis*-(fluorenylmethyl)-diisopropylamine phosphoramidite (**2**) solutions. Trimethyl phosphate (0.290 mL, 0.350 mg, 2.5 mmol) was pipetted into a 10 mL volumetric flask and the flask was made up to the mark with anhydrous DMF.

6.2.4.1.2 Standardized solution containing NMP and activator (SOLUTION A)

A solution containing the tetrabutylammonium salt of nucleoside monophosphate (see section 6.2.1.1) and activator was prepared by first measuring the concentration by quantitative ^{31}P NMR spectroscopy (see section 6.4.1.2) then adjusting the concentration to the desired, standardized value.

First, 5'-NMP $TBA_{1.2}H_{0.8}$ (**4**) (~5 mmol, ~1.0 equiv.) was dissolved in anhydrous DMF (20 mL) to prepare a solution of ~ 0.25 mol·L^{-1}. An aliquot of this solution (0.15 mL measured using a micropipette) was added to a standardized solution of trimethyl phosphate (0.15 mL, 0.25 mol·L^{-1}, see section 6.2.4.1.1 for preparation details). The mixture was transferred to an NMR tube with D_2O lock tube (sealed capillary containing D_2O) and the relative concentrations of the NMP TBA salt and trimethyl phosphate were compared by using a single repetition NMR program with d1= 51.5 s + a.t= 18 s to ensure complete relaxation of all ^{31}P nuclei. Based on the ratio of the integral of the NMP signal to the integral of the trimethyl phosphate signal, an aliquot of the NMP stock solution in DMF was further diluted, to obtain a standardized solution of NMP in DMF of concentration 0.05 mol·L^{-1}. 5-(ethylthio)-1*H*-tetrazole (65.0 mg, 0.5 mmol, 2 equiv.) was added to the NMP solution to prepare a solution with 0.05 mol·L^{-1} of the tetrabutylammonium salt of NMP and 0.010 mol·L^{-1} of activator. The trimethyl phosphate stock solution (section see section 6.2.4.1.1) was then diluted to 0.05 mol·L^{-1} to compare it to the NMP TBA salt solution containing activator and confirm correct dilution: An aliquot of analyte solution (0.15 mL measured using a micropipette) was added to a volumetric solution of trimethyl phosphate (0.15 mL, 0.05 mol·L^{-1}). The mixture was transferred to an NMR tube with D_2O lock tube and the relative concentrations of the NMP TBA salt and trimethyl phosphate were compared by using a single repetition NMR program with d1= 51.5 s + a.t= 18 s to ensure complete relaxation of all ^{31}P nuclei. At this stage, the ^{31}P signals for NMP and trimethyl phosphate had identical within ±0.0015 error integral sizes, thus confirming the concentration of NMP in

solution A to be 0.05 mol·L^{-1} (±0.0015 error estimate based on signal to noise ratio (SNR) of ^{31}P NMR spectrum).

[SNR has been calculated as the average peak height divided by the amplitude of the noise in the baseline. SNR = P_{SIGNAL}/P_{NOISE}, where P is average signal amplitude. Given two signals, A(internal standard) and B (our compound), the error has been calculated following the formula:$|\Delta R| = 1/SNR_B + R/SNR_B$, where peak height ratio R is R = A/B.][195]

6.2.4.1.3 Standardized solution of *bis*-(fluorenylmethyl)-diisopropylamine phosphoramidite (2). (SOLUTION B)

Volumetric solutions containing *bis*-(fluorenylmethyl)-diisopropylamine phosphoramidite (**2**) (see section 6.1.1.3.2) were prepared by quantitative ^{31}P NMR spectroscopy (section 6.4, 6.4.1.2).

A stock solution of *bis*-(fluorenylmethyl)-diisopropylamine phosphoramidite (**2**) (~5 mmol, ~0.25 mol·L^{-1}) in anhydrous DMF (20 mL) was prepared. An aliquot of this solution (0.15 mL measured using a micropipette) was added to a standardized solution of trimethyl phosphate (0.15 mL, 0.25 mol·L^{-1}, see section 6.2.4.1.1 for preparation details). The mixture was transferred to an NMR tube with D_2O lock tube and the relative concentrations of *bis*-(fluorenylmethyl)-diisopropylamine phosphoramidite (**2**) and trimethyl phosphate were compared by using an NMR program with d1= 51.5 s + a.t= 18 s to ensure complete relaxation of all ^{31}P nuclei. Based on the ratio of the integral of the phosphoramidite signal to the integral of the trimethyl phosphate signal, an aliquot of the phosphoramidite stock solution in DMF was further diluted to obtain a standardized solution of *bis*-(fluorenylmethyl)-diisopropylamine phosphoramidite (**2**) DMF with a concentration of 0.065 mol·L^{-1} in 5 mL. The trimethyl phosphate stock solution (section 1.2.3.2.1.1) was then diluted to 0.065 mol·L^{-1} to compare it with the *bis*-(fluorenylmethyl)-diisopropylamine phosphoramidite (**2**) solution and confirm correct dilution: An aliquot of analyte solution (0.15 mL measured using a micropipette) was added to a volumetric solution of trimethyl phosphate (0.15 mL, 0.065 mol·L^{-1}). The mixture was transferred to an NMR tube with D_2O lock tube and the relative concentrations of the *bis*-(fluorenylmethyl)-diisopropylamine phosphoramidite (**2**) and trimethyl phosphate were compared by using a single repetition NMR program with d1= 51.5

s + a.t= 18 s to ensure complete relaxation of all ^{31}P nuclei. At this stage, the ^{31}P signals for *bis*-(fluorenylmethyl)-diisopropylamine phosphoramidite (**2**) and trimethyl phosphate had equal within ±0.001 error integral sizes, thus confirming the concentration of *bis*-(fluorenylmethyl)-diisopropylamine phosphoramidite (**2**) reagent in solution B to be 0.065 mol·L^{-1} (±0.001 error estimate based on signal to noise of NMR).

6.2.4.2 Semi-Continuous Flow syntheses of Nucleoside Diphosphates

In this section, the procedure for the syntheses of ADP performed in a 0.27 mL chip reactor (see section 6.2.4.2.1) will be reported. The synthesis of ADP and UDP performed using a 2.5 mL coil reactor will then be reported in section 6.2.4.2.2 (for more details see Chapter 4, sections 4.2.2.3.2.2 and 4.2.2.4.

6.2.4.2.1 Flow Syntheses of bis-piperidinium ADP (7) using a 0.27 mL chip reactor

The following two procedures describe the optimised processes for delivery of ADP and UDP on scales of ~ 150 mg of substrate.

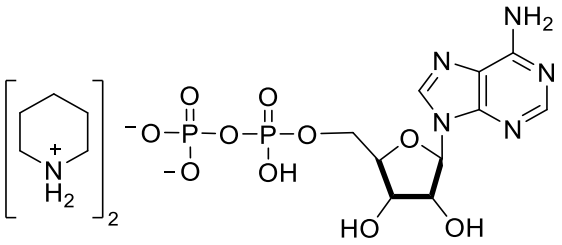

SOLUTION A [5'-AMP $TBA_{1.2}$ $H_{0.8}$ (0.05 mol·L^{-1}, 5 mL, 1.0 equiv.) (**4**) with 5-(ethylthio)-1*H*-tetrazole (65.0 mg, 0.5 mmol, 2 equiv.) in anhydrous DMF] and SOLUTION B [*bis*-(fluorenylmethyl)-diisopropylamine phosphoramidite (0.065 mol·L^{-1}, 5 mL, 1.3 equiv.) **(2)** in anhydrous DMF] were pumped from their flasks through suction needles at flow rate A (FRA = 0.040 mL·min^{-1}) and flow rate B (FRB = FRA) using pumps A and B, respectively, and mixed in a 0.27 mL chip *Uniqsis* FlowSyn system under temperature control at 25 °C. After establishing stable flow (approximately 2 coil volumes), the resulting coupling mixture was then quenched directly into a solution of *t*BuOOH 70% in H_2O (0.17 mL, 1.25 mmol, 5 equiv.) in dry DMF (2.5 mL). Following complete oxidation as determined by ^{31}P NMR

spectroscopy, the Fm protecting groups were cleaved with piperidine in DMF (0.625 mL of a 5% v/v solution) After deprotection, the product was precipitated by addition of Et_2O. The precipitate was isolated by centrifugation, washed with Et_2O and dried *in vacuo.* The resulting materials were analysed by ^{31}P NMR spectroscopy which showed 98% consumption of AMP after the oxidation step and 90% conversion of AMP after the deprotection step.

6.2.4.2.2 Flow Synthesis of P(III)-P(V) Intermediate using 2.5 mL coil reactor and exploration of different oxidation and Fm-deprotection conditions

The coupling step in the ADP synthesis reported in section 6.2.2.1 **Errore. L'origine riferimento non è stata trovata.** proved to be effective and reliable enough to be translated to a reactor that was ~10 times larger. This allowed us to increase the quantities of reagents (see Chapter 4) and deliver larger quantities of P(III)-P(V) intermediate (**8**), with consistently high levels of consumption of AMP and formation of the P(III)-P(V) intermediate (**8**). The resulting material formed the basis of several sets of experiments to explore the effects of different oxidants, different oxidant stoichiometries and, thereafter, different amine bases to effect Fm-deprotection. Summaries of the results of these experiments are provided in the following sections and flowcharts therein.

6.2.4.2.2.1 Preparation of P(III)-P(V) Intermediate (8) for Optimisations of Oxidation and Fm-deprotection Steps

SOLUTION A [5'-AMP $TBA_{1.2}$ $H_{0.8}$, 0.05 mol·L^{-1}, 20 mL, 1.0 equiv.) (**4**) and 5-(ethylthio)-1*H*-tetrazole (2 equiv.) in anhydrous DMF] and SOLUTION B [*bis*-(fluorenylmethyl)-diisopropylamine phosphoramidite (0.065 mol·L^{-1}, 20 mL, 1.3 equiv.) (**2**) in anhydrous DMF] were pumped from their flasks through suction needles at flow rates A (FRA = 0.3 mL·min^{-1}) and flow rate B (FRB = FRA) from pumps A and B, respectively, and mixed in a 2.5 mL coil (PTFE), under temperature control at 25 °C. After establishing stable flow (approximately 2 coil volumes) the resulting coupling mixture was then quenched into a solution of oxidant (see sections 6.2.4.2.2.1.1, 6.2.4.2.2.1.2 and 6.2.4.2.2.1.3). Thereafter, when optimal conditions for oxidation had been explored, the resulting P(V)-P(V) intermediate (**9**) was subjected to a range of different Fm-deprotection strategies (see section 6.2.4.2.2.1.3)).

Several sets of experiments were carried out as listed in the synthesis of ADP piperidinium (**6**) salt from 5'-AMP $TBA_{1.2}H_{0.8}$ (**4**):

- Exploration of use of *t*BuOOH oxidant stoichiometry (see *Table 20*, see section 6.2.4.2.2.1.2);
- Test of different oxidants (see *Table 21*, see section 6.2.4.2.2.1.3);
- Screening of different deprotection stirring timing (see
- *Table 22*, see section 6.2.4.2.2.1.3);
- Test of different piperidine equivalents and temperature in the deprotection step (see *Table 23*, see section 6.2.4.2.2.1.36.2.4.2.2.1.3);
- Screening of different bases in the deprotection step (see *Table 24*, see section 6.2.4.2.2.1.3).

6.2.4.2.2.1.1. Exploration of use of *t*BuOOH oxidant stoichiometry

Two separate runs of the procedure described in section 6.2.4.2.2.1 were performed, and the resulting coupling mixture was then quenched into a solution of *t*BuOOH 70% in H_2O (see *Table 20*) in dry DMF (2.5 mL). Following complete oxidation, as determined by ^{31}P NMR spectroscopy, the Fm protecting groups were cleaved with 5% v/v piperidine in DMF (2 mL). After deprotection, the product was precipitated by addition of Et_2O. The precipitate was isolated by centrifugation or filtration, washed with Et_2O and dried *in vacuo.*

Entry	*t*BuOOH 70%in H_2O (eq.)[a]	Consumption of AMP after oxidation (%)[b]	Consumption of AMP after deprotection (%)[b]
1	5	97	87
2	1.3	98	92

Legend: a eq.: equivalents; b (%) Conversion rate by 31P NMR.

Table 20: Varying number of equivalents of *t*BuOOH oxidant for the synthesis of ADP piperidinium salt (**7**) from 5'-AMP $TBA_{1.2}H_{0.8}$ (**4**).

6.2.4.2.2.1.2 Exploration of use of different Oxidants

A flow ADP synthesis using the procedure described in section 6.2.4.2.2.1 was performed, and the resulting coupling mixture was then split into 3 portions of 12 mL each and each portion was quenched into a solutions of different oxidant (see *Table 21*) in dry DMF (2.5 mL). Following complete oxidation, as determined by ^{31}P NMR spectroscopy, the Fm protecting groups were cleaved with 5% v/v piperidine in DMF (2 mL). After deprotection, the product was precipitated by addition of Et_2O. The precipitate was isolated by centrifugation or filtration, washed with Et_2O and dried in vacuo.

One flow coupling reaction split in three portions (12 mL) to explore the use of different oxidant reagents:

5'-AMP $TBA_{1.2}H_{0.8}$ (4) (mmol·mL^{-1})[a]	Activator (eq.)[b]	Amidite (2) (eq.)[b]
0.05	2	1.3

Entry	Oxidant reagent (eq.)[b]	Consumption of AMP before dep.(%)[d]	Consumption of AMP after dep.(%)[d]
1	*m*CPBA (1.3 eq.)	77	50
2	*t*BuOOH 5 M in decane (1.3 eq.)	~99	60
3	*t*BuOOH 70% in H_2O (0.95 eq.)	~99	56

a C: concentration. b eq.: equivalents. c %v/v.: percentage solute volume over solution volume d Conversion rate by ^{31}P NMR.

Table 21: Experiments exploring different oxidants for the synthesis of ADP (**7**) from 5'-AMP $TBA_{1.2}$ $H_{0.8}$ (**4**).

6.2.4.2.2.1.3 Optimisation of the Fm-deprotection step

In this set of experiments, I explored conditions for the Fm-deprotection step, analysing reaction time (see *Table 22),* piperidine stoichiometry, temperature (see *Table 23*) and different bases (see *Table 24*). For each experiment, a flow ADP synthesis using the procedure described in section 6.2.4.2.2.1 was performed. After establishing stable flow (approximately 2 coil volumes) the resulting coupling mixture was then quenched into a solution of oxidant and after complete oxidation, as determined by ^{31}P NMR spectroscopy, the Fm protecting groups were cleaved following different procedures, see details in

Table 22, Table 23, Table 24.

After deprotection, the product was precipitated by addition of Et_2O. The precipitate was isolated by centrifugation or filtration, washed with Et_2O and dried in vacuo. The results obtained are reported in

Table 22, Table 23, Table 24.

One flow coupling reaction split into 3 portions (12 mL each) to explore piperidine deprotection time.

5'-AMP $TBA_{1.2}H_{0.8}$ (4) (mmol·mL^{-1})[a]	Activator (eq.)[b]	Amidite (2) (eq.)[b]	*t*BuOOH 70% in H_2O (eq.)[b]
0.05	2	1.3	1.3

Entry	Piperidine 5% v/v[c] stirring time	Consumption of AMP before dep.(%)[d]	Consumption of AMP after dep.(%)[d]
1	~ few seconds	~98	92
2	~1 min		93
3	10 min		93

a C: concentration. b eq.: equivalents. c %v/v.: percentage solute volume over solution volume d Conversion rate by ^{31}P NMR.

Table 22: Experiments exploring different piperidine deprotection step times piperidine in the synthesis of ADP (**7**) from 5'-AMP $TBA_{1.2}H_{0.8}$ (**4**).

One flow coupling reaction split in 4 portions (10 mL) to explore the use of piperidine equivalents and temperature:

5'-AMP $TBA_{1.2}H_{0.8}$ (4) ($mmol \cdot mL^{-1}$)[a]	Activator (eq.)[b]	Amidite (2) (eq.)[b]	*t*BuOOH 5 M in decane (eq.)[b]
0.05	2	1.3	5

Entry	piperidine (eq.)[b]	temperature (°C)[c]	Consumption of AMP before dep.(%)[d]	Consumption of AMP after dep.(%)[d]
1	5	25	96	76
2	10			80
3	15			82
4	15	0		81

a C: concentration. b eq.: equivalents. c °C: degree Celsius. d Conversion rate by ^{31}P NMR.

Table 23: Experiments exploring piperidine stoichiometry and temperature of the deprotection step for the synthesis of ADP (**7**) from 5'-AMP $TBA_{1.2}H_{0.8}$ (**4**).

One flow coupling reaction split in 6 portions (5 mL) to explore different deprotection bases:

5'-AMP $TBA_{1.2}H_{0.8}$ (4) (mmol·mL^{-1})[a]	Activator (eq.)[b]	Amidite (2) (eq.)[b]	*t*BuOOH 5M in decane (eq.)[b]
0.05	2	1.3	5

Entry	Base 5% v/v	Consumption of AMP before dep.(%)[c]	Consumption of AMP after dep.(%)[c]
1	Piperidine	~ 99	83
2	DBU		~ 98
3	TMG		~ 98
4	Morpholine		83
5	Triethylamine		92
6	Hünig's base		75

a C: concentration. b eq.: equivalents. c Conversion rate by ^{31}P NMR.

Table 24: Experiments exploring different bases for the deprotection step of the synthesis of ADP (**7**) from 5'-AMP $TBA_{1.2}H_{0.8}$ (**4**).

6.2.4.2.2.2 Flow Synthesis of ADP using 2.5 mL coil reactor using procedure adapted from section 6.2.4.2.2.1

After conducting studies to optimize the one pot three step synthesis of ADP (see sections 6.2.4.2.2, 6.2.4.2.2.1) further comparative studies between TMG and piperidine as deprotecting agents were performed. I found the resulting ADP piperidinium and TMG salts to be quite insoluble in H_2O. Thus, to purify the crude reaction mixture using anion exchange chromatography, I performed cation exchange to Na salts to facilitate chromatography column loading. The procedures for the synthesis, batch cation exchange and anion exchange chromatography, and the scale up reaction are reported below. The synthesis of ADP was performed on the scale of ~2 g of substrate (for more details see Chapter 4, section 4.2.2.3.2.2).

6.2.4.2.2.2.1 Synthesis of Na ADP using piperidine as deprotecting base (10)

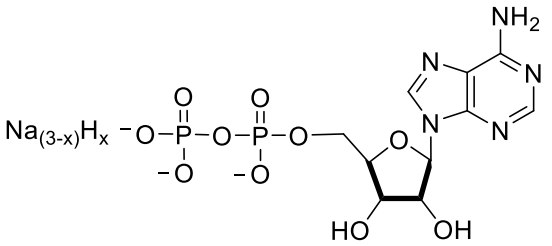

SOLUTION A [(5'-AMP $TBA_{1.2}$ $H_{0.8}$, 0.05 mol·L^{-1}, 20 mL, 1.0 equiv.) (**4**) and 5-(ethylthio)-1*H*-tetrazole 2 equiv.) in anhydrous DMF] and SOLUTION B [*bis*-(fluorenylmethyl)-diisopropylamine phosphoramidite (0.065 mol·L^{-1}, 20 mL, 1.3 equiv.) **(2)** in anhydrous DMF] were pumped from their flasks through suction needles at flow rate A (FRA = 0.30 mL·min^{-1}) and flow rate B (FRB = FRA) from pumps A and B, respectively, and mixed in a 2.5 mL coil reactor under temperature control at 25 °C. The resulting coupling mixture was then quenched into a solution of *t*BuOOH 5 M in decane (0.25 mL, 1.3 mmol, 1.3 equiv.) in dry DMF (2.5 mL). Analysis by ^{31}P NMR spectroscopy at this point showed complete consumption of P(III) species and 98% consumption of AMP. The Fm protecting groups were cleaved with 5% v/v piperidine in DMF (2 mL) and the product was precipitated by addition of Et_2O. The precipitate was isolated by centrifugation, washed with Et_2O and dried *in vacuo.* The residue was cation exchanged via suspension in a solution of NaI in acetone/H_2O (10 mL of a 5 M solution in 9:1 acetone-water). The mixture was stirred overnight at room temperature, the solid was collected by filtration, dried, and analysed by ^{31}P NMR spectroscopy. Integration of the signals showed 92% consumption of AMP.

6.2.4.2.2.2.2 Synthesis of Na ADP using TMG as deprotecting base (10)

SOLUTION A [5-AMP $TBA_{1.2}H_{0.8}$ (0.05 mol·L^{-1}, 20 mL, 1.0 equiv.) (**4**) and 5-(ethylthio)-1*H*-tetrazole (2 equiv.) in anhydrous DMF] and SOLUTION B [*bis*-(fluorenylmethyl)-diisopropylamine phosphoramidite (0.065 mol·L^{-1}, 20 mL, 1.3 equiv.) (**2**) in anhydrous DMF] were pumped from their flasks through suction needles at flow rate A (FRA = 0.30 mL·min^{-1}) and flow rate B (FRB = FRA) from pumps A and B, respectively, and mixed in a 2.5 mL coil reactor under temperature control at 25 °C. The resulting coupling mixture was then quenched into a solution of *t*BuOOH 5 M in decane (0.25 mL, 1.3 mmol, 1.3 equiv.) in

dry DMF (2.5 mL). Analysis by ^{31}P NMR spectroscopy at this point showed complete consumption of P(III) species and 99% consumption of AMP. The Fm protecting groups were cleaved with 5% v/v TMG in DMF (2 mL). After deprotection, the product was precipitated upon addition of Et_2O. The residue was cation exchanged via suspension in a solution of NaI in acetone/ H_2O (10 mL of a 5 M solution in 9:1 acetone-water). After filtration, the solid was analysed by ^{31}P NMR spectrum and showed 97% consumption of AMP.

6.2.4.2.2.2.3 Scale up of synthesis of triethylammonium ADP salt using TMG as deprotecting base (11)

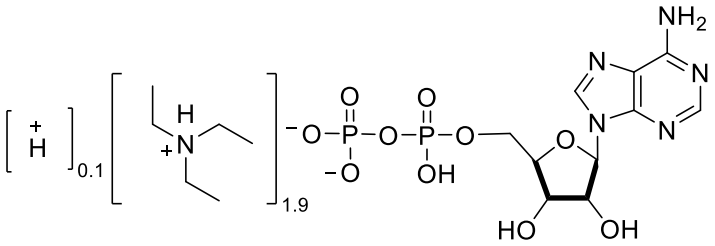

SOLUTION A [5'-AMP $TBA_{1.2}$ $H_{0.8}$ (0.05 mol·L^{-1}, 60 mL, 1.0 equiv.) (**4**) and 5-(ethylthio)-1*H*-tetrazole (2 equiv.) in anhydrous DMF] and SOLUTION B [*bis*-(fluorenylmethyl)-diisopropylamine phosphoramidite (0.065 mol·L^{-1}, 60 mL, 1.3 equiv.) **(2)** in anhydrous DMF] were pumped from their flasks through suction needles at flow rate A (FRA = 0.30 mL·min^{-1}) and flow rate B (FRB = FRA) from pumps A and B, respectively, and mixed in a 2.5 mL coil reactor under temperature control at 25 °C. After establishing stable flow (approximately 2 coil volumes), the resulting coupling mixture was then quenched into a solution of *t*BuOOH 5 M in decane (0.80 mL, 3.9 mmol, 1.3 equiv.) in dry DMF (2.5 mL). Analysis by ^{31}P NMR spectroscopy at this point showed complete consumption of P(III) species and 95% consumption of AMP. The Fm protecting groups were cleaved with 5% v/v TMG in DMF (6 mL). After deprotection, the product was precipitated by addition of Et_2O. The precipitate was isolated by centrifugation, washed with Et_2O and dried *in vacuo.* The residue was cation exchanged by suspension in a solution of NaI in acetone/ H_2O (10 mL of a 5 M solution in 9:1 acetone-water). The mixture was stirred overnight at room temperature. After filtration, the solid was purified by anion exchange chromatography on a 100 g RediSep Rf Gold® Amine column, with a linear gradient from 0-1 M TEAB buffer pH 8, and a flow rate of 30 mL/min, followed by freeze drying. 5'-ADP $(Et_3NH)_{1.4}H_{0.6}$ was collected (1.0 g, 1.8 mmol, 65%).

^{31}P NMR (162 MHz, DMSO-d6): δP = 2.95 (s), –6.46- – 6.58 (d, speciation, J= 19.5 Hz), –7.84- – 7.96 (d, J= 19.5 Hz), –8.23 - – 8.35 (d, J= 19.5 Hz).

^{1}H NMR (600 MHz, DMSO-d6): δH = 8.40 (s, 1H), 8.11 (s, 1H), 7.25 (s, NH_2), 8.57 (d, J= 4.5 MHz. 1H), 4.45-4.40 (m, 1H), 4.29 (app t, J= 6.5 MHz. 1H), 4.0-3.91 (m, 3H), 2.77-2.74 (m, 17H), 1.04 (t, J= 7.2 Hz, 26H).

^{13}C NMR (151 MHz, DMSO-d6): δC = 156.40 (C), 153.04 (C), 149.83 (C), 139.52 (C), 119.23 (C), 87.72 (CH), 83.71 (CH), 74.58 (CH), 69.92 (CH), 64,23 (CH_2), 45.73 (CH_3×2), 11.41, 10.0(CH_2×2).

HR-MS calculated for $C_{10}H_{16}N_5O_{10}P_2$ 428.0357, found 428.0372 (Δ = –0.8 mDa; –1.9 ppm).

HPLC analysis of isolated material with UV detection (254 nm) showed the isolated material to >99% homogeneous.

6.2.3.2.2.4 Synthesis of *bis*-piperidinium UDP (12) on a 2.5 mL coil reactor

The following procedure describes the synthesis of UDP using ~ 500 mg of UMP substrate, based on the procedure for the preparation of ADP described in section 6.2.4.2.2.2.1 (for more details see section 4.2.2.4).

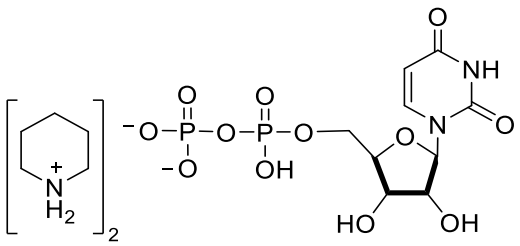

SOLUTION A [5'-UMP $TBA_{1.6}$ $H_{0.4}$ (0.05 mol·L^{-1}, 20 mL, 1.0 equiv.) (**5**) with 5-(ethylthio)-1*H*-tetrazole (2 equiv.) in anhydrous DMF] and SOLUTION B [*bis*-(fluorenylmethyl)-diisopropylamine phosphoramidite (0.065 mol·L^{-1}, 20 mL, 1.3 equiv.) in anhydrous DMF] **(2)** were pumped from their flasks through suction needles at flow rate A (FRA = 0.30 mL·min^{-1}) and flow rate B (FRB = FRA) from pumps A and B, respectively, and mixed in a 2.5 mL coil reactor under temperature control at 25 °C. After establishing stable flow (approximately 2 coil volumes), the resulting coupling mixture was then quenched into a solution of *t*BuOOH 5 M in decane (0.25 mL, 1.3 mmol, 1.3 equiv.) in dry DMF (2.5 mL).

Analysis by ^{31}P NMR spectroscopy at this point showed complete consumption of P(III) species and 90% consumption of UMP. The Fm protecting groups were cleaved with 5% v/v piperidine in DMF (1.5 mL). After deprotection, the product was precipitated by addition of Et_2O. The ^{31}P NMR spectra after deprotection showed 85% consumption of UMP.

6.2.4.2.2 Attempted Semi-Continuous Flow synthesis of *bis*-piperidinium CDP (13)

CDP synthesis is considered separately because, contrary to what I experienced for the synthesis of ADP and UDP, I encountered solubility problems both in the preparation of the 5'-CMP $TBA_{1.2}H_{0.8}$ stock solution and in the execution of the reaction in flow (see Chapter 4, section 4.2.2.4). For the preparation of trimethyl phosphate solution see section 6.2.4.1.1 and for the preparation of SOLUTION B see section 6.2.4.1.3.

6.2.4.2.3.1 Volumetric solution of CMP (SOLUTION A)

A solution containing 5'-CMP $TBA_{1.2}H_{0.8}$ (**6**) (see section 6.2.1.3) was prepared by first estimating, and then adjusting, its concentration by quantitative ^{31}P NMR spectroscopy (see section 6.4, 6.4.1.2).

First, 5'-CMP $TBA_{1.2}H_{0.8}$ (**6**) (~5 mmol, ~1.0 equiv.) was dissolved in anhydrous DMF (20 mL) to prepare a solution of ~ 0.25 mol·L^{-1}. An aliquot of this solution (0.15 mL measured using a micropipette) was added to a standardized solution of trimethyl phosphate (0.15 mL, 0.25 mol·L^{-1}, see section 6.2.4.1.1 for preparation details). The mixture was transferred to an NMR tube with D_2O lock tube and the relative concentrations of the 5'-CMP $TBA_{1.2}H_{0.8}$ (**6**) and trimethyl phosphate were compared by using an NMR program with d1= 51.5 s + a.t= 18 s to ensure complete relaxation of all ^{31}P nuclei. Based on the ratio of CMP signal to triethyl phosphate, the stock solution in DMF was further diluted, to obtain a standardized solution of CMP in DMF of concentration 0.05 mol·L^{-1}. The trimethyl phosphate stock solution (see section 6.2.4.1.1 for preparation details).) was then diluted to 0.05 mol·L^{-1} to compare it with the concentration of the 5'-CMP $TBA_{1.2}H_{0.8}$ solution to confirm correct dilution. An aliquot (0.15 mL measured using a micropipette) was added to a volumetric solution of trimethyl

phosphate (0.15 mL, 0.05 mol·L^{-1}, see section 6.2.4.1.1 for preparation details). The mixture was transferred to an NMR tube with D_2O lock tube and the relative concentrations of the 5'-CMP $TBA_{1.2}H_{0.8}$ (**6**) and trimethyl phosphate were compared by using an NMR program with d1= 51.5 s + a.t= 18 s to ensure complete relaxation of all ^{31}P nuclei (see section 6.4, 6.4.1). At this stage, the ^{31}P signals for CMP and trimethyl phosphate showed identical integral sizes, thus confirming the concentration of CMP in solution A to be 0.05 mol·L^{-1} (±0.0015 error estimate based on signal to noise of NMR).

6.2.4.2.3.2 Attempted flow coupling of 5'-CMP $TBA_{1.2}H_{0.8}$ (6) with *bis*-(fluorenylmethyl)-diisopropylamine phosphoramidite (2) for the synthesis of bis-piperidinium CDP (13)

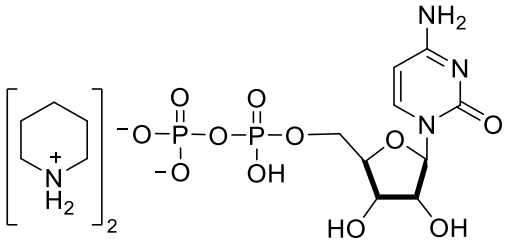

The following experiments show the attempted synthesis of bis-piperidinium CDP (**14**) into a flow system, as described in Chapter 4, see section 4.2.2.4, see results detail in *Table 25*. After the coupling step performed in flow, the solution was quench and the resulting analysed by ^{31}P NMR spectroscopy. Due the low-rate conversion of CMP and the clogging issues occurred during the synthesis, the deprotection step and the subsequent ^{31}P NMR spectroscopy analysis of the deprotected product has never been performed.

SOLUTION A [5'-CMP $TBA_{1.2}H_{0.8}$ salt (0.05 mol·L^{-1}, 1.0 equiv.) (**6**) and SOLUTION B [*bis*-(fluorenylmethyl)-diisopropylamine phosphoramidite (0.065 mol·L^{-1}, 1.3 equiv.) (**2**) with 5-(ethylthio)-1*H*-tetrazole (2 equiv.)] were dissolved in anhydrous DMF] were pumped from their flasks through suction needles at flow rate (FRA = FRB) using pumps A and B, respectively and mixed in a reactor under temperature control (see *Table 25* for details of reactor type, flow rates and temperatures). After establishing stable flow (approximately 2 coil volumes), the resulting coupling mixture was then quenched into a solution of *t*BuOOH 70% in H_2O (0.17 mL, 1.25 mmol, 5 equiv.) in dry DMF (2.5 mL) and the resulting then analysed by ^{31}P NMR spectroscopy.

Entry	Reactor	$FR_A=FR_B$ ($mL \cdot min^{-1}$)[a]	T (°C)[b]	RT (min)[d]	5'-CMP $TBA_{1.2}H_{0.8}$ (6) ($mol \cdot L^{-1}$)[e]	Conv. after ox. (%)[f]
1	0.27 mL Chip	0.04	25	3	0.10	CLOG
2	2.5 mL Coil	0.3	25	4	0.05	65
4	2.5 mL Coil	0.3	25	4	0.025	40
5	2.5 mL Coil	0.3	50	4	0.025	26

Legend: a FR: flow rate each pump. b T: reaction temperature in the first coil. c R1: residence time of the first reaction step. e C: concentration. f conversion analysed by ^{31}P NMR.

Table 25: Semi Continuous Flow synthesis experiments of bis-piperidinium CDP.

6.3 Workflow for the One Pot Three Step synthesis of tris-piperidinium ATP

The synthesis of *tris*-piperidinium ATP from 5'-ADP $TBA_{0.2}H_{0.8}$ (**15**) was used to test the effectiveness of the phosphitylating reagent (**2**) (see section 6.1.1.3.2). Yields were not recorded, however, outcomes based on NMR spectra are reported in Chapter 4, section 4.2.1.

6.3.1 Adenosine diphosphate $TBA_{0.2}H_{0.8}$ (15)

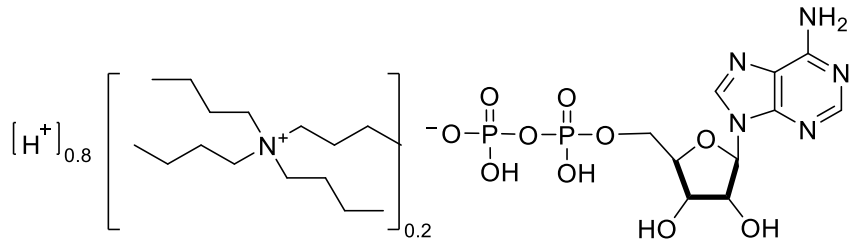

5'-ADP (acid form, 1.2 g, 2.8 mmol) was dissolved in distilled H_2O (4 mL) at room temperature. Tetra-*n*-butylammonium hydroxide (40% w/v solution in water, 0.145 g, 0.56 mmol, 0.2 equiv.) was added to the solution and the mixture was stirred for 20 min. The product was isolated as a white solid by overnight freeze drying (1.24 g, 93%).

^{31}P NMR (242.65 MHz, D_2O): δP = –10.83 (d, J=19.9 Hz), –11.31 (d, J=19.9 Hz).

^{1}H NMR (599.242 MHz, D_2O): δH= 8.45 (s, 1H), 8.27 (s, 1H), 6.0 (d, J=5.3 Hz, 1H), 4.59 (t, J = 5.3 Hz, 1H), 4.41 - 4.39 (m,1H), 4.28 - 4.26 (m, 1H), 4.22 – 4.17 (m, 1H), 4.16 – 4.13 (m, 1H), 4.11 – 4.02 (m, 1H), 3.06 – 3.03 (m, 3H), 1.55 – 1.47 (m, 3H), 1.24 - 1.17 (h, J=7.4 Hz, 3H), 0.79 (t, J= 7.4 Hz, 4 H).

^{13}C NMR (150.72 MHz, D_2O) δ 149.78 (C), 148.14 (C), 144.79 (C), 142.26 (C), 118.26 (C), 87.79 (CH), 84.13 (d,$^{4}J_{C,P}$= 9.05 Hz, CH), 74.69 (CH), 70.14 (CH), 64.87 (d,$^{3}J_{C,P}$= 5.40 Hz, CH_2), 58.06 -58.02 (m, CH_2), 23.04 (CH_2), 19.07-19.05 (m, CH_2), 12.72 (CH_3).

HR-MS calculated for $C_{10}H_{16}N_5O_{10}P_2$ 428.0357, found 428.0372 (Δ = –1.5 mDa; –3.5 ppm).

6.3.2 Synthesis of tris-piperidinium ATP (16)

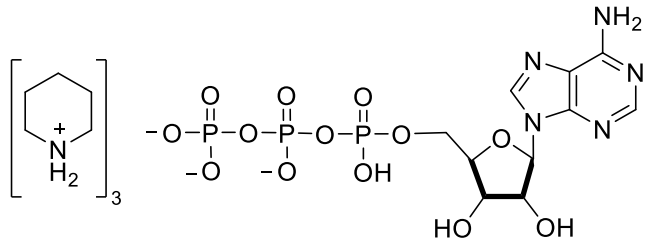

5'-ADP $TBA_{0.2}H_{0.8}$ (**15**) (0.1 g, 0.21 mmol) was suspended in DMF (99.8%, 1.00 mL). *Bis*-(fluorenylmethyl)-diisopropylamine phosphoramidite (0.117 g, 0.34 mmol, 1.6 equiv.) was dissolved in DMF (0.5 mL) and the solution was added to the reaction mixture, followed by 5-(ethylthio)-1*H*-tetrazole (0.055 g, 0.42 mmol, 2 equiv.). The reaction mixture was stirred for 5 min. and then *m*CPBA (0.0725 g, 0.42 mmol, 2 equiv.) was added and the mixture was stirred for 10 min. The bis-Fm-protected ATP was than precipitated by addition of Et_2O-*hexane* (5:1, 4 mL) and the suspension was centrifuged. The solid was collected, washed with Et_2O and dissolved in DMSO (1.5 mL). Piperidine solution (75 μL of a 5% v/v solution) was added to the reaction solution and the mixture was stirred for 10 min. After deprotection, the title compound was precipitated by addition of Et_2O (4 mL). The precipitate was isolated by centrifugation or filtration, washed with Et_2O and dried in vacuo The crude compound was then analysed without further purification via ^{31}P NMR spectroscopy and the ^{31}P NMR spectrum showed 79 % consumption of ADP.

^{31}P NMR (162 MHz, CD_3OD): δP = 3.87 (s), 1.78 (s), 0.09 (s), –6.1 (d, J=18.6 Hz), –6.7 (d, J=21.3 Hz), –9.9 (d, J= 21.1 Hz), –10.3 (d, J=18.0 Hz), –20.18 (t, J= 18.7 Hz).

6.4 ^{31}P NMR spectroscopy experiments

In this section quantitative and non-quantitative NMR spectroscopy studies, using single acquisitions or time courses, which were extensively discussed in the Chapter 4, section 4.2.2.2, are reported. Non-time course Nuclear Magnetic Resonance (NMR) spectra for determination of the concentrations of stock solutions were recorded on a Bruker Neo-400 spectrometer with operating frequencies of 400.20 MHz for ^{1}H, 100.63 MHz for ^{13}C and 162.00 MHz for ^{31}P at 25°C. Nuclear Magnetic Resonance (NMR) time course spectra were recorded on a Varian DD2-500 operating spectrometer with operating frequencies of 499.53 MHz for ^{1}H and 202.21 MHz for ^{31}P at 25 °C. The Time course studies were performed on the two reaction steps ('coupling' and 'oxidation') illustrated in *Figure 71*

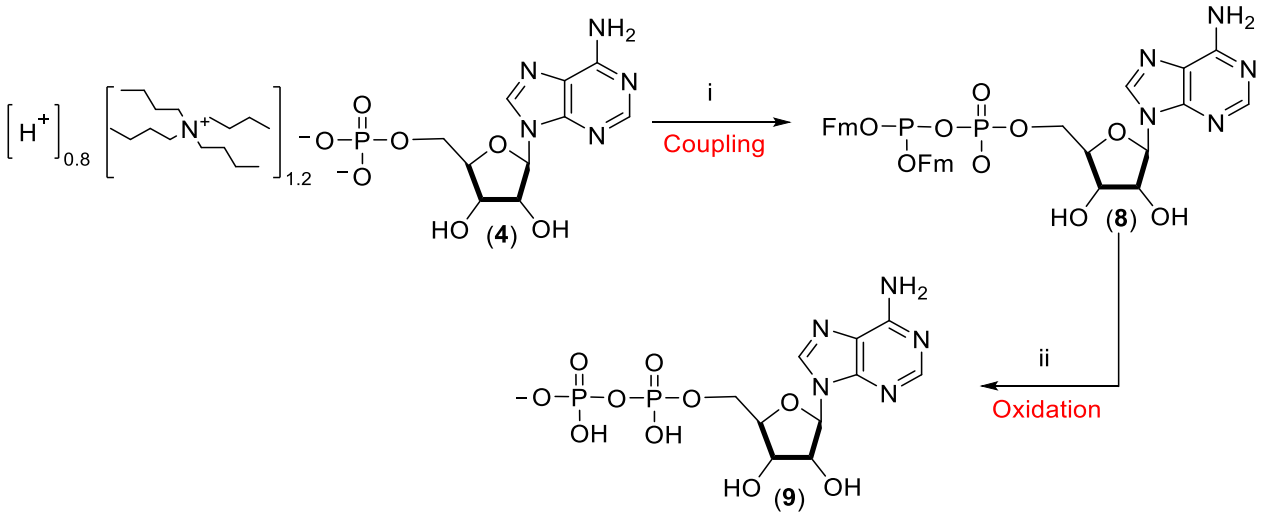

Reagents and conditions: i) bis-fluorenylmethyl diisopropylamine phosphoramidite (2), 5-(ethylthio)-1H-tetrazole, wet DMF, 25 °C. ii) tBuOOH, DMF, 25 °C.

Figure 71: Conversion of AMP to P(III)-P(V) anhydride (**8**) (i) and from P(III)-P(V) anhydride (**8**) to P(V)-P(V) anhydride (**9**) following Jessen's method.

6.4.1 Measurement of the ^{31}P T_1 relaxation times of the oxidation step reaction of P(V)-P(V) intermediate (9) (see Chapter 4, section 4.2.2.2.3.1)

In the following procedure, I reported how I performed the ^{31}P NMR spectra to calculate the spin-lattice T_1 constants of all reaction players using a Varian DD2-500 MHz spectrometer at 25 ºC.

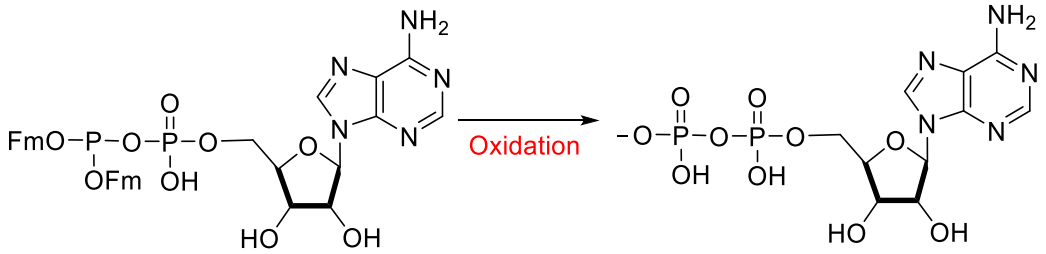

(**8**) (**9**)

In a vial, 5'-AMP $TBA_{1.2}$ $H_{0.8}$ salt (0.088 g, 0.14 mmol) (**4**) was dissolved in DMF (0.375 mL). 5-(ethylthio)-1*H*-tetrazole (from 1.3 to 2 equiv.) was added to the solution. *Bis*-(fluorenylmethyl)-diisopropylamine phosphoramidite (**2**) (mass adjusted based on purity level measured by ^{31}P NMR spectroscopy, 0.18 mmol, 1.3 equiv.) dissolved in DMF (0.375 mL) was then added to the AMP solution. The reaction mixture was shaken at room temperature over a period of 10 min. Then *t*BuOOH 5 M in decane (36 µL, 0.18 mmol,1.3 equiv.) was added. The mixture then was transferred to an NMR tube with D_2O lock tube and trimethyl phosphate as standard in D_2O (0.00 ppm) (20 mg, 17 µl, 0.14 mmol, 1 equiv.) was added. The T_1 relaxation times of the phosphorus nuclei were measured by recording the inversion recovery ^{31}P NMR spectra in a series of experiments involving different recovery times ranging from 100 ms to 20 s. The ^{31}P signals were integrated and their intensities were plotted against the delay time to give the T_1 relaxation times.

Peak	^{31}P (ppm)	T_1 (s)
P(III) reagent (**2**)	146.11	0.88 ± 0.01
Trimethyl phosphate	0.00	8.25 ± 0/07
5'-AMP $TBA_{1.2}H_{0.8}$ (**4**)	–2.25	0.69 ± 0.02
P(V)-P(V) anhydride (**9**)	–12.50	0.40 ± 0.01
P(V)-P(V) anhydride (**9**)	–13.01	0.44 ± 0.02
P(III)-P(V) anhydride (**8**)	–12.82	0.53 ± 0.01
P(III)-P(V) anhydride (**8**)	125.18	0.54 ± 0.01

Table 26: T_1 values for the oxidant reaction. Data calculated using a 500 MHz spectrometer at 25 °C.

Based on the results obtained (see *Table 26*), the next set of experiments described in 6.4.1.1 were conducted by acquiring a single transient ^{31}P experiment with an acquisition time of 1.5 s and d1 of 3.5 s This single-scan acquisition was followed by 10 s waiting time before acquiring a new ^{31}P experiment.

6.4.1.1 ^{31}P NMR spectroscopy time course experiments carried out with T_1 relaxation time studies

In this section quantitative NMR spectroscopy, time course and single acquisition studies are reported. The time course studies were performed with a D_2O lock tube or DMF-d7 on the two steps illustrated in *Figure 71* (see Chapter 4, section 4.2.2.2.3.2). Single acquisition studies were performed with a D_2O lock tube to analyse the stock solution stabilities (see section 6.2.4.1 for preparation details), before performing the flow syntheses of NDPs (see section 6.2,6.2.3, 6.2.4 and Chapter 4, section 4.2.2.2.3.2 for more details).

6.4.1.1.1 Kinetic studies of the coupling reaction of P(III)-P(V) intermediate (8) with *bis*-(fluorenylmethyl)-diisopropylamine phosphoramidite (2) in D_2O

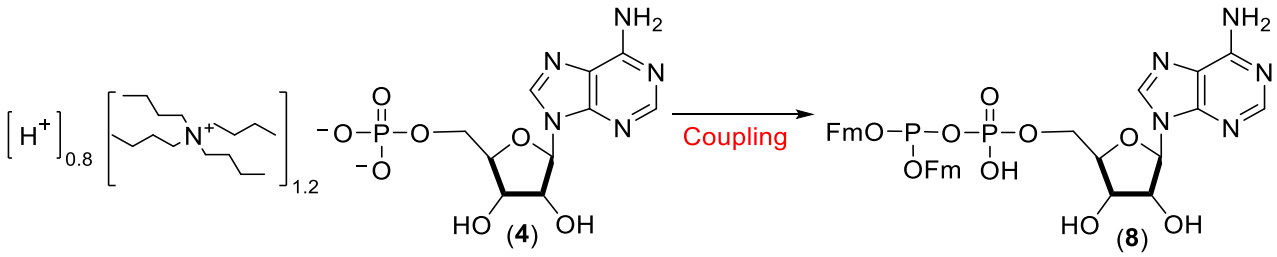

5'-AMP $TBA_{1.2}H_{0.8}$ (0.088 g, 0.14 mmol) (**4**) was dissolved in DMF (0.375 mL) and 5-(ethylthio)-1*H*-tetrazole (from 1.3 to 2 equiv.) was added to the solution. *Bis*-(fluorenylmethyl)-diisopropylamine phosphoramidite (**2**) (mass adjusted based on purity level measured by ^{31}P NMR spectroscopy, 0.18 mmol, 1.3 equiv.) dissolved in DMF (0.375 mL) was then added to the nucleotide solution. The reaction mixture was shaken at room temperature and transferred to an NMR tube with D_2O lock tube and trimethyl phosphate as standard (0.00 ppm) (20 mg, 17 µl, 0.14 mmol, 1 equiv.). The ^{31}P NMR spectrum was recorded at 25 °C with a single scan (nt=1) and relaxation delay (d1) of 3.5 s between acquisitions over a period of 100 min.

6.4.1.1.2 Kinetic studies of the oxidation step of P(V)-P(V) intermediate (9) in D_2O

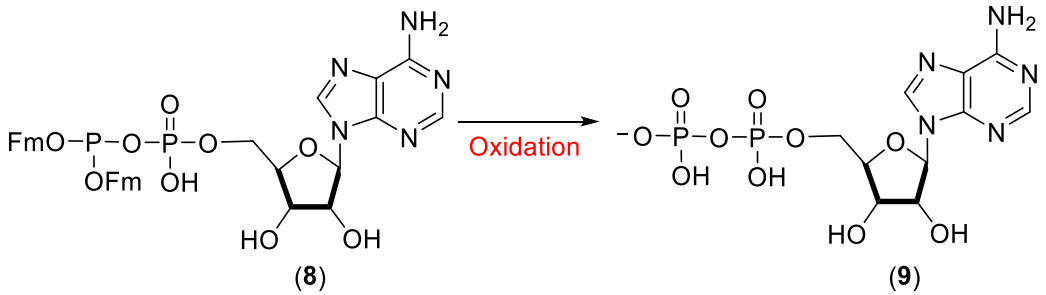

After the coupling step described in section 6.4.1.1.1, *t*BuOOH (5 M in decane, 36 µL, 0.18 mmol, 1.3 equiv.) was added to the solution directly in the NMR tube and the NMR spectrometer was set to record ^{31}P spectra at 25 °C with a single scan (nt=1) and a relaxation delay (d1) of 3.5 s between acquisitions over a period of 100 min.

6.4.1.1.3 Kinetics studies of the coupling step of P(III)-P(V) intermediate (8) with *bis*-(fluorenylmethyl)-diisopropylamine phosphoramidite (2) in DMF-d7

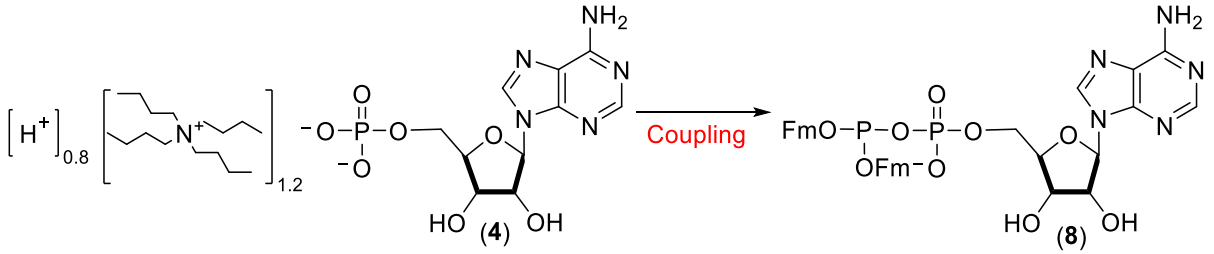

In a vial, 5'-AMP $TBA_{1.2}H_{0.8}$ (0.088 g, 0.14 mmol) (**4**) was dissolved in DMF-d7 (0.375 mL). 5-(ethylthio)-1*H*-tetrazole (from 1.3 to 2 equiv.) was added to the solution. *Bis*-(fluorenylmethyl)-diisopropylamine phosphoramidite (**2**) (mass adjusted based on purity level measured by ^{31}P NMR spectroscopy, 0.18 mmol, 1.3 equiv.) dissolved in DMF-d7 (0.375 mL) was then added to the nucleotide solution. The reaction mixture was shaken at room temperature and transferred to an NMR tube with trimethyl phosphate as internal standard (20 mg, 17 µl, 0.14 mmol, 1 equiv.). An array of ^{31}P NMR spectra was recorded at 25 °C with a single scan (nt=1) and a relaxation delay (d1) of 3.5 s between acquisitions over a period of 100 min.

6.4.1.1.4 Kinetics studies of the oxidation step of P(V)-P(V) intermediate (9) in DMF-d7

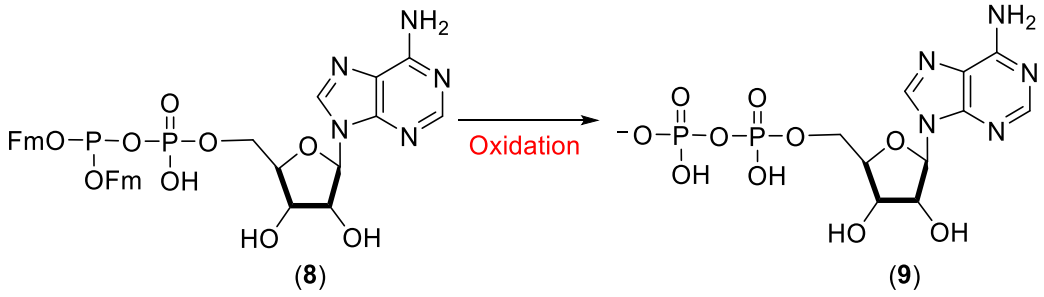

In a vial, 5'-AMP $TBA_{1.2}$ $H_{0.8}$ (0.088 g, 0.14 mmol) (**4**) was dissolved in DMF-d7 (0.375 mL). 5-(ethylthio)-1*H*-tetrazole (from 1.3 to 2 equiv.) was added to the solution. *Bis*-(fluorenylmethyl)-diisopropylamine phosphoramidite (**2**) (mass adjusted based on purity level measured by ^{31}P NMR spectroscopy, 0.18 mmol, 1.3 equiv.) dissolved in DMF (0.375 mL) was then added to the nucleotide solution. The reaction mixture was shaken at room temperature over a period of 10 min and *t*BuOOH 5 M in decane (36 µL, 0.18 mmol, 1.3 equiv.) was added to the solution. The oxidation mixture was then transferred to an NMR tube

with trimethyl phosphate as internal standard (0.00 ppm) (20 mg, 17 µl, 0.14 mmol, 1 equiv.). The NMR experiments were set to record ^{31}P spectra at 25 °C with a single scan (nt=1) and a relaxation delay (d1) of 3.5 s between acquisitions over a period of 100 min.

6.4.1.2 ^{31}P NMR Spectroscopy Studies of the Stock Solution Stabilities (see section 6.2.4.1 for solution preparation details)

Stock solutions were analysed periodically to study their stability. This was done by adding trimethyl phosphate as a reference of known concentration to a sample containing the stock solution and acquiring a ^{31}P NMR spectrum with decoupling active only during the acquisition. ^{31}P T_1s were measured to ensure that the integrals were quantitative, as the repetition time (the acquisition time plus d1) should be longer than $5T_1$ for all species under analysis. Furthermore, the sample spent more than $5T_1$ (~ 4 min) inside the spectrometer during the locking, tuning, and shimming. This period is ~30 times longer than the longest $5T_1$ [trimethyl phosphate (8.25 s)], and thus it allowed the complete polarization of all nuclei before acquiring scans.

6.4.2 ^{31}P NMR Spectroscopy Time Course Experiments carried out prior to detailed T1 relaxation time studies

In this section preliminary, non-quantitative ^{31}P NMR kinetics experiments are reported. The described methods were adopted to analyse the conversion of AMP pyridinium salt to ADP in DMSO-d6 (see Chapter 4, section 4.2.2.2.1).

6.4.2.1 Kinetic studies of the coupling step reaction of AMP with *bis*-(fluorenylmethyl)-diisopropylamine phosphoramidite (2) in DMSO- d6

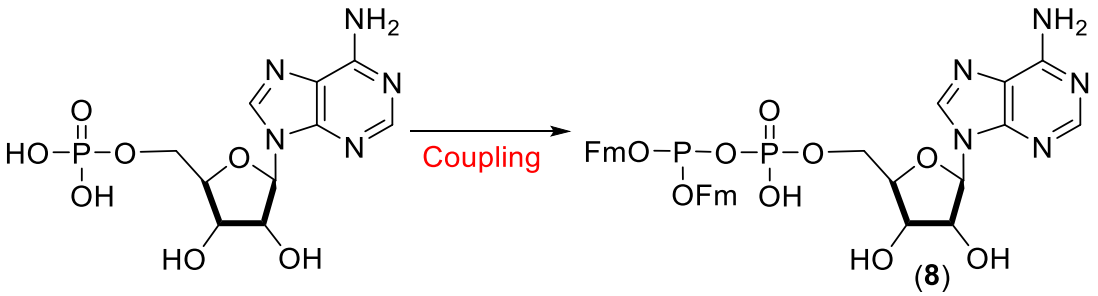

In a vial, 5'-AMP (acid form, 0.050 g, 0.14 mmol), pyridine (12 µl, 1.2 equiv.) and 5-(ethylthio)-1*H*-tetrazole (from 1.3 to 2 equiv.) were dissolved in DMSO-d6 (0.375 mL). *Bis*-(fluorenylmethyl)-diisopropylamine phosphoramidite (**2**) (mass adjusted based on purity level measured by ^{31}P NMR spectroscopy, 0.17 mmol, 1.2 equiv.) dissolved in DMSO-d6 (0.375 mL) was then added to the nucleotide solution. The reaction mixture was shaken at room temperature and transferred to an NMR tube with trimethyl phosphate as internal standard (20 mg, 17 µl, 0.14 mmol, 1 equiv.). The NMR experiments were set to record ^{31}P spectra at 25 °C with a single scan (nt=1) and a relaxation delay (d1) of 2 s between acquisitions over a period of 3 h 50 mins.

6.4.2.2 Kinetics of the oxidation step of the conversion of AMP to ADP using *bis*-(fluorenylmethyl)-diisopropylamine phosphoramidite (2) and 5-(ethylthio)-1*H*-tetrazole in DMSO- d6 with *m*CPBA as oxidant

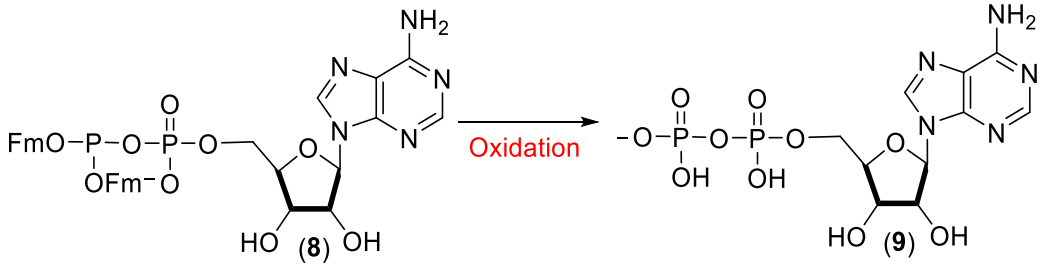

In a vial, 5'-AMP (acid form, 0.050 g, 0.14 mmol), pyridine (12 µl, 0.17 mmol, 1.2 equiv.) and 5-(ethylthio)-1*H*-tetrazole (from 1.3 to 2 equiv.) were dissolved in DMSO-d6 (0.375 mL). *Bis*-(fluorenylmethyl)-diisopropylamine phosphoramidite (**2**) (mass adjusted based on purity level measured by ^{31}P NMR spectroscopy, 0.17 mmol, 1.2 equiv.) DMSO-d6 (0.375 mL) was then added to the nucleotide solution. The reaction mixture was shaken at room temperature for 10 min. *m*-CPBA (31 mg, 0.18 mmol, 1.3 equiv.) was added to the solution (the vial warmed significantly). The reaction mixture was shaken at room temperature and transferred to an NMR tube with trimethyl phosphate as internal standard (20 mg, 17 µl, .0.14 mmol, 1 equiv.). NMR experiments were set to record ^{31}P spectra at 25 °C with a single scan (nt=1) and a relaxation delay (d1) of 2 s between acquisitions over a period of 3 h and 50 mins.

7 Appendix

The COVID-19 pandemic had significant impacts on research activity. Social distancing and the inability to room-share prevented the timely use of NMR kinetic methods and flow systems that were key elements of the main thesis project. On this basis, two 'side projects' based on the syntheses of a phosphate-containing thiamine mimic and a nucleoside analogue were engaged, and progress towards these synthetic targets is briefly reported in this chapter. The first project was a collaboration with Jacob Murray,[196] who was a PhD candidate in Professor AnnMarie O'Donoghue's research group. Our task was to (pyro)phosphorylate a 1,2,4-triazolium mimic (**22**) of thiamine and purify these phosphorylated species. In one aspect, I adopted Jessen's phosphorylation method[1, 145] and used the phosphitylating reagent prepared using the approach described in Chapter 4 of this thesis. After our preliminary studies, Jacob Murray[196] continued to optimise the methods and their ultimate outcome is reported in his thesis. The second project follows on from the work of Rebecca Sweeney, who completed an M. Chem. project in the Hodgson laboratory. Rebecca's work followed on from the work of Ziona Juer, who was a summer project student in the laboratory. The goal of the project was the incorporation of unnatural amino acids (UNAAs) via *in vitro* translation. The element addressed by Juer, Sweeney and in this thesis is the synthesis of the 2',3'-cis-aminothiol analogue of uridine (**35**), which has been reported in the literature.[197, 198] Further details of each project are provided in sections 7.1.1and 7.2.1.

7.1 Synthesis and purification of mono- and diphosphates of a triazolium mimic of thiamine

7.1.1 Introduction

Industrial Chemistry has been an engine of innovation and continuous growth, however, copious amounts of waste have been generated by out-dated processes. Since the 1990s more attention has been paid to the need to reduce environmental pollution and to limit the use and production of toxic, hazardous substances. The demand for cleaner chemistry led to the birth of the Green Chemistry movement.[156] At this new frontier, enzymatic catalysis (biocatalysis) is an essential tool.[157, 199-203] Many enzymes, however, are not accessible in large enough quantities for practical applications and have a narrow substrate scope. An important aspect in the use of enzymes as catalysts has been overcoming these two limiting factors, which has been achieved in part through high-throughput DNA sequencing, enzyme engineering and optimization reached in the last twenty years.[204-206] Biocatalytic applications continue to develop at a rapid rate, finding wide industrial uses in a cost-effective manner.[207]

Many enzymes depend on the presence of cofactors for catalytic activity. Cofactors can be metal ions, metal-organic complexes and organic molecules.[208, 209] One of the most represented cofactor-dependent enzyme families is thiamine diphosphate-(ThDP-)-dependent enzymes, which take part in numerous biosynthetic pathways and catalyse a broad range of reactions. Most importantly, they are involved in the making and breaking of C–C bonds.[210-212] Concurrent with enzymology studies delineating the mode of action of ThDP-dependent enzymes,[213] chemists designed small molecules related to thiamine, namely, N-heterocyclic carbenes (NHCs), which have similar reaction mechanisms.[214-218] The triazolylidene molecular class in particular shows remarkable activity across a diverse range of catalytic processes.[219-223] A biological understanding of the mechanism of thiamine catalysis, combined with the chemical synthesis of small molecule thiamine analogues, led to the discovery of new enzymatic activities to perform desired non-natural functions.[213]

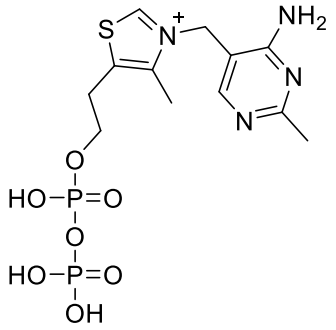

Figure 72: Thiamine diphosphate structure (**24**)

7.1.1 Aim of the project

As reported in the Foreword of this chapter (see section **7**), this project was a collaboration with Jacob Murray, PhD candidate in Prof. AnnMarie O' Donoghue's research group, and they dealt with the synthesis of the 1,2,4-triazolium mimic (**20**). I focussed our attention on the phosphorylation of the triazolium substrate (**20)** and purification of mono- (**21**) and diphosphate (**22**) systems, as shown in *Figure 73*.

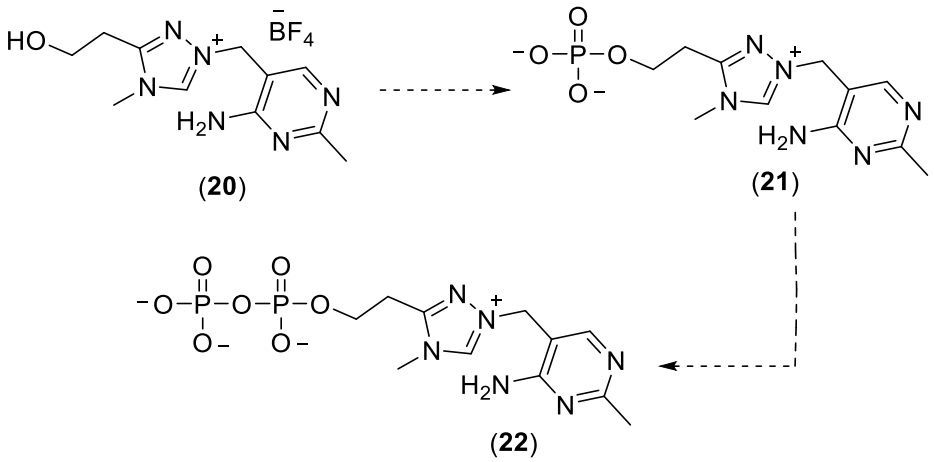

Figure 73: Planned synthetic route for the preparation of mono- (**21**) and di-phosphorylated (**22**) triazolium mimics of thiamine.

Thiamine phosphates and derivatives are synthetized primarily through enzymatic methods,[224-226] whereas chemically, the thiazole/pyrimidine coupling and phosphorylation steps are challenging.[227] However, owing to the non-natural nature of our mimic system, I chose two different synthetic chemical phosphorylation approaches based upon related literature precedents:

- Direct conversion of triazolium mimic (**20**) to its diphosphate using polyphosphoric acid (PPA) as the phosphorylating agent (*Figure 74*).[227]

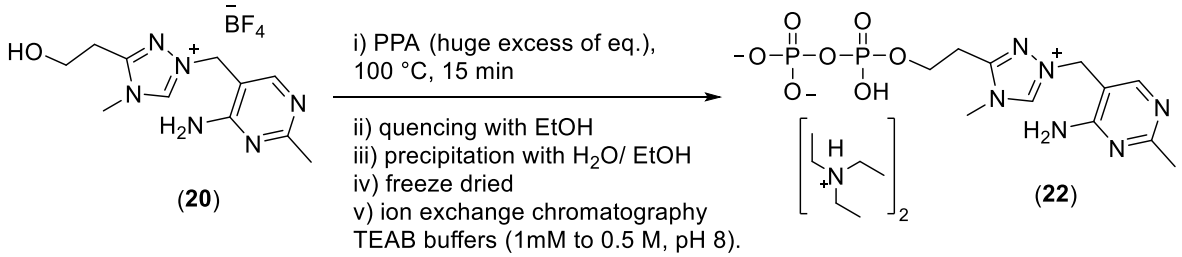

Figure 74: First synthetic strategy for the synthesis of 1-[(4-amino-2-methylpyrimidin-5-yl)methyl]-3-(2-hydroxyethyl)-4-methyl-4*H*-1,2,4-triazol-1-ium diphosphate (**22**) following the strategy proposed by Matsukawa et al.

- Two-step synthesis passing through the synthesis of monophosphate (**21**), using $POCl_3$ as the reagent for the first phosphorylation step [228] (*Figure 75*). and the phosphitylating agent *bis*-(fluorenylmethyl)-diisopropylamine phosphoramidite (**2**) in the second coupling step.[35, 36]

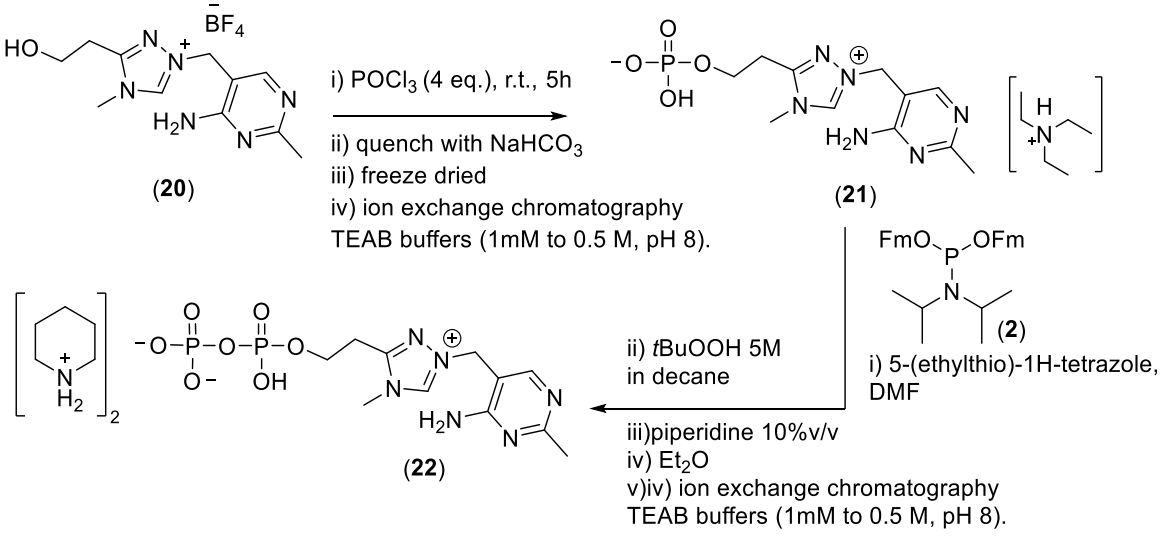

Figure 75: Synthesis of monophosphate compound (**21**) and subsequent formation of diphosphate (**22**).

7.1.2 Results and discussion

After preliminary tests were carried out with commercially sourced thiamine hydrochloride as a model starting material, the direct synthesis of the triazolium thiamine diphosphate mimic (**22**) was conducted as a solvent-free reaction on the mimic compound (**21**), at 100 °C for 15 min. based on the literature (*Figure 74*). The subsequent treatment with ethanol after reaction quenching and then with an ethanolic solution is essential to remove as much inorganic phosphate as possible, to facilitate purification of the compound. The oily crude material was purified using anion exchange chromatography. At first, I tried to reproduce a published purification method[33], adopting a Capto Q strong anion-exchange column (particle size 90 µm) as the stationary phase and 1 mM KH_2PO_4 and 0.5 M KH_2PO_4, pH 6, as the mobile phase. A linear gradient was initiated 10 min. after the injection going from 0% to 100% 0.5 M KH_2PO_4 at a rate of 5% of 0.5 M KH_2PO_4 per minute, with a flow rate of 1.0 mL/min. This method proved to be effective for the purification of the thiamine diphosphate compound (**24**), but not for the monophosphate (**23**), which eluted in the void volume with the starting material. Separation of polar molecules using ion-exchange chromatography is based on their charges, which depend on the pH of the buffer, which should be between the pK_a and the isoelectric point. Based on this assumption, to optimize their purification, I first modified the buffer solution pH, from 6 to 8, in order to have the phosphate moiety fully charged. This allowed us to successfully separate the starting material from the monophosphate, which at this stage eluted at 10% 0.5 M KH_2PO_4 buffer. Since the diphosphate elutes at 20% of 0.5 M KH_2PO_4 buffer, I then focused on improving the resolution of the purification, opting for a step-gradient run (0%, 10%, 20% of 0.5 M KH_2PO_4 buffer). Despite effectively separating the compounds, they were not pure due the presence of inorganic phosphate in the elution buffer. Given that the inorganic phosphate was present as a result of the chosen buffer (based on literature precedent), I decided to use an alternative eluent system, consisting of a gradient between 1 mM triethylammonium bicarbonate (TEAB) and 0.5 M TEAB buffer with a pH in the range between 7 and 8. Subsequent runs were then carried out following the same protocol in terms of gradient and flowrate, however, the presence of inorganic phosphate was still detected by ^{31}P NMR, suggesting co-elution of phosphate by-product derived from excess polyphosphoric acid. Different flow rates and gradients were tested (i.e., step-gradient run 0%, 20%, 40% for 10 minutes each) without any improvement on the results. Washing with ethanolic solution was therefore not sufficient to remove all inorganic phosphate from the crude reaction mixture, thus making the purification more difficult than expected. Based on

these preliminary experiments and on the analyses conducted, the conversion of the starting material into monophosphate (**21**) and diphosphate (**22**) products was not very high (≤ 20%), and, considering the amounts of by-products generated, the reaction yield and purification seemed to be unworkably low.

Therefore, I decided to try a second synthetic strategy of isolating the monophosphate to optimize the second phosphorylation step for the diphosphate synthesis (see *Figure 75*). During the first step of the sequence, the substrate (**20**) was stirred in phosphorus(V) oxychloride for 6 h at room temperature, with a conversion of starting material into monophosphate of *ca.* 90% based on the ^{1}H NMR spectrum. Despite gaining promising purification results with Capto Q media, I found that the length of the purification process was significant, especially because of the low sample loading capacity (total ionic capacity 0.16–0.22 mmol Cl^-/mL medium). Our choice, therefore, was to exploit the use of a 5.5 g RediSep Rf Gold® Amine column, a linear gradient between H_2O and 1 M TEAB buffer (pH 7-8), and a flow rate of 13 mL/min with a linear gradient run (35 CV). The column adopted on the Teledyne system was a weak anion-exchange column, rather than strong anion exchange. At first, I attempted the purification of commercial standards of thiamine, thiamine monophosphate and thiamine diphosphate with satisfactory results (as reported in *Figure 76*).

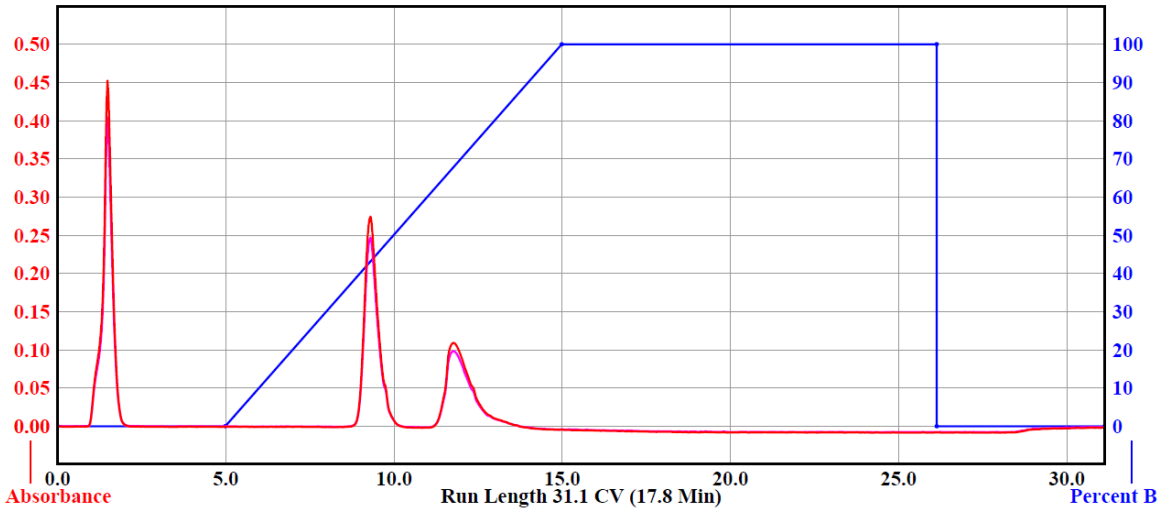

Figure 76: Chromatogram of thiamine, thiamine monophosphate and thiamine diphosphate during anion exchange purification on a 15.5 g RediSep Rf Gold® Amine column, H_2O and 1 M TEAB buffer pH 8 of 30 mL/min (31 CV). In details, the first peak corresponds to thiamine, the second one to thiamine monophosphate and the third one to thiamine diphosphate.

However, the subsequent purification of the crude monophosphate of the triazolium mimic (**21**) did not give positive results since the monophosphate was found to elute in the void volume with the starting material (**20**). This reduction in retention may be due to a different charge state of the analyte, compared to the thiamine system, at the chosen elution pH. In response, I decided to adopt a larger column—15.5 g RediSep Rf Gold® Amine column, instead of 5.5 g—while maintaining the same linear gradient profile of H_2O and 1 M TEAB buffer pH 8, and a flow rate of 30 mL/min (31 CV) over 20 min (as shown in *Figure 77*).

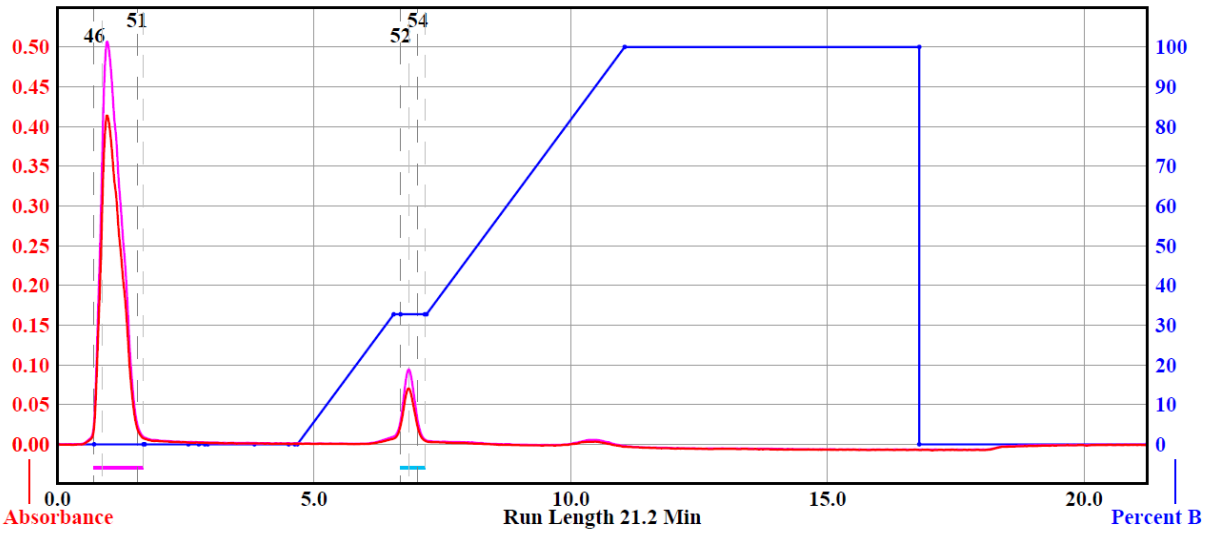

Figure 77: Chromatogram of triazolium mimic monophosphate crude purified by anion exchange chromatography on 15.5 g RediSep Rf Gold® Amine column, H_2O and 1 M TEAB buffer pH 8 of 30 mL/min (31 CV). The second peak corresponds to the triazolium mimic monophosphate.

Pleasingly, the purity of the resolved monophosphate was confirmed by ^{31}P NMR spectroscopy. This material and the associated protocol were used as the starting points for the synthesis of the diphosphate, which was pursued by Jacob Murray.[196]

7.1.3 Conclusions

These preliminary, but still satisfying results were the forerunner of further work carried out by Jacob Murray, who tested and improved the two-step synthetic method and the purification procedure, obtaining both mono- and di-phosphates of the triazolium mimic with excellent yields. The Jessen method[1], with reagent being prepared using a batch approach (see Chapter 4, section 4.1), proved to be efficient for the delivery of the diphosphate (**22**), demonstrating its wider applicability.

7.1.4 General experimental procedures

Unless otherwise stated, all solvents were purchased from Fisher Scientific and used without further purification. Dry solvents were purchased from Sigma Aldrich and used without further purification. Substrates, their precursors, and reagents were purchased from either Alfa Aesar, Sigma-Aldrich, TCI, Carbosynth or Acros Organics. Flash chromatography was performed on two different chromatographic systems: an ÄKTA Prime Plus was used for Capto Q strong anion-exchange chromatography (particle size 90 µm), and a Teledyne CombiFlash NextGen 100 system was used for RediSep Rf Gold® Amine weak anion-exchange (5.5/15 g) chromatography. Here I I report only the purification performed on a Teledyne CombiFlash NextGen 100 system. Nuclear Magnetic Resonance (NMR) spectra were recorded on a Bruker Neo-400 spectrometer with operating frequencies of 400.20 MHz for ^{1}H, 100.63 MHz for ^{13}C and 162.00 MHz for ^{31}P at 25 °C and on a Varian VNMRS-600 spectrometer with operating frequencies of 599.242 MHz for ^{1}H, 92.01 MHz for ^{2}H, 150.72 MHz for ^{13}C and 242.65 MHz for ^{31}P at 25 °C. The analytical data collected for the thiamine monophosphate and diphosphate (^{1}H and ^{31}P NMR spectra) that were prepared to validate our synthetic approaches corresponded directly to those for the commercially sourced compounds.

7.1.4.1 Synthesis of Thiamine Monophosphate (23): 3-[(4-Amino-2-methylpyrimidin-5-yl)methyl]-4-methyl-thiazol-3-ium monophosphate

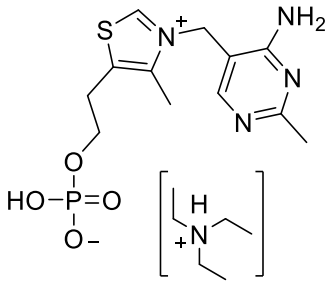

Thiamine hydrochloride (0.226 g, 0.59 mmol) was stirred in phosphorus(V) oxychloride (0.22 mL, 2.36 mmol, 4 equiv.) for 6 h at room temperature. The solid crude material was quenched with 1 M $NaHCO_3$ solution, and the resulting solution was lyophilised. The crude material was suspended in ethanol and insoluble sodium phosphate was removed by filtration. The solvent was removed under vacuum to obtain a yellow solid. Purification was carried out by

weak ion exchange chromatography using a 5.5 g RediSep Rf Gold® Amine column with a stepwise gradient of TEAB buffers (1 mM to 1 M, pH 8) and 13 mL/min flow rate. Mass recovery 41%.

^{1}H NMR (400 MHz, D_2O): δH= 7.57 (s, 1H), 5.33 (s, 2H), 3.09 (ap. q., *J*= 11.8, 6.2 Hz, 2H), 3.25 (s, 2H) 3.15 (t, *J*= 5.70 Hz, 2H), 2.51 (s, 3H), 2.44 (s, 3H).

^{31}P NMR (162 MHz, D_2O): δP =2.69 (t, *J*= 5.9 Hz monophosphate 82%), 1.19 (s, phosphate 18%).

(Similar NMR data were also observed with commercial thiamine monophosphate, except for the presence of triethylammonium ions.)

7.1.4.2 Synthesis of Thiamine Pyrophosphate (24): 3-[(4-Amino-2-methylpyrimidin-5-yl)methyl]-4-methyl-thiazol-3-ium diphosphate

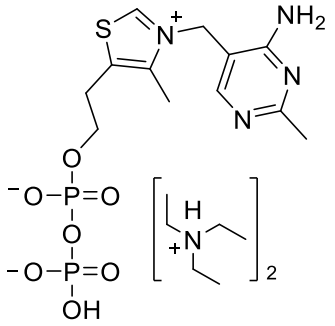

Thiamine hydrochloride (0.1 g, 0.30 mmol) and polyphosphoric acid (0.366 g, 4.36 mmol, 14 equiv.) were heated at 100 ºC for 10-15 min. until the gummy mixture turned from white to yellow. The mixture was cooled, and the precipitate was removed by filtration. The solid was taken up in water (1.5 ml), then ethanol was added (5 ml) and the mixture was stored at –18 ºC overnight. The solid material was collected by filtration, redissolved in water, and the pH of the solution was adjusted to pH 8. The solution was then subjected to purification on weak ion exchange chromatography using a 5.5 g RediSep Rf Gold® Amine column with a stepwise gradient of TEAB buffers (1 mM to 0.5 M, pH 8) and 13 mL/min flow rate. Mass recovery 35%.

^{1}H NMR (400 MHz, D_2O): δH= 9.56 (s, 1H), 7.83 (s, 1H), 5.45 (s, 2H), 3.09 (ap. q., *J*= 11.8, 6.2 Hz, 2H, CH_2OP), 3.23-3.20 (m, 2H), 2.51 (s, 3H), 2.44 (s, 3H).

^{31}P NMR (162 MHz, D_2O): δP = –10.80 (d, J=19.6 Hz), –11.21 (d, J=19.7 Hz).

(Similar NMR data were also observed with commercial thiamine pyrophosphate, except for the presence of triethylammonium ions.)

7.1.4.3 Synthesis of Thiamine Monophosphate analogue (21): 1-[(4-amino-2-methylpyrimidin-5-yl)methyl]-3-(2-hydroxyethyl)-4-methyl-4H-1,2,4-triazol-1-ium monophosphate

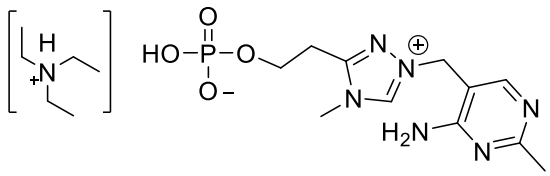

Substate (**20**) (0.1 g, 0.30 mmol) was stirred in phosphorus(V) oxychloride (0.185 g, 1.2 mmol, 4 equiv.) for 6 h at room temperature. The solid crude material was quenched with 1 M $NaHCO_3$ solution, and the resulting solution was lyophilised. The crude material was suspended in ethanol and insoluble sodium phosphate was removed by filtration. The solution was dried under vacuum to obtain a yellow solid. The solution was then subjected to purification on weak ion exchange chromatography using a 15.5 g RediSep Rf Gold® Amine column, with a linear gradient of 1 M TEAB buffer pH 8, and a flow rate of 30 mL/min. Mass recovery 42%.

^{1} H NMR (600 MHz, D_2O) δH: 8.05 (s, 1H), 5.32 (s, 2H), 3.92 (app q, *J*= 13, 12.8 MHz, 2H), 3.76 (s, 3H), 3.06 (t, *J*=6.2, 5.7 MHz, 2H), 2.29 (s, 3H)

^{31}P NMR (162 MHz, D_2O): δP =2.20 (s).

7.1.4.4. Synthesis of Thiamine Diphosphate analogue (22): 1-[(4-amino-2-methylpyrimidin-5-yl)methyl]-3-(2-hydroxyethyl)-4-methyl-4H-1,2,4-triazol-1-ium diphosphate

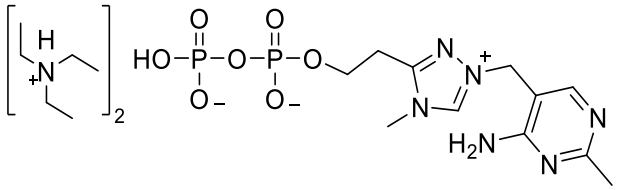

Substate (**20**) (0.05 g, 0.15 mmol) and polyphosphoric acid (0.183, 2.18mmol, 14 equiv.) were heated at 100 ºC for 10-15 min. until the sticky solid turned from white to yellow. The mixture was cooled, and the precipitate was removed by filtration. The solid was taken up in water (1.5 ml), then ethanol was added (5 ml) and the mixture was stored at –18 ºC overnight. The solid material was collected by filtration, redissolved in water, and the pH of the solution was adjusted to pH 8. The solution was then subjected to purification on weak ion exchange chromatography using a 5.5 g RediSep Rf Gold® Amine column with a stepwise gradient of TEAB buffers (1 mM to 0.5 M, pH 8) and 13 mL/min flow rate. Mass recovery 37%.

^{1} H NMR (600 MHz, D_2O) δH: 8.10 (s, 1H), 5.36 (s, 2H,), 4.18(app q, *J*= 13, 12.8 Hz, 2H), 3.81 (s, 3H), 3.18 (m,2H), 2.33 (s, 3H).

^{13}C NMR (150 MHz, D_2O) δC= 168.8 (C), 162.1 (C), 157.2 (C), 155.6 (CH), 142.2 (CH), 105.6 (C), 62.0 (CH_2), 49.5 (CH_2), 33.3 (CH_3), 25.4 (CH_2), 24.0 (CH_3).

^{31}P NMR (276 MHz, D_2O) δP= –6.05 (d, 21.9 Hz), –10.84 (d, 21.1 Hz).

HR-MS calculated for $C_{11}H_{19}N_6O_7P_2^+$: 409.08, found (32%, M+), 431.41.

7.2 A Chemical approach to the introduction of non-natural amino acids into proteins

7.2.1 Introduction

The incorporation of unnatural amino acids (UNAAs) in protein engineering is a key tool in synthetic biology, that could provide proteins with novel physicochemical properties and biological functions.[229-233]

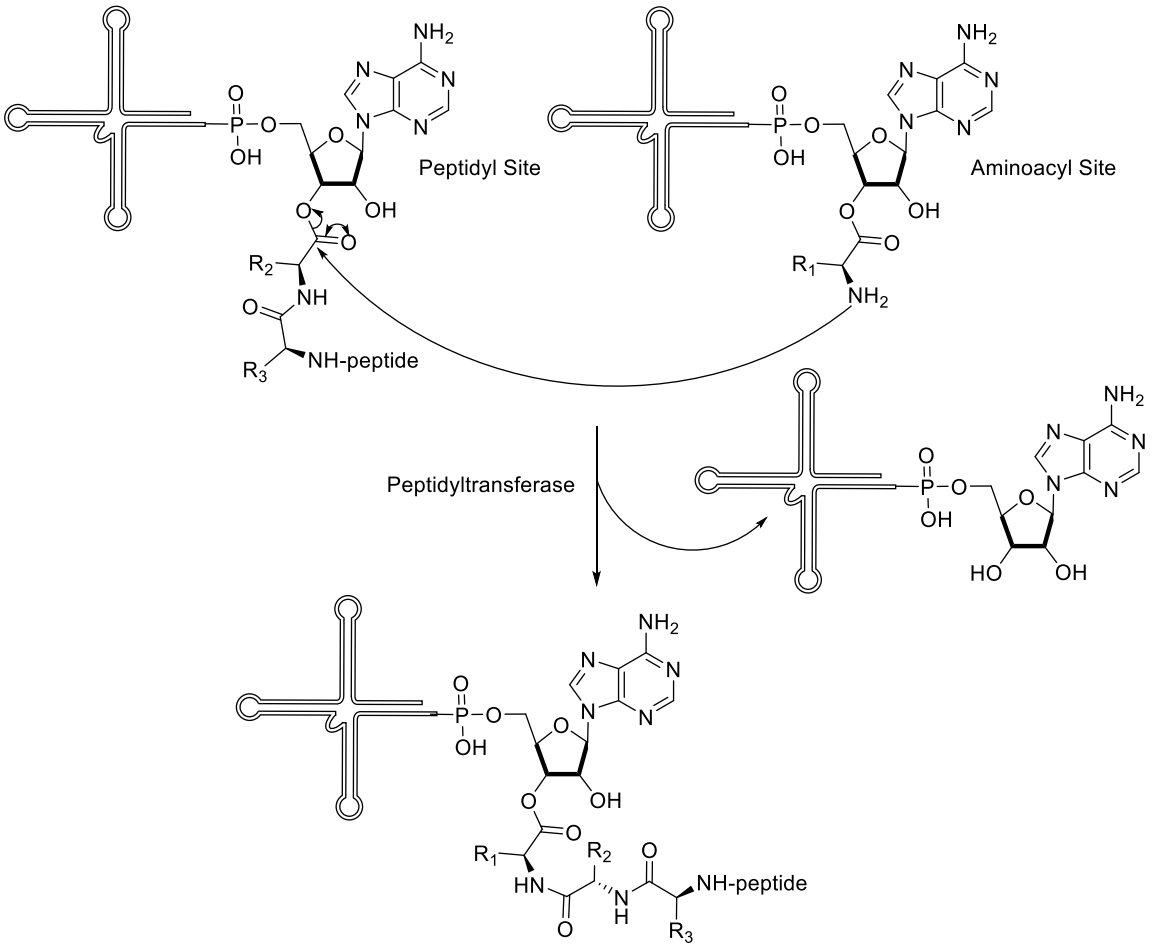

Figure 78: Chemical mechanism of peptide bond formation during the elongation phase of ribosomal protein synthesis.

The central reaction in protein synthesis involves the delivery of an aminoacyl-tRNA to the acceptor site on the ribosome, with its identity being specified by messenger RNA (mRNA). The function of aminoacyl-tRNA synthesis is to match amino acids with tRNAs containing the corresponding anticodon. The ribosomal peptidyl transferase activity normally cleaves the

ester bond connecting the amino acid and the 3'-terminal adenosine of tRNA to form a peptide bond between the carbonyl group of the peptidyl chain and the amino group on the adjoining aminoacyl-tRNA[234, 235] (see *Figure 78)*. In summary, all aminoacyl-tRNA synthetases (aaRS) lead to ligation of amino acids to their cognate tRNAs; where each aaRS reacts with a specific amino acid, tRNA, and a molecule of ATP[236] (see *Figure 79)*.

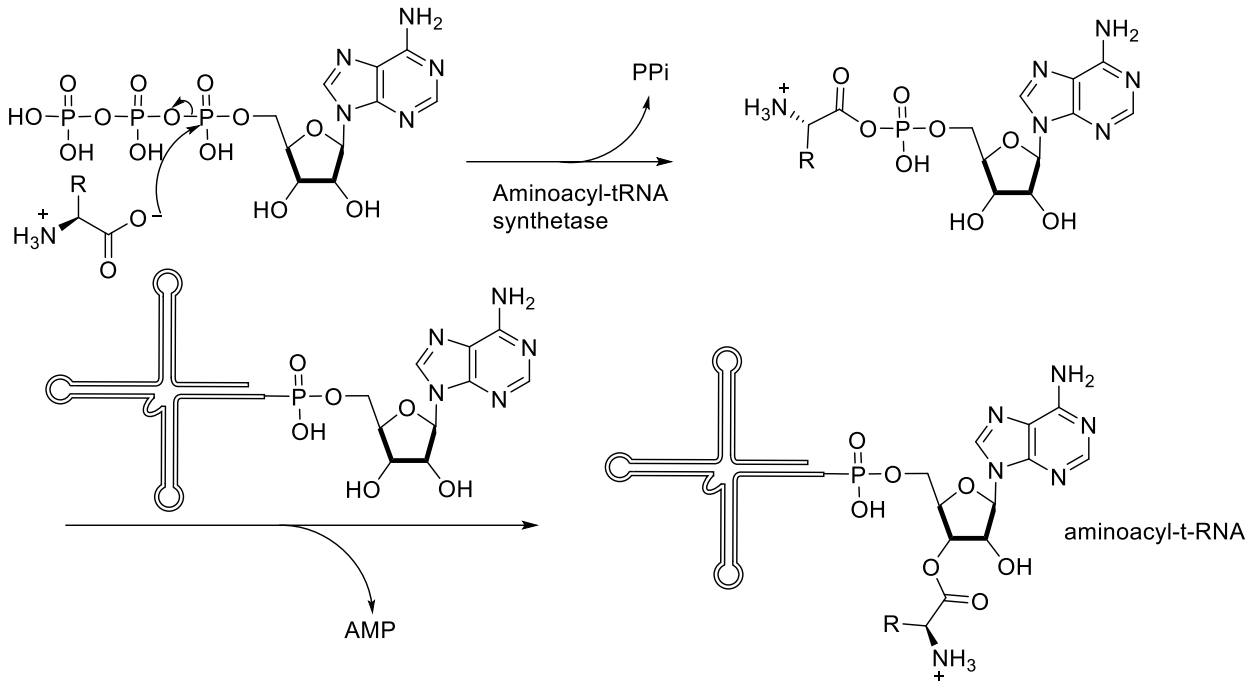

Figure 79: Mechanism of aminoacyl-tRNA synthesis.

Several methods have been developed to incorporate unnatural amino acids site-specifically into proteins *in vivo*, but they require the addition of new components to the biosynthetic machinery including a codon that does not encode any of the common 20 amino acids (often through suppression of a stop codon), an orthogonal tRNA / aminoacyl-tRNA synthetase and an unnatural amino acid.[229, 230, 233, 237-245] The major drawbacks of *in vivo* UNAA incorporation strategies[246-249]are the cytotoxicity of the foreign biological components and the low permeability of cell membranes to UNAAs. Moreover, these systems are only useful for introducing a small number of UNAAs into a single protein. To overcome these problems, incorporation of UNAAs using cell-free protein synthesis (CFPS) systems forms the basis of *in vitro* studies.[231, 243, 249-256] CFPS is the synthesis of proteins *in vitro* without using intact, living cells. The open environment of the CFPS allows the direct addition of new components into the biochemical systems. These cell-free systems are not constrained by cell-viability requirements, so it is possible to use linear DNA fragments for a target gene expression, avoiding time-consuming gene cloning steps required for *in vivo* protein synthesis. The most

used methods of incorporating UNAAs into CFPS systems are the Global Suppression Method (GSM) and the Orthogonal Translation System (OTS). The OTS is more widely used than the GSM due to its greater site-specific UNAA incorporation, resembling the *in vivo* incorporation strategies, through its use of orthogonal aaRS/tRNA pairs. Whilst in the GSM, auxotrophic strains are prepared to make the UNAA extracts. This strategy utilises native biological machinery to incorporate multiple identical UNAAs into a single protein. While, if more orthogonal translation pairs can be identified, another strategy, the Frame-shift Suppression Strategy, may become the preferred method due to its ability to incorporate multiple distinct UNAAs into protein thanks to the creation of an enlarged codon with four or five nucleotides.[231, 238, 254] However, expensive reagents, the lack of scalable systems hindering cell-free protein production at an adequate scale and restrictions on the incorporation of multiple distinct UNAAs into a single protein remain the biggest drawbacks. Chemical approaches towards the delivery of aminoacyl tRNAs have been explored, however, they are very challenging because of the low nucleophilicity of the hydroxyl groups, as well as the lability of the ester bonds that form between the tRNA molecules and the amino acids.[257]

7.2.2 Aim of the project

The main hypothesis of the work described here hinges on the fact that an NH_2 group is a better nucleophile than an OH group, due to nitrogen being more nucleophilic than oxygen (see *Figure 80*).[234, 249,258-263] However, amide-linked amino-acyl-aminodeoxyadenosine analogues are unable to donate the amino acids and incorporate them into a growing polypeptide chain because the inert nature of amide bonds causes the de-acylation of these systems to be very slow. For example, the antibiotic Puromycin, amino nucleoside with a similar structure to the terminal adenosine residue of aa-tRNA, inhibits protein synthesis by ribosome-catalysed incorporation into the C-terminus of elongating nascent chains, blocking extension and resulting in premature termination of translation (see *Figure 80*). [262, 264]

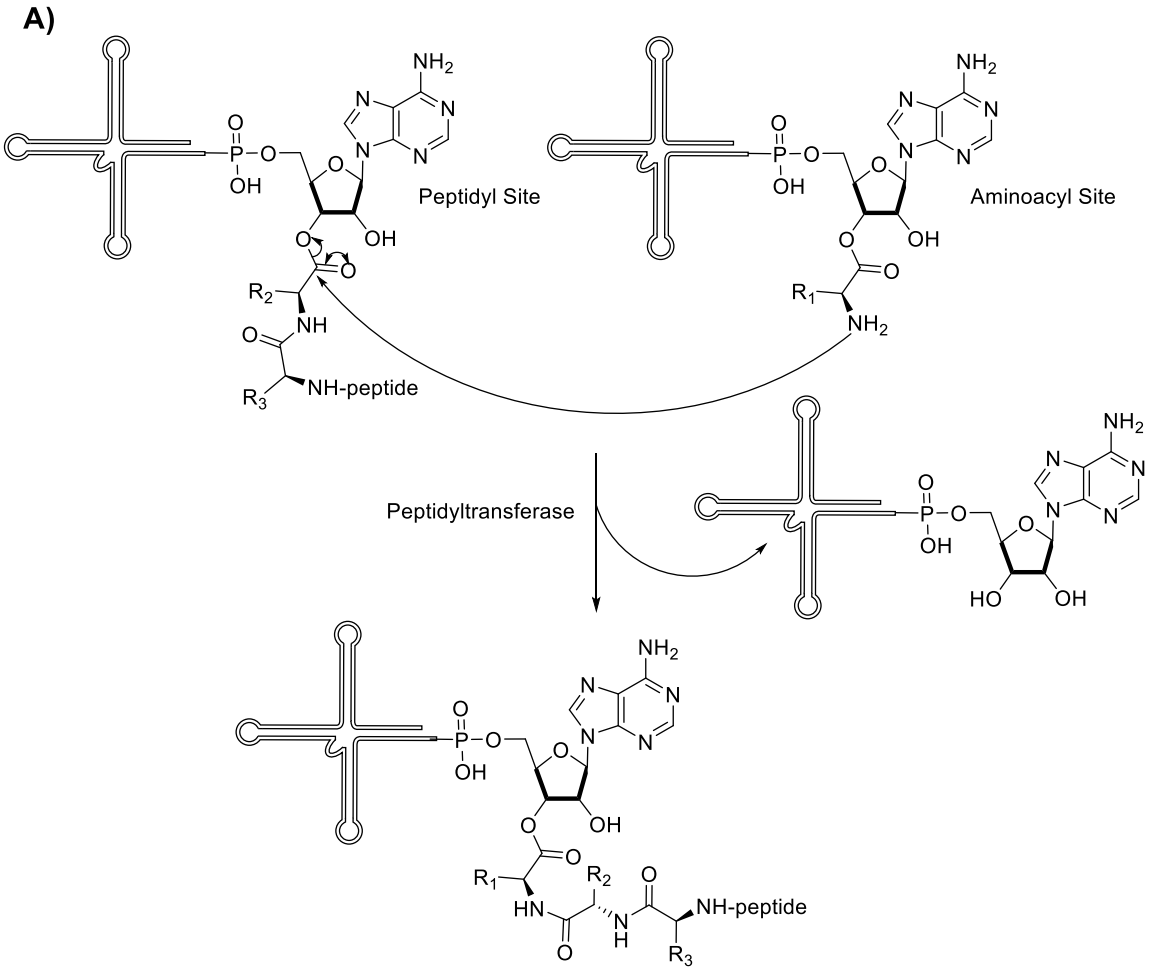

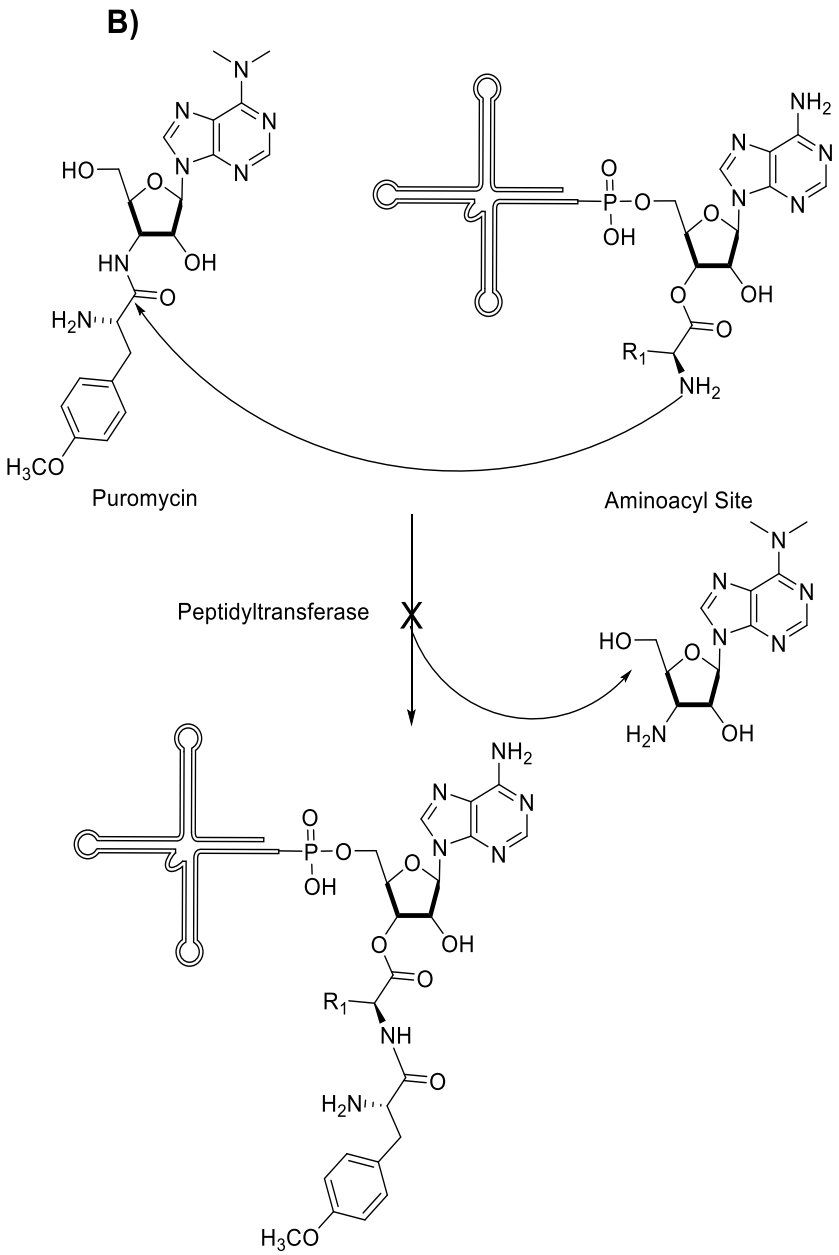

Figure 80: Comparison between the mechanisms of peptide bond formation and the mechanism of action of puromycin. (A) Peptide bond formation's mechanism. (B) Puromycin's action mechanism.

The rationale behind this project is to impart the advantages of having a nitrogen nucleophile at the 3'-RNA terminus, which should facilitate acylation, while simultaneously decreasing the stability of the aa-tRNA amide bond to allow deacylation on the ribosome.

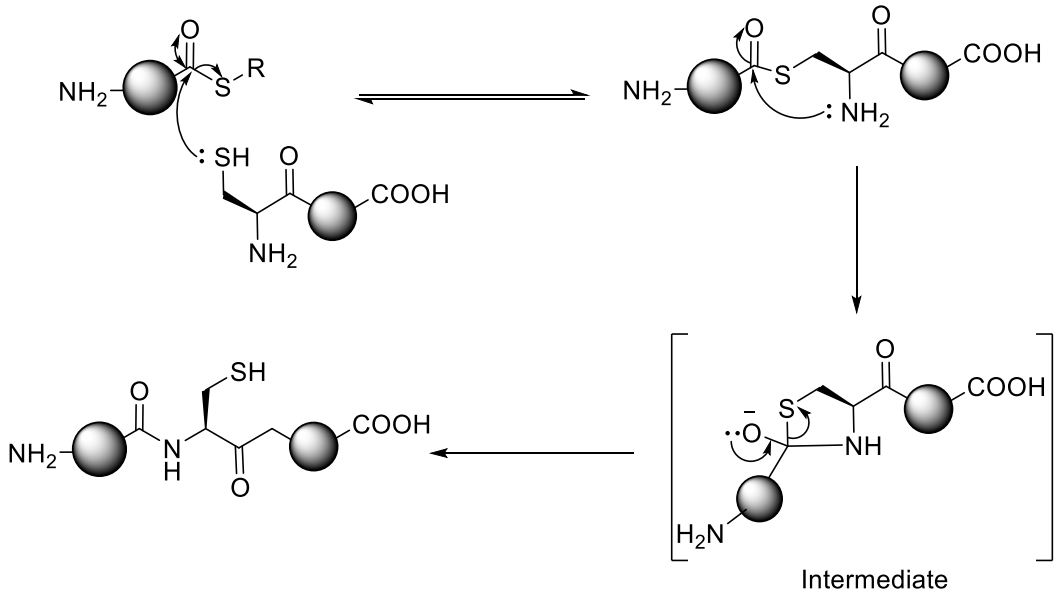

Figure 81: Mechanism of Native Chemical Ligation.

Native Chemical Ligation (NCL), see *Figure 81*, is one of the most commonly employed methods for peptide ligation, that takes inspiration from biological processes such as protein ubiquitination, intein-mediated protein splicing, sortase-mediated protein modification and transglutamination. NCL exploits S-to-N acyl transfer as a key step to introduce an amide bond.[265-269] I Ihypothesize that the use of a ribonucleoside analogue containing a cis-aminothiol system may afford a solution to the deacylation problem (see *Figure 82*) given that *N-S* acyl shifts are known to be reversible.[270] The equilibrium of *N-S*/*S-N* acyl shifts is thermodynamically favoured in the direction of amide product formation, and the thermodynamic driving force is amide bond formation. In addition, there are several methods of forcing the equilibrium to favour thioester formation.[271, 272] For example, in protein splicing, the formation of the thioester intermediate involves a thermodynamically unfavourable reversible *N-S* acyl shift. Eukaryotic systems can shift this equilibrium in favour of *N-S* acyl transfer by inducing a conformational rearrangement of the intein.[273]

In our case, if migration to S were to occur on the ribosome, there would be two potential N-based acceptors, namely the donating nucleoside-N or the N of the P-site peptidyl-tRNA, where transfer to the latter would be irreversible.

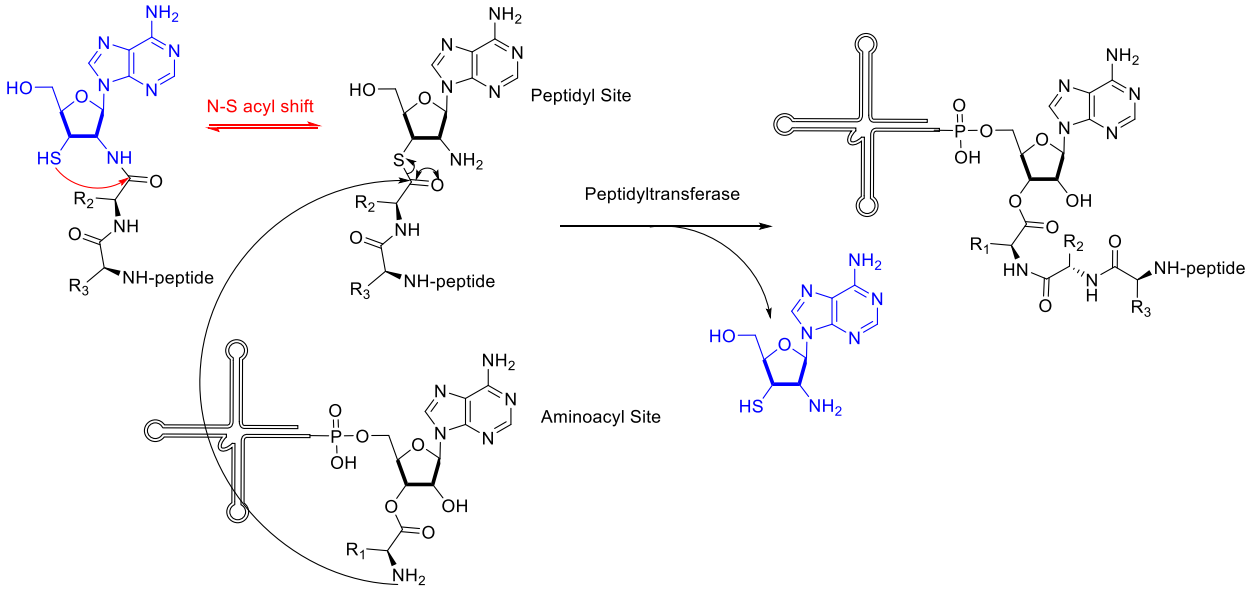

Figure 82: Potential mechanism for peptide bond formation for the cis-aminothiol-based aa-tRNA, utilising an N-S acyl shift.

I hypothesise that the presence of a cis-aminothiol system should provide a framework for N-S migration of acyl groups, and this may render N-aminoacylation on the nucleoside reversible. I aim to synthesize a 2'-3'-cis-aminothiol analogue of a ribonucleoside and then explore its ability to undergo aminoacylation and deacylation. I report our efforts towards the synthesis of 2',3'-cis-aminothiol analogue of uridine (**35**), the first synthesis of a ribonucleoside analogue bearing a 2'-3'-cis-aminothiol system, see *Figure 83*.[197] If this analogue can be efficiently acylated and thereafter deacylated, this strategy will be adapted to prepare a cis-aminothiol-adenosine analogue that mimics the natural 3'-terminus of tRNA. Subsequently, an aminothiol-based tRNA, prepared via ligation of cis-aminothiol adenosine to tRNA, will be used for the in vitro translation of proteins containing UNAAs.

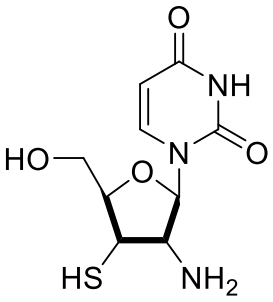

Figure 83: 2',3'-cis-aminothiol analogue of uridine (**35**).

7.2.3 Results and Discussion

The aim of the work described below was to perform the reported literature synthesis of molecule (**35**), see *Figure 84*, and, if time permitted, test whether the analogue could undergo aminoacylation and subsequent deacylation. At the point of engaging this project, Rebecca Sweeney had progressed to mesylate (**30**). In addition, she had overcome problems associated with the conversion of ribo-configured (**27**) to xylo-configured (**29**). The synthesis had to be re-started in order to have enough material to explore steps beyond (**30**). I planned to achieve a firm, reliable, scaled route through to (**32**) before moving on to (**33**) and (**34**). As (**32**) is fully protected, I hoped for greater stability in contrast to the partially protected, and fully deprotected (**35**), where (**35**) is likely to be susceptible to disulphide bond formation. In the following report, details of the synthetic process for the scaled-up synthesis of (**30**) are given. I will then discuss the attempted synthesis of (**31**), however, during this phase of the project, access to facilities became available, and the main project, described in Chapter 4 was resumed.

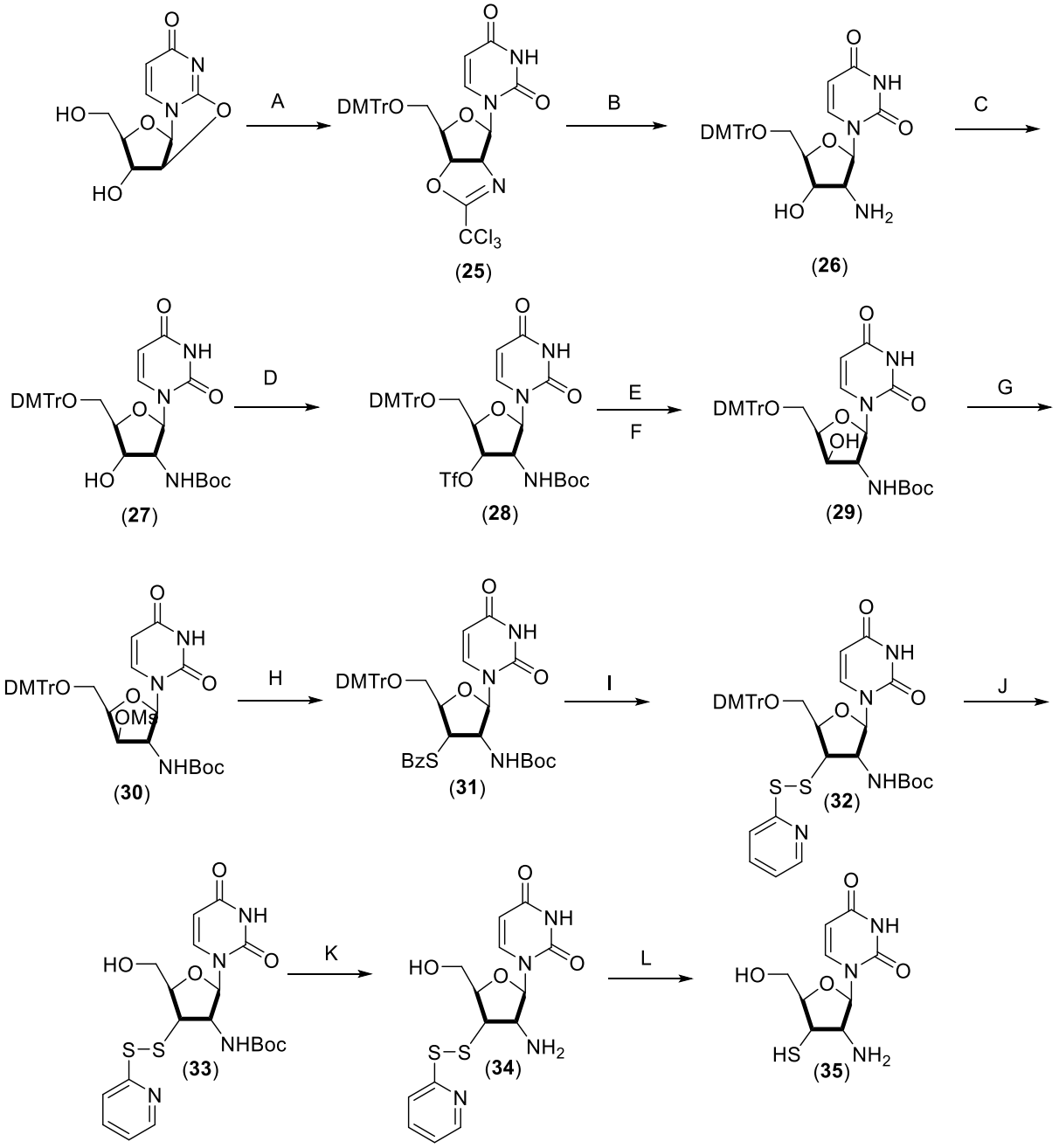

Reaction conditions: (A) (1) DMTr-Cl, DMAP, dry pyridine, dry DMF, 16 h, under N_2; (2) Cl_3CCN, Et_3N, reflux, 24 h, (B) 6 N NaOH, EtOH, reflux, 16 h; (C) Boc-ON,Et_3N,dry dioxane, 40 °C, 16 h, under N_2; (D) $(CF_3SO_2)_2O$, dry pyridine, dry CH_2Cl_2, –78 °C to rt, 18 h, under N2; (E) 6 N NaOH (1.1 equiv), EtOH, rt, 16 h; (F) 6 N NaOH (2.0 equiv), EtOH, rt, 16 h; (G) $MeSO_2Cl$, pyridine, rt, 16 h (H) Sodium thiobenzoate, DMF, 100 °C, 16 h; (I) (1) 40% aqueous $MeNH_2$, rt, 16 h, (2) aldrithiol, DMF, 60 °C, 16 h (J), 3% trichloroacetic acid in acetonitrile, rt, 0.5 h; (K) 30% trifluoroacetic acid in CH_2Cl_2, rt, 1 h; (L) dithiothreitol, THF, rt, 1 h.

Figure 84: Synthetic route towards 2'-3'-cis-aminothiol uridine analogue (**35**) following the methods outline by McGee at al.[198], and Dai at al.[197].

Reasonable yields were reported by McGee *et al.*[198] for the two different strategies for synthesising compound (**25**). The strategy was to isolate each reaction intermediate of the three reactions that led to the formation of (**25**). After regioselective trityl protection of the 5'-

OH group of anhydrouridine, synthesis of imidate intermediate (**25**) occurred by reaction with trichloroacetonitrile, first at room temperature followed by reflux. At last, the 3′-imidate was dissolved in dioxane with 1 equiv. of sodium hydride to eliminate trichloroimidate and regenerate the 5'-protected anhydrouridine. McGee et al.[198] reacted the crude protected anhydrouridine (**25**) in neat trichloroacetonitrile with catalytic triethylamine to overcome the reversibility of 3′- imidate formation under basic conditions.

Initially, I followed the "non-isolation method", where an overnight regioselective trityl protection on the 5'-OH group of anhydrouridine was performed, followed by a liquid-liquid extraction-based work up. After I evaporated the organic layer, the crude reaction mixture was reacted directly with trichloroacetonitrile, in the presence of Et_3N to form oxazoline moiety (**25**) in a yield of 30%, which is significantly lower than the 80% yield reported in the literature. I postulated that one of the possible explanations for this poor mass recovery is the acid lability of the dimethoxytrityl protecting group, causing degradation of the product during chromatographic purification on silica gel.

Despite the low recovery levels, cyclic trichloroacetimidate (**25**) was suspended in EtOH and aqueous 6 N NaOH solution was added dropwise, and the reaction was stirred at 80 °C overnight. The solvent was removed under vacuum and the residue was redissolved in CH_2Cl_2 and washed with saturated NH_4Cl solution. The organic layer was dried under vacuum and the residue was purified by column chromatography to afford compound (**26**) in a yield of 70%. (**26**) was then subjected to Boc-protection on the 2'-NH_2 to form compound (**27**). The overnight reaction reported by Dai and Piccirilli[197] involved the use of Boc-ON in the presence of Et_3N in dioxane at 50 °C. Due to the 38% yield observed in our hands, and the observation by TLC analysis of multiple products, I chose to change the reaction conditions. Specifically, di-tert-butyl-dicarbonate was used as the protecting reagent in dry CH_2Cl_2 at room temperature. These changes afforded compound (**27**) in 3 h in a yield of 60%.

The synthesis of compound (**28**) involved a very exothermic reaction between the nucleoside starting material (**27**) and triflic anhydride. Nucleophilic attack of the 3'-OH group of (**27**) upon the sulfur atom of triflic anhydride is rapid because of the high electrophilicity of the triflic anhydride reagent. The yield of this reaction (25%) appears to be limited by product instability. The white solid (**28**) likely undergoes decomposition during the purification process. The route towards compound (**29**) from (**28**) was developed by a Rebecca Violet Sweeney, initially following the procedure of Piccirilli *et al.*[197], who attempted a one-pot approach.

The synthesis involved the isolation of an intermediate (**36)** as shown in *Figure 85*.

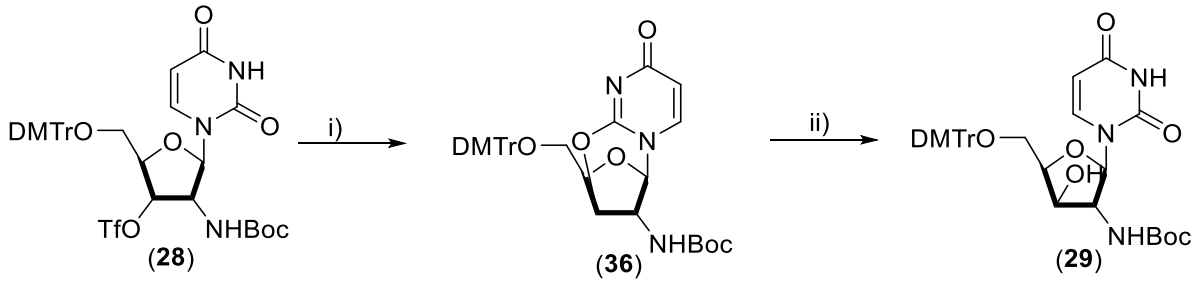

Reagents and conditions:(i) 6 N NaOH (1.1 equiv.), EtOH, rt, 16 h; (ii) 6 N NaOH (2.0 equiv.).

Figure 85: Multi-step synthesis of the xylose derivative (**29**) as described by Piccirilli and co-workers.[197]

Rebecca Sweeney explored different synthetic routes ('one-pot' and multi-step) to obtain compound (**29**), eventually in a good yield. In these two steps she observed that the treatment of an ethanolic solution of (**28**) with NaOH solution can yield an array of products. This is because there are several electrophilic positions on the ribose sugar and the uracil base where a hydroxide ion could attack as a nucleophile. There was ^{1}H NMR evidence to suggest that by-products included 2',3'- or 3',4'-unsaturated nucleosides, formed *via* E2 elimination of triflate from (**28**). Through varying NaOH concentrations and trying different workup methods, Rebecca was able to optimise a "one-pot" synthesis method for compound (**29**), avoiding isolation of the anhydrouridine intermediate (**36**). (**28**) was treated with 1 equivalent of NaOH for 18 h and a further 1.5 equivalents of NaOH. Compound (**29**) was then isolated with a yield of 43% after column chromatography.

The methods developed by Sweeney were adopted and repeated on larger scale by the thesis author upon to the formation of mesylate (**30**). Mesylation on the 3'-OH of (**29**) was required to convert the OH group into a better leaving group, to allow its subsequent nucleophilic displacement (S_N2) by sodium thiobenzoate (**37**). Unfortunately, Sweeney's research activity was impacted as well by COVID-19 pandemic, and she was not able to continue. She attempted the synthesis on a small scale, on ~50 mg of starting material, leading to ~30 mg of (**30**). On the basis of this, I scaled the reaction up and ~ 300 mg of 3'-OMs system (**30**) was prepared in good yield (62%). Subsequently, sodium thiobenzoate (**37**) was prepared by neutralising thiobenzoic acid with NaOH (1 equiv.) in aqueous solution. Sodium thiobenzoate was isolated by freeze drying the aqueous solution to afford a yellow solid. The first reaction attempt was on a small scale, starting from 100 mg of mesylate compound (**30**), but the material recovered from an initial attempt at chromatographic purification was impure and

only obtained in small quantities. Sodium thiobenzoate appears to hydrolyse rapidly, thus during a second reaction attempt, it was added slowly over the course of 4 h to a DMF solution of (**30**), followed by overnight stirring. The reaction was then cooled down and a CH_2Cl_2/$NaHCO_3$ partition was performed. The organic layer was dried under vacuum and the residue was purified by chromatography to afford a white solid. From the ^1H NMR analysis of the residue, it was found that the solid was a mixture of product and starting material, with similar R_f values. Based on this observation, I concluded that our initial strategy to follow the course of reaction using the TLC was not reliable.

At this point, some of the restrictive measures to contain the COVID-19 pandemic were relaxed. As a result, the primary research project was resumed, and the project reported in this section was paused.

7.2.4 Conclusions and future works

The synthesis of fully protected reaction intermediate (**30**) was achieved. with 1 g of material being isolated over several reaction attempts (see *Figure 86*). The conversion into the 3'-thiobenzoyl derivative (**31**) has been attempted two times but further measures are needed in the synthetic process.

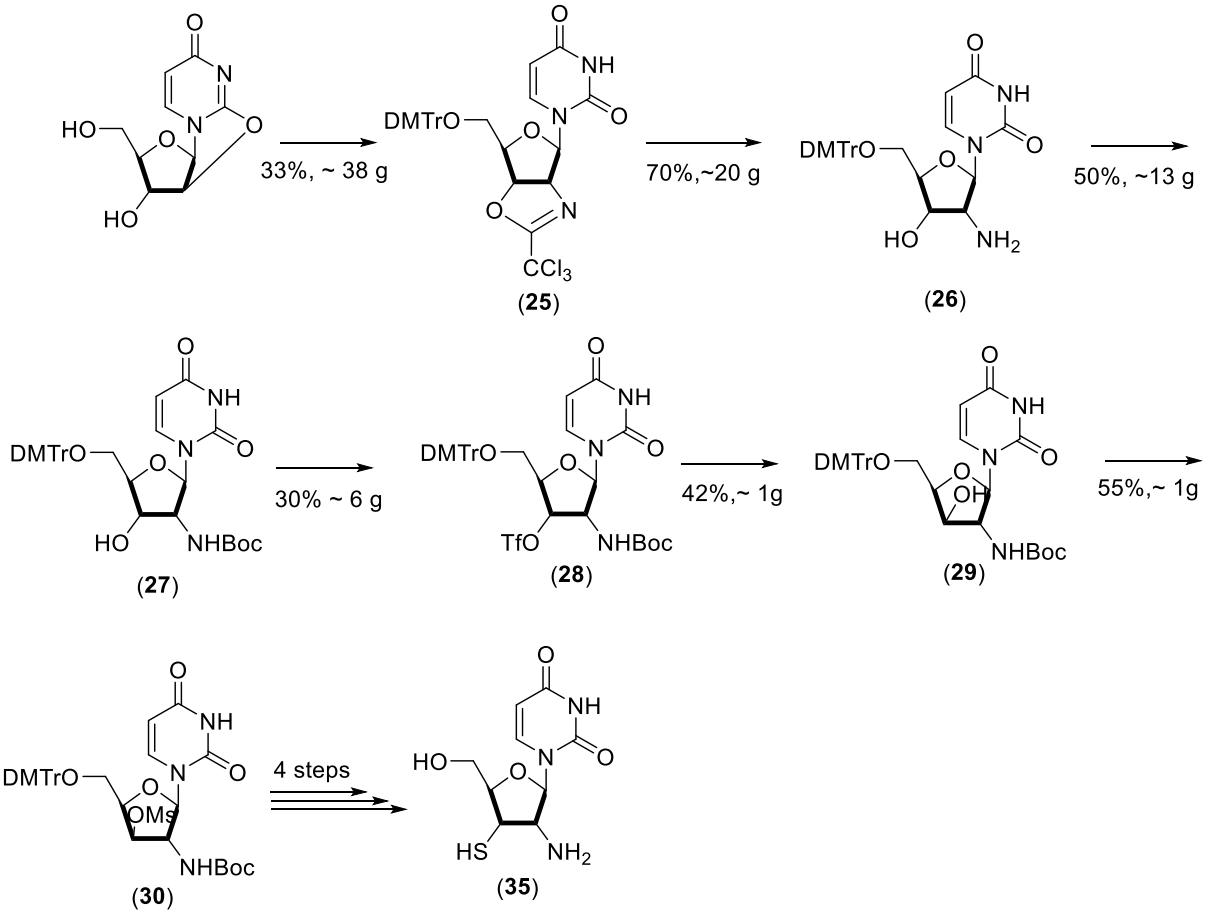

Figure 86: Synthetic route towards 2'-3'-cis-aminothiol uridine analogue (**35**) with the details of the grams synthetized and the overall yields over each reaction attempts.

Carrying out the subsequent conversion into the 3'-pyridyl sulphide before deprotection to get 2′,3′-dideoxy-2′-amino-3′-thiouridine (**35**), and trying to get results more in line with the yields published by Piccirilli,[197] must be the key future plans. The project was adopted to buffer a period of forced unproductivity and remains incomplete. The characterizations presented below are thus, incomplete, and NMR analyses show traces of residual solvents. The partial data and findings are reported to allow subsequent researchers in the Hodgson group to engage more productively with the project in the future. Once the synthesis is completed, it is anticipated that readily-accessible NHS esters could be used in the aminoacylation assays, and their effectiveness could be

monitored by LC-MS and NMR spectroscopy. The same assays will also be deployed to measure diacylation. If these studies show effective acylation and deacylation, an aminothiol-based tRNA will be prepared via ligation of 2',3'-cis-aminothiol adenosine 5'-triphosphate to tRNA. Thereafter, acylation conditions will be explored, followed by the *in vitro* translation of proteins containing non-natural amino acids.

7.2.5 General experimental procedures

Unless otherwise stated, all solvents were purchased from Fisher Scientific and used without further purification. Dry solvents were purchased from Sigma Aldrich and used without further purification. Substrates, their precursors, and reagents were purchased from either Alfa Aesar, Sigma-Aldrich, TCI, Carbosynth or Acros Organics.All reactions using air sensitive, or moisture sensitive reagents were carried out under a nitrogen atmosphere. Flash chromatography was performed on a Teledyne CombiFlash NextGen 100 system. Nuclear Magnetic Resonance (NMR) spectra were recorded on a Bruker Neo-400 spectrometer with operating frequencies of 400.20 MHz for ^{1}H, at 25°C. The spectroscopic data of the compounds synthesised during this research match those described in the literature.[197]

7.2.5.1 Synthesis of 5'-O-(4,4'-Dimethoxytrityl)-2'-N,3'-O-(2-(trichloromethyl)o1zolino)-2'-deoxy-1-(β-D-ribofuranosyl)uracil (25)

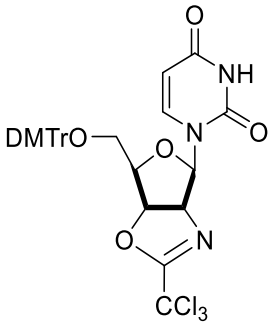

Under an inert atmosphere, anhydrous pyridine (15 mL) and anhydrous DMF (12 mL) were added to a mixture of 2,2'-anhydrouridine (4.45 g, 19.0 mmol), 4,4'-dimethoxytrityl chloride (7.1 g, 21.0 mmol, 1.05 equiv.) and catalytic DMAP (0.019 g, 0.1 equiv.). The reaction mixture was stirred overnight at room temperature under an inert atmosphere, and then evaporated to dryness *in vacuo*. The concentrated reaction mixture was partitioned between CH_2Cl_2 (25 mL) and water (25 mL), and the organic phase was washed with 10% $NaHCO_3$ solution (2 × 20 mL) and brine (2 × 20 mL), dried with $MgSO_4$ and filtered. The solvents were removed *in vacuo*, and the crude residue was then co-evaporated with toluene to afford a sticky red oil. Trichloroacetonitrile (13.3 mL, 133.0 mmol, 7 equiv.) and Et_3N (0.3 mL, 2.47 mmol, 0.13 equiv.) were added to the oil, and the reaction mixture was then refluxed overnight (16 h) at 115 °C. The solvents were removed *in vacuo*, leaving a viscous black oil,

and the crude material was purified by column chromatography on silica gel (20-80% EtOAc in hexane) to afford (**25**) (5.18 g, 7.7 mmol, 40%) as a white powder.

^{1}H NMR (400 MHz, $CDCl_3$): δH = 8.7 (s, 1H, -NH), 7.44-7.35 (m, 3H, Ar-H), 7.33-7.16 (m, 8H, Ar-H), 6.85-6.80 (dd, J = 8.8, 2.6 Hz 4H, Ar-H), 5.75 (d, J = 2.3 Hz, 1H, 1'-H), 5.65 (dd, J = 8.1, 2.3 Hz, 1H, =CHR), 5.31 (dd, J = 8.6, 4.4 Hz, 1H, 3'-H), 5.16 (dd, J = 8.5, 2.3 Hz, 1H, 2'-H), 4.36-4.31 (m, 1H, 4'-H), 3.80 (d, J = 1.8 Hz, 6H, Ar-OCH_3), 3.60 (dd, J = 10.3, 6.7 Hz, 1H, 5'-H), 3.46 (dd, J = 10.3, 3.7 Hz, 1H, 5'-H).

7.2.5.2 Synthesis of Amino-5'-O-(4,4'-dimethoxytrityl)-2'-deoxyuridine (26)

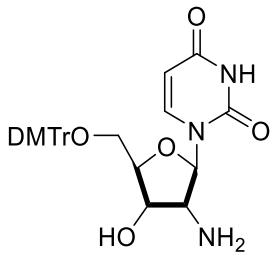

5'-O-(4,4'-Dimethoxytrityl)-2'-N,3'-O-(2-(trichloromethyl)o1zolino)-2'-deoxy-1-(β-D-ribofuranosyl)uracil (**25**) (5.38 g, 7.7 mmol) was dissolved in ethanol (20 mL), and NaOH solution (6 M, 10 mL) was added slowly. The reaction mixture was then refluxed at 108 °C. After cooling, the reaction mixture was evaporated to dryness *in vacuo*, and the crude residue was partitioned between CH_2Cl_2 (20 mL) and saturated ammonium chloride (20 mL). The aqueous phase was extracted with CH_2Cl_2 (3 × 20 mL), and combined organic phases were dried with $MgSO_4$, and filtered. The solvents were then removed *in vacuo* and the crude material was purified by column chromatography on silica gel (1-6% MeOH/CH_2Cl_2 containing 1% Et_3N), to afford compound (**26**) (4.00 g, 7.3 mmol, 95%) as a white foam.

^{1}H NMR (400 MHz, $CDCl_3$): δH = 7.75 (d, J = 8.3 Hz, 1H, =CHR), 7.36-7.34 (m, 2H, Ar-H), 7.28-7.24 (m, 8H, Ar-H), 7.24-7.19 (m, 1H, Ar-H), 6.81-6.84 (m, 4H, Ar-H), 5.88 (d, J = 6.2 Hz, 1H, 1'-H), 5.38 (d, J = 8.6 Hz, 1H, =CHR), 4.20-4.18 (m, 2H, 3',4'-H), 3.78 (s, 6H, Ar-OCH_3), 3.58 (dd, J = 6.5, 5.1 Hz, 2'-H), 3.39-3.45 (m, 2H, 5'-H).

7.2.5.3 Synthesis of 2-Deoxy-2-(tert-butyloxycarbonyl) amino-5-O-(4,4'-dimethoxytrityl)uridine (27)

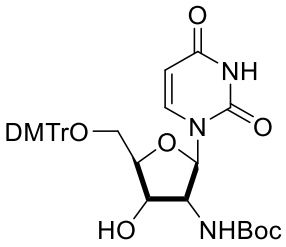

Under an inert atmosphere, 2'-Amino-5'-O-(4,4'-dimethoxytrityl)-2'-deoxyuridine (**26**) (3.54 g, 6.48 mmol) was dissolved in anhydrous dioxane (30 mL). Boc-ON (1.76 g, 7.14 mmol, 1.1 equiv.) and Et_3N (1.5 mL, 7.14 mmol, 1.1 equiv.) were then added, and the reaction mixture was heated overnight at 50 °C. The solvents were removed in vacuo, and the crude residue was partitioned [197]between CH_2Cl_2 (30 mL) and 10% $NaHCO_3$ solution (30 mL). The organic phase was washed with brine (3 × 20 mL), dried with Na_2SO_4, and the solvents were removed *in vacuo*. The crude material was purified by column chromatography on silica gel (0-2% MeOH/CH_2Cl_2 containing 0.2% Et_3N), to afford (**27**) (1.64 g, 2.5 mmol, 38%) as a white solid.

^{1}H NMR (400 MHz, $(CD_3)_2SO$): δH = 11.35 (br s, 1H, -NH), 7.62 (d, J = 8.2 Hz, 1H, =CHR), 7.40 (d, J = 7.6 Hz 2H, Ar-H), 7.32 (t, J = 7.5 Hz, 2H, Ar-H), 7.29-7.23 (m, 5H, Ar-H), 6.90 (d, J = 8.9 Hz, 4H, Ar-H), 6.63 (d, J = 8.8 Hz, 1H, 1'-H), 5.85 (s, 1H,3'-H), 5.61 (s, 1H), 5.46 (d, J = 7.2 Hz, 1H=CHR), 4.27 (q, J = 7.5, 1H, 2'-H), 4.13 (br s, 1H), 4.00-3.97 (m, 1H, 4'-H), 3.75 (s, 6H, Ar-OCH_3), 3.27-3.24 (m, 1H, 5'-H), 3.24-3.20 (m, 1H, 5'-H), 1.38 (s, 9H, $C(CH_3)_3$).

7.2.5.3.1. Modification of the method reported by Piccirilli et all.[197]

Under an inert atmosphere, 2'-Amino-5'-O-(4,4'-dimethoxytrityl)-2'-deoxyuridine (**26**) (4.2 g, 7.7 mmol) was dissolved in anhydrous CH_2Cl_2 (35 mL). Di-tert-butyl-dicarbonate (1.8 g, 8.5 mmol, 1.1 equiv.) and Et_3N (1.1 mL, 8.5 mmol, 1.1 equiv.) were then added, and the reaction mixture was stirred overnight (16 h) at 25 °C. The solvents were removed in vacuo, and the crude residue was partitioned between CH_2Cl_2 (30 mL) and 10% $NaHCO_3$ solution (30 mL). The organic phase was washed with brine (3 × 20 mL), dried with Na_2SO_4, and the solvents were removed *in vacuo*. The crude material was purified by column chromatography

on silica gel (0-2% MeOH/CH_2Cl_2 containing 0.2% Et_3N), to afford 2-deoxy-2-(tert-butyloxycarbonyl) amino-5-O-(4,4'-dimethoxytrityl)uridine (**27**) (3.5 g, 5.4 mmol, 70%) as a white solid.

^{1}H NMR (400 MHz, $(CD_3)_2SO$): δH = 11.35 (br s, 1H, -NH), 7.62 (d, J = 8.2 Hz, 1H, =CHR), 7.40 (d, J = 7.6 Hz 2H, Ar-H), 7.32 (t, J = 7.5 Hz, 2H, Ar-H), 7.29-7.23 (m, 5H, Ar-H), 6.90 (d, J = 8.9 Hz, 4H, Ar-H), 6.63 (d, J = 8.8 Hz, 1H, 1'-H), 5.85 (s, 1H,3'-H), 5.61 (s, 1H), 5.46 (d, J = 7.2 Hz, 1H=CHR), 4.27 (q, J = 7.5, 1H, 2'-H), 4.13 (br s, 1H), 4.00-3.97 (m, 1H, 4'-H), 3.75 (s, 6H, Ar-OCH_3), 3.27-3.24 (m, 1H, 5'-H), 3.24-3.20 (m, 1H, 5'-H), 1.38 (s, 9H, $C(CH_3)_3$).

7.2.5.4 Synthesis of 2-Deoxy-2-(tert-butyloxycarbonyl)amino-3'-O'trifluoromethanesulfonyl-5'-O-(4,4- dimethoxytrityl)uridine (28)

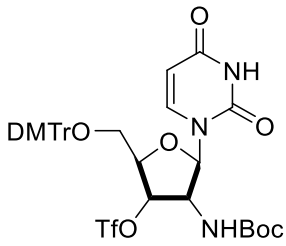

Under an inert atmosphere, 2-Deoxy-2-(tert-butyloxycarbonyl) amino-5-O-(4,4'-dimethoxytrityl)uridine (**27**) (2.7 g, 4.20 mmol) was dissolved in anhydrous pyridine (15 mL) and anhydrous CH_2Cl_2 (15 mL). The solution was cooled to –78 °C, and triflic anhydride (1.06 mL, 6.31 mmol, 1.5 equiv.) was added dropwise. The reaction mixture was then stirred overnight (16 h) at room temperature. MeOH (0.7 mL) was added to quench the reaction, and the solvents were then removed *in vacuo*. The residue was dissolved in CH_2Cl_2, and the solution was washed with 10% $NaHCO_3$ solution (3 × 20 mL) and brine (3 × 20 mL). The organic phase was dried with Na_2SO_4, and the solvents were removed *in vacuo*. The crude material was purified by column chromatography on silica gel (1% MeOH/CH_2Cl_2 containing 0.2% Et_3N), to afford (**28**) (1.28 g, 1.6 mmol, 38%) as a yellow solid.

^{1}H NMR (400 MHz, $CDCl_3$): δH = 8.68 (s, 1H, -NH), 7.44 (d, J = 8.9 Hz, 1H, =CHR) 7.33-7.17 (m, 9H, Ar-H), 6.80 (d, J = 8.2 Hz 4H, Ar-H), 6.10 (d, J = 9.6 Hz, 1H, 1'-H), 5.38 (dd, J = 7.9, 2.1 Hz, 1H, =CHR), 5.40-5.35 (m, 1H, 3'-H), 4.68-4.62 (m, 1H, 2'-H), 4.35-4.34 (m, 1H, 4'-H) 3.73 (s, 6H, Ar-OCH_3), 3.48 (d, J = 2.6 Hz, 2H, 5-H), 1.39 (s, 9H, $C(CH_3)_3$).

7.2.5.5 Synthesis of 2-Deoxy-2-(tert-butyloxycarbonyl)amino-5-O-(4,4-dimethoxytrityl)-3,O'-anhydrouridine (29)

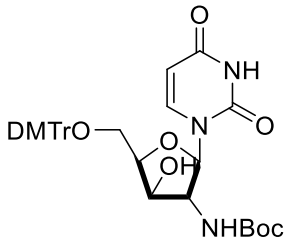

2-Deoxy-2-(tert-butyloxycarbonyl)amino-3'-O'trifluoromethanesulfonyl-5'-O-(4,4-dimethoxytrityl)uridine (**28**) (1.28 g, 1.64 mmol) was dissolved in ethanol (24 mL) and NaOH solution (6 M, 270 µl, 1 equiv.) was added slowly. The reaction mixture was stirred overnight at room temperature, and TLC analyses showed complete consumption of compound (**28**) after 20 h and formation of suspected (**36**). Additional NaOH solution (6 M, 410 µl, 1.5 equiv.) was added dropwise, and the reaction mixture was stirred at room temperature. Monitoring of the reaction by TLC analyses, showed conversion of (**36**) into (**29**) after 24 h. The reaction mixture was concentrated to 5 mL *in vacuo*, and then neutralised (pH ~ 7) with sodium dihydrogen phosphate solution, this induced precipitation of the crude product. The solid crude residue was collected by filtration and then dissolved in MeOH, and silica gel (1-2 g) was added. The crude material was dry loaded onto a pre-prepared silica gel chromatography column and material was eluted (30-80% EtOAc in hexane), to afford compound (**29**) (0.39 g, 0.6 mmol, 37%) as a white solid.

^{1}H NMR (400 MHz, CD_3OD): 7.83 (d, J= 7.3 Hz, 1H, =CHR), 7.46-7.48 (m, 2H, Ar-H), 7.40-7.35 (m, 4H, Ar-H), 7.31-7.28 (m, 2H, Ar-H) , 7.24-7.20 (m, 1H, Ar-H) 6.86 (dd, J =9.0, 1.2 Hz, 4H, Ar-H), 5.9 (d, J = 4.0 Hz, 1H, 1'-H), 5.50 (m, 1H, =CHR), 4.34(m,1H, 4'-H), 4.13 (br s, 1H, 3'-H), 4.04 (br s, 1H, 2'-H), 3.82 (s, 6H, Ar-OCH_3), 3.62 (dd, J = 10.1, 6.0 Hz, 1H, 5'-H), 5'-H, 3.36 (dd, J = 10.5, 3.6 Hz 1H, 5'-H), 1.46 (s, 9H, $C(CH_3)_3$).

7.2.5.6 Synthesis of 2'-Deoxy-2-(tert-butyloxycarbonyl)amino–5'-O-(4,4'-dimethoxytrityl)-3'-β-uridine (30)

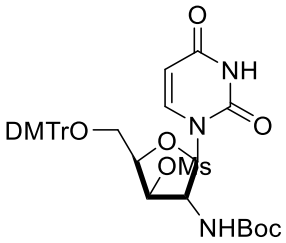

Under an inert atmosphere, 2-deoxy-2-(tert-butyloxycarbonyl)amino-5-O-(4,4-dimethoxytrityl)-3,O'-anhydrouridine (**29**) (0.30 g, 0.46 mmol) was dissolved in anhydrous pyridine (2 mL), and the solution was cooled to 0 °C. Methanesulfonyl chloride (25 µl, 3.22 mmol, 7.2 equiv.) was then added, and the reaction mixture was stirred overnight at room temperature. The reaction was quenched with MeOH (30 µl), and the solvents were removed *in vacuo*. The crude material was then co-evaporated with toluene (× 2), and the dried residue was partitioned between CH_2Cl_2 (10 mL) and 10% $NaHCO_3$ solution (10 mL). The organic phase was washed with brine (3 × 5 mL), dried with Na_2SO_4, and the solvents were then removed *in vacuo*. The crude material was purified by column chromatography on silica gel (30-80% EtOAc in hexane), to afford compound (**30)** (0.207 mg, 0.28 mmol, 62%) as a yellow foam.

^{1}H NMR (400 MHz, $CDCl_3$): 8.85 (s, 1H, -NH), 7.57 (d, J= 8.2 Hz, 1H, =CHR), 7.48-7.46 (m, 2H, Ar-H), 7.38-7.31 (m, 7H, Ar-H), 7.23-7.27 (m, 1H, Ar-H) 6.86 (d, J =8.9 Hz, 4H, Ar-H), 6.04 (d, J = 4.8 Hz, 1H), 5.58 (d, J = 8.2 Hz, 1H, =CHR), 5.19 (dd, J= 3.7, 1.5 Hz), 4.50 (q, J= 5.0 Hz 1H), 4.26 (br s, 1H), 3.81 (s, 6H, Ar-OCH_3), 3.62 (dd, J = 11.4, 5.4 Hz, 1H), 46 (dd, J = 10.4, 3.8 Hz, 1H), 3.07 (s, 3H, OSO_2CH_3), 1.46 (s, 9H, $C(CH_3)_3$).

7.2.5.7 Attempted Synthesis of 2'-Deoxy-2-(tert-butyloxycarbonyl)amino3'-deovy-3'a-benzoylthio-5''-O-(4,4'-dimethoxytrityl)-uridine (31)

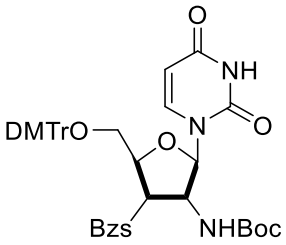

Under an inert atmosphere, (**30**) (0.140 g, 0.19 mmol) was dissolved in anhydrous DMF (2.8 mL), and the solution warmed up to 100 °C. Sodium thiobenzoate (**37**) was slowly added over 4h,0.120 g, 0.76 mmol, 4 equiv.) and the reaction mixture was stirred overnight at 100 °C. The reaction was diluted in CH_2Cl_2 (10 mL) and washed with dilute $NaHCO_3$ solution (2 × 10 mL) and brine (2 × 10 mL). The organic phase was dried with Na_2SO_4, and the solvents were removed in vacuo. The crude material was purified by column chromatography on silica gel (1-3% MeOH/CH_2Cl_2).

7.2.5.8 Synthesis Sodium thiobenzoate (37)

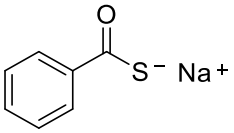

Thiobenzoic acid (1g, 7.2 mmol) was added to 2 mL of H_2O. Solid NaOH (0.290 g, 7.2 mmol) was then added to the mixture and the solution was stirred for 10 min. After checking the pH level (in a range between 6-7), the compound was dried overnight to afford compound (**35**) as a yellow solid (1.10 gr, 6.9 mmol, 96% of yield).

(The analytical data reported above correspond to those reported in the literature).[197]

8 Supporting information index

Each data file in the “Supporting information” is reported with the number and name of the compound it refers to, followed by the analytical method acronym, NMR, HR-MS and IR (infrared spectroscopy), (i.e., (1) N,N-diisopropylphosphoramide dichloridite NMR).

The analysed data are converted to PDF files.

Normal folders are also reported with the number and name of the compound they refer to and contain NMR spectroscopy raw data.

Zip folders are reported using the same filename labelling system and, contain additional IR raw data and related PDF file analysis not reported in the main document. IR spectra were obtained using a Perkin Elmer Spectrum Two UATR Two FT-IR Spectrometer (neat, ATR sampling).

9 Bibliography

(1) Jessen, H. J.; Ahmed, N.; Hofer, A. Phosphate esters and anhydrides--recent strategies targeting nature's favoured modifications. *Organic & Biomolecular Chemistry* **2014**, *12* (22), 3526-3530. DOI: 10.1039/c4ob00478g.
(2) Bialy, L.; Waldmann, H. Total synthesis and biological evaluation of the protein phosphatase 2A inhibitor cytostatin and analogues. *Chemistry* **2004**, *10* (11), 2759-2780. DOI: 10.1002/chem.200305543 (acccessed 2020/05/18).
(3) Caron, J.; Lepeltier, E.; Reddy, L. H.; Lepetre-Mouelhi, S.; Wack, S.; Bourgaux, C.; Couvreur, P.; Desmaele, D. Squalenoyl Gemcitabine Monophosphate: Synthesis, Characterisation of Nanoassemblies and Biological Evaluation. *European Journal of Organic Chemistry* **2011**, *2011* (14), 2615-2628. DOI: 10.1002/ejoc.201100036 (acccessed 2020/05/19).
(4) Ouellette, R. J.; Rawn, J. D. Nucleosides, Nucleotides, and Nucleic Acids. In *Organic Chemistry*, **2018**; pp 973-1000.
(5) Reichard, P. Interactions between Deoxyribonucleotide and DNA-Synthesis. *Annual Review of Biochemistry* **1988**, *57*, 349-374. DOI: DOI 10.1146/annurev.bi.57.070188.002025.
(6) Kornberg, A.; Baker, T. A. *DNA replication.*; W.H. Freeman and Company, 1992.
(7) Wright, J. A.; Chan, A. K.; Choy, B. K.; Hurta, R. A.; McClarty, G. A.; Tagger, A. Y. Regulation and drug resistance mechanisms of mammalian ribonucleotide reductase, and the significance to DNA synthesis. *Biochemistry and Cell Biology* **1990**, *68* (12), 1364-1371. DOI: 10.1139/o90-199.
(8) Yang, L.; Arora, K.; Beard, W. A.; Wilson, S. H.; Schlick, T. Critical Role of Magnesium Ions in DNA Polymerase β's Closing and Active Site Assembly. *Journal of the American Chemical Society* **2004**, *126* (27), 8441-8453. DOI: 10.1021/ja049412o.
(9) Cox, A. L.; Nelson, M. M.; Lehninger, D. L. *Lehninger Principles Of Biochemistry. 7th Edition.*; W.H. Freeman, **2017**.
(10) Lam, E. Nucleic Acids and Proteins. In *Plant Biochemistry*, **1997**; pp 315-352.
(11) Bonora, M.; Patergnani, S.; Rimessi, A.; De Marchi, E.; Suski, J. M.; Bononi, A.; Giorgi, C.; Marchi, S.; Missiroli, S.; Poletti, F.; et al. ATP synthesis and storage. *Purinergic Signalling* **2012**, *8* (3), 343-357. DOI: 10.1007/s11302-012-9305-8.
(12) Krebs, H. A. The citric acid cycle and the Szent-Gyorgyi cycle in pigeon breast muscle. *Biochemical Journal* **1940**, *34* (5), 775-779. DOI: 10.1042/bj0340775.
(13) Melendez-Hevia, E.; Waddell, T. G.; Cascante, M. The puzzle of the Krebs citric acid cycle: assembling the pieces of chemically feasible reactions, and opportunism in the design of metabolic pathways during evolution. *Journal of Molecular Evolution* **1996**, *43* (3), 293-303. DOI: 10.1007/BF02338838.
(14) Lipmann, F. Metabolic Generation and Utilization of Phosphate Bond Energy. In *Advances in Enzymology and Related Areas of Molecular Biology*, F. F. Nord, C. H. W. Ed.; Vol. 1; 1941; pp 99-162.
(15) Lenaz, G.; Genova, M. L. Structure and organization of mitochondrial respiratory complexes: a new understanding of an old subject. *Antioxidants & Redox Signaling* **2010**, *12* (8), 961-1008. DOI: 10.1089/ars.2009.2704 (acccessed 2020/05/16).
(16) Dhar-Chowdhury, P.; Malester, B.; Rajacic, P.; Coetzee, W. A. The regulation of ion channels and transporters by glycolytically derived ATP. *Cellular and Molecular Life Sciences* **2007**, *64* (23), 3069-3083. DOI: 10.1007/s00018-007-7332-3.
(17) Potter, L. R. Guanylyl cyclase structure, function and regulation. *Cellular Signalling* **2011**, *23* (12), 1921-1926. DOI: 10.1016/j.cellsig.2011.09.001.
(18) Beste, K. Y.; Spangler, C. M.; Burhenne, H.; Koch, K. W.; Shen, Y.; Tang, W. J.; Kaever, V.; Seifert, R. Nucleotidyl cyclase activity of particulate guanylyl cyclase A: comparison with particulate guanylyl cyclases E and F, soluble guanylyl cyclase and bacterial adenylyl cyclases CyaA and edema factor. *PLoS One* **2013**, *8* (7), e70223. DOI: 10.1371/journal.pone.0070223.
(19) Hardman, J. G.; Sutherland, E. W. Guanyl Cyclase, an Enzyme Catalyzing the Formation of Guanosine 3', 5'-Monophosphate fromGuanosine Triphosphate. *Journal of Biological Chemistry* **1969**, *244* (10), 8363-6370.
(20) Stone, J. R.; Marletta, M. A. Spectral and kinetic studies on the activation of soluble guanylate cyclase by nitric oxide. *Biochemistry* **1996**, *35* (4), 1093-1099. DOI: 10.1021/bi9519718.

(21) Friebe, A.; Sandner, P.; Schmidtko, A. cGMP: a unique 2nd messenger molecule - recent developments in cGMP research and development. *Naunyn-Schmiedeberg's Archives of Pharmacology* **2020**, *393* (2), 287-302. DOI: 10.1007/s00210-019-01779-z.
(22) Di Virgilio, F.; Chiozzi, P.; Ferrari, D.; Falzoni, S.; Sanz, J. M.; Morelli, A.; Torboli, M.; Bolognesi, G.; Baricordi, O. R. Nucleotide receptors: an emerging family of regulatory molecules in blood cells. *Blood* **2001**, *97* (3), 587-600. DOI: 10.1182/blood.v97.3.587.
(23) Burnstock, G. Purine and pyrimidine receptors. *Cellular and Molecular Life Sciences* **2007**, *64* (12), 1471-1483. DOI: 10.1007/s00018-007-6497-0.
(24) Zimmermann, H. Extracellular ATP and other nucleotides-ubiquitous triggers of intercellular messenger release. *Purinergic Signalling* **2016**, *12* (1), 25-57. DOI: 10.1007/s11302-015-9483-2.
(25) Doudna, J. A.; Charpentier, E. The new frontier of genome engineering with CRISPR-Cas9. *Science* **2014**, *346* (6213), 1258096. DOI: 10.1126/science.1258096 (acccessed 2022/12/15).
(26) Ran, F. A.; Hsu, P. D.; Wright, J.; Agarwala, V.; Scott, D. A.; Zhang, F. Genome engineering using the CRISPR-Cas9 system. *Nature Protocols* **2013**, *8* (11), 2281-2308. DOI: 10.1038/nprot.2013.143.
(27) Hsu, Patrick D.; Lander, Eric S.; Zhang, F. Development and Applications of CRISPR-Cas9 for Genome Engineering. *Cell* **2014**, *157* (6), 1262-1278. DOI: https://doi.org/10.1016/j.cell.2014.05.010.
(28) Watson, J. D.; Crick, F. H. Molecular structure of nucleic acids; a structure for deoxyribose nucleic acid. *Nature* **1953**, *171* (4356), 737-738. DOI: 10.1038/171737a0 From NLM.
(29) Zallen, D. T. Despite Franklin's work, Wilkins earned his Nobel. In *Nature*, Vol. 425; 2003; p 15.
(30) Heather, J. M.; Chain, B. The sequence of sequencers: The history of sequencing DNA. *Genomics* **2016**, *107* (1), 1-8. DOI: 10.1016/j.ygeno.2015.11.003 PubMed.
(31) Shendure, J.; Balasubramanian, S.; Church, G. M.; Gilbert, W.; Rogers, J.; Schloss, J. A.; Waterston, R. H. DNA sequencing at 40: past, present and future. *Nature* **2017**, *550* (7676), 345-353. DOI: 10.1038/nature24286.
(32) Su, Z.; Ning, B.; Fang, H.; Hong, H.; Perkins, R.; Tong, W.; Shi, L. Next-generation sequencing and its applications in molecular diagnostics. *Expert Review of Molecular Diagnostics* **2011**, *11* (3), 333-343. DOI: 10.1586/erm.11.3.
(33) Shendure, J.; Ji, H. Next-generation DNA sequencing. *Nature Biotechnology* **2008**, *26* (10), 1135-1145. DOI: 10.1038/nbt1486.
(34) Hutchison, C. A., 3rd. DNA sequencing: bench to bedside and beyond. *Nucleic Acids Research* **2007**, *35* (18), 6227-6237. DOI: 10.1093/nar/gkm688.
(35) Sanger, F., Nicklen,S. and Coulson,A.R. DNA sequencing with chain-terminating inhibitors. *Proc. Natl Acad. Sci.* **1977**, *74*, 5463–5467.
(36) Hutchison, C. A. DNA sequencing: bench to bedside and beyondy. *Nucleic Acids Research* **2007**, *18*, 6227–6237. DOI: 10.1093/nar/gkm688.
(37) Sanger, F.; Coulson, A. R. A rapid method for determining sequences in DNA by primed synthesis with DNA polymerase. *Journal of Molecular Biology* **1975**, *94* (3), 441-448. DOI: https://doi.org/10.1016/0022-2836(75)90213-2.
(38) Sanger, F.; Brownlee, G. G.; Barrell, B. G. A two-dimensional fractionation procedure for radioactive nucleotides. *Journal of Molecular Biology* **1965**, *13* (2), 373-IN374. DOI: https://doi.org/10.1016/S0022-2836(65)80104-8.
(39) Maxam, A. M.; Gilbert, W. A new method for sequencing DNA. *Proceedings of the National Academy of Sciences* **1977**, *74* (2), 560-564. DOI: 10.1073/pnas.74.2.560 (acccessed 2022/12/15).
(40) B., Z. Bacteriophage T7 DNA polymerase - sequenase. *Frontiers in Microbiology* **2014**, *5* (181). DOI: 10.3389/fmicb.2014.00181.
(41) Shendure J., J. H. Next-generation DNA sequencing. *Nature Biotechnology* **2008**, *10*, 1135-1145. DOI: 10.1038/nbt1486.
(42) Shen, C.-H. Chapter 11 - Techniques in Sequencing. In *Diagnostic Molecular Biology*, Shen, C.-H. Ed.; Academic Press, **2019**; pp 277-302.
(43) Malke, H. PCR Technology: Principles and Applications for DNA Amplification. *Journal of Basic Microbiology* **1990**, *30* (10), 736-736. DOI: 10.1002/jobm.3620301009 (acccessed 2020/05/17).
(44) Bartlett, J. M. S.; Stirling, D. A Short History of the Polymerase Chain Reaction. In *PCR Protocols*, Bartlett, J. M. S., Stirling, D. Eds.; Humana Press, **2003**; pp 3-6.
(45) Templeton, N. S. The polymerase chain reaction. History, methods, and applications. *Diagnostic Molecular Pathoogyl* **1992**, *1* (1), 58-72. DOI: 10.1097/00019606-199203000-00008 From NLM.

(46) Mullis, K. B. The unusual origin of the polymerase chain reaction. *Scientific American* **1990**, *262* (4), 56-61, 64-55. DOI: 10.1038/scientificamerican0490-56.
(47) Garibyan L, A. N. Polymerase chain reaction. *Journal of Investigative Dermatology* **2013**, *133* (3), 1-4. DOI: 10.1038/jid.2013.1.
(48) Behjati, S.; Tarpey, P. S. What is next generation sequencing? *Archives of disease in childhood: education and practice edition* **2013**, *98* (6), 236-238. DOI: 10.1136/archdischild-2013-304340 From NLM.
(49) Metzker, M. L. Sequencing technologies - the next generation. *Nature Reviews Genetics* **2010**, *11* (1), 31-46. DOI: 10.1038/nrg2626.
(50) Wold, B.; Myers, R. M. Sequence census methods for functional genomics. *Nature Methods* **2008**, *5* (1), 19-21. DOI: 10.1038/nmeth1157.
(51) King, C.; Scott-Horton, T. Pyrosequencing: a simple method for accurate genotyping. *Journal of Visualized Experiments* **2008**, (11). DOI: 10.3791/630 From NLM.
(52) Margulies, M.; Egholm, M.; Altman, W. E.; Attiya, S.; Bader, J. S.; Bemben, L. A.; Berka, J.; Braverman, M. S.; Chen, Y.-J.; Chen, Z.; et al. Genome sequencing in microfabricated high-density picolitre reactors. *Nature* **2005**, *437* (7057), 376-380. DOI: 10.1038/nature03959.
(53) Meyer, M.; Kircher, M. Illumina sequencing library preparation for highly multiplexed target capture and sequencing. *Cold Spring Harbor Protocols* **2010**, *2010* (6), pdb.prot5448. DOI: 10.1101/pdb.prot5448 From NLM.
(54) Thompson, J. F.; Steinmann, K. E. Single molecule sequencing with a HeliScope genetic analysis system. *Current Protocols in Molecular Biology* **2010**, *Chapter 7*, Unit7.10. DOI: 10.1002/0471142727.mb0710s92 From NLM.
(55) Schatz, M. C.; Delcher, A. L.; Salzberg, S. L. Assembly of large genomes using second-generation sequencing. *Genome Research* **2010**, *20* (9), 1165-1173. DOI: 10.1101/gr.101360.109 From NLM.
(56) Schadt, E. E.; Turner, S.; Kasarskis, A. A window into third-generation sequencing. *Human Molecular Genetics* **2010**, *19* (R2), R227-240. DOI: 10.1093/hmg/ddq416 From NLM.
(57) Gut, I. G. New sequencing technologies. *Clinical and Translational Oncology* **2013**, *15* (11), 879-881. DOI: 10.1007/s12094-013-1073-6 From NLM.
(58) Quail, M. A.; Smith, M.; Coupland, P.; Otto, T. D.; Harris, S. R.; Connor, T. R.; Bertoni, A.; Swerdlow, H. P.; Gu, Y. A tale of three next generation sequencing platforms: comparison of Ion Torrent, Pacific Biosciences and Illumina MiSeq sequencers. *BMC Genomics* **2012**, *13*, 341. DOI: 10.1186/1471-2164-13-341 From NLM.
(59) Niedringhaus, T. P.; Milanova, D.; Kerby, M. B.; Snyder, M. P.; Barron, A. E. Landscape of Next-Generation Sequencing Technologies. *Analytical Chemistry* **2011**, *83* (12), 4327-4341. DOI: 10.1021/ac2010857.
(60) van Dijk, E. L.; Auger, H.; Jaszczyszyn, Y.; Thermes, C. Ten years of next-generation sequencing technology. *Trends in Genetics* **2014**, *30* (9), 418-426. DOI: https://doi.org/10.1016/j.tig.2014.07.001.
(61) Ke, R.; Mignardi, M.; Hauling, T.; Nilsson, M. Fourth Generation of Next-Generation Sequencing Technologies: Promise and Consequences. *Human Mutation* **2016**, *37* (12), 1363-1367, https://doi.org/10.1002/humu.23051. DOI: https://doi.org/10.1002/humu.23051 (acccessed 2022/12/16).
(62) Balasubramanian, S. Sequencing nucleic acids: from chemistry to medicine. *Chemical Communications* **2011**, *47* (26), 7281-7286. DOI: 10.1039/c1cc11078k.
(63) Boudreau, R. L.; Martins, I.; Davidson, B. L. Artificial microRNAs as siRNA shuttles: improved safety as compared to shRNAs in vitro and in vivo. *Molecular therapy : the journal of the American Society of Gene Therapy* **2009**, *17* (1), 169-175. DOI: 10.1038/mt.2008.231 PubMed.
(64) Davidson, B. L.; McCray, P. B. Current prospects for RNA interference-based therapies. *Nature Reviews Genetics* **2011**, *12* (5), 329-340. DOI: 10.1038/nrg2968.
(65) Metzker, M. L. Sequencing technologies — the next generation. *Nature Reviews Genetics* **2010**, *11* (1), 31-46. DOI: 10.1038/nrg2626.
(66) *The BioBricks Foundation*. [http://biobricks.org] (accessed.
(67) Shetty, R. P.; Endy, D.; Knight, T. F. Engineering BioBrick vectors from BioBrick parts. *Journal of Biological Engineering* **2008**, *2* (1), 5. DOI: 10.1186/1754-1611-2-5.

(68) Hillson, N.; Caddick, M.; Cai, Y.; Carrasco, J. A.; Chang, M. W.; Curach, N. C.; Bell, D. J.; Le Feuvre, R.; Friedman, D. C.; Fu, X.; et al. Building a global alliance of biofoundries. *Nature Communications* **2019**, *10* (1), 2040. DOI: 10.1038/s41467-019-10079-2.
(69) Chao, R.; Mishra, S.; Si, T.; Zhao, H. Engineering biological systems using automated biofoundries. *Metabolic engineering* **2017**, *42*, 98-108. DOI: 10.1016/j.ymben.2017.06.003 PubMed.
(70) Durbin, R. M.; Altshuler, D.; Abecasis, G. R.; Bentley, D. R.; Chakravarti, A.; Clark, A. G.; Collins, F. S.; De La Vega, F. M.; Donnelly, P.; Egholm, M.; et al. A map of human genome variation from population-scale sequencing. *Nature* **2010**, *467* (7319), 1061-1073. DOI: 10.1038/nature09534.
(71) McKenna, C. E.; Kashemirov, B. A.; Peterson, L. W.; Goodman, M. F. Modifications to the dNTP triphosphate moiety: From mechanistic probes for DNA polymerases to antiviral and anti-cancer drug design. *Biochimica et Biophysica Acta (BBA) - Proteins and Proteomics* **2010**, *1804* (5), 1223-1230. DOI: https://doi.org/10.1016/j.bbapap.2010.01.005.
(72) Berdis, A. J. DNA Polymerases as Therapeutic Targets. *Biochemistry* **2008**, *47* (32), 8253-8260. DOI: 10.1021/bi801179f.
(73) Hodgson, D. R.; Schroder, M. Chemical approaches towards unravelling kinase-mediated signalling pathways. *Chemical Society Reviews* **2011**, *40* (3), 1211-1223, 10.1039/C0CS00020E. DOI: 10.1039/c0cs00020e.
(74) Gille, A.; Guo, J.; Mou, T.-C.; Doughty, M. B.; Lushington, G. H.; Seifert, R. Differential interactions of G-proteins and adenylyl cyclase with nucleoside 5'-triphosphates, nucleoside 5'-[gamma-thio]triphosphates and nucleoside 5'-[beta,gamma-imido]triphosphates. *Biochemical pharmacology* **2005**, *71* (1-2), 89-97. DOI: 10.1016/j.bcp.2005.10.006 PubMed.
(75) Jacobson, K. A.; Jarvis, M. F.; Williams, M. Purine and Pyrimidine (P2) Receptors as Drug Targets. *Journal of Medicinal Chemistry* **2002**, *45* (19), 4057-4093. DOI: 10.1021/jm020046y.
(76) Elliott, T. S.; Slowey, A.; Ye, Y.; Conway, S. J. The use of phosphate bioisosteres in medicinal chemistry and chemical biology. *Medicinal Chemistry Communications* **2012**, *3* (7), 735-751, 10.1039/C2MD20079A. DOI: 10.1039/C2MD20079A.
(77) Camarasa, M.-J. Prodrugs of Nucleoside Triphosphates as a Sound and Challenging Approach: A Pioneering Work That Opens a New Era in the Direct Intracellular Delivery of Nucleoside Triphosphates. *ChemMedChem* **2018**, *13* (18), 1885-1889. DOI: 10.1002/cmdc.201800454 (acccessed 2020/05/16).
(78) Meier, C. Nucleoside diphosphate and triphosphate prodrugs - An unsolvable task? *Antiviral chemistry & chemotherapy* **2017**, *25* (3), 69-82. DOI: 10.1177/2040206617738656.
(79) Camarasa, M. J. Prodrugs of Nucleoside Triphosphates as a Sound and Challenging Approach: A Pioneering Work That Opens a New Era in the Direct Intracellular Delivery of Nucleoside Triphosphates. *ChemMedChem* **2018**, *13* (18), 1885-1889. DOI: 10.1002/cmdc.201800454 (acccessed 2020/05/16).
(80) McKenna, C. E.; Kashemirov, B. A.; Peterson, L. W.; Goodman, M. F. Modifications to the dNTP triphosphate moiety: from mechanistic probes for DNA polymerases to antiviral and anti-cancer drug design. *Biochimica et Biophysica Acta* **2010**, *1804* (5), 1223-1230. DOI: 10.1016/j.bbapap.2010.01.005.
(81) Pradere, U.; Garnier-Amblard, E. C.; Coats, S. J.; Amblard, F.; Schinazi, R. F. Synthesis of Nucleoside Phosphate and Phosphonate Prodrugs. *Chemical Reviews* **2014**, *114* (18), 9154-9218. DOI: 10.1021/cr5002035.
(82) Hecker, S. J.; Erion, M. D. Prodrugs of Phosphates and Phosphonates. *Journal of Medicinal Chemistry* **2008**, *51* (8), 2328-2345. DOI: 10.1021/jm701260b.
(83) De Clercq, E.; Field, H. J. Antiviral prodrugs – the development of successful prodrug strategies for antiviral chemotherapy. *British Journal of Pharmacology* **2006**, *147* (1), 1-11, https://doi.org/10.1038/sj.bjp.0706446. DOI: https://doi.org/10.1038/sj.bjp.0706446 (acccessed 2022/12/16).
(84) Rachwalak, M.; Romanowska, J.; Sobkowski, M.; Stawinski, J. Nucleoside Di- and Triphosphates as a New Generation of Anti-HIV Pronucleotides. Chemical and Biological Aspects. In *Applied Sciences*, 2021; Vol. 11.
(85) Gisch, N.; Balzarini, J.; Meier, C. 5-Diacetoxymethyl-cycloSal-d4TMP—A prototype of enzymatically activated cycloSal-pronucleotides. *Nucleosides, Nucleotides & Nucleic Acids* **2007**, *26* (6-7), 861-864. DOI: 10.1080/15257770701504025.

(86) Meier, C. cycloSal phosphates as chemical Trojan horses for intracellular nucleotide and glycosylmonophosphate delivery - Chemistry meets biology. *European Journal of Organic Chemistry* **2006**, *2006* (5), 1081-1102. DOI: 10.1002/ejoc.200500671.
(87) Warnecke, S.; Meier, C. Synthesis of nucleoside Di- and triphosphates and dinucleoside polyphosphates with cycloSal-nucleotides. *Journal of Organic Chemistry* **2009**, *74* (8), 3024-3030. DOI: 10.1021/jo802348h.
(88) Seley, K. L.; Zhang, L.; Hagos, A. "Fleximers". Design and Synthesis of Two Novel Split Nucleosides. *Organic Letters* **2001**, *3* (20), 3209-3210. DOI: 10.1021/ol0165443.
(89) Seley, K. L.; Zhang, L.; Hagos, A.; Quirk, S. "Fleximers". Design and synthesis of a new class of novel shape-modified nucleosides(1). *Journal of Organic Chemistry* **2002**, *67* (10), 3365-3373. DOI: 10.1021/jo0255476 From NLM.
(90) Seley, K. L.; Salim, S.; Zhang, L.; O'Daniel, P. I. "Molecular chameleons". Design and synthesis of a second series of flexible nucleosides. *Journal of Organic Chemistry* **2005**, *70* (5), 1612-1619. DOI: 10.1021/jo048218h From NLM.
(91) Mehellou, Y. B., J.; McGuigan, C. . Aryloxy phosphoramidate triesters: a technology for delivering monophosphorylated nucleosides and sugars into cells. *ChemMedChem* **2009**, *4*, 1779–17791. DOI: 10.1002/cmdc.200900289.
(92) Mehellou, Y.; Rattan, H. S.; Balzarini, J. The ProTide Prodrug Technology: From the Concept to the Clinic. *Journal of Medicinal Chemistry* **2018**, *61* (6), 2211-2226. DOI: 10.1021/acs.jmedchem.7b00734.
(93) Serpi, M.; Pertusati, F. An overview of ProTide technology and its implications to drug discovery. *Expert Opinion Drug Discovery* **2021**, *16* (10), 1149-1161. DOI: 10.1080/17460441.2021.1922385 From NLM.
(94) Alanazi, A. S.; James, E.; Mehellou, Y. The ProTide Prodrug Technology: Where Next? *ACS Medicinal Chemistry Letters* **2019**, *10* (1), 2-5. DOI: 10.1021/acsmedchemlett.8b00586.
(95) Slusarczyk, M.; Serpi, M.; Pertusati, F. Phosphoramidates and phosphonamidates (ProTides) with antiviral activity. *Antiviral Chemistry and Chemotherapy* **2018**, *26*, 2040206618775243. DOI: 10.1177/2040206618775243 (acccessed 2022/12/16).
(96) Gollnest, T.; de Oliveira, T. D.; Schols, D.; Balzarini, J.; Meier, C. Lipophilic prodrugs of nucleoside triphosphates as biochemical probes and potential antivirals. *Nature Communications* **2015**, *6* (1), 8716. DOI: 10.1038/ncomms9716.
(97) Weising, S.; Sterrenberg, V.; Schols, D.; Meier, C. Synthesis and Antiviral Evaluation of TriPPPro-AbacavirTP, TriPPPro-CarbovirTP, and Their 1',2'-cis-Disubstituted Analogues. *ChemMedChem* **2018**, *13* (17), 1771-1778. DOI: 10.1002/cmdc.201800361 From NLM.
(98) Jessen, H. J.; Schulz, T.; Balzarini, J.; Meier, C. Bioreversible Protection of Nucleoside Diphosphates. *Angewandte Chemie International Edition* **2008**, *47* (45), 8719-8722, https://doi.org/10.1002/anie.200803100. DOI: https://doi.org/10.1002/anie.200803100 (acccessed 2022/12/16).
(99) Pertenbreiter, F.; Balzarini, J.; Meier, C. Nucleoside Mono- and Diphosphate Prodrugs of 2′,3′-Dideoxyuridine and 2′,3′-Dideoxy-2′,3′-didehydrouridine. *ChemMedChem* **2015**, *10* (1), 94-106, https://doi.org/10.1002/cmdc.201402295. DOI: https://doi.org/10.1002/cmdc.201402295 (acccessed 2022/12/16).
(100) Ciotti, M.; Ciccozzi, M.; Terrinoni, A.; Jiang, W.-C.; Wang, C.-B.; Bernardini, S. The COVID-19 pandemic. *Critical Reviews in Clinical Laboratory Sciences* **2020**, *57* (6), 365-388. DOI: 10.1080/10408363.2020.1783198.
(101) World Health, O. *Coronavirus disease (COVID-19), 12 October 2020*; World Health Organization, Geneva, 2020. https://apps.who.int/iris/handle/10665/336034.
(102) Velavan, T. P.; Meyer, C. G. The COVID-19 epidemic. In *Tropical Medicine & International Health*, Vol. 25; **2020**; pp 278-280.
(103) La Marca, A.; Capuzzo, M.; Paglia, T.; Roli, L.; Trenti, T.; Nelson, S. M. Testing for SARS-CoV-2 (COVID-19): a systematic review and clinical guide to molecular and serological in-vitro diagnostic assays. *Reproductive Biomedicine Online* **2020**, *41* (3), 483-499. DOI: 10.1016/j.rbmo.2020.06.001 From NLM.
(104) Böger, B.; Fachi, M. M.; Vilhena, R. O.; Cobre, A. F.; Tonin, F. S.; Pontarolo, R. Systematic review with meta-analysis of the accuracy of diagnostic tests for COVID-19. *American Journal of Infection Control* **2021**, *49* (1), 21-29. DOI: 10.1016/j.ajic.2020.07.011 From NLM.

(105) Yang, L.; Liu, S.; Liu, J.; Zhang, Z.; Wan, X.; Huang, B.; Chen, Y.; Zhang, Y. COVID-19: immunopathogenesis and Immunotherapeutics. *Signal Transduction and Targeted Therapy* **2020**, *5* (1), 128. DOI: 10.1038/s41392-020-00243-2.
(106) Ndwandwe, D.; Wiysonge, C. S. COVID-19 vaccines. *Current Opinion in Immunology* **2021**, *71*, 111-116. DOI: https://doi.org/10.1016/j.coi.2021.07.003.
(107) Felsenstein, S.; Herbert, J. A.; McNamara, P. S.; Hedrich, C. M. COVID-19: Immunology and treatment options. *Clinical Immunology* **2020**, *215*, 108448. DOI: https://doi.org/10.1016/j.clim.2020.108448.
(108) Stasi, C.; Fallani, S.; Voller, F.; Silvestri, C. Treatment for COVID-19: An overview. *European Journal of Pharmacology* **2020**, *889*, 173644. DOI: https://doi.org/10.1016/j.ejphar.2020.173644.
(109) Beigel, J. H.; Tomashek, K. M.; Dodd, L. E.; Mehta, A. K.; Zingman, B. S.; Kalil, A. C.; Hohmann, E.; Chu, H. Y.; Luetkemeyer, A.; Kline, S.; et al. Remdesivir for the Treatment of Covid-19 — Final Report. *New England Journal of Medicine* **2020**, *383* (19), 1813-1826. DOI: 10.1056/NEJMoa2007764 (acccessed 2022/12/13).
(110) Frediansyah, A.; Nainu, F.; Dhama, K.; Mudatsir, M.; Harapan, H. Remdesivir and its antiviral activity against COVID-19: A systematic review. *Clinical Epidemiology and Global Health* **2021**, *9*, 123-127. DOI: 10.1016/j.cegh.2020.07.011 From NLM.
(111) Roy, B.; Depaix, A.; Perigaud, C.; Peyrottes, S. Recent Trends in Nucleotide Synthesis. *Chemical Reviews* **2016**, *116* (14), 7854-7897. DOI: 10.1021/acs.chemrev.6b00174.
(112) Ahmadibeni, Y.; Parang, K. Selective diphosphorylation, dithiodiphosphorylation, triphosphorylation, and trithiotriphosphorylation of unprotected carbohydrates and nucleosides. *Organic Letters* **2005**, *7* (25), 5589-5592. DOI: 10.1021/ol0521432.
(113) Tonn, V. C.; Meier, C. Solid-phase synthesis of (poly)phosphorylated nucleosides and conjugates. *Chemistry* **2011**, *17* (35), 9832-9842. DOI: 10.1002/chem.201101291.
(114) Schoetzau, T.; Holletz, T.; Cech, D. A facile solid phase synthesis of 2'- and 3'-aminonucleoside triphosphates. *Chemical Communications* **1996**, (3), 387-388, 10.1039/CC9960000387. DOI: DOI 10.1039/cc9960000387.
(115) Gaur, R. K.; Sproat, B. S.; Krupp, G. Novel solid phase synthesis of 2'-o-methylribonucleoside 5'-triphosphates and their α-thio analogues. *Tetrahedron Letters* **1992**, *33* (23), 3301-3304. DOI: 10.1016/s0040-4039(00)92072-0.
(116) Khorana, H. G.; Todd, A. R. 465. Studies on phosphorylation. Part XI. The reaction between carbodi-imides and acid esters of phosphoric acid. A new method for the preparation of pyrophosphates. *Journal of the Chemical Society (Resumed)* **1953**, (0), 2257-2260, 10.1039/JR9530002257. DOI: 10.1039/JR9530002257.
(117) Khorana, H. Carbodiimides. Part V. 1 A Novel Synthesis of Adenosine Di-and Triphosphate and P1, P2-Diadenosine-5'-pyrophosphate. *Journal of the American Chemical Society* **1954**, *76* (13), 3517-3522.
(118) Moffatt, J. G.; Khorana, H. G. Nucleoside Polyphosphates. X.1The Synthesis and Some Reactions of Nucleoside-5' Phosphoromorpholidates and Related Compounds. Improved Methods for the Preparation of Nucleoside-5' Polyphosphates1. *Journal of the American Chemical Society* **1961**, *83* (3), 649-658. DOI: 10.1021/ja01464a034.
(119) Vanboom, J. H.; Crea, R.; Luyten, W. C.; Vink, A. B. 2,2,2-Tribromoethyl Phosphoromorpholinochloridate - Convenient Reagent for Synthesis of Ribonucleoside Mono-Phosphates, Di-Phosphates and Tri-Phosphates. *Tetrahedron Letters* **1975**, *16* (32), 2779-2782.
(120) Mohamady, S.; Desoky, A.; Taylor, S. D. Sulfonyl imidazolium salts as reagents for the rapid and efficient synthesis of nucleoside polyphosphates and their conjugates. *Organic Letters* **2012**, *14* (1), 402-405. DOI: 10.1021/ol203178k.
(121) Wu, W.; Freel Meyers, C. L.; Borch, R. F. A novel method for the preparation of nucleoside triphosphates from activated nucleoside phosphoramidates. *Organic Letters* **2004**, *6* (13), 2257-2260. DOI: 10.1021/ol049267j.
(122) Davisson, V. J.; Davis, D. R.; Dixit, V. M.; Poulter, C. D. Synthesis of nucleotide 5'-diphosphates from 5'-O-tosyl nucleosides. *The Journal of Organic Chemistry* **1987**, *52* (9), 1794-1801. DOI: 10.1021/jo00385a026.
(123) Korhonen, H. J.; Bolt, H. L.; Hodgson, D. R. W. A procedure for the preparation and isolation of nucleoside-5'-diphosphates. *Beilstein Journal of Organic Chemistry* **2015**, *11*, 469-472. DOI: 10.3762/bjoc.11.52.

(124) Sun, Q.; Gong, S.; Sun, J.; Liu, S.; Xiao, Q.; Pu, S. A P(V)-N activation strategy for the synthesis of nucleoside polyphosphates. *Journal of Organic Chemistry* **2013**, *78* (17), 8417-8426. DOI: 10.1021/jo4011156.
(125) Liao, J.-Y.; Bala, S.; Ngor, A. K.; Yik, E. J.; Chaput, J. C. P(V) Reagents for the Scalable Synthesis of Natural and Modified Nucleoside Triphosphates. *Journal of the American Chemical Society* **2019**, *141* (34), 13286-13289. DOI: 10.1021/jacs.9b04728.
(126) Kore, A. R.; Parmar, G. Convenient Synthesis of Nucleoside-5′-Diphosphates from the Corresponding Ribonucleoside-5′-phosphoroimidazole. *Synthetic Communications* **2006**, *36* (22), 3393-3399. DOI: 10.1080/00397910600941448.
(127) Bogachev, V. S. Synthesis of deoxynucleoside 5'-triphosphates using trifluoroacetic anhydride as an activating reagent. *Bioorganicheskaya Khimiya* **1996**, *22* (9), 699-705.
(128) Hoard, D. E.; Ott, D. G. Conversion of Mono- and Oligodeoxyribonucleotides to 5'-Triphosphates. *Journal of the American Chemical Society* **1965**, *87* (8), 1785-1788.
(129) Hoard, D. E.; Ott, D. G. Conversion of Mono- and Oligodeoxyribonucleotides to 5'-Triphosphates1. *Journal of the American Chemical Society* **1965**, *87* (8), 1785-1788. DOI: 10.1021/ja01086a031.
(130) Moffatt, J. G.; Khorana, H. G. Nucleoside Polyphosphates. X.1 The Synthesis and Some Reactions of Nucleoside-5' Phosphoromorpholidates and Related Compounds. Improved Methods for the Preparation of Nucleoside-5' Polyphosphates1. *Journal of the American Chemical Society* **1961**, *83* (3), 649-658. DOI: 10.1021/ja01464a034.
(131) CooK, K. B. a. D. Synthesis of Nucleoside Triphosphate. *Chem. Rev.* **2000**, *100*, 2047-2059.
(132) Bogachev, V. S. Synthesis of Deoxynucleoside 5′-Triphosphates Using Trifluoroacetic Anhydride as an Activating Reagent. *Bioorganic Chemistry* **1996**, *22* (9), 699−705.
(133) Svetlana V. Vasilyeva , B. I. B., Dmitrii A. Konevetz & Vladimir N. Silnikov Synthesis of Novel Nucleoside 5′-Triphosphates and Phosphoramidites Containing Alkyne or Amino Groups for the Postsynthetic Functionalization of Nucleic Acids. *Nucleosides, Nucleotides and Nucleic Acids* **2011**, *30* (10), 753-767. DOI: 10.1080/15257770.2011.595379.
(134) Depaix, A.; Peyrottes, S.; Roy, B. Water-Medium Synthesis of Nucleoside 5′-Polyphosphates. *Current Protocols in Nucleic Acid Chemistry* **2017**, *69* (1), 13.16.11-13.16.11, https://doi.org/10.1002/cpnc.30. DOI: https://doi.org/10.1002/cpnc.30 (acccessed 2023/01/09).
(135) Sun, Q.; Edathil, J. P.; Wu, R.; Smidansky, E. D.; Cameron, C. E.; Peterson, B. R. One-pot synthesis of nucleoside 5'-triphosphates from nucleoside 5'-H-phosphonates. *Organic Letters* **2008**, *10* (9), 1703-1706. DOI: 10.1021/ol8003029 PubMed.
(136) Sun, Q.; Gong, S.; Sun, J.; Wang, C.; Liu, S.; Liu, G.; Ma, C. Efficient synthesis of nucleoside 5′-triphosphates and their β,γ-bridging oxygen-modified analogs from nucleoside 5′-phosphates. *Tetrahedron Letters* **2014**, *55* (13), 2114-2118. DOI: 10.1016/j.tetlet.2014.02.031.
(137) Masaharu Yoshikawa, T. K. a. T. T. Studies of Phosphorylation. Selective Phosphorylation of Unprotected Nucleosides. *Bulletin of the Chemical Society* **1969**, *42*, 3505-3508.
(138) Yoshikawa, M.; Kato, T.; Takenishi, T. A novel method for phosphorylation of nucleosides to 5'-nucleotides. *Tetrahedron Letters* **1967**, *50* (50), 5065-5068. DOI: 10.1016/s0040-4039(01)89915-9.
(139) Ludwig, J. A new route to nucleoside 5'-triphosphates. *Acta Biochimica et Biophysica* **1981**, *16*, 131-133.
(140) Ikemoto, T., Haze, A., Hatano, H., Kitamoto, Y., Ishida, M., & Nara, K. Phosphorylation of Nucleosides with Phosphorus Oxychloride in Trialkyl Phosphate. *Chemical & Pharmaceutical Bulletin*, 1995; Vol. 43, pp 210-215.
(141) Gillerman, I.; Fischer, B. An Improved One-Pot Synthesis of Nucleoside 5′-Triphosphate Analogues. *Nucleosides, Nucleotides and Nucleic Acids* **2010**, *29* (3), 245-256. DOI: 10.1080/15257771003709569.
(142) Kore, A. R. S., M.; Senthilvelan, A.; Srinivasan, B. . An Improved Protection-Free One-Pot Chemical Synthesis of 2′-Deoxynucleoside-5′-triphosphates. *Nucleosides, Nucleotides, Nucleic Acids Res.* **2012**, *31* (5), 423−431.
(143) Ludwig, J.; Eckstein, F. Rapid and efficient synthesis of nucleoside 5'-0-(1-thiotriphosphates), 5'-triphosphates and 2',3'-cyclophosphorothioates using 2-chloro-4H-1,3,2-benzodioxaphosphorin-4-one. *The Journal of Organic Chemistry* **1989**, *54* (3), 631-635. DOI: 10.1021/jo00264a024.

(144) Caton-Williams, J.; Lin, L.; Smith, M.; Huang, Z. Convenient synthesis of nucleoside 5'-triphosphates for RNA transcription. *Chemical Communications* **2011**, *47* (28), 8142-8144. DOI: 10.1039/c1cc12201k.
(145) Cremosnik, G. S.; Hofer, A.; Jessen, H. J. Iterative synthesis of nucleoside oligophosphates with phosphoramidites. *Angewandte Chemie-International Edition* **2014**, *53* (1), 286-289. DOI: 10.1002/anie.201306265.
(146) Warnecke, S.; Meier, C. Synthesis of Nucleoside Di- and Triphosphates and Dinucleoside Polyphosphates with cycloSal-Nucleotides. *The Journal of Organic Chemistry* **2009**, *74* (8), 3024-3030. DOI: 10.1021/jo802348h.
(147) Meier, C.; Ruppel, M. F. H.; Vukadinovic, D.; Balzarini, J. "Lock-in"-cycloSal-Pronucleotides - A New Generation of Chemical Trojan Horses? *Mini Reviews in Medicinal Chemistry* **2004**, *4* (4), 383-394. DOI: 10.2174/1389557043403972.
(148) Meier, C. cycloSal Phosphates as Chemical Trojan Horses for Intracellular Nucleotide and Glycosylmonophosphate Delivery — Chemistry Meets Biology. *European Journal of Organic Chemistry*. **2006**, (1081). DOI: https://doi.org/10.1002/ejoc.200500671.
(149) McQuade, D. T.; Seeberger, P. H. Applying Flow Chemistry: Methods, Materials, and Multistep Synthesis. *The Journal of Organic Chemistry* **2013**, *78* (13), 6384-6389. DOI: 10.1021/jo400583m.
(150) Wegner, J.; Ceylan, S.; Kirschning, A. Flow Chemistry – A Key Enabling Technology for (Multistep) Organic Synthesis. *Advanced Synthesis & Catalysis* **2012**, *354* (1), 17-57, https://doi.org/10.1002/adsc.201100584. DOI: https://doi.org/10.1002/adsc.201100584 (acccessed 2022/01/11).
(151) Baxendale, I. R.; Brocken, L.; Mallia, C. J. Flow chemistry approaches directed at improving chemical synthesis. *Green Processing and Synthesis* **2013**, *2* (3), 211-230. DOI: doi:10.1515/gps-2013-0029.
(152) Plutschack, M. B.; Pieber, B.; Gilmore, K.; Seeberger, P. H. The Hitchhiker's Guide to Flow Chemistry. *Chemical Reviews* **2017**, *117* (18), 11796-11893. DOI: 10.1021/acs.chemrev.7b00183.
(153) Baxendale, I. R. The integration of flow reactors into synthetic organic chemistry. *Journal of Chemical Technology & Biotechnology* **2013**, *88* (4), 519-552, https://doi.org/10.1002/jctb.4012. DOI: https://doi.org/10.1002/jctb.4012 (acccessed 2022/01/11).
(154) Song, F.; Zhang, J.; Zhao, Y.; Chen, W.; Li, L.; Xi, Z. Synthesis and antitumor activity of inositol phosphotriester analogues. *Organic & Biomolecular Chemistry* **2012**, *10* (18), 3642-3654, 10.1039/C2OB00031H. DOI: 10.1039/c2ob00031h.
(155) Dunetz, J. R.; Magano, J.; Weisenburger, G. A. Large-Scale Applications of Amide Coupling Reagents for the Synthesis of Pharmaceuticals. *Organic Process Research & Development* **2016**, *20* (2), 140-177. DOI: 10.1021/op500305s.
(156) Anastas, P.; Eghbali, N. Green Chemistry: Principles and Practice. *Chemical Society Reviews* **2010**, *39* (1), 301-312, 10.1039/B918763B. DOI: 10.1039/B918763B.
(157) Sheldon, R. A. Green solvents for sustainable organic synthesis: state of the art. *Green Chemistry* **2005**, *7* (5), 267-278, 10.1039/B418069K. DOI: 10.1039/B418069K.
(158) Jessop, P. G. Searching for green solvents. *Green Chemistry* **2011**, *13* (6), 1391-1398, 10.1039/C0GC00797H. DOI: 10.1039/C0GC00797H.
(159) Gu, Y.; Jérôme, F. Bio-based solvents: an emerging generation of fluids for the design of eco-efficient processes in catalysis and organic chemistry. *Chemical Society Reviews* **2013**, *42* (24), 9550-9570, 10.1039/C3CS60241A. DOI: 10.1039/C3CS60241A.
(160) Byrne, F. P.; Jin, S.; Paggiola, G.; Petchey, T. H. M.; Clark, J. H.; Farmer, T. J.; Hunt, A. J.; Robert McElroy, C.; Sherwood, J. Tools and techniques for solvent selection: green solvent selection guides. *Sustainable Chemical Processes* **2016**, *4* (1), 7. DOI: 10.1186/s40508-016-0051-z.
(161) Chemat, F.; Abert Vian, M.; Ravi, H. K.; Khadhraoui, B.; Hilali, S.; Perino, S.; Tixier, A.-S. F. Review of Alternative Solvents for Green Extraction of Food and Natural Products: Panorama, Principles, Applications and Prospects. *Molecules (Basel, Switzerland)* **2019**, *24* (16), 3007. DOI: 10.3390/molecules24163007 PubMed.
(162) Cvjetko Bubalo, M.; Vidović, S.; Radojčić Redovniković, I.; Jokić, S. Green solvents for green technologies. *Journal of Chemical Technology & Biotechnology* **2015**, *90* (9), 1631-1639, https://doi.org/10.1002/jctb.4668. DOI: https://doi.org/10.1002/jctb.4668 (acccessed 2022/03/28).
(163) Henderson, R. K.; Jiménez-González, C.; Constable, D. J. C.; Alston, S. R.; Inglis, G. G. A.; Fisher, G.; Sherwood, J.; Binks, S. P.; Curzons, A. D. Expanding GSK's solvent selection guide –

embedding sustainability into solvent selection starting at medicinal chemistry. *Green Chemistry* **2011**, *13* (4), 854-862, 10.1039/C0GC00918K. DOI: 10.1039/C0GC00918K.
(164) Pace, V.; Hoyos, P.; Castoldi, L.; Domínguez de María, P.; Alcántara, A. R. 2-Methyltetrahydrofuran (2-MeTHF): a biomass-derived solvent with broad application in organic chemistry. *ChemSusChem* **2012**, *5* (8), 1369-1379. DOI: 10.1002/cssc.201100780 From NLM.
(165) Ogawa, A.; Curran, D. P. Benzotrifluoride: A Useful Alternative Solvent for Organic Reactions Currently Conducted in Dichloromethane and Related Solvents. *The Journal of Organic Chemistry* **1997**, *62* (3), 450-451. DOI: 10.1021/jo9620324.
(166) Camp, J. E. Bio-available Solvent Cyrene: Synthesis, Derivatization, and Applications. *ChemSusChem* **2018**, *11* (18), 3048-3055. DOI: 10.1002/cssc.201801420 PubMed.
(167) Sherwood, J.; De bruyn, M.; Constantinou, A.; Moity, L.; McElroy, C. R.; Farmer, T. J.; Duncan, T.; Raverty, W.; Hunt, A. J.; Clark, J. H. Dihydrolevoglucosenone (Cyrene) as a bio-based alternative for dipolar aprotic solvents. *Chemical Communications* **2014**, *50* (68), 9650-9652, 10.1039/C4CC04133J. DOI: 10.1039/C4CC04133J.
(168) Brouwer, T.; Schuur, B. Dihydrolevoglucosenone (Cyrene), a Biobased Solvent for Liquid–Liquid Extraction Applications. *ACS Sustainable Chemistry & Engineering* **2020**, *8* (39), 14807-14817. DOI: 10.1021/acssuschemeng.0c04159.
(169) Milescu, R. A.; Zhenova, A.; Vastano, M.; Gammons, R.; Lin, S.; Lau, C. H.; Clark, J. H.; McElroy, C. R.; Pellis, A. Polymer Chemistry Applications of Cyrene and its Derivative Cygnet 0.0 as Safer Replacements for Polar Aprotic Solvents. *ChemSusChem* **2021**, *14* (16), 3367-3381. DOI: 10.1002/cssc.202101125 From NLM.
(170) Marino, T.; Galiano, F.; Molino, A.; Figoli, A. New frontiers in sustainable membrane preparation: Cyrene™ as green bioderived solvent. *Journal of Membrane Science* **2019**, *580*, 224-234.
(171) Amigues, E. J.; Hardacre, C.; Keane, G.; Migaud, M. E. Solvent-modulated reactivity of PCl3 with amines. *Green Chemistry* **2008**, *10* (6), 660-669, 10.1039/B718849H. DOI: 10.1039/B718849H.
(172) Gukathasan, R.; Massoudipour, M.; Gupta, I.; Chowdhury, A.; Pulst, S.; Ratnam, S.; Sanghvi, Y. S.; Laneman, S. A. Large-scale synthesis of high purity "Phos reagent" useful for oligonucleotide therapeutics. *Journal of Organometallic Chemistry* **2005**, *690* (10), 2603-2607. DOI: https://doi.org/10.1016/j.jorganchem.2004.10.014.
(173) Morodo, R., Bianchi, P. and Monbaliu, J.-C.M. (2020), Continuous Flow Organophosphorus Chemistry. European Journal of Organic Chemistry, 2020: 5236-5277. https://doi.org/10.1002/ejoc.202000430
(174) Taylor, C. J.; Baker, A.; Chapman, M. R.; Reynolds, W. R.; Jolley, K. E.; Clemens, G.; Smith, G. E.; Blacker, A. J.; Chamberlain, T. W.; Christie, S. D. R.; et al. Flow chemistry for process optimisation using design of experiments. *Journal of Flow Chemistry* **2021**, *11* (1), 75-86. DOI: 10.1007/s41981-020-00135-0.
(175) Alfonsi, K.; Colberg, J.; Dunn, P. J.; Fevig, T.; Jennings, S.; Johnson, T. A.; Kleine, H. P.; Knight, C.; Nagy, M. A.; Perry, D. A.; et al. Green chemistry tools to influence a medicinal chemistry and research chemistry based organisation. *Green Chemistry* **2008**, *10* (1), 31-36, 10.1039/B711717E. DOI: 10.1039/B711717E.
(176) Baselt, R. C.; Cravey, R. H. *Disposition of toxic drugs and chemicals in man*; Biomedical publications Davis, CA, 1982.
(177) Scailteur, V.; Lauwerys, R. R. Dimethylformamide (DMF) hepatotoxicity. *Toxicology* **1987**, *43* (3), 231-238. DOI: https://doi.org/10.1016/0300-483X(87)90082-5.
(178) Monticelli, S.; Castoldi, L.; Murgia, I.; Senatore, R.; Mazzeo, E.; Wackerlig, J.; Urban, E.; Langer, T.; Pace, V. Recent advancements on the use of 2-methyltetrahydrofuran in organometallic chemistry. *Monatshefte für Chemie* **2017**, *148* (1), 37-48. DOI: 10.1007/s00706-016-1879-3 From NLM.
(179) Laraman, F. J.; Fisk, H.; Whittaker, D. T. E.; Cherryman, J. H.; Diorazio, L. J. Investigating the Activation Kinetics of Phosphoramidites for Oligonucleotide Synthesis. *Organic Process Research & Development* **2022**, *26* (3), 764-772. DOI: 10.1021/acs.oprd.1c00195.
(180) Ben-Tal, Y.; Boaler, P. J.; Dale, H. J. A.; Dooley, R. E.; Fohn, N. A.; Gao, Y.; García-Domínguez, A.; Grant, K. M.; Hall, A. M. R.; Hayes, H. L. D. Mechanistic analysis by NMR spectroscopy: A users guide. *Progress in nuclear magnetic resonance spectroscopy* **2022**.
(181) Davies, S. R.; Jones, K.; Goldys, A.; Alamgir, M.; Chan, B. K. H.; Elgindy, C.; Mitchell, P. S. R.; Tarrant, G. J.; Krishnaswami, M. R.; Luo, Y. Purity assessment of organic calibration standards

using a combination of quantitative NMR and mass balance. *Analytical and Bioanalytical Chemistry* **2015**, *407* (11), 3103-3113.
(182) Wei, R.; Dickson, C. L.; Uhrín, D.; Lloyd-Jones, G. C. Rapid Estimation of T1 for Quantitative NMR. *The Journal of Organic Chemistry* **2021**, *86* (13), 9023-9029. DOI: 10.1021/acs.joc.1c01007.
(183) Dalitz, F.; Cudaj, M.; Maiwald, M.; Guthausen, G. Process and reaction monitoring by low-field NMR spectroscopy. *Progress in nuclear magnetic resonance spectroscopy* **2012**, *60* (2012), 52-70.
(184) Lakrimi, M.; Thomas, A. M.; Hutton, G.; Kruip, M.; Slade, R.; Davis, P.; Johnstone, A. J.; Longfield, M. J.; Blakes, H.; Calvert, S. The principles and evolution of magnetic resonance imaging. 2011, IOP Publishing: Vol. 286, p 012016.
(185) Schmidt, V. F.; Arnone, F.; Dietrich, O.; Seidensticker, M.; Armbruster, M.; Ricke, J.; Kazmierczak, P. M. Artifact reduction of coaxial needles in magnetic resonance imaging-guided abdominal interventions at 1.5 T: a phantom study. *Scientific Reports* **2021**, *11* (1), 22963. DOI: 10.1038/s41598-021-02434-5.
(186) Ernst, R. R.; Anderson, W. A. Application of Fourier transform spectroscopy to magnetic resonance. *Review of Scientific Instruments* **1966**, *37* (1), 93-102.
(187) Sanders, J. A. CHAPTER 4 - Magnetic Resonance Imaging. In *Functional Brain Imaging*, Orrison, W. W., Lewine, J. D., Sanders, J. A., Hartshorne, M. F. Eds.; Mosby, 1995; pp 145-186.
(188) Shoulders, B. High-Resolution NMR Techniques in Organic Chemistry. Tetrahedron Organic Chemistry Series Volume 19 By Timothy D. W. Claridge (Dyson Perrins Laborotory, Oxford). Pergamon: Oxford. 1999. ix + 384 pp. Hardbound $134.50, ISBN 0-08-042799-5. Paperback $49.50, ISBN 0-08-042798-7. *Journal of the American Chemical Society* **2000**, *122* (33), 8104-8104. DOI: 10.1021/ja004717y.
(189) Sanders, J. A.; Orrison, W. W. CHAPTER 7 - Functional Magnetic Resonance Imaging. In *Functional Brain Imaging*, Orrison, W. W., Lewine, J. D., Sanders, J. A., Hartshorne, M. F. Eds.; Mosby, 1995; pp 239-326.
(190) Couch, D. A.; Howarth, O. W.; Moore, P. Kinetic studies by stopped-flow pulse Fourier transform nuclear magnetic resonance. *Journal of Physics E: Scientific Instruments* **1975**, *8* (10), 831. DOI: 10.1088/0022-3735/8/10/012.
(191) Tshepelevitsh, S.; Kütt, A.; Lõkov, M.; Kaljurand, I.; Saame, J.; Heering, A.; Plieger, P. G.; Vianello, R.; Leito, I. On the Basicity of Organic Bases in Different Media. *European Journal of Organic Chemistry* **2019**, *2019* (40), 6735-6748, https://doi.org/10.1002/ejoc.201900956. DOI: https://doi.org/10.1002/ejoc.201900956 (acccessed 2022/11/18).
(192) Raczyńska, E. D.; Laurence, C.; Nicolet, P. Hydrogen bonding basicity of amidines. *Journal of the Chemical Society, Perkin Transactions 2* **1988**, (8), 1491-1494, 10.1039/P29880001491. DOI: 10.1039/P29880001491.
(193) Shriner, R. L.; Neumann, F. W. The Chemistry of the Amidines. *Chemical Reviews* **1944**, *35* (3), 351-425. DOI: 10.1021/cr60112a002.
(194) Ishikawa, T. Guanidine Chemistry. *Chemical and Pharmaceutical Bulletin* **2010**, *58* (12), 1555-1564. DOI: 10.1248/cpb.58.1555.
(195) https://nmr.chem.ucsb.edu/protocols/SNR.html (accessed.
(196) Jacob, M. 1,2,4-Triazoliums: Applications in Biocatalysis, Organocatalysis and Stable Radical Synthesis. Durham University, 2023.
(197) Dai, Q.; Piccirilli, J. A. Efficient Synthesis of 2‘,3‘-Dideoxy-2‘-amino-3‘-thiouridine. *Organic Letters* **2004**, *6* (13), 2169-2172. DOI: 10.1021/ol049366x.
(198) McGee, D. P. C.; Vaughn-Settle, A.; Vargeese, C.; Zhai, Y. 2‘-Amino-2‘-deoxyuridine via an Intramolecular Cyclization of a Trichloroacetimidate. *The Journal of Organic Chemistry* **1996**, *61* (2), 781-785. DOI: 10.1021/jo9510548.
(199) Fryszkowska, A.; Devine, P. N. Biocatalysis in drug discovery and development. *Current Opinion in Chemical Biology* **2020**, *55*, 151-160. DOI: https://doi.org/10.1016/j.cbpa.2020.01.012.
(200) Arnold, F. H. Directed Evolution: Bringing New Chemistry to Life. *Angewandte Chemie International Edition* **2018**, *57* (16), 4143-4148, https://doi.org/10.1002/anie.201708408. DOI: https://doi.org/10.1002/anie.201708408 (acccessed 2021/06/04).
(201) Sheldon, R. A.; Woodley, J. M. Role of Biocatalysis in Sustainable Chemistry. *Chemical Reviews* **2018**, *118* (2), 801-838. DOI: 10.1021/acs.chemrev.7b00203 From NLM.
(202) Wu, S.; Snajdrova, R.; Moore, J. C.; Baldenius, K.; Bornscheuer, U. T. Biocatalysis: Enzymatic Synthesis for Industrial Applications. *Angewandte Chemie International Edition* **2021**, *60* (1), 88-119,

https://doi.org/10.1002/anie.202006648. DOI: https://doi.org/10.1002/anie.202006648 (acccessed 2021/06/04).
(203) Reetz, M. T. Biocatalysis in Organic Chemistry and Biotechnology: Past, Present, and Future. *Journal of the American Chemical Society* **2013**, *135* (34), 12480-12496. DOI: 10.1021/ja405051f.
(204) Turner, N. J. Directed evolution drives the next generation of biocatalysts. *Nature Chemical Biology* **2009**, *5* (8), 567-573. DOI: 10.1038/nchembio.203 From NLM.
(205) Luetz, S.; Giver, L.; Lalonde, J. Engineered enzymes for chemical production. *Biotechnology & Bioengineering* **2008**, *101* (4), 647-653. DOI: 10.1002/bit.22077 From NLM.
(206) Woodley, J. M. Protein engineering of enzymes for process applications. *Current Opinion in Chemical Biology* **2013**, *17* (2), 310-316. DOI: 10.1016/j.cbpa.2013.03.017 From NLM.
(207) Schmid, A.; Dordick, J. S.; Hauer, B.; Kiener, A.; Wubbolts, M.; Witholt, B. Industrial biocatalysis today and tomorrow. *Nature* **2001**, *409* (6817), 258-268. DOI: 10.1038/35051736 PubMed.
(208) Richter, M. Functional diversity of organic molecule enzyme cofactors. *Natural Product Reports* **2013**, *30* (10), 1324-1345, 10.1039/C3NP70045C. DOI: 10.1039/C3NP70045C.
(209) Rokita, S. The Organic Chemistry of Enzyme-Catalyzed Reactions By Richard B. Silverman (Northwestern University). Academic Press: San Diego. 2000. xviii + 718 pp. $89.95. ISBN 0-12-643745-9. *Journal of the American Chemical Society* **2000**, *122* (33), 8103-8104. DOI: 10.1021/ja004710g.
(210) Kluger, R.; Tittmann, K. Thiamin Diphosphate Catalysis: Enzymic and Nonenzymic Covalent Intermediates. *Chemical Reviews* **2008**, *108* (6), 1797-1833. DOI: 10.1021/cr068444m.
(211) Müller, M.; Gocke, D.; Pohl, M. Thiamin diphosphate in biological chemistry: exploitation of diverse thiamin diphosphate-dependent enzymes for asymmetric chemoenzymatic synthesis. *The FEBS Journal* **2009**, *276* (11), 2894-2904, https://doi.org/10.1111/j.1742-4658.2009.07017.x. DOI: https://doi.org/10.1111/j.1742-4658.2009.07017.x (acccessed 2021/06/04).
(212) Pohl, M.; Sprenger, G. A.; Müller, M. A new perspective on thiamine catalysis. *Current Opinion in Biotechnology* **2004**, *15* (4), 335-342. DOI: https://doi.org/10.1016/j.copbio.2004.06.002.
(213) Prier, C. K.; Arnold, F. H. Chemomimetic Biocatalysis: Exploiting the Synthetic Potential of Cofactor-Dependent Enzymes To Create New Catalysts. *Journal of the American Chemical Society* **2015**, *137* (44), 13992-14006. DOI: 10.1021/jacs.5b09348.
(214) Hopkinson, M. N.; Richter, C.; Schedler, M.; Glorius, F. An overview of N-heterocyclic carbenes. *Nature* **2014**, *510* (7506), 485-496. DOI: 10.1038/nature13384 From NLM.
(215) Flanigan, D. M.; Romanov-Michailidis, F.; White, N. A.; Rovis, T. Organocatalytic Reactions Enabled by N-Heterocyclic Carbenes. *Chemical Reviews* **2015**, *115* (17), 9307-9387. DOI: 10.1021/acs.chemrev.5b00060 From NLM.
(216) Breslow, R. On the Mechanism of Thiamine Action. IV.1 Evidence from Studies on Model Systems. *Journal of the American Chemical Society* **1958**, *80* (14), 3719-3726. DOI: 10.1021/ja01547a064.
(217) Enders, D.; Niemeier, O.; Henseler, A. Organocatalysis by N-Heterocyclic Carbenes. *Chemical Reviews* **2007**, *107* (12), 5606-5655. DOI: 10.1021/cr068372z.
(218) Bugaut, X.; Glorius, F. Organocatalytic umpolung: N-heterocyclic carbenes and beyond. *Chemical Society Reviews* **2012**, *41* (9), 3511-3522, 10.1039/C2CS15333E. DOI: 10.1039/C2CS15333E.
(219) Massey, R. S.; Collett, C. J.; Lindsay, A. G.; Smith, A. D.; O'Donoghue, A. C. Proton Transfer Reactions of Triazol-3-ylidenes: Kinetic Acidities and Carbon Acid pKa Values for Twenty Triazolium Salts in Aqueous Solution. *Journal of the American Chemical Society* **2012**, *134* (50), 20421-20432. DOI: 10.1021/ja308420c.
(220) Collett, C. J.; Massey, R. S.; Maguire, O. R.; Batsanov, A. S.; O'Donoghue, A. C.; Smith, A. D. Mechanistic insights into the triazolylidene-catalysed Stetter and benzoin reactions: role of the N-aryl substituent. *Chemical Science* **2013**, *4* (4), 1514-1522, 10.1039/C2SC22137C. DOI: 10.1039/C2SC22137C.
(221) Massey, R. S.; Murray, J.; Collett, C. J.; Zhu, J.; Smith, A. D.; O'Donoghue, A. C. Kinetic and structure–activity studies of the triazolium ion-catalysed benzoin condensation. *Organic & Biomolecular Chemistry* **2021**, *19* (2), 387-393, 10.1039/D0OB02207A. DOI: 10.1039/D0OB02207A.

(222) DiRocco, D. A.; Oberg, K. M.; Rovis, T. Isolable Analogues of the Breslow Intermediate Derived from Chiral Triazolylidene Carbenes. *Journal of the American Chemical Society* **2012**, *134* (14), 6143-6145. DOI: 10.1021/ja302031v.
(223) Higgins, E. M.; Sherwood, J. A.; Lindsay, A. G.; Armstrong, J.; Massey, R. S.; Alder, R. W.; O'Donoghue, A. C. pKas of the conjugate acids of N-heterocyclic carbenes in water. *Chemical Communications* **2011**, *47* (5), 1559-1561, 10.1039/C0CC03367G. DOI: 10.1039/C0CC03367G.
(224) Melnick, J. S.; Sprinz, K. I.; Reddick, J. J.; Kinsland, C.; Begley, T. P. An efficient enzymatic synthesis of thiamin pyrophosphate. *Bioorganic & Medicinal Chemistry Letters* **2003**, *13* (22), 4139-4141. DOI: https://doi.org/10.1016/j.bmcl.2003.07.026.
(225) Nosaka, K.; Kaneko, Y.; Nishimura, H.; Iwashima, A. Isolation and characterization of a thiamin pyrophosphokinase gene, THI80, from Saccharomyces cerevisiae. *Journal of Biological Chemistry* **1993**, *268* (23), 17440-17447. From NLM.
(226) Begley, T. P.; Downs, D. M.; Ealick, S. E.; McLafferty, F. W.; Van Loon, A. P. G. M.; Taylor, S.; Campobasso, N.; Chiu, H. J.; Kinsland, C.; Reddick, J. J.; et al. Thiamin biosynthesis in prokaryotes. *Archives of Microbiology* **1999**, *171* (5), 293-300, Short Survey. DOI: 10.1007/s002030050713 Scopus.
(227) Matsukawa, T.; Hirano, H.; Yurugi, S. [25] Preparation of thiamine derivatives and analogs. In *Methods in Enzymology*, Vol. 18; Academic Press, 1970; pp 141-162.
(228) K., C.; R., C.; E., M. M.; P., R.; T., R.; S., V. Selective solvent free phosphorylation. 12-08-2016.
(229) Noren, C. J.; Anthony-Cahill, S. J.; Griffith, M. C.; Schultz, P. G. A general method for site-specific incorporation of unnatural amino acids into proteins. *Science* **1989**, *244* (4901), 182. DOI: 10.1126/science.2649980.
(230) Dougherty, D. A. Unnatural amino acids as probes of protein structure and function. *Current Opinion in Chemical Biology* **2000**, *4* (6), 645-652. DOI: https://doi.org/10.1016/S1367-5931(00)00148-4.
(231) Gao, W.; Cho, E.; Liu, Y.; Lu, Y. Advances and Challenges in Cell-Free Incorporation of Unnatural Amino Acids Into Proteins. *Frontiers in Pharmacology* **2019**, *10*, 611, 10.3389/fphar.2019.00611.
(232) Liu, W.; Brock, A.; Chen, S.; Chen, S.; Schultz, P. G. Genetic incorporation of unnatural amino acids into proteins in mammalian cells. *Nature Methods* **2007**, *4* (3), 239-244. DOI: 10.1038/nmeth1016.
(233) Kim, C. H.; Axup, J. Y.; Schultz, P. G. Protein conjugation with genetically encoded unnatural amino acids. *Current Opinion in Chemical Biology* **2013**, *17* (3), 412-419. DOI: https://doi.org/10.1016/j.cbpa.2013.04.017.
(234) Fraser, T. H.; Rich, A. Synthesis and aminoacylation of 3'-amino-3'-deoxy transfer RNA and its activity in ribosomal protein synthesis. *National Academy of Sciences U S A* **1973**, *70* (9), 2671-2675. DOI: 10.1073/pnas.70.9.2671 From NLM.
(235) Ibba, M.; Söll, D. Aminoacyl-tRNA Synthesis. *Annual Review of Biochemistry* **2000**, *69* (1), 617-650. DOI: 10.1146/annurev.biochem.69.1.617 (acccessed 2021/06/06).
(236) Pang, Y. L. J.; Poruri, K.; Martinis, S. A. tRNA synthetase: tRNA aminoacylation and beyond. *Wiley interdisciplinary reviews. RNA* **2014**, *5* (4), 461-480. DOI: 10.1002/wrna.1224 PubMed.
(237) Munier, R.; Cohen, G. N. [Incorporation of structural analogues of amino acids into bacterial proteins during their synthesis in vivo]. *Biochimica et Biophysica Acta* **1959**, *31* (2), 378-391. DOI: 10.1016/0006-3002(59)90011-3 From NLM.
(238) Liu, C. C.; Schultz, P. G. Adding New Chemistries to the Genetic Code. *Annual Review of Biochemistry* **2010**, *79* (1), 413-444. DOI: 10.1146/annurev.biochem.052308.105824 (acccessed 2021/06/07).
(239) Xiao, H.; Chatterjee, A.; Choi, S. H.; Bajjuri, K. M.; Sinha, S. C.; Schultz, P. G. Genetic incorporation of multiple unnatural amino acids into proteins in mammalian cells. *Angewandte Chemie International Edition in English* **2013**, *52* (52), 14080-14083. DOI: 10.1002/anie.201308137 From NLM.
(240) Chatterjee, A.; Xiao, H.; Bollong, M.; Ai, H.-W.; Schultz, P. G. Efficient viral delivery system for unnatural amino acid mutagenesis in mammalian cells. *Proceedings of the National Academy of Sciences* **2013**, *110* (29), 11803. DOI: 10.1073/pnas.1309584110.

(241) Hoesl, M. G.; Budisa, N. Recent advances in genetic code engineering in Escherichia coli. *Current Opinion in Biotechnology* **2012**, *23* (5), 751-757. DOI: https://doi.org/10.1016/j.copbio.2011.12.027.
(242) Wang, L.; Brock, A.; Herberich, B.; Schultz, P. G. Expanding the genetic code of Escherichia coli. *Science* **2001**, *292* (5516), 498-500. DOI: 10.1126/science.1060077 From NLM.
(243) Xie, J.; Schultz, P. G. Adding amino acids to the genetic repertoire. *Current Opinion in Chemical Biology* **2005**, *9* (6), 548-554. DOI: https://doi.org/10.1016/j.cbpa.2005.10.011.
(244) Kobayashi, T.; Nureki, O.; Ishitani, R.; Yaremchuk, A.; Tukalo, M.; Cusack, S.; Sakamoto, K.; Yokoyama, S. Structural basis for orthogonal tRNA specificities of tyrosyl-tRNA synthetases for genetic code expansion. *Nature Structural & Molecular Biology* **2003**, *10* (6), 425-432. DOI: 10.1038/nsb934.
(245) Normanly, J.; Kleina, L. G.; Masson, J.-M.; Abelson, J.; Miller, J. H. Construction of Escherichia coli amber suppressor tRNA genes: III. Determination of tRNA specificity. *Journal of Molecular Biology* **1990**, *213* (4), 719-726. DOI: https://doi.org/10.1016/S0022-2836(05)80258-X.
(246) Rackham, O.; Chin, J. W. A network of orthogonal ribosome·mRNA pairs. *Nature Chemical Biology* **2005**, *1* (3), 159-166. DOI: 10.1038/nchembio719.
(247) Wang, K.; Neumann, H.; Peak-Chew, S. Y.; Chin, J. W. Evolved orthogonal ribosomes enhance the efficiency of synthetic genetic code expansion. *Nature Biotechnology* **2007**, *25* (7), 770-777. DOI: 10.1038/nbt1314.
(248) Fried, S. D.; Schmied, W. H.; Uttamapinant, C.; Chin, J. W. Ribosome Subunit Stapling for Orthogonal Translation in E. coli. *Angewandte Chemie International Edition in English* **2015**, *54* (43), 12791-12794. DOI: 10.1002/anie.201506311 PubMed.
(249) Terasaka, N.; Hayashi, G.; Katoh, T.; Suga, H. An orthogonal ribosome-tRNA pair via engineering of the peptidyl transferase center. *Nature Chemical Biology* **2014**, *10* (7), 555-557. DOI: 10.1038/nchembio.1549.
(250) Cornish, V. W.; Mendel, D.; Schultz, P. G. Probing Protein Structure and Function with an Expanded Genetic Code. *Angewandte Chemie International Edition in English* **1995**, *34* (6), 621-633, https://doi.org/10.1002/anie.199506211. DOI: https://doi.org/10.1002/anie.199506211 (acccessed 2021/06/07).
(251) Taira, H.; Fukushima, M.; Hohsaka, T.; Sisido, M. Four-base codon-mediated incorporation of non-natural amino acids into proteins in a eukaryotic cell-free translation system. *Journal of Bioscience and Bioengineering* **2005**, *99* (5), 473-476. DOI: 10.1263/jbb.99.473 From NLM.
(252) Hong, S. H.; Kwon, Y.-C.; Jewett, M. C. Non-standard amino acid incorporation into proteins using Escherichia coli cell-free protein synthesis. *Frontiers in chemistry* **2014**, *2*, 34-34. DOI: 10.3389/fchem.2014.00034 PubMed.
(253) Soye, B. J. D.; Patel, J. R.; Isaacs, F. J.; Jewett, M. C. Repurposing the translation apparatus for synthetic biology. Current Opinion in Chemical Biology **2015**, *28*, 83-90. DOI: 10.1016/j.cbpa.2015.06.008 From NLM.
(254) Ellman, J.; Mendel, D.; Anthony-Cahill, S.; Noren, C. J.; Schultz, P. G. [15] Biosynthetic method for introducing unnatural amino acids site-specifically into proteins. In *Methods in Enzymology*, Vol. 202; Academic Press, 1991; pp 301-336.
(255) Jewett, M. C.; Calhoun, K. A.; Voloshin, A.; Wuu, J. J.; Swartz, J. R. An integrated cell-free metabolic platform for protein production and synthetic biology. *Molecular systems biology* **2008**, *4*, 220-220. DOI: 10.1038/msb.2008.57 PubMed.
(256) Jewett, M. C.; Fritz, B. R.; Timmerman, L. E.; Church, G. M. In vitro integration of ribosomal RNA synthesis, ribosome assembly, and translation. *Molecular systems biology* **2013**, *9*, 678-678. DOI: 10.1038/msb.2013.31 PubMed.
(257) Hecht, S. M.; Alford, B. L.; Kuroda, Y.; Kitano, S. "Chemical aminoacylation" of tRNA's. *Journal of Biological Chemistry* **1978**, *253* (13), 4517-4520. DOI: https://doi.org/10.1016/S0021-9258(17)30417-9.
(258) Gamper, H.; Hou, Y. M. tRNA 3'-amino-tailing for stable amino acid attachment. *Rna* **2018**, *24* (12), 1878-1885. DOI: 10.1261/rna.068015.118 From NLM.
(259) Cho, H. D.; Oyelere, A. K.; Strobel, S. A.; Weiner, A. M. Use of nucleotide analogs by class I and class II CCA-adding enzymes (tRNA nucleotidyltransferase): deciphering the basis for nucleotide selection. *Rna* **2003**, *9* (8), 970-981. DOI: 10.1261/rna.2110903 From NLM.

(260) Sprinzl, M. Chemistry of aminoacylation and peptide bond formation on the 3'terminus of tRNA. *Journal of Biosciences* **2006**, *31* (4), 489-496. DOI: 10.1007/bf02705188 From NLM.
(261) Goodman, C. A.; Pierre, P.; Hornberger, T. A. Imaging of protein synthesis with puromycin. *Proceedings of the National Academy of Sciences* **2012**, *109* (17), E989. DOI: 10.1073/pnas.1202000109.
(262) Liu, J.; Xu, Y.; Stoleru, D.; Salic, A. Imaging protein synthesis in cells and tissues with an alkyne analog of puromycin. *Proceedings of the National Academy of Sciences* **2012**, *109* (2), 413. DOI: 10.1073/pnas.1111561108.
(263) Katoh, T.; Suga, H. Flexizyme-catalyzed synthesis of 3′-aminoacyl-NH-tRNAs. *Nucleic Acids Research* **2019**, *47* (9), e54-e54. DOI: 10.1093/nar/gkz143 (acccessed 6/7/2021).
(264) Nguyen-Trung, N. Q.; Botta, O.; Terenzi, S.; Strazewski, P. A Practical Route to 3‘-Amino-3‘-deoxyadenosine Derivatives and Puromycin Analogues. *The Journal of Organic Chemistry* **2003**, *68* (5), 2038-2041. DOI: 10.1021/jo026627c.
(265) Burke, H. M.; McSweeney, L.; Scanlan, E. M. Exploring chemoselective S-to-N acyl transfer reactions in synthesis and chemical biology. *Nature Communications* **2017**, *8* (1), 15655. DOI: 10.1038/ncomms15655.
(266) Kent, S. Origin of the chemical ligation concept for the total synthesis of enzymes (proteins). *Peptide Science* **2010**, *94* (4), iv-ix, https://doi.org/10.1002/bip.21492. DOI: https://doi.org/10.1002/bip.21492 (acccessed 2021/06/07).
(267) Dawson, P. E.; Muir, T. W.; Clark-Lewis, I.; Kent, S. B. Synthesis of proteins by native chemical ligation. *Science* **1994**, *266* (5186), 776. DOI: 10.1126/science.7973629.
(268) Pattabiraman, V. R.; Bode, J. W. Rethinking amide bond synthesis. *Nature* **2011**, *480* (7378), 471-479. DOI: 10.1038/nature10702.
(269) Muir, T. W.; Sondhi, D.; Cole, P. A. Expressed protein ligation: A general method for protein engineering. *Proceedings of the National Academy of Sciences* **1998**, *95* (12), 6705. DOI: 10.1073/pnas.95.12.6705.
(270) Macmillan, D.; Adams, A.; Premdjee, B. Shifting Native Chemical Ligation into Reverse through N→S Acyl Transfer. *Israel Journal of Chemistry* **2011**, *51* (8-9), 885-899, https://doi.org/10.1002/ijch.201100084. DOI: https://doi.org/10.1002/ijch.201100084 (acccessed 2023/02/14).
(271) Cowper, B.; Shariff, L.; Chen, W.; Gibson, S. M.; Di, W.-L.; Macmillan, D. Expanding the scope of N → S acyl transfer in native peptide sequences. *Organic & Biomolecular Chemistry* **2015**, *13* (27), 7469-7476, 10.1039/C5OB01029B. DOI: 10.1039/C5OB01029B.
(272) Melnyk, O.; Agouridas, V. From protein total synthesis to peptide transamidation and metathesis: playing with the reversibility of N,S-acyl or N,Se-acyl migration reactions. *Current Opinion in Chemical Biology* **2014**, *22*, 137-145. DOI: 10.1016/j.cbpa.2014.09.030 From NLM.
(273) Noren, C. J.; Wang, J.; Perler, F. B. Dissecting the Chemistry of Protein Splicing and Its Applications. *Angewandte Chemie International Edition in English* **2000**, *39* (3), 450-466. DOI: 10.1002/(sici)1521-3773(20000204)39:3<450::aid-anie450>3.0.co;2-f PubMed.